

A solution NMR methodology enabling the elucidation of small molecule-phospholipid membrane adhesion and passive permeation parameters.

Angela Serrano-Sanchez, Matthew Rice, Joseph Cassar, Lisa J. White, Precious I. A. Popoola, Gary Thompson, Jennifer R. Hiscock and Jose L. Ortega-Roldan*

Contents

General experimental for chemical synthesis and compound characterisation	2
High-resolution mass spectrometry studies	2
Chemical synthesis	2
Experimental for the permeation/membrane adhesion assay.....	4
24-Hour Incubation.....	5
1D ¹ H CPMG spectra.....	8
T1 and T2 spin relaxation data for reference compounds	100
NMR characterisation	111
References	114

General experimental for chemical synthesis and compound characterisation

A positive pressure of nitrogen and oven dried glassware were used for all reactions. All solvents and starting materials were purchased from known chemical suppliers or available stores and used without any further purification unless specifically stipulated. The NMR spectra were obtained using a Bruker AV2 400 MHz or AVNEO 400 MHz spectrometer. The data was processed using Topspin software. NMR Chemical shift values are reported in parts per million (ppm) and calibrated to the centre of the residual solvent peak set (s = singlet, br = broad, d = doublet, t = triplet, q = quartet, m = multiplet). The melting point for each compound was measured using Stuart SMP10 melting point apparatus. High resolution mass spectrometry was performed using a Bruker microTOF-Q mass spectrometer and spectra recorded and processed using Bruker's Compass Data Analysis software. Infrared spectra were obtained using a Shimadzu IR-Affinity-1 model Infrared spectrometer. The data are analysed in wavenumbers (cm^{-1}) using IRsolution software.

High-resolution mass spectrometry studies

Chemical samples were dissolved in HPLC-grade methanol at a concentration of 1 mg/mL before being further diluted 1 in 100 in methanol. 10 μL of the sample was injected into a flowing stream of 10 mM ammonium acetate in 95% methanol in water (flow rate: 0.02 mL/min) and the flow directed into the electrospray source of the mass spectrometer. Mass spectra were acquired in the negative ion mode and data processed in Bruker's Compass Data Analysis software.

Chemical synthesis

29: This compound was synthesized in line with our previously published method.¹ ^1H NMR (400 MHz, 298.15 K, $\text{DMSO-}d_6$): δ : 12.64 (s, 1H), 9.28 (s, 1H), 7.59 (d, $J = 2.92$ Hz, 4H), 6.56 (t, $J = 5.48$ Hz, 1H), 3.81 (d, $J = 5.60$ Hz, 2H).

30: This compound was synthesised in line with our previously published methods². Proton NMR were found to match our previously published.¹ ^1H NMR (400 MHz, 298.15 K, $\text{DMSO-}d_6$): δ : 10.41 (s, 1H), 7.70 (d, $J = 8.60$ Hz, 2H), 7.48 (d, $J = 8.68$ Hz, 2H), 6.85 (s, 1H), 3.17 - 3.13 (m, 8H), 1.59 - 1.51 (m, 8H), 1.34 - 1.25 (m, 8H), 0.92 (t, $J = 7.24$ Hz, 12H).

32: This compound was synthesised in line with our previously published methods². Proton NMR were found to match our previously published values.¹ ^1H NMR (400 MHz, 298.15 K, $\text{DMSO-}d_6$): δ : 10.24 (s, 1H), 8.18 (t, $J = 5.20$ Hz, 1H), 7.77 (d, $J = 8.48$ Hz, 2H), 7.67 (d, $J = 8.56$ Hz, 2H), 4.23 (d, $J = 5.24$ Hz, 2H).

57: *D*-phenylalanine *tert*-butyl ester hydrochloride (0.52 g, 2.0 mmol) was added to a stirring solution of 1-isocyanato-4-(trifluoromethyl) benzene (0.29 mL, 2.00 mmol) in pyridine (10 mL) and left at RT overnight. The mixture was then taken to dryness, then dissolved in chloroform (5 mL), followed by dropwise additions of hexane, resulting in precipitation. Zinc bromide (2.25 g, 10 mmol) was added to a solution of the precipitate (0.51 g, 1.25 mmol) in dichloromethane (5 mL) and stirred at RT for 24 hours. Water (20 mL) was added, and the mixture was stirred at RT for further 4 hours, before removal of the precipitate via filtration. Tetrabutylammonium hydroxide (1 M) in methanol (1.25 mL, 1.25 mM) was added to the precipitate and taken to dryness. The pure product was obtained by flash chromatography, 100 % ethyl acetate followed by 100 % methanol, as a brown solid with a yield of 54 % (0.28 g, 0.47 mmol); Melting point: > 200 °C; ^1H NMR (400 MHz, 298 K, $\text{DMSO-}d_6$): δ : 10.28 (s, 1H), 7.72 (d, $J = 8.48$ Hz, 2H), 7.48 (d, $J = 8.68$ Hz, 2H), 7.17 - 7.09 (m, 5H), 6.89 (s, 1H), 3.97 (s, 1H), 3.35 - 2.98 (m, 10 H), 1.60 - 1.51 (m, 8H), 1.35 - 1.27 (m, 8H), 0.93 (t, $J = 7.24$ Hz, 12H); $^{13}\text{C}\{^1\text{H}\}$ NMR (100 MHz, 298 K, $\text{DMSO-}d_6$): δ : 173.2 (CO), 155.2 (CO), 145.9 (ArC), 140.2 (ArC), 130.1 (ArCH), 127.9 (ArCH), 126.7 (ArCH), 126.0 (q, $J = 3.52$ Hz, CF_3), 125.9 (ArCH), 123.9 (ArC), 120.7 - 119.7 (q, $J = 46.7$ Hz, ArC), 117.3 (ArCH), 57.9 (t, $J = 4.99$ Hz, CH_2); 56.7 (CH), 39.1 (CH_2), 23.5 (CH_2), 19.7 (CH_2), 13.9 (CH_3); IR (film): $\nu = 2962$ (NH stretch), 1695, 1487, 1319, 881; HRMS for the carboxylate urea ($\text{C}_{17}\text{H}_{14}\text{F}_3\text{N}_2\text{O}_3^-$) (ESI⁻): m/z : act: 351.0937 [M]⁻ cal: 351.0962 [M]⁻.

60: This compound was synthesised in line with our previously published methods². Proton NMR were found to match our previously published.³ ¹H NMR (400 MHz, 298.15 K, DMSO-*d*₆): δ : 9.98 (s, 1H), 7.87 (t, *J* = 9.08 Hz, 1H, 4H), 7.65 (d, *J* = 8.76 Hz, 2H), 7.31 (d, *J* = 1.08 Hz, 1H), 6.62 (s, 1H), 3.31 (s, 2H), 3.17 – 3.13 (m, 8H), 2.44 (s, 3H), 1.59 – 1.51 (m, 8H), 1.33 – 1.27 (m, 8H), 0.92 (t, *J* = 7.28, 12H).

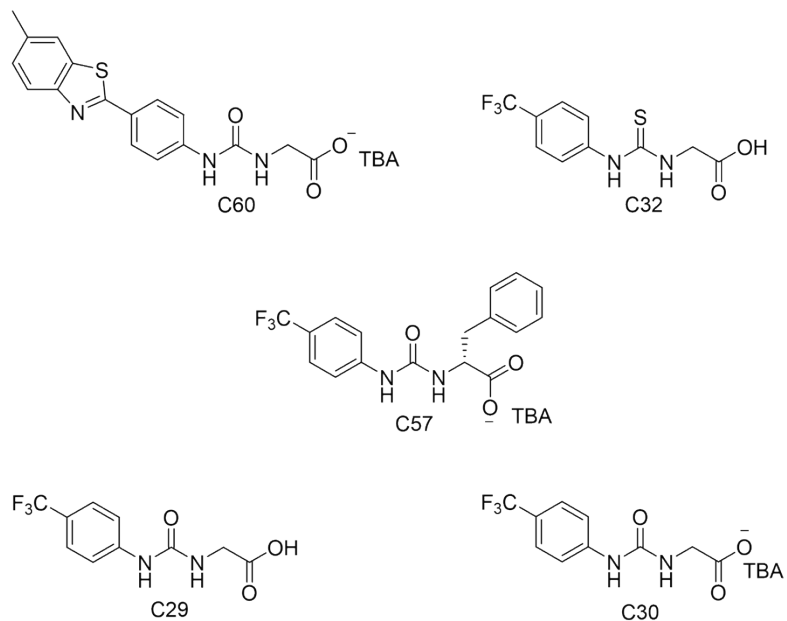


Figure S1. Chemical structures of SSAs C29, C30, C32, C57 and C60. TBA = Tetrabutylammonium.

Experimental for the permeation/membrane adhesion assay

Preparation of inner membranes vesicles. The Gram-negative bacterial strain of *E. coli* DH5 α was used for lipid extraction following the method described previously⁴. The resulting lipid film created by drying the solvent with nitrogen or using a rotavapor was rehydrated with buffer and then sonicated for 1 h. Finally, multilamellar vesicles were extruded through a membrane with a pore size of 1000 nm to make empty unilamellar vesicles.

Preparation of stock solutions. Firstly, approximately 400 μ M of a stock solution was prepared for each antimicrobial compound to be tested by dissolving the required amount of the compound into 350 μ L of DMSO-d₆. For the SSA compounds in each sample, 400 μ M of a 5 mM stock solution was prepared dissolving the required amount of the compound into HEPES buffer (10 mM HEPES and 10 mM NaCl pH 7.4) at 90C by sonicating. As control samples, 400 μ M of a stock solution of glucose and indole were prepared as well as 400 μ M of manganese stock for the titrations.

NMR sample preparation. Samples were brought to a total final volume of 300 μ L and transferred to a 3 mm NMR tube, containing 5% D₂O, 0.01 mM of DSS, 30 μ L of the lipid vesicles (20 mg/mL) and the reference or SSA compounds tested individually.

NMR acquisition. The 1D ¹H NMR and ¹H CPMG spectra were collected using a Bruker Avance III spectrometer at a proton frequency of 600 MHz and recorded at 298 K. This spectrometer is equipped with a QCIP cryoprobe with a standard ³¹P pre-amplifier without enhanced sensitivity from cryogenic cooling⁴. 1D ¹H NMR spectra were acquired using the standard zgprcpmg pulse sequence from the Bruker library, though it was modified with an excitation water suppression element (1D ¹H WATERGATE) to ensure elimination of water signal for all experiments. That was achieved with 3-9-19 watergate sequence using 1 ms pulses. The following acquisition parameters were used: spectral width of 12 ppm, relaxation delay of 10 μ s and acquisition time of 1.02 s at a power of 7.9W. All data was collected with 16384 points and receiver gain was set to 256 with an accumulation time of 32 scans and 8 dummy scans. The CPMG element was collected at three different CPMG spin-lock times: 20 ms, 50 ms and 150 ms; after a selection process between 20 ms and 300 ms. The rest of parameters were the same as the 1D ¹H NMR experiment except the relaxation delay that was 1 ms and an acquisition time of 1.02 s.

The 24-hour incubation test was carried out using the same samples with ¹H CPMG spectra being collected after 30 minutes of incubation and then again after 24 hours of incubation.

NMR Data Collection and Processing. TOPSPIN 3.6.1 was used to collect the NMR data. All spectra were automatically or manually corrected for phase and baseline distortions using a polynomial function and calibrated to the centre of DSS peak (at 0 ppm) using MestReNova software.

Data interpretation. The intensities of well resolved peaks on the CPMG spectra of each compound were calculated using MestReNova and used in equations 1 and 2 to calculate PF and MAF values. Errors are determined based on the baseline error of the spectra used in equations 1 and 2. The selection of CPMG spin-lock time depends on the T₁ and T₂ contribution, which can lead to different effects on the intensity of the NMR peaks in the presence of vesicles and/or the solvent PRE reagent. For molecules associating more tightly with the membrane, longer CPMG spin-locks results in the loss of the NMR signals due to broadening. For all the molecules tested we found that a CPMG spin-lock of 150mS works best at distinguishing small molecules with different levels of membrane association/permeation.

24-Hour Incubation

Table S1. A table containing the calculated permeability factors (PF) and membrane adhesion factors (MAF) for glucose after 30-minute and 24-hour incubation times.

ms	30-Minute Incubation				24-Hour Incubation			
	20	50	150	300	20	50	150	300
PF	1.06	0.70	0.92	0.96	1.39	1.08	1.07	1.18
MAF	0.93	1.42	0.97	0.94	0.70	0.91	0.83	0.71

Table S2. A table containing the calculated permeability factors (PF) and membrane adhesion factors (MAF) for glucose after 30-minute and 24-hour incubation times.

ms	30-Minute Incubation				24-Hour Incubation			
	20	50	150	300	20	50	150	300
PF	1.00	1.08	1.29	1.66	1.01	1.13	1.29	1.58
MIF	0.99	0.97	0.95	0.97	0.94	0.94	0.95	0.96

1D ¹H CPMG Spectra

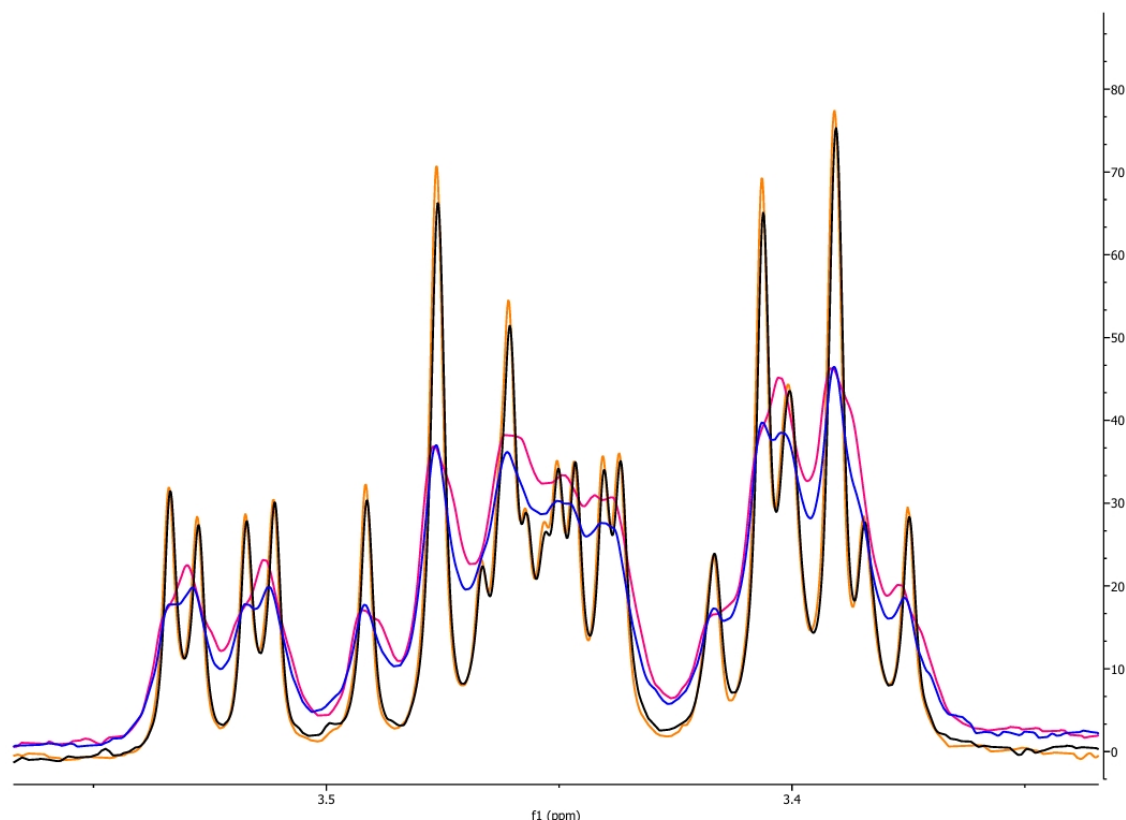


Figure S2. Proton 1D CPMG NMR spectra collected with a spin-lock time of 150 ms of the reference compound glucose (500 μM) after a 30-minute incubation period in the absence of *E. coli* lipids (orange), in the presence of Mn²⁺ (pink), in the presence of *E. coli* vesicles (black) and in the presence of both *E. coli* lipids and Mn²⁺ (blue).

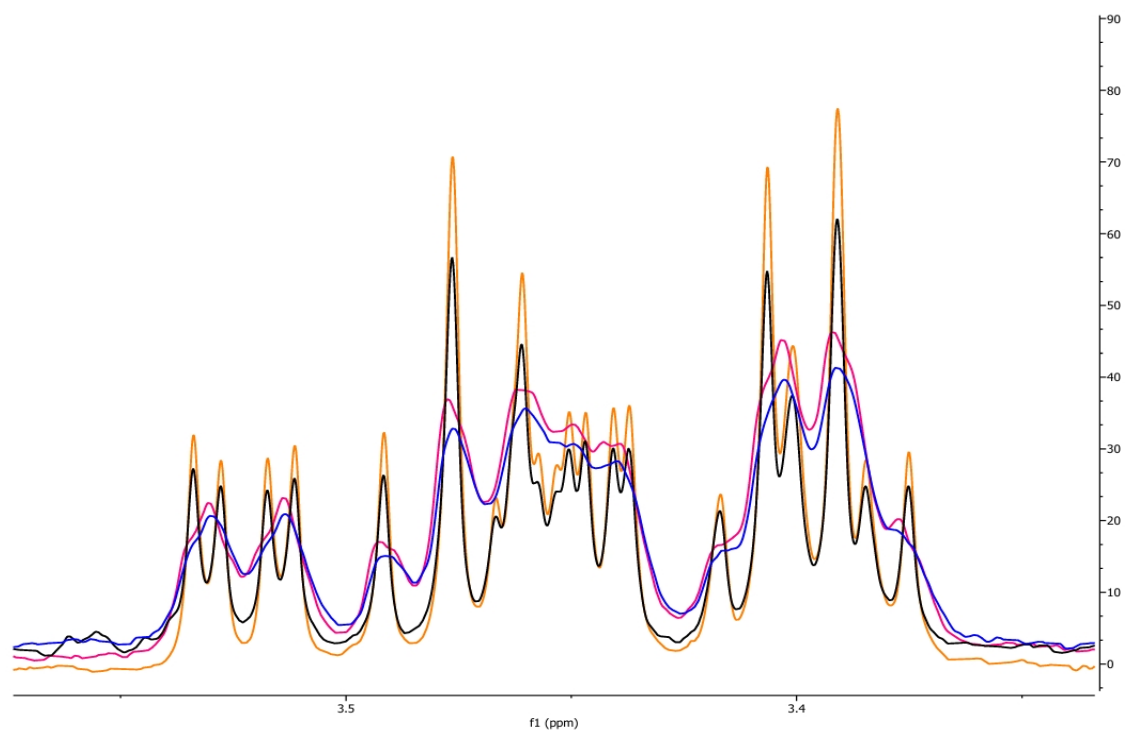


Figure S3. Proton 1D CPMG NMR spectra collected with a spin-lock time of 150 ms of the reference compound glucose (500 μM) after a 24-hour incubation period in the absence of *E. coli* lipids (orange), in the presence of Mn^{2+} (pink), in the presence of *E. coli* vesicles (black) and in the presence of both *E. coli* lipids and Mn^{2+} (blue).

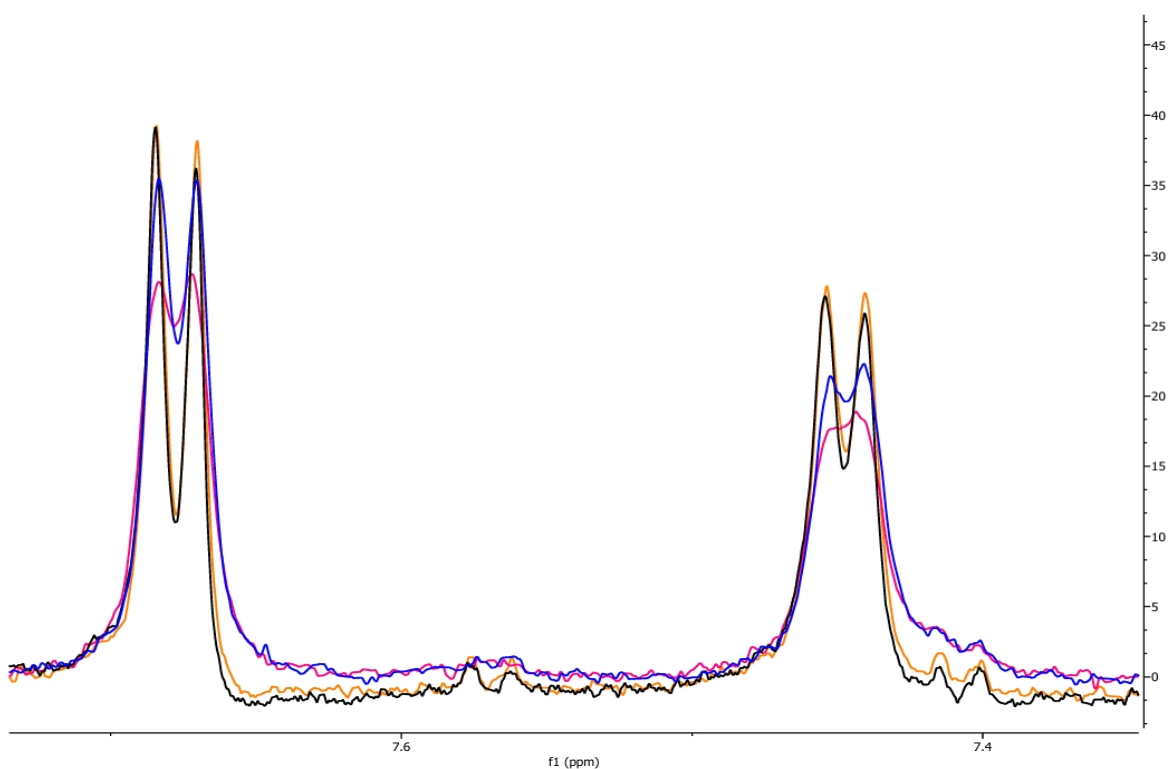


Figure S4. Proton 1D CPMG NMR spectra collected with a spin-lock time of 150 ms of the reference compound C32 (200 μM) after a 30-minute incubation period in the absence of *E. coli* lipids (orange), in the presence of Mn^{2+} (pink), in the presence of *E. coli* vesicles (black) and in the presence of both *E. coli* lipids and Mn^{2+} (blue).

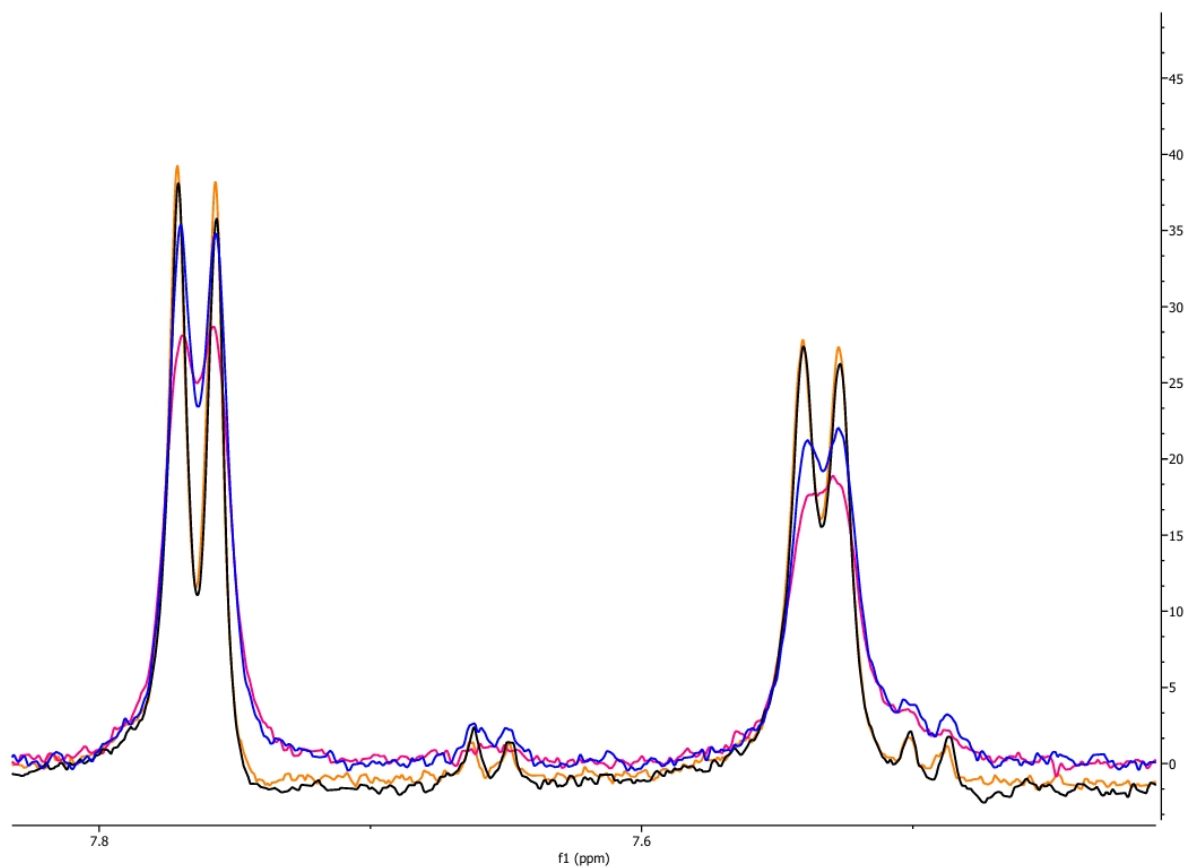


Figure S5. Proton 1D CPMG NMR spectra collected with a spin-lock time of 150 ms of the reference compound C32 (200 μM) after a 24-hour incubation period in the absence of *E. coli* lipids (orange), in the presence of Mn²⁺ (pink), in the presence of *E. coli* vesicles (black) and in the presence of both *E. coli* lipids and Mn²⁺ (blue).

1D ^1H CPMG spectra

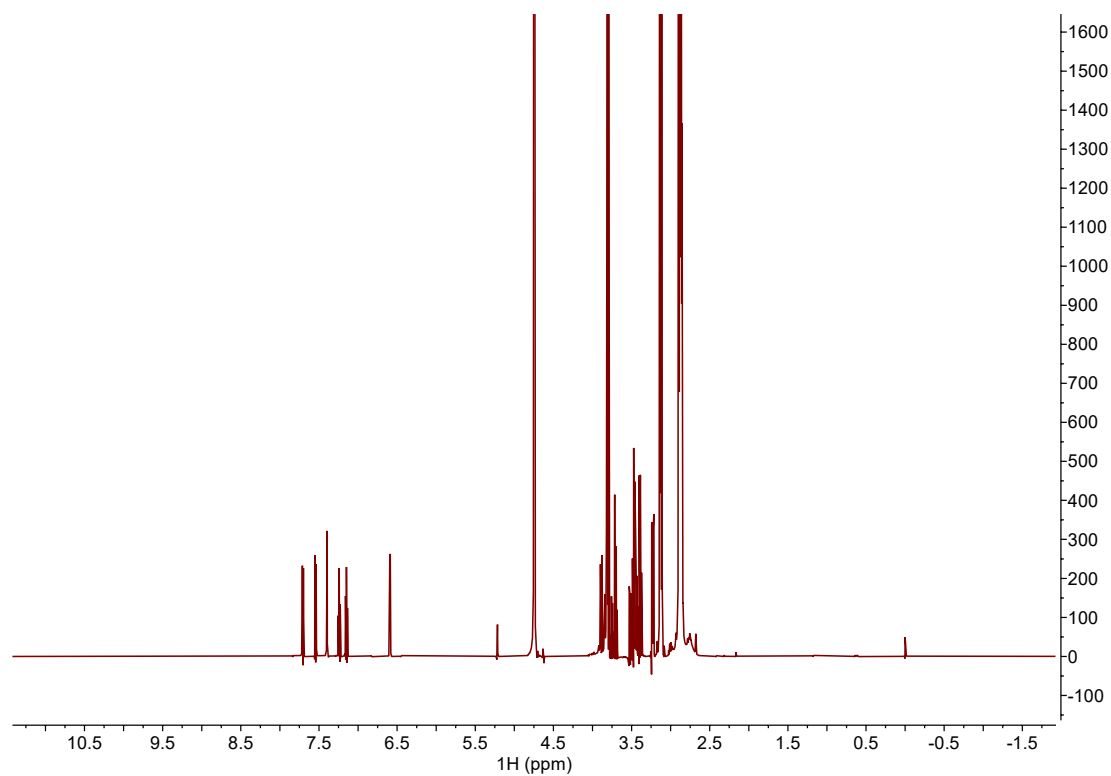


Figure S6. Proton 1D CPMG NMR spectrum of 4 mM glucose and 2 mM indole collected with a spin-lock time of 20 ms at 298K.

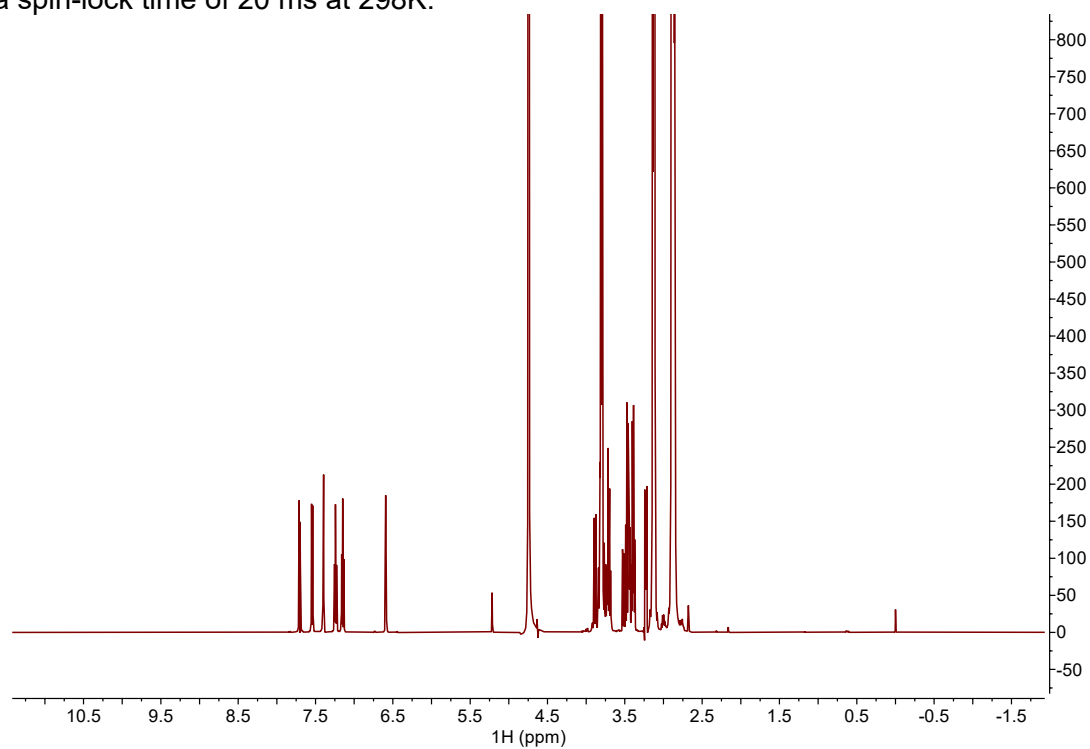


Figure S7. Proton 1D CPMG NMR spectrum of 4 mM glucose and 2 mM indole collected with a spin-lock time of 50 ms at 298K.

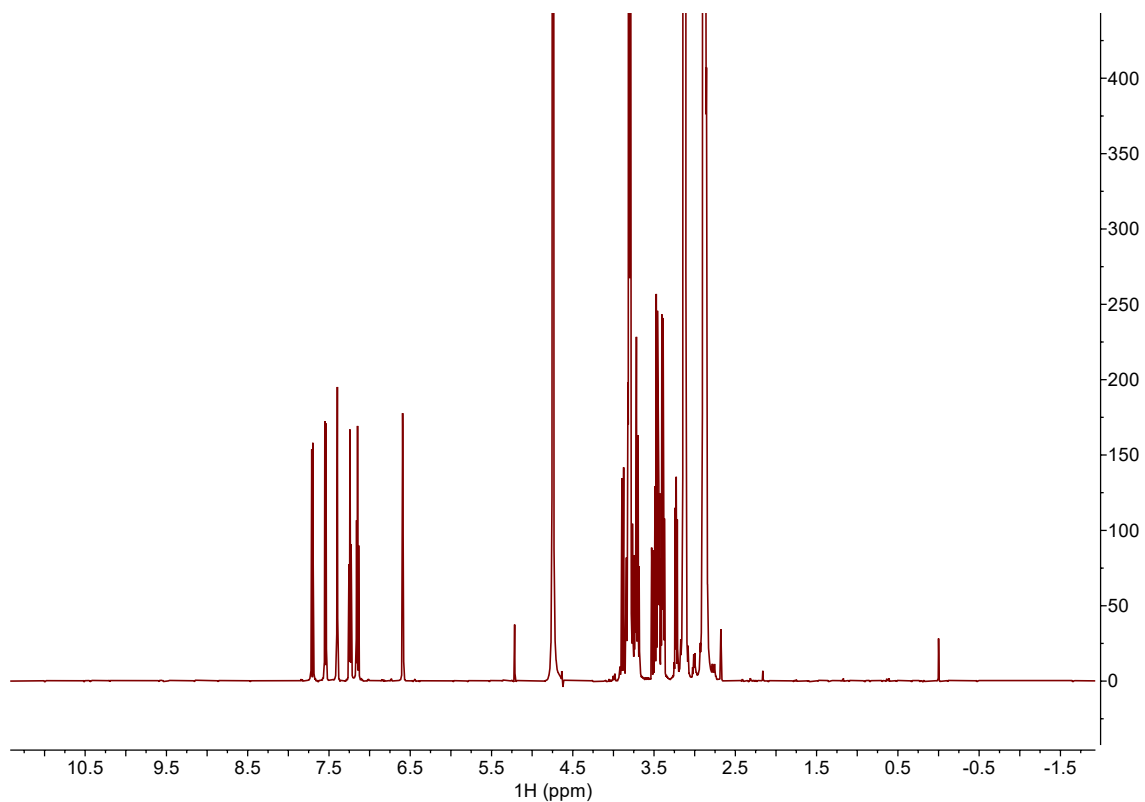


Figure S8. Proton 1D CPMG NMR spectrum of 4 mM glucose and 2 mM indole collected with a spin-lock time of 150 ms at 298K.

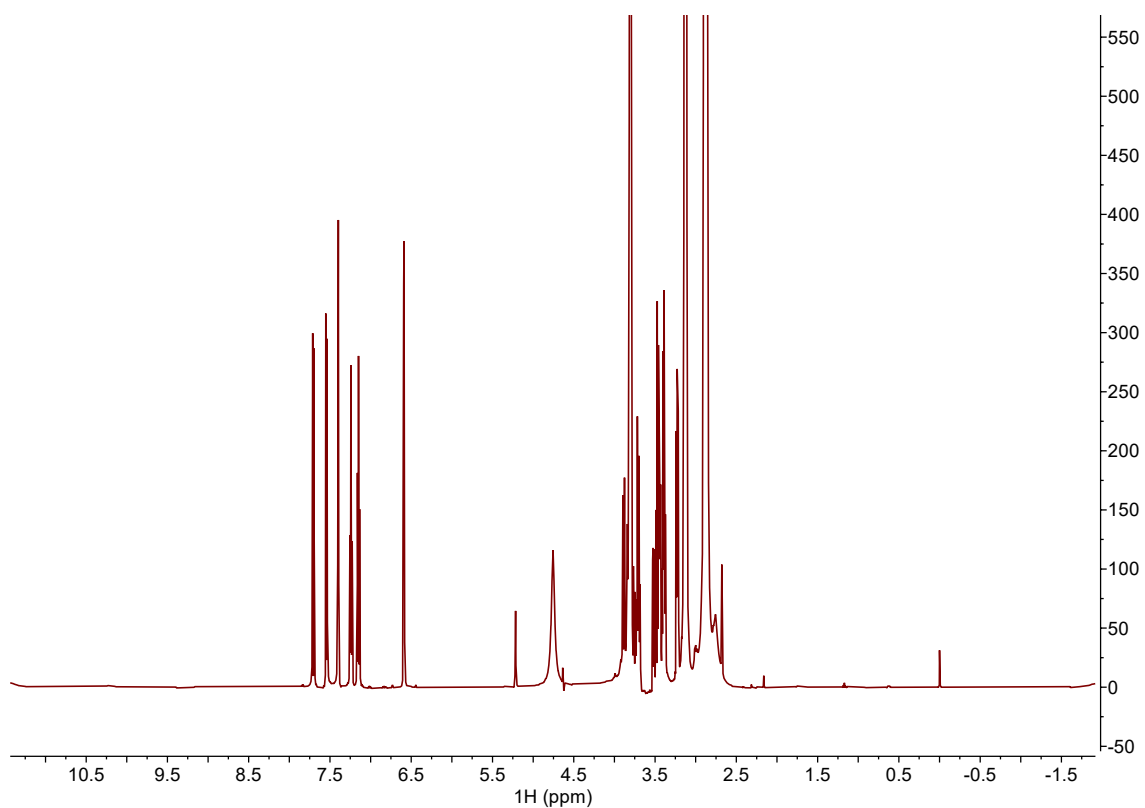


Figure S9. Proton 1D CPMG NMR spectrum of 4 mM glucose and 2 mM indole with the addition of 0.5 mM Mn²⁺ collected with a spin-lock time of 20 ms at 298K.

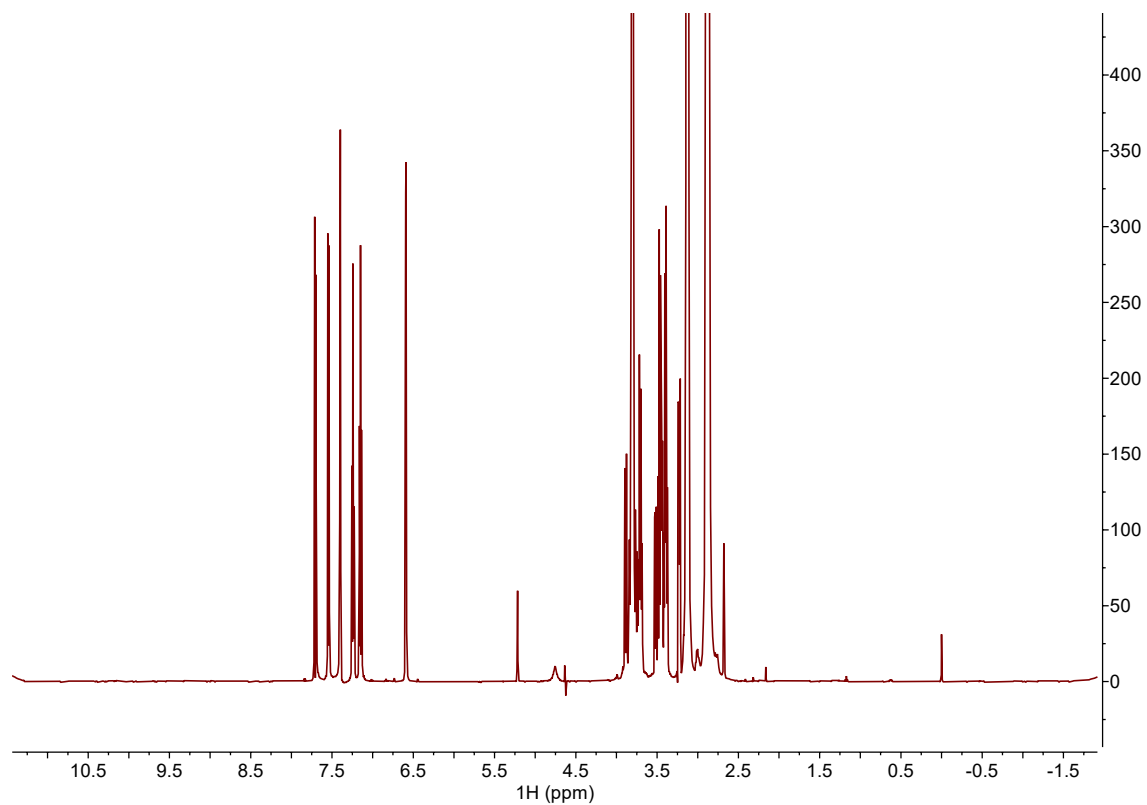


Figure S10. Proton 1D CPMG NMR spectrum of 4 mM glucose and 2 mM indole with the addition of 0.5 mM Mn^{2+} collected with a spin-lock time of 50 ms at 298K.

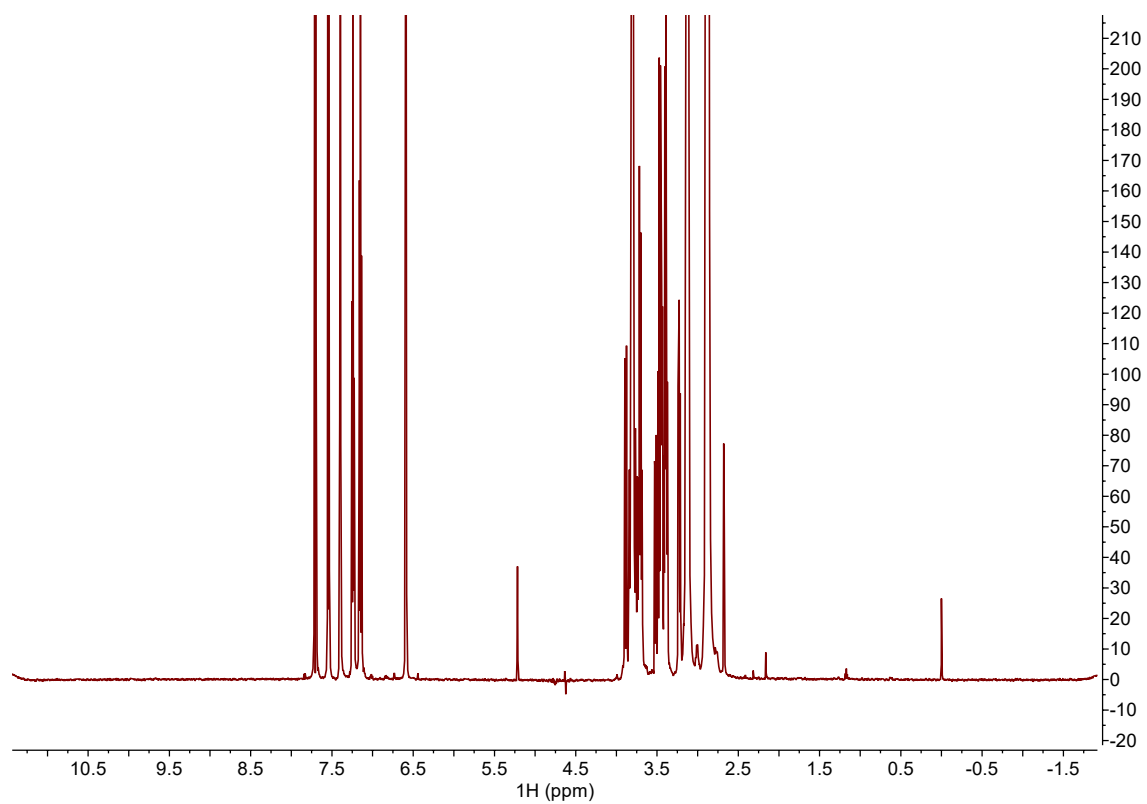


Figure S11. Proton 1D CPMG NMR spectrum of 4 mM glucose and 2 mM indole with the addition of 0.5 mM Mn^{2+} collected with a spin-lock time of 150 ms at 298K.

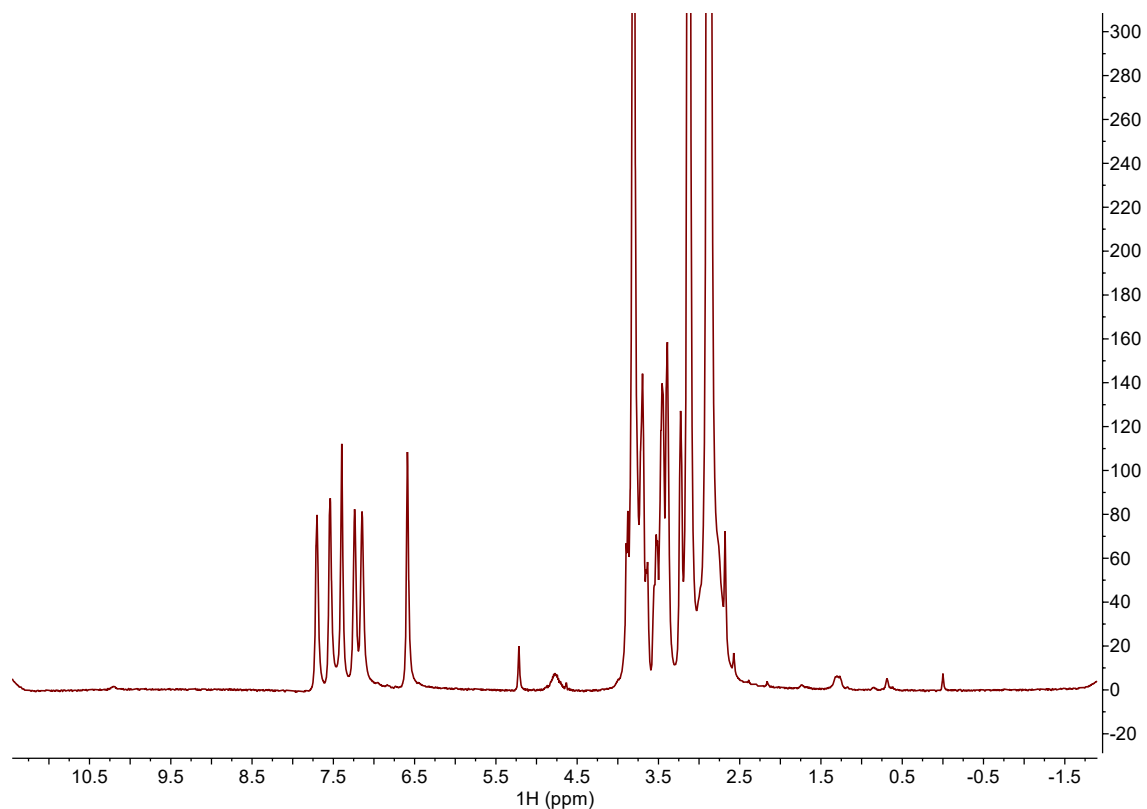


Figure S12. Proton 1D CPMG NMR spectrum of 4 mM glucose and 2 mM indole with the addition of 2 mM Mn^{2+} collected with a spin-lock time of 20 ms at 298K.

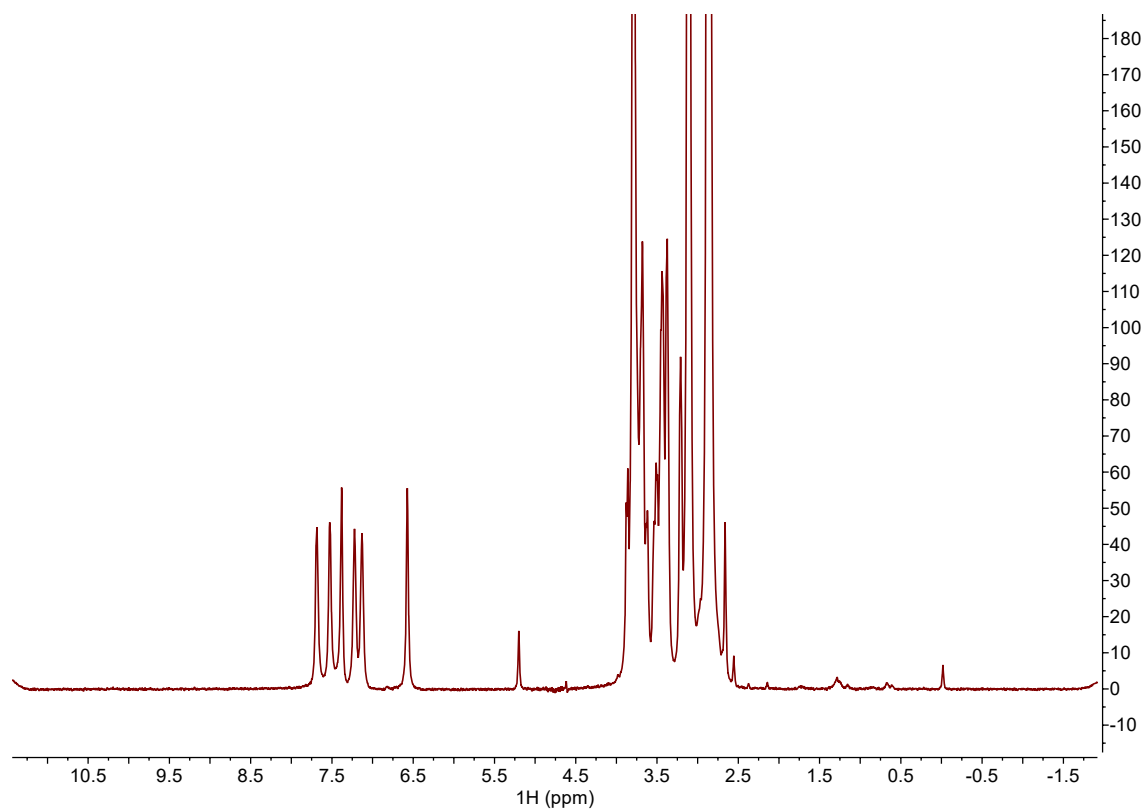


Figure S13. Proton 1D CPMG NMR spectrum of 4 mM glucose and 2 mM indole with the addition of 2 mM Mn^{2+} collected with a spin-lock time of 50 ms at 298K.

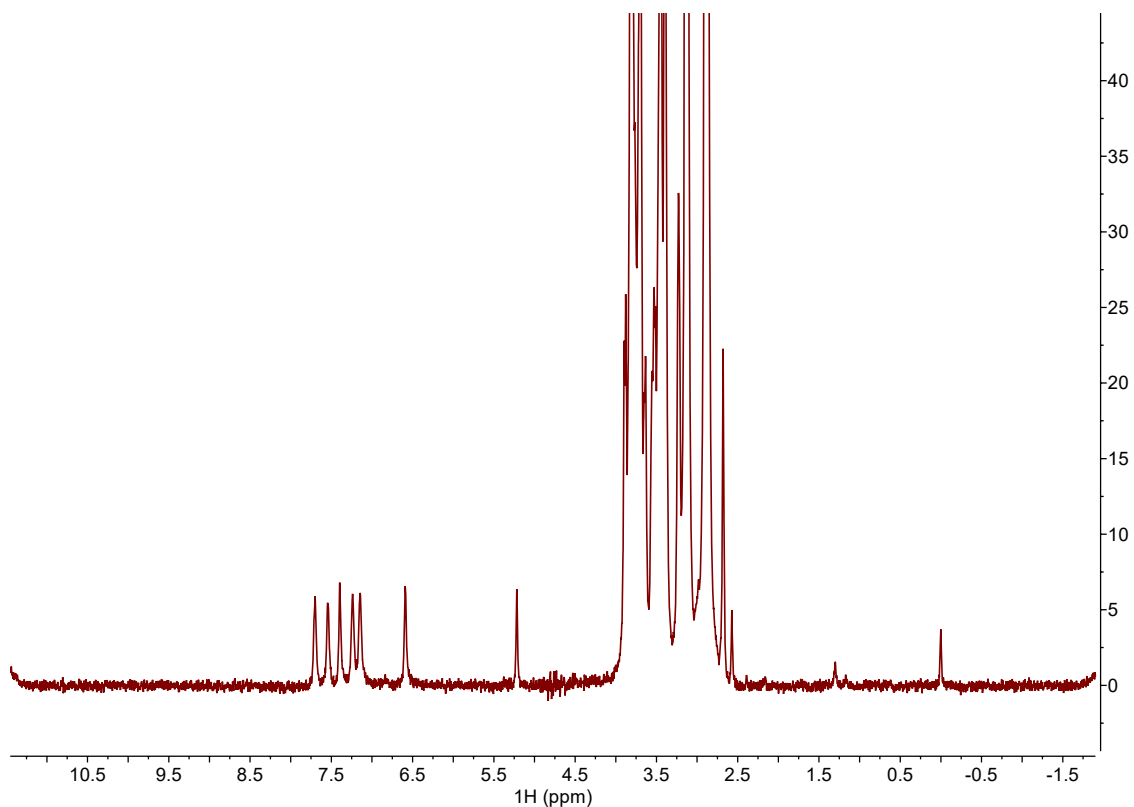


Figure S14. Proton 1D CPMG NMR spectrum of 4 mM glucose and 2 mM indole with the addition of 2 mM Mn^{2+} collected with a spin-lock time of 150 ms at 298K.

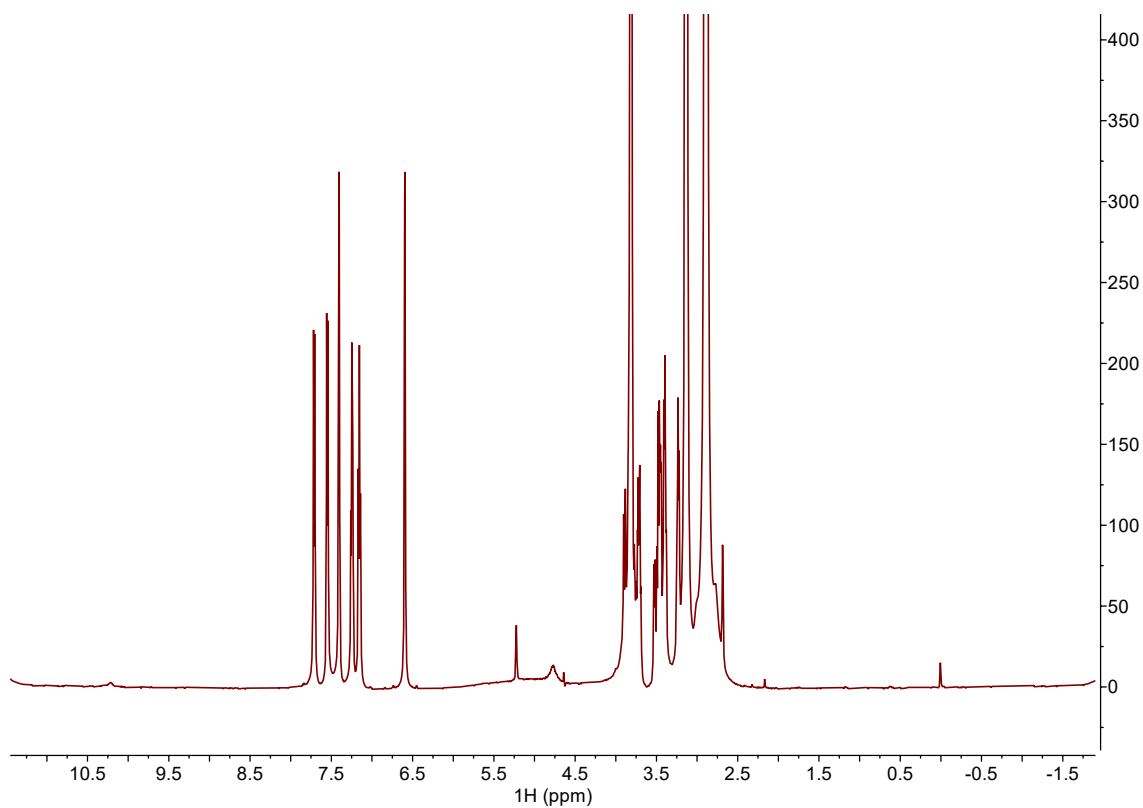


Figure S15. Proton 1D CPMG NMR spectrum of 4 mM glucose and 2 mM indole with the addition of 4 mM Mn^{2+} collected with a spin-lock time of 20 ms at 298K.

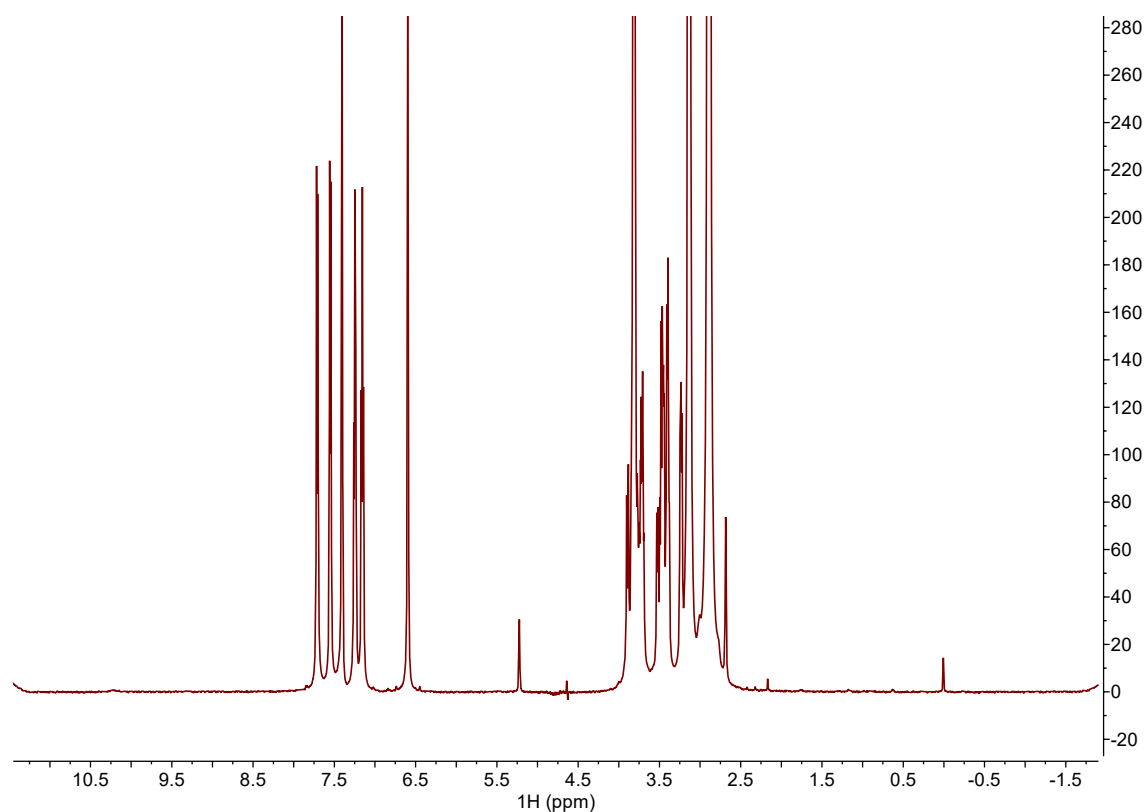


Figure S16. Proton 1D CPMG NMR spectrum of 4 mM glucose and 2 mM indole with the addition of 4 mM Mn^{2+} collected with a spin-lock time of 50 ms at 298K.

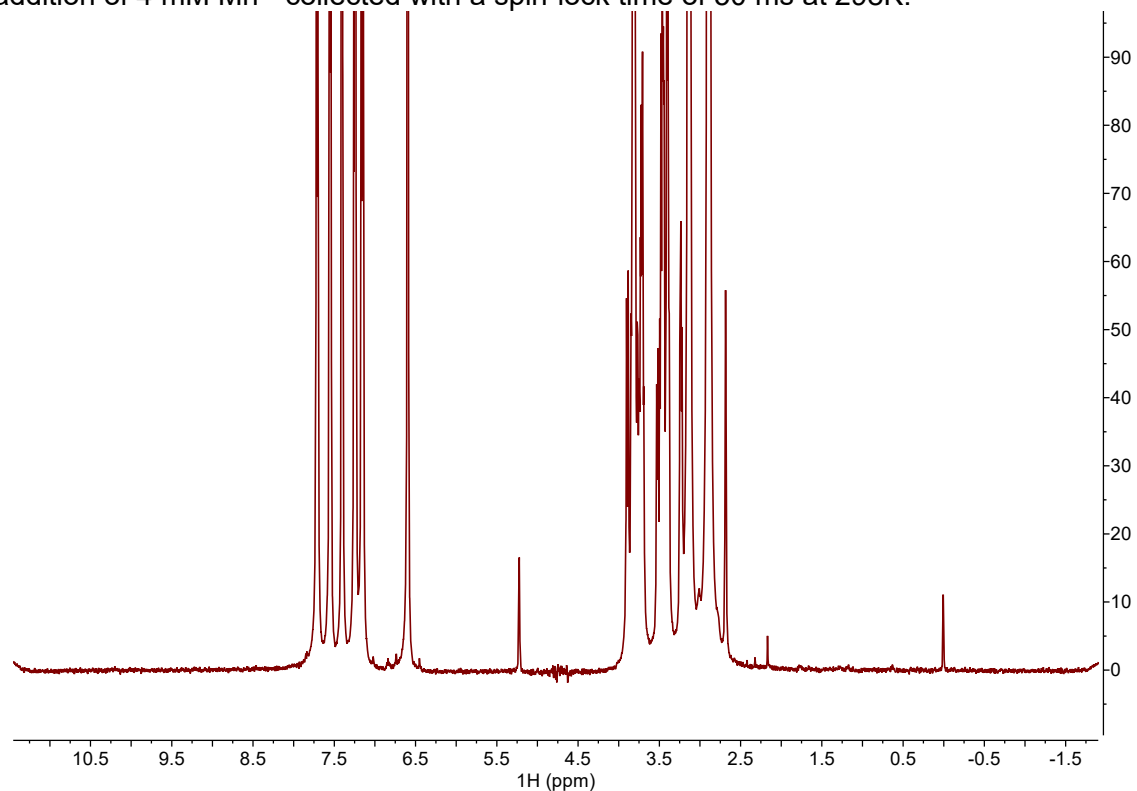


Figure S17. Proton 1D CPMG NMR spectrum of 4 mM glucose and 2 mM indole with the addition of 4 mM Mn^{2+} collected with a spin-lock time of 150 ms at 298K.

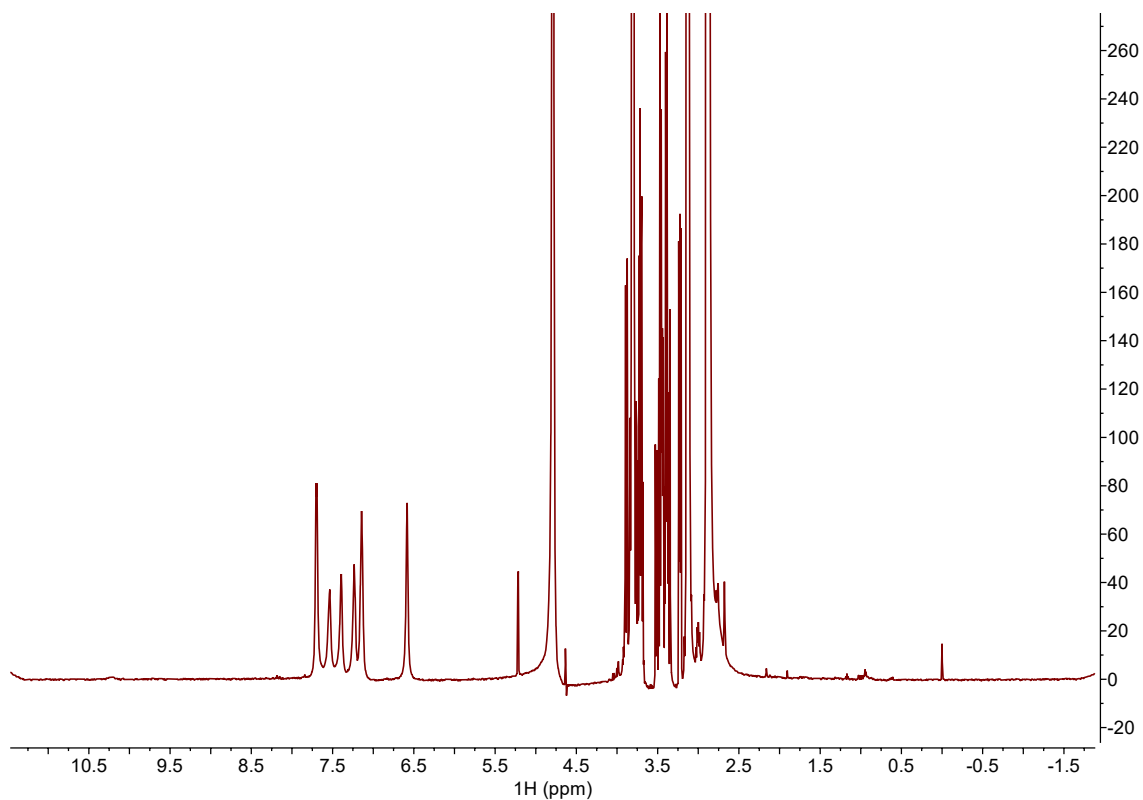


Figure S18. Proton 1D CPMG NMR spectrum of 4 mM glucose and 2 mM indole in the presence of *E. coli* lipid vesicles without the addition of Mn^{2+} collected with a spin-lock time of 20 ms at 298K.

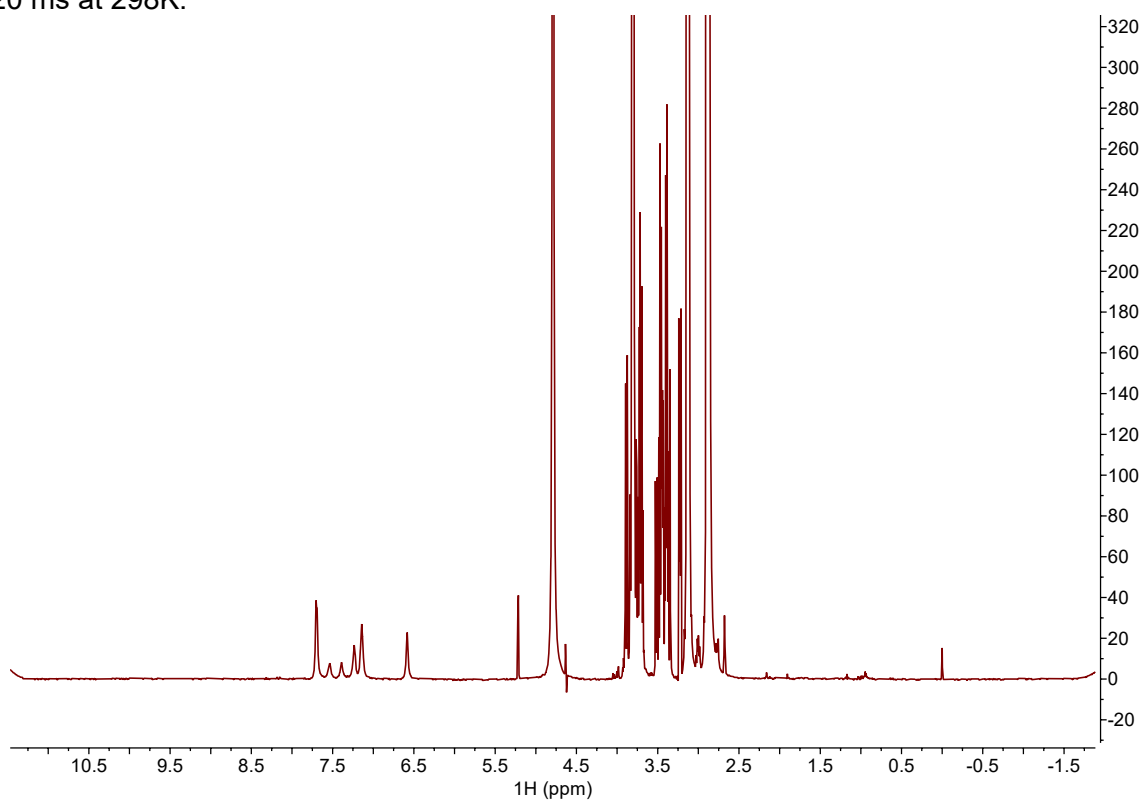


Figure S19. Proton 1D CPMG NMR spectrum of 4 mM glucose and 2 mM indole in the presence of *E. coli* lipid vesicles without the addition of Mn^{2+} collected with a spin-lock time of 50 ms at 298K.

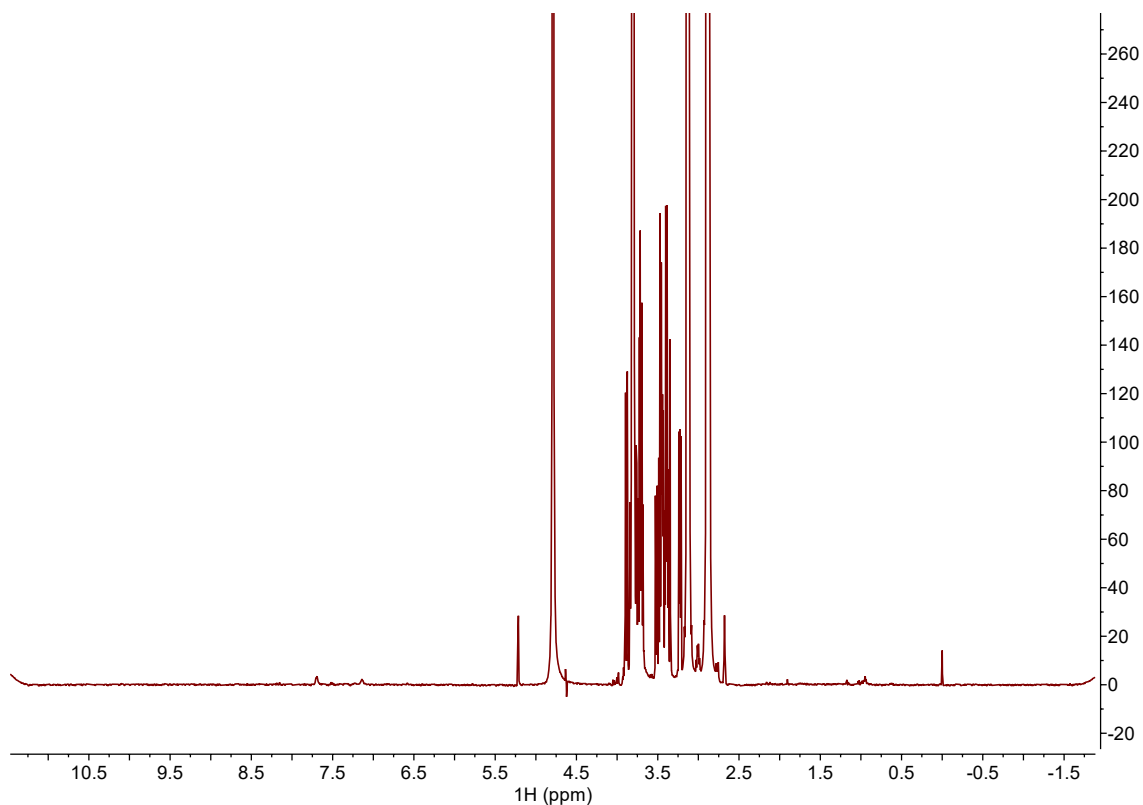


Figure S20. Proton 1D CPMG NMR spectrum of 4 mM glucose and 2 mM indole in the presence of *E. coli* lipid vesicles without the addition of Mn^{2+} collected with a spin-lock time of 150 ms at 298K.

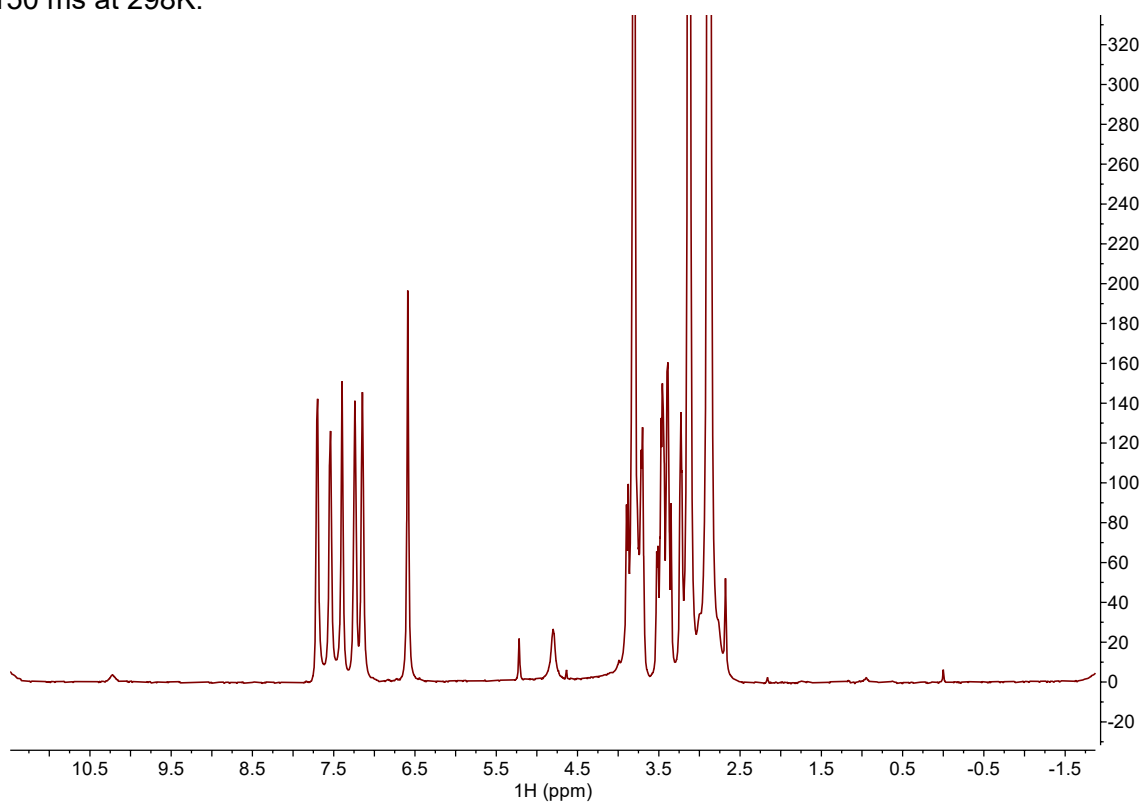


Figure S21. Proton 1D CPMG NMR spectrum of 4 mM glucose and 2 mM indole in the presence of *E. coli* lipid vesicles with the addition of 0.5 mM Mn^{2+} collected with a spin-lock time of 20 ms at 298K.

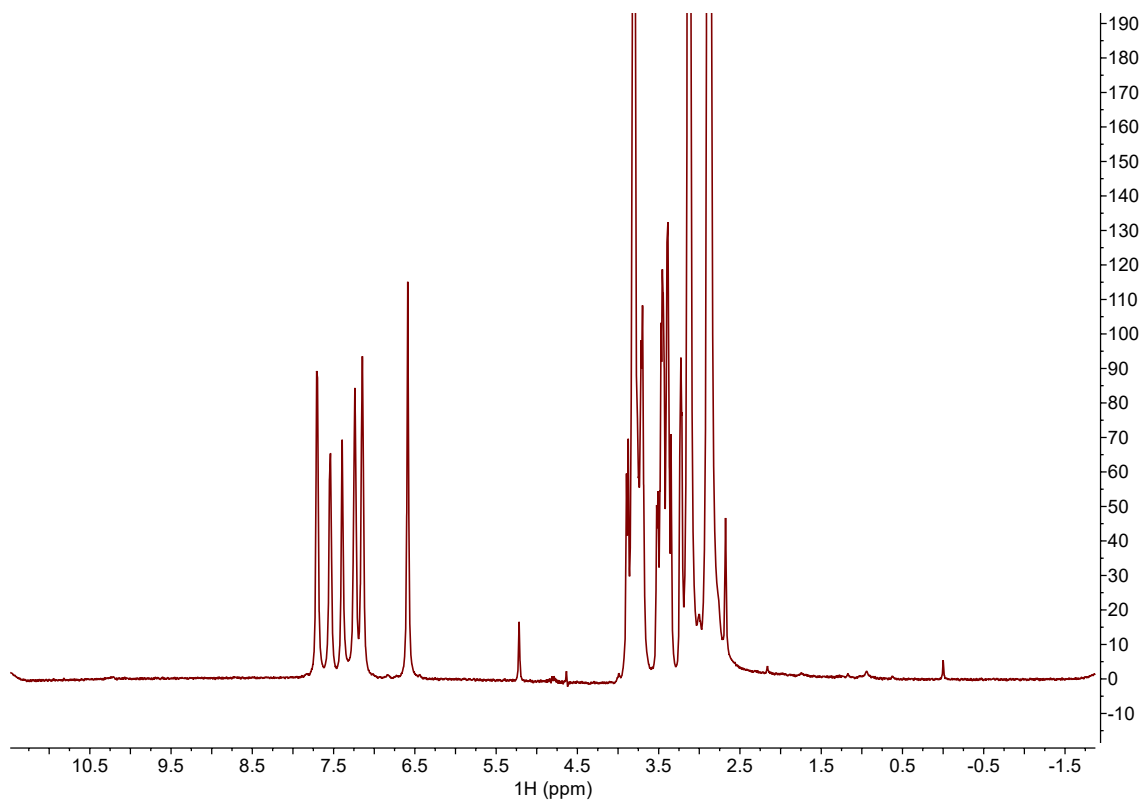


Figure S22. Proton 1D CPMG NMR spectrum of 4 mM glucose and 2 mM indole in the presence of *E. coli* lipid vesicles with the addition of 0.5 mM Mn^{2+} collected with a spin-lock time of 50 ms at 298K.

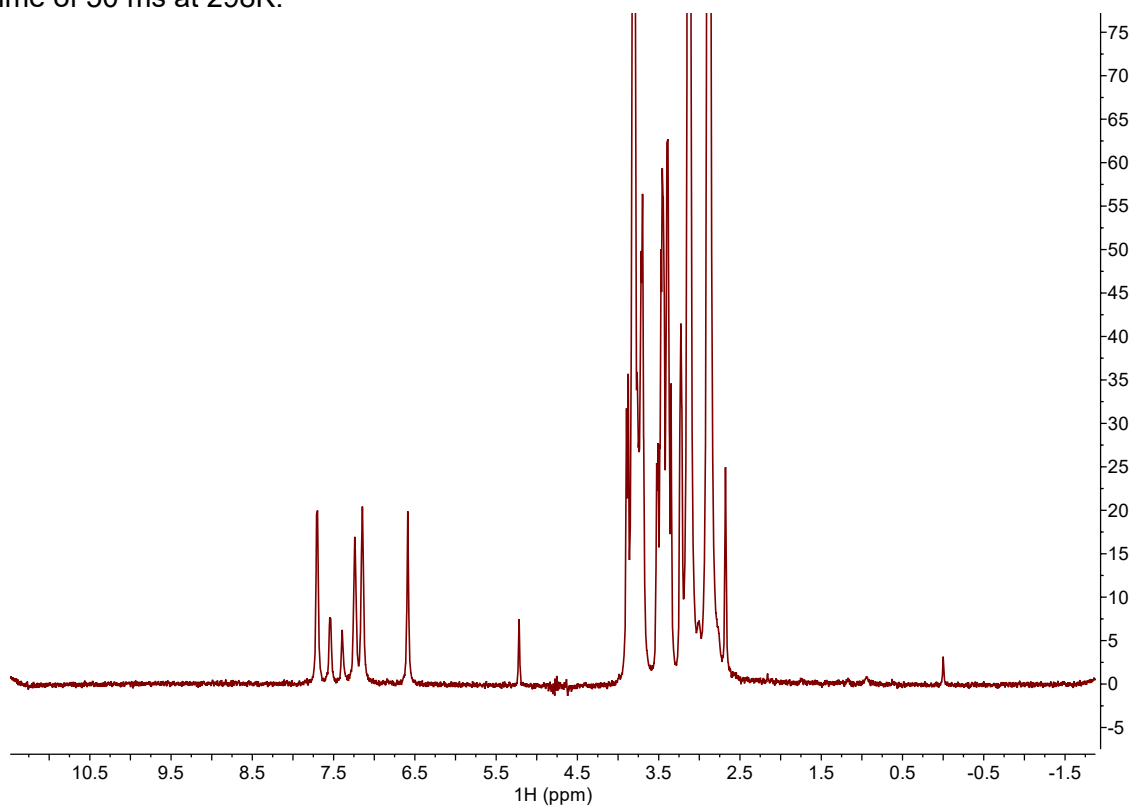


Figure S23. Proton 1D CPMG NMR spectrum of 4 mM glucose and 2 mM indole in the presence of *E. coli* lipid vesicles with the addition of 0.5 mM Mn^{2+} collected with a spin-lock time of 150 ms at 298K.

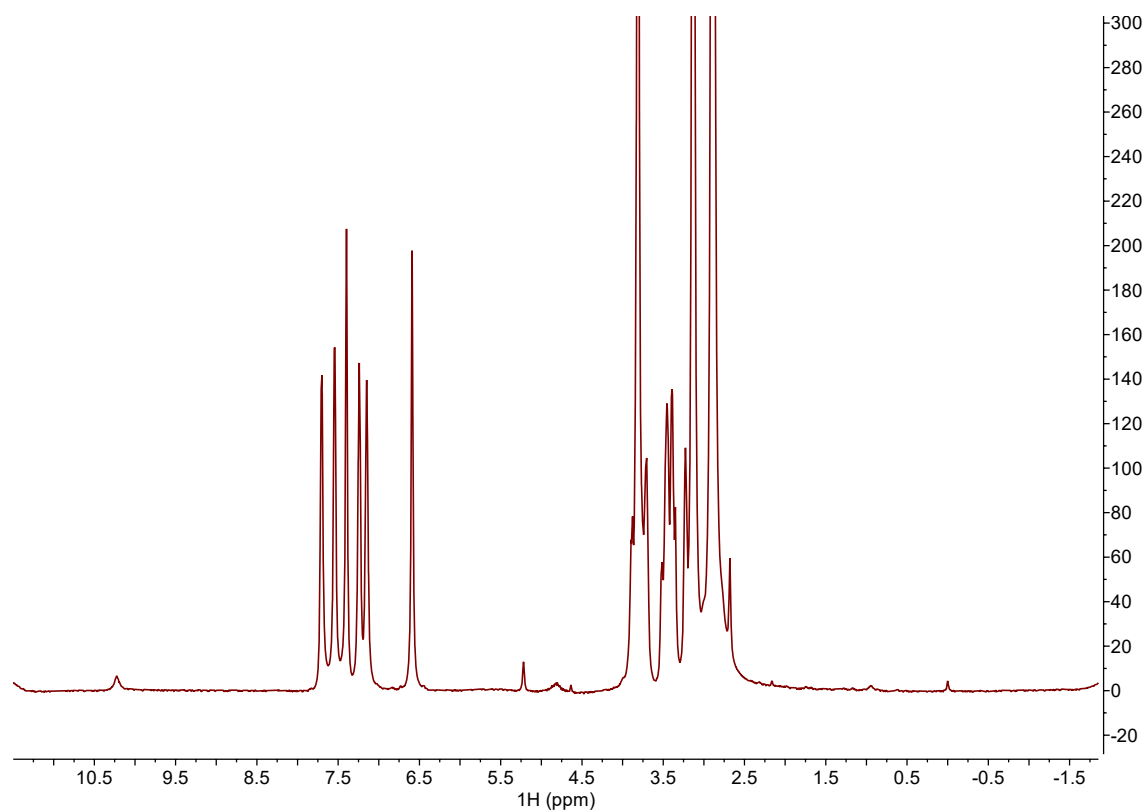


Figure S24. Proton 1D CPMG NMR spectrum of 4 mM glucose and 2 mM indole in the presence of *E. coli* lipid vesicles with the addition of 2 mM Mn^{2+} collected with a spin-lock time of 20 ms at 298K.

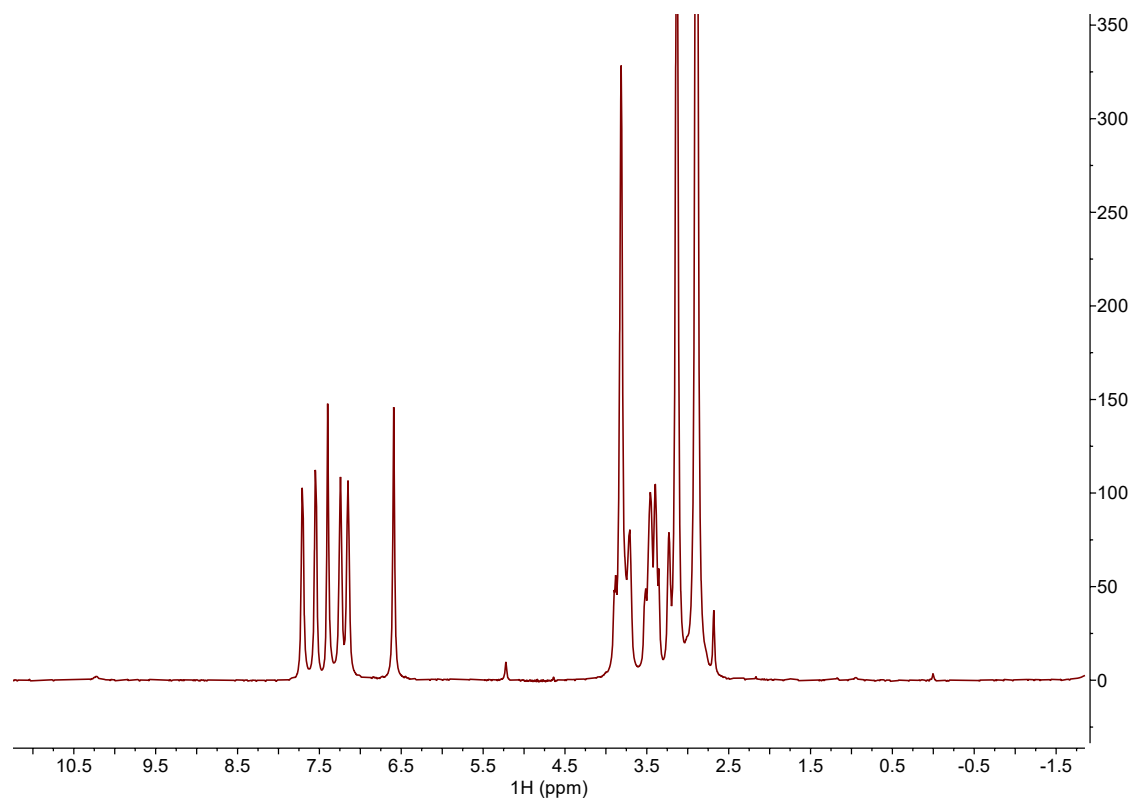


Figure S25. Proton 1D CPMG NMR spectrum of 4 mM glucose and 2 mM indole in the presence of *E. coli* lipid vesicles with the addition of 2 mM Mn^{2+} collected with a spin-lock time of 50 ms at 298K.

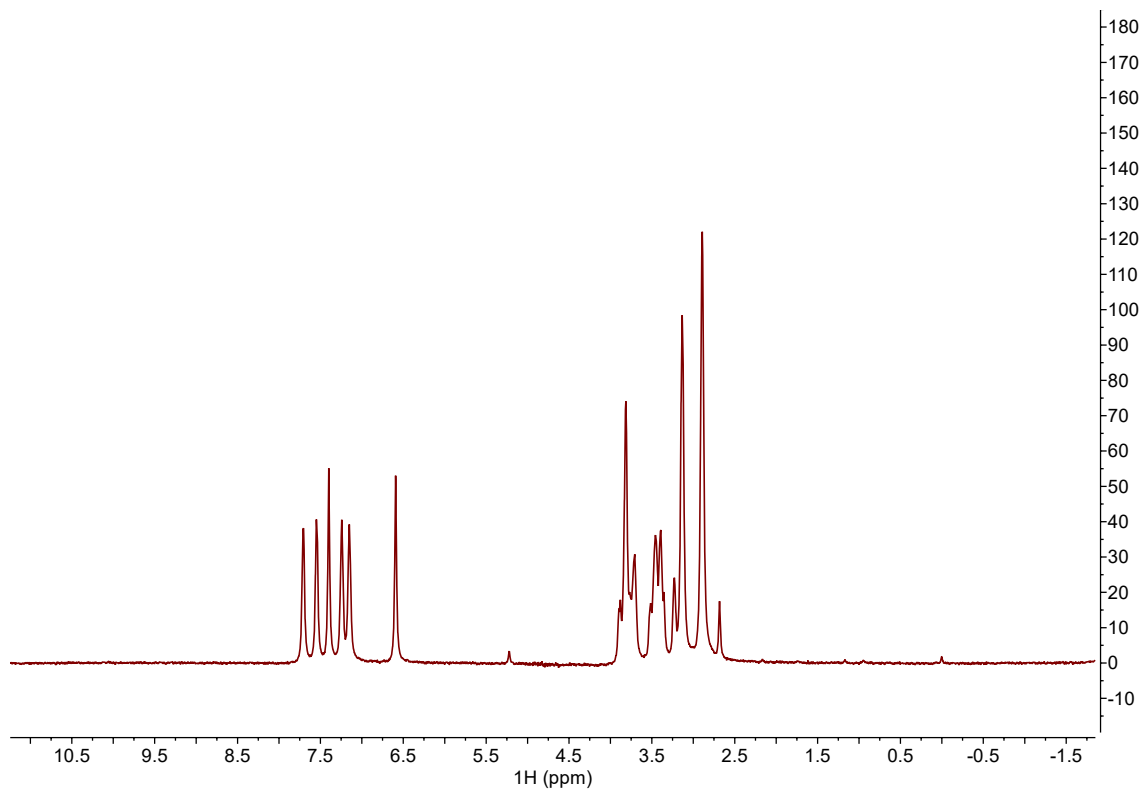


Figure S26. Proton 1D CPMG NMR spectrum of 4 mM glucose and 2 mM indole in the presence of *E. coli* lipid vesicles with the addition of 2 mM Mn^{2+} collected with a spin-lock time of 150 ms at 298K.

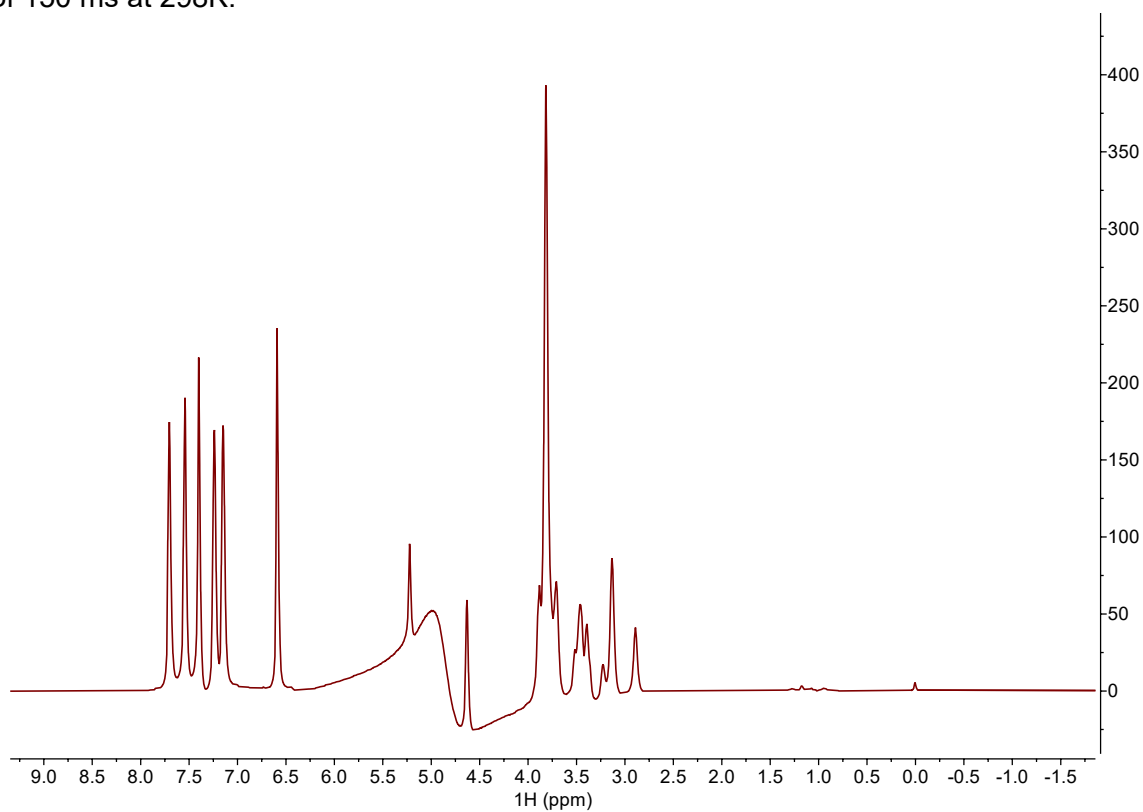


Figure S27. Proton 1D CPMG NMR spectrum of 4 mM glucose and 2 mM indole in the presence of *E. coli* lipid vesicles with the addition of 4 mM Mn^{2+} collected with a spin-lock time of 20 ms at 298K.

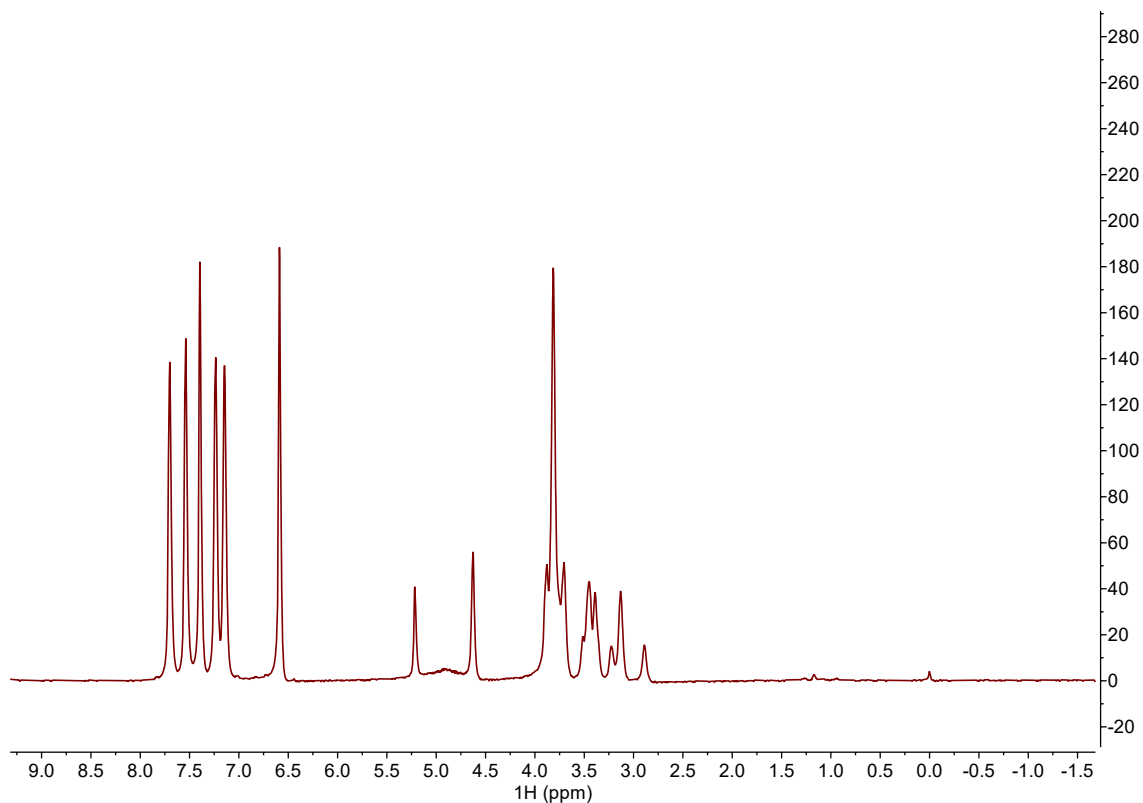


Figure S28. Proton 1D CPMG NMR spectrum of 4 mM glucose and 2 mM indole in the presence of *E. coli* lipid vesicles with the addition of 4 mM Mn^{2+} collected with a spin-lock time of 50 ms at 298K.

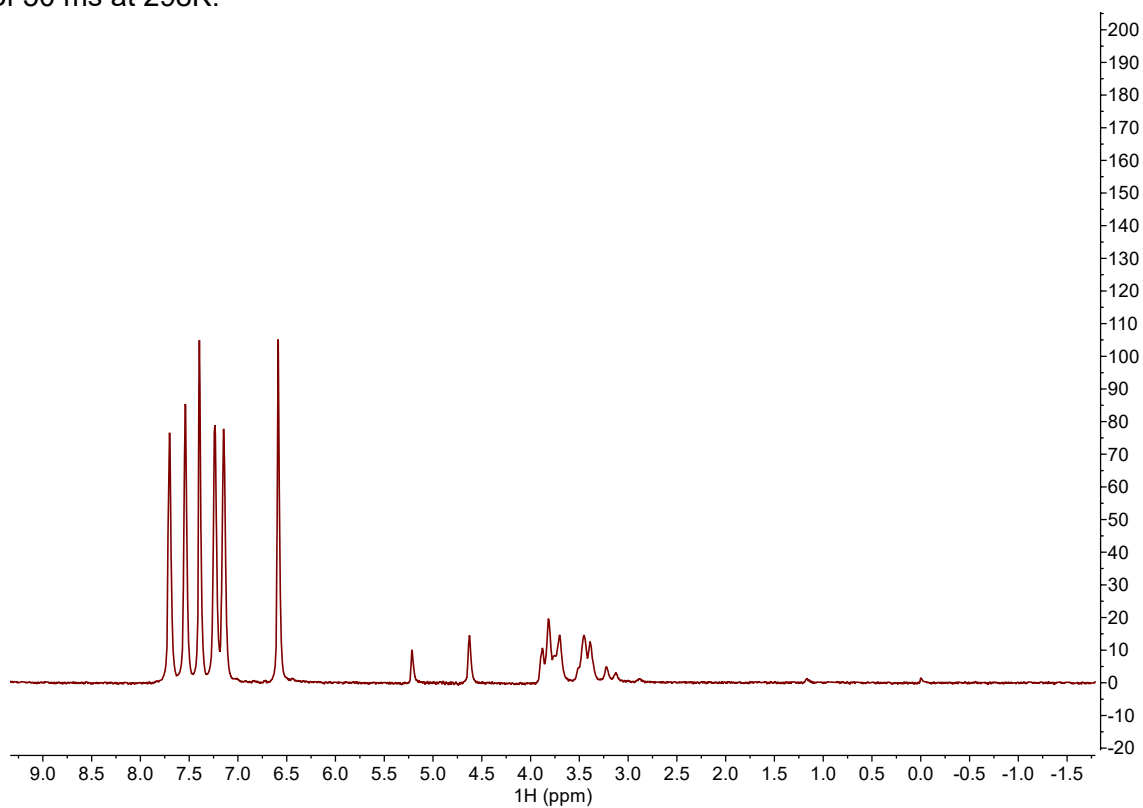


Figure S29. Proton 1D CPMG NMR spectrum of 4 mM glucose and 2 mM indole in the presence of *E. coli* lipid vesicles with the addition of 4 mM Mn^{2+} collected with a spin-lock time of 150 ms at 298K.

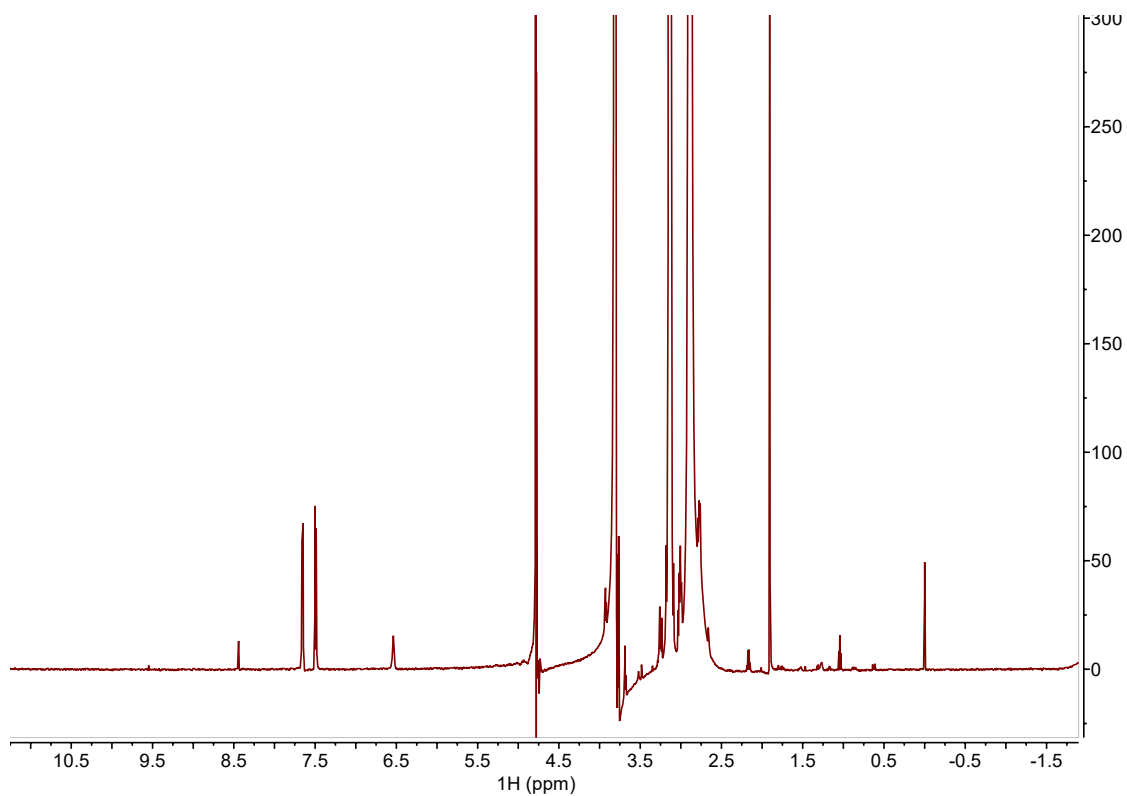


Figure S30. Proton 1D CPMG NMR spectrum of 0.4 mM C29 collected with a spin-lock time of 20 ms at 298K.

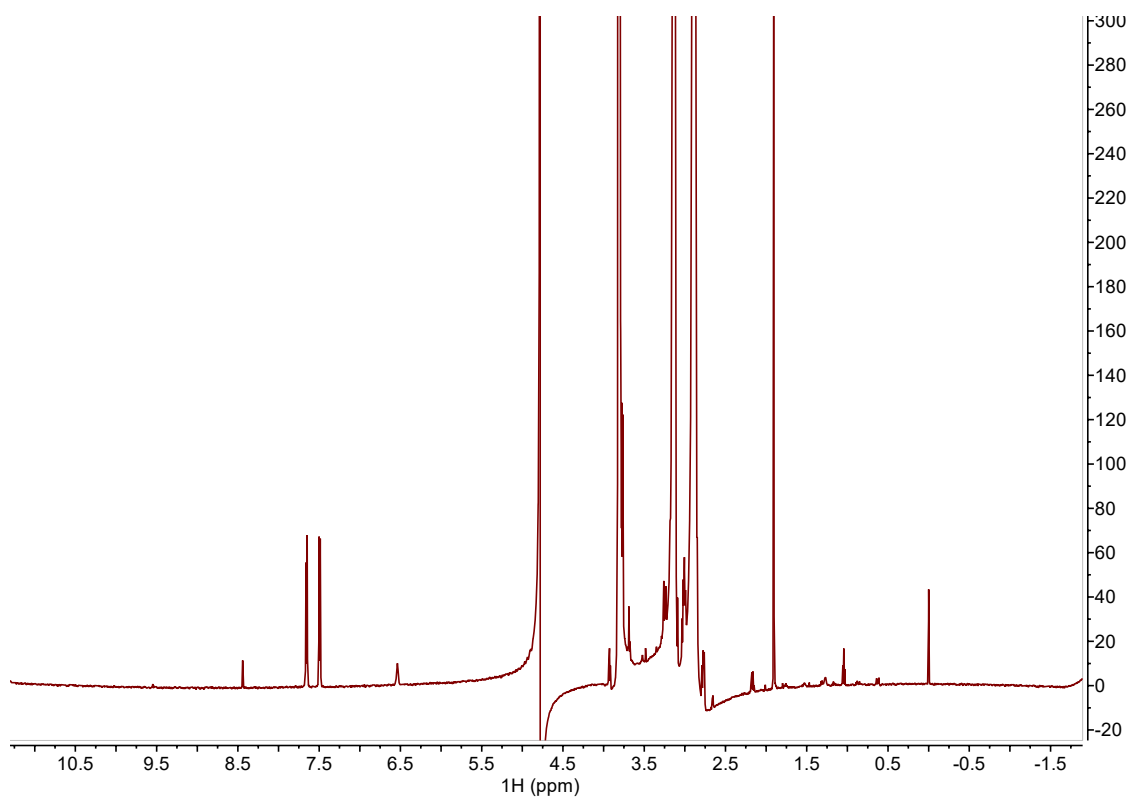


Figure S31. Proton 1D CPMG NMR spectrum of 0.4 mM C29 collected with a spin-lock time of 50 ms at 298K.

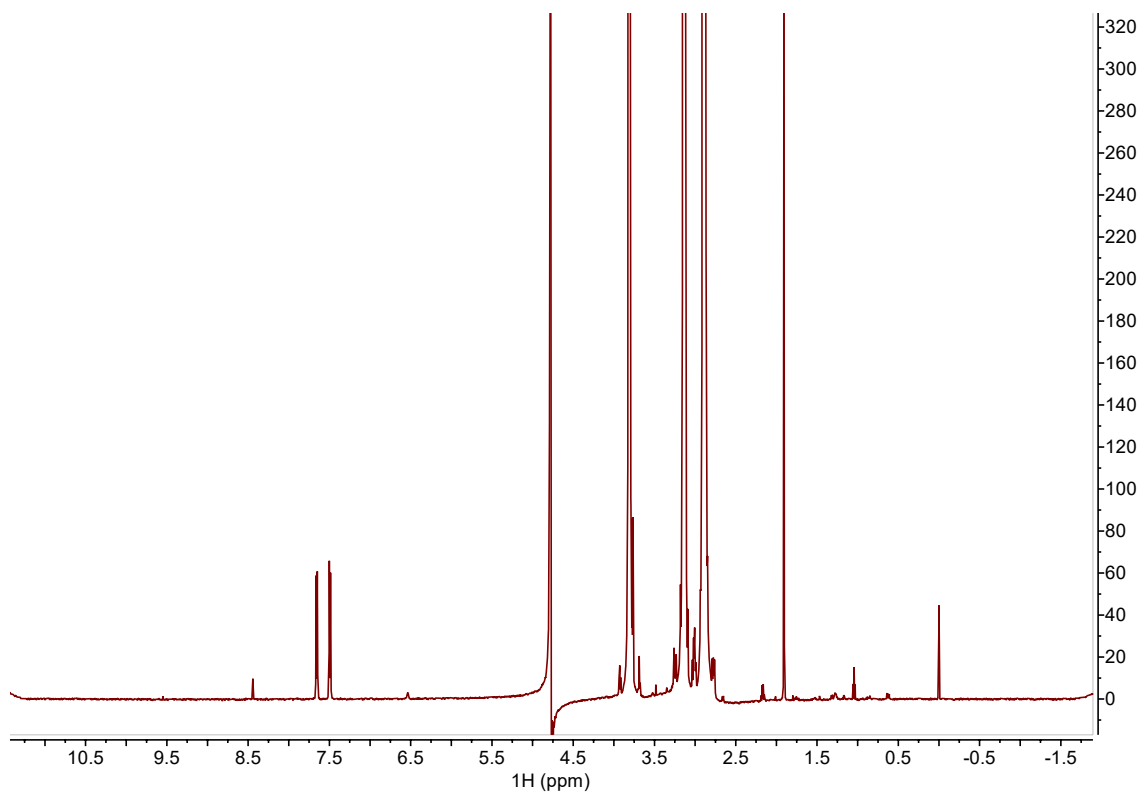


Figure S32. Proton 1D CPMG NMR spectrum of 0.4 mM C29 collected with a spin-lock time of 150 ms at 298K.

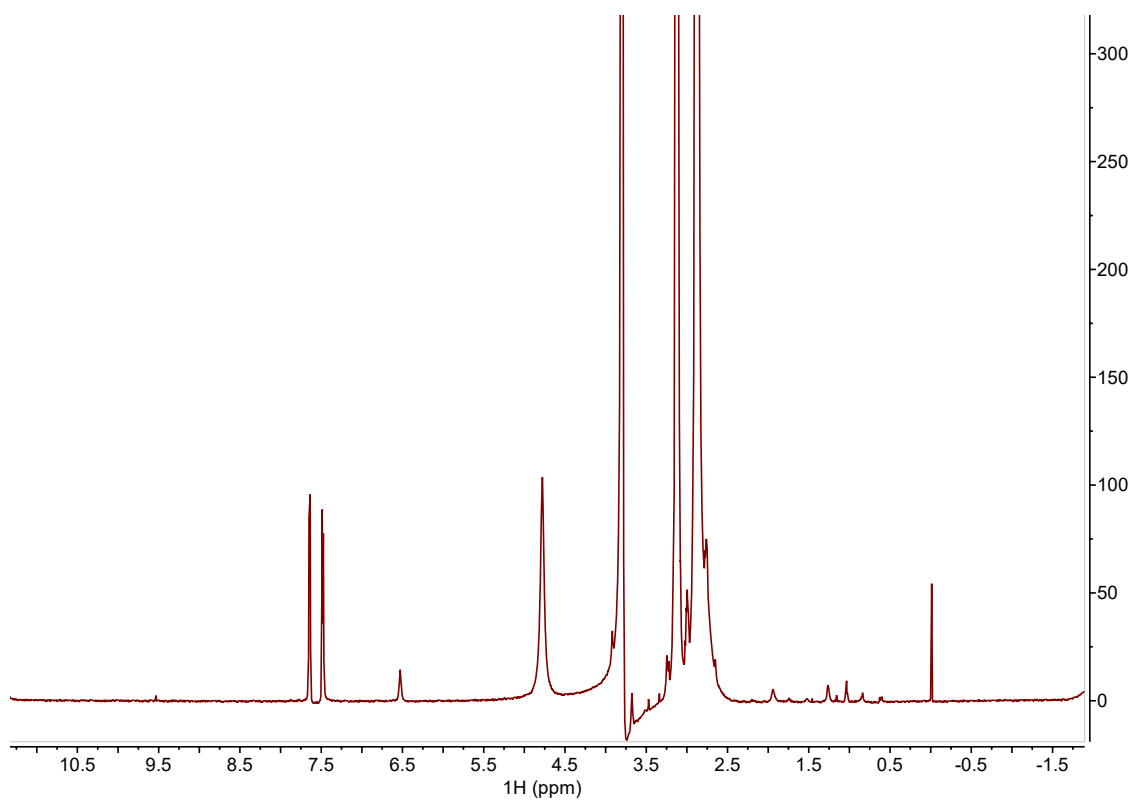


Figure S33. Proton 1D CPMG NMR spectrum of 0.4 mM C29 with the addition of 0.5mM Mn²⁺ collected with a spin-lock time of 20 ms at 298K.

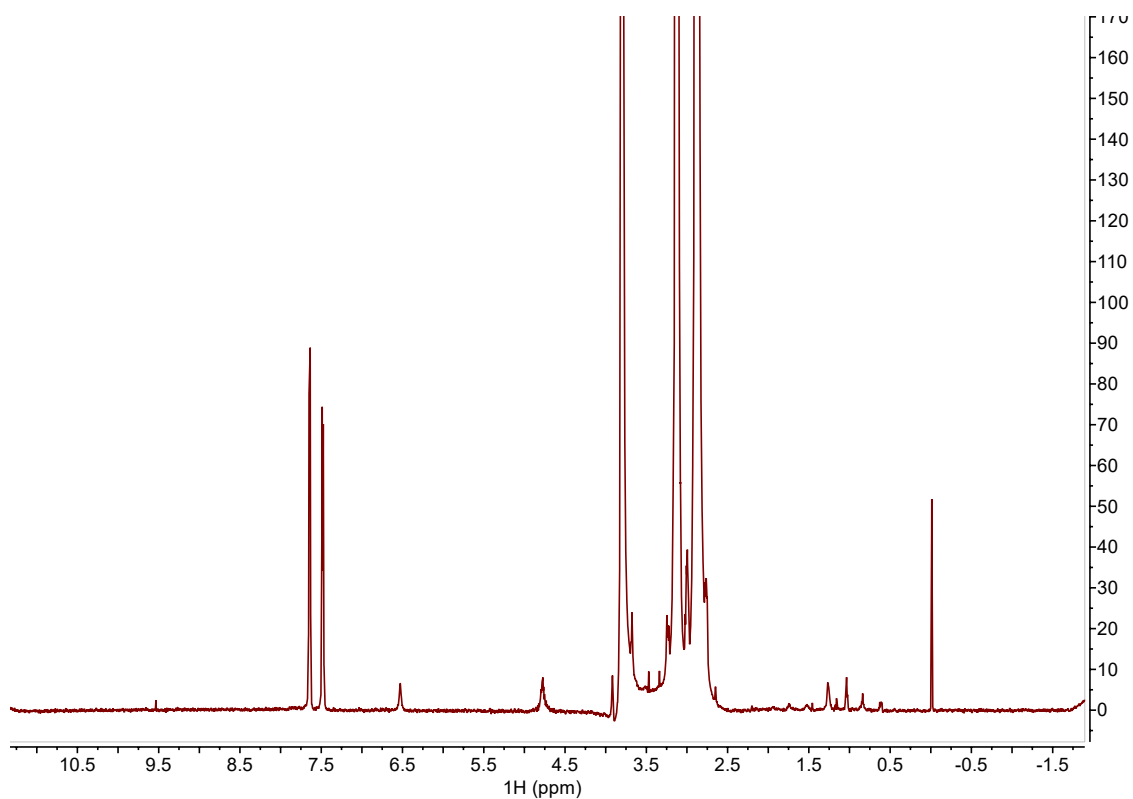


Figure S34. Proton 1D CPMG NMR spectrum of 0.4 mM C29 with the addition of 0.5 mM Mn^{2+} collected with a spin-lock time of 50 ms at 298K.

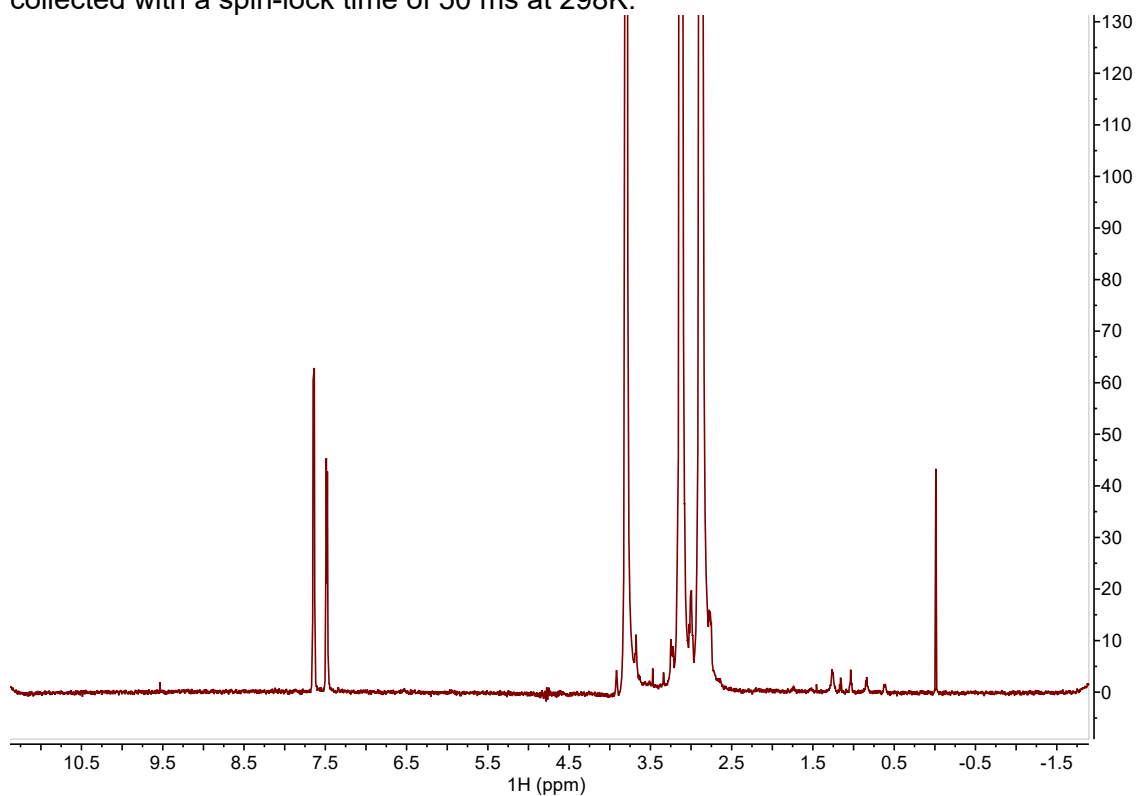
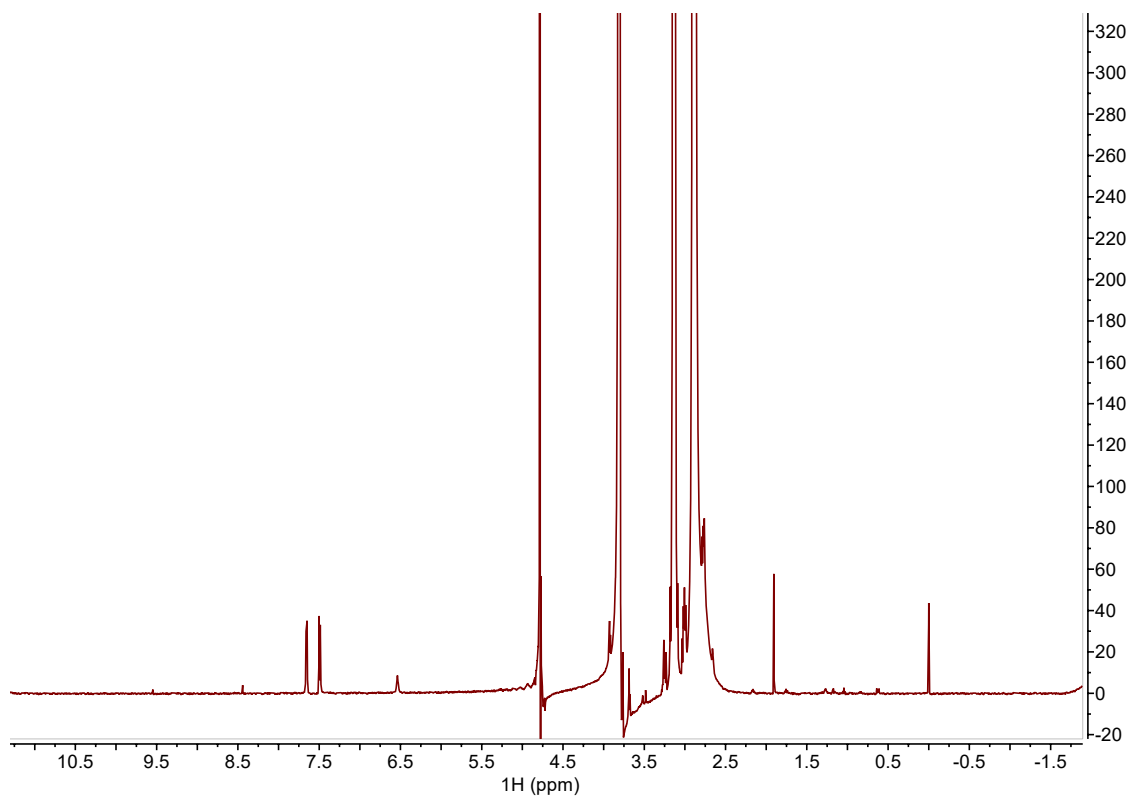


Figure S35. Proton 1D CPMG NMR spectrum of 0.4 mM C29 with the addition of 0.5 mM Mn^{2+} collected with a spin-lock time of 150 ms at 298K.



Fi

Figure S36. Proton 1D CPMG NMR spectrum of 0.2 mM C29 in the presence of *E. coli* lipid vesicles collected with a spin-lock time of 20 ms at 298K.

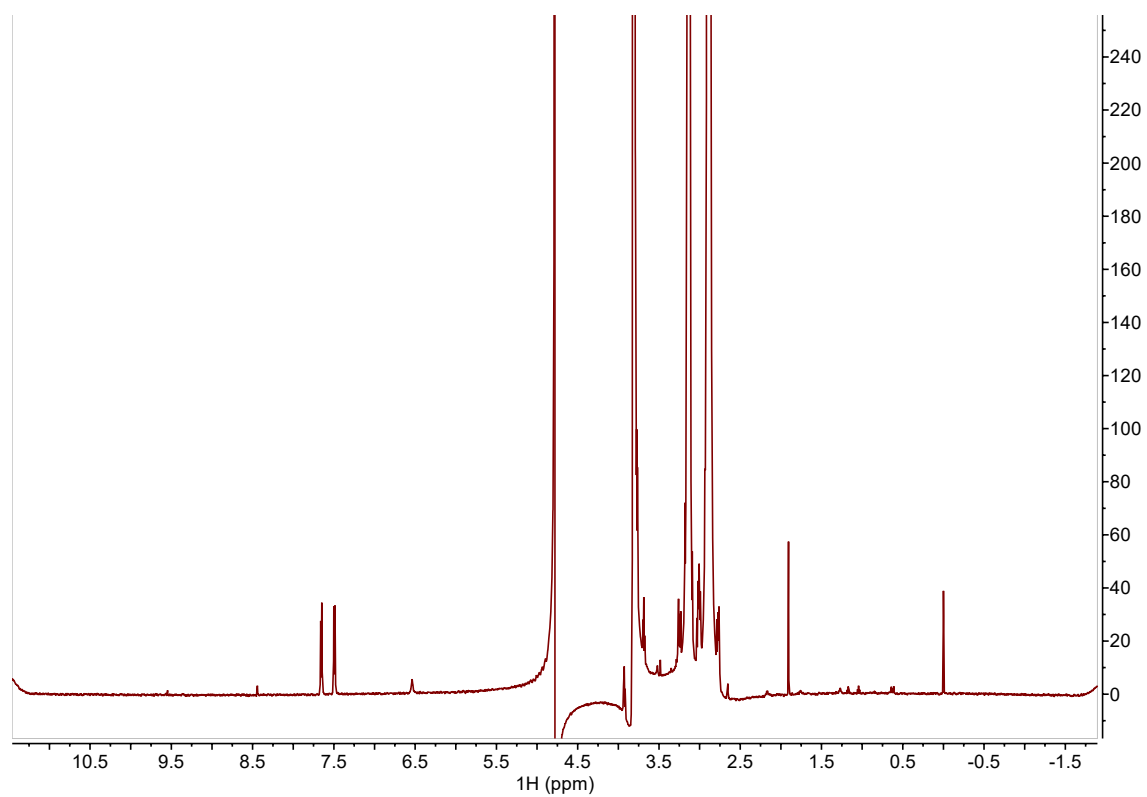


Figure S37. Proton 1D CPMG NMR spectrum of 0.2 mM C29 in the presence of *E. coli* lipid vesicles collected with a spin-lock time of 50 ms at 298K.

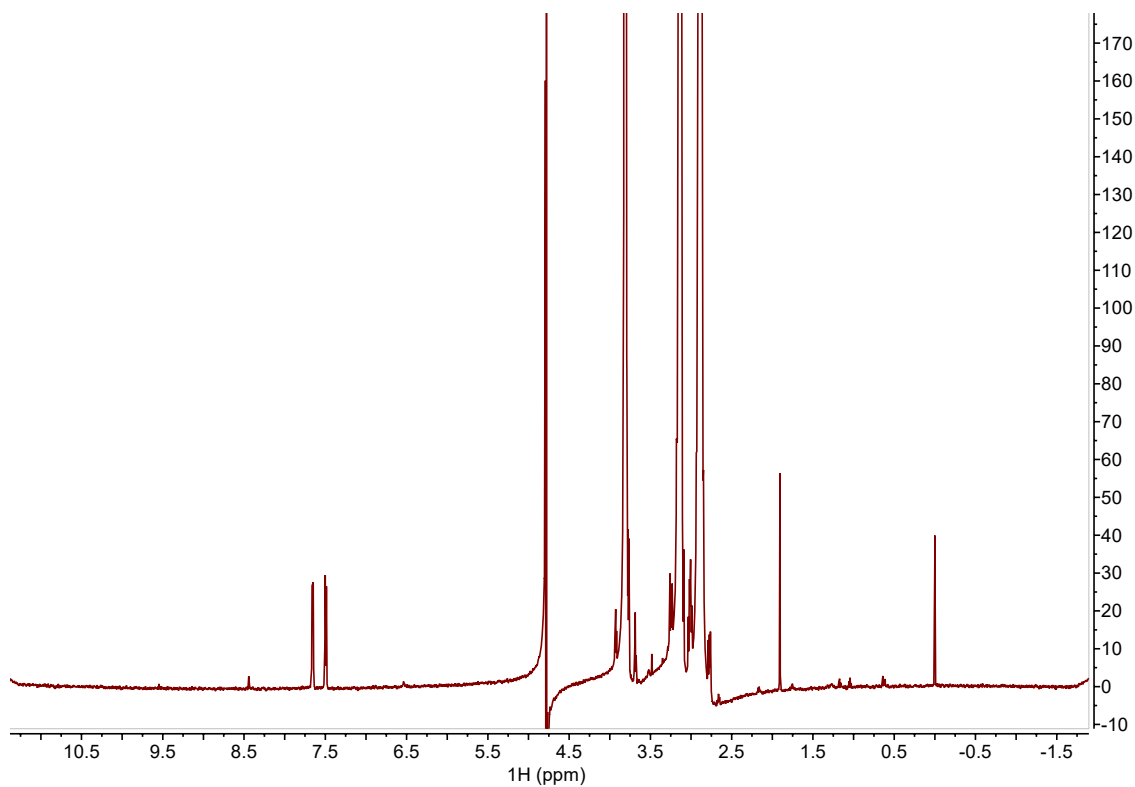


Figure S38. Proton 1D CPMG NMR spectrum of 0.2 mM C29 in the presence of *E. coli* lipid vesicles collected with a spin-lock time of 150 ms at 298K.

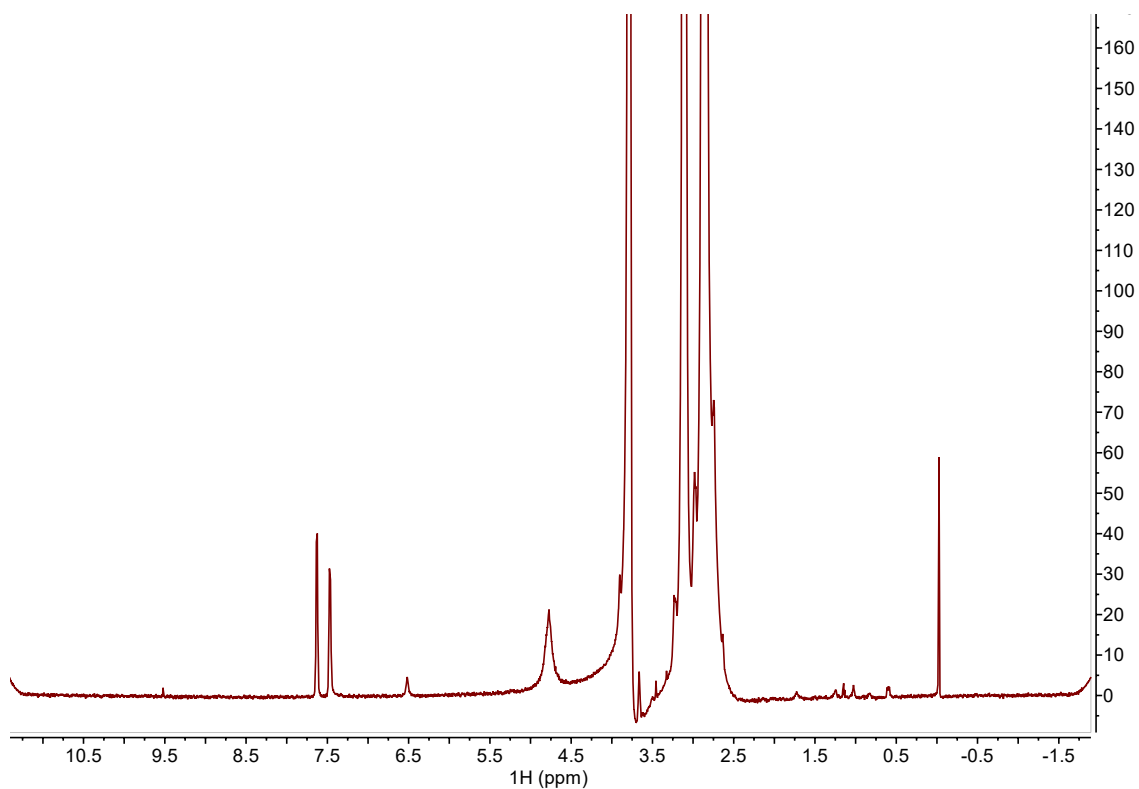


Figure S39. Proton 1D CPMG NMR spectrum of 0.2 mM C29 in the presence of *E. coli* lipid vesicles with the addition of 0.5 mM Mn^{2+} collected with a spin-lock time of 20 ms at 298K.

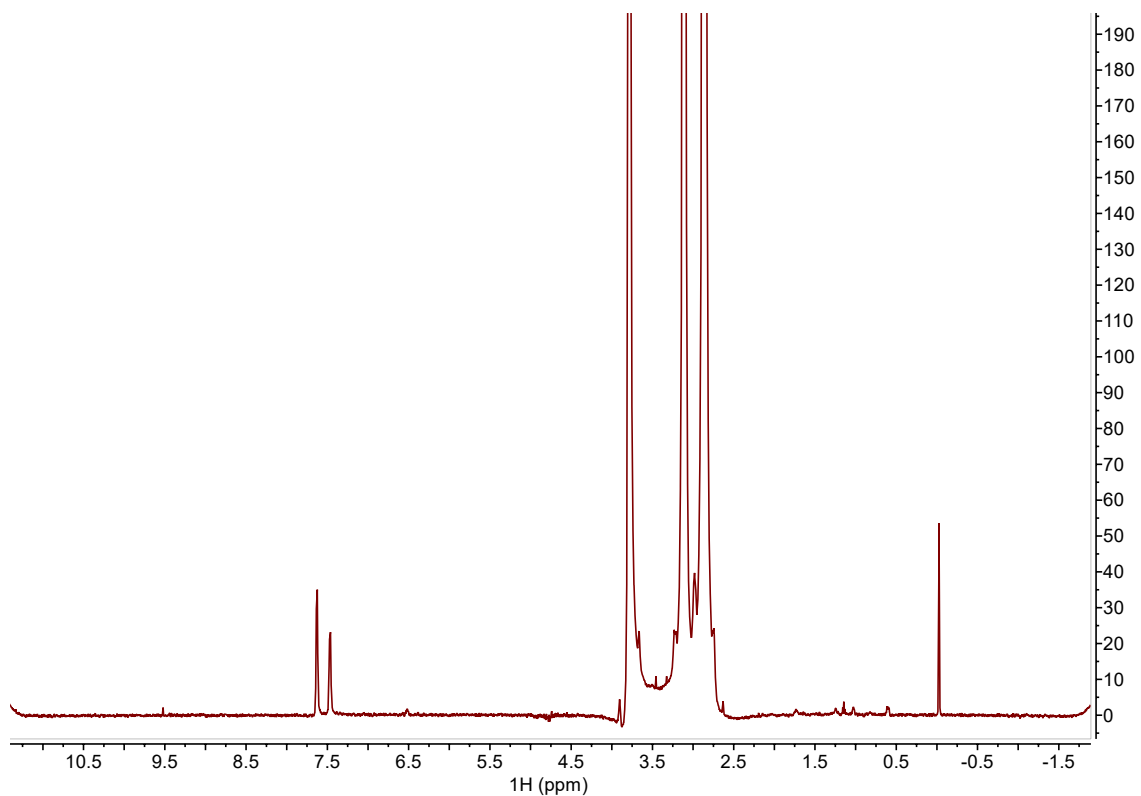


Figure S40. Proton 1D CPMG NMR spectrum of 0.2 mM C29 in the presence of *E. coli* lipid vesicles with the addition of 0.5 mM Mn^{2+} collected with a spin-lock time of 50 ms at 298K.

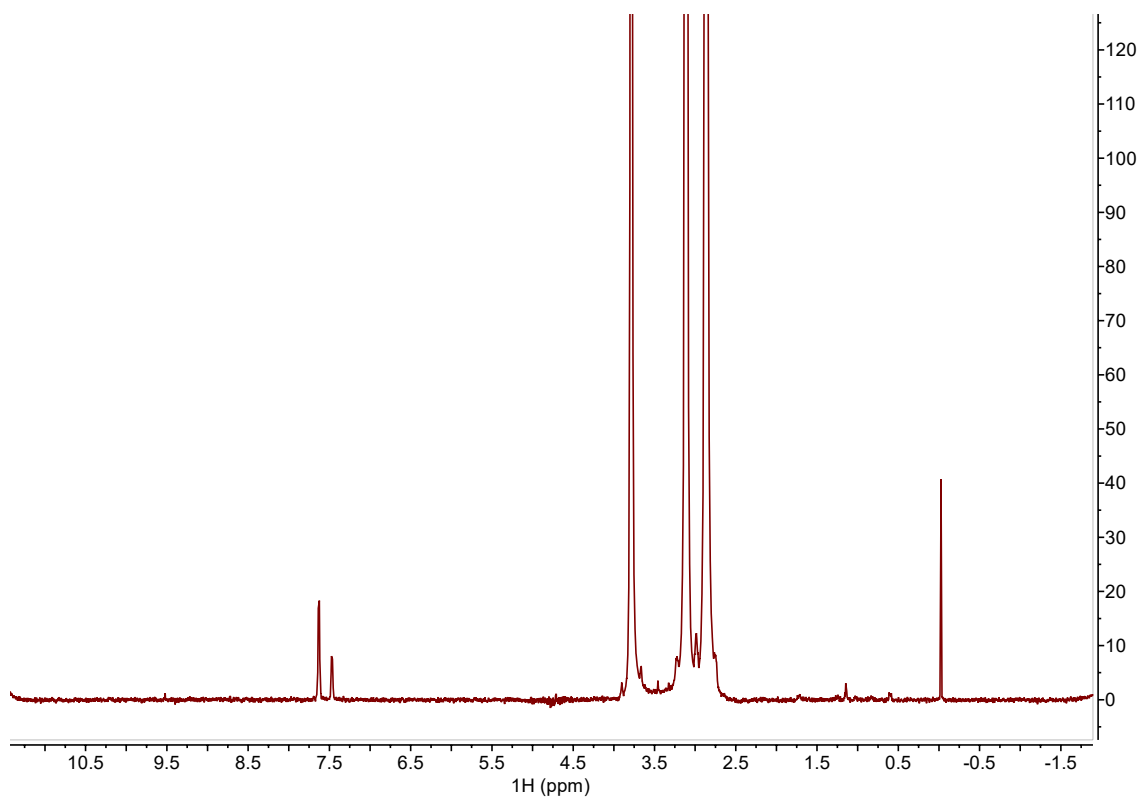


Figure S41. Proton 1D CPMG NMR spectrum of 0.2 mM C29 in the presence of *E. coli* lipid vesicles with the addition of 0.5 mM Mn^{2+} collected with a spin-lock time of 150 ms at 298K.

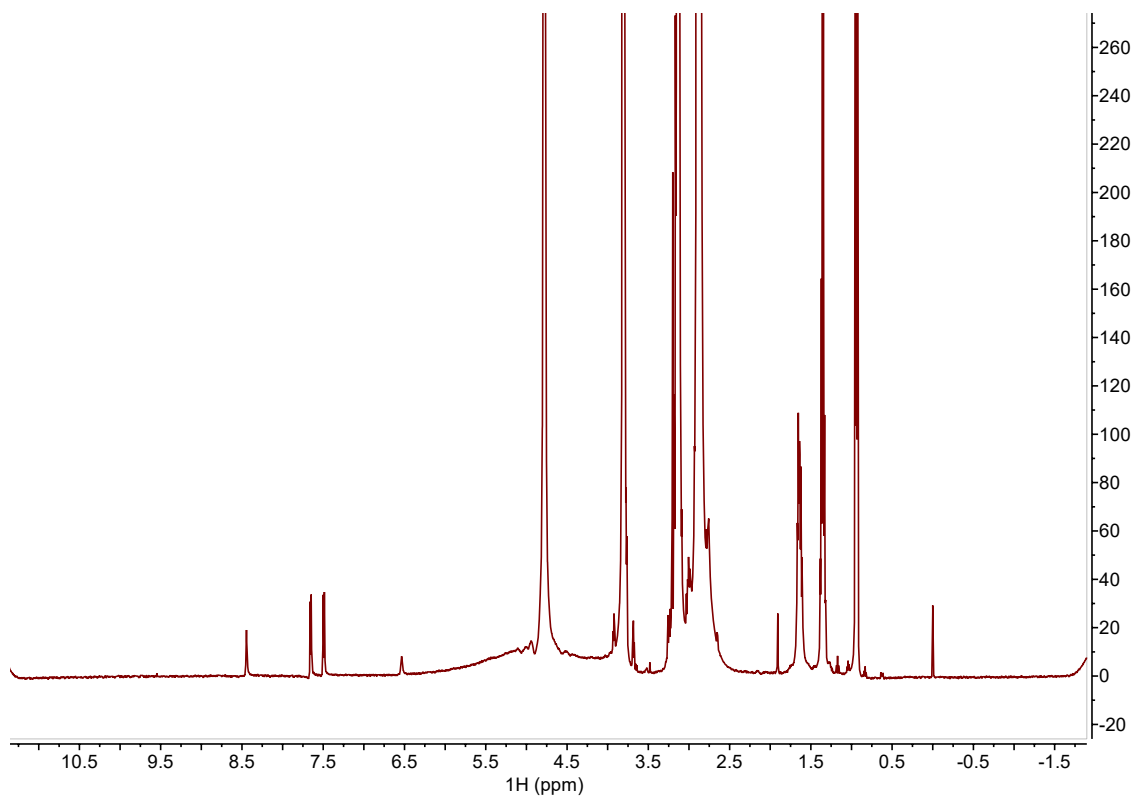


Figure S42. Proton 1D CPMG NMR spectrum of 0.4 mM C30 collected with a spin-lock time of 20 ms at 298K.

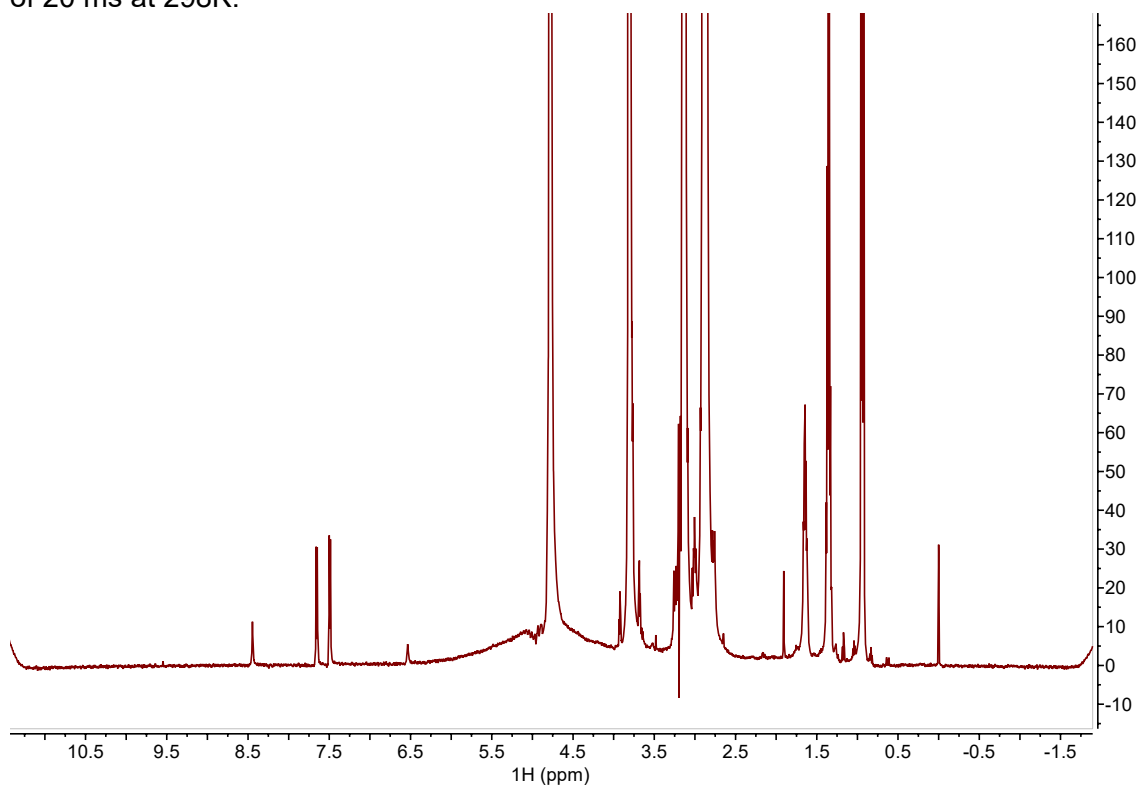


Figure S43. Proton 1D CPMG NMR spectrum of 0.4 mM C30 collected with a spin-lock time of 50 ms at 298K.

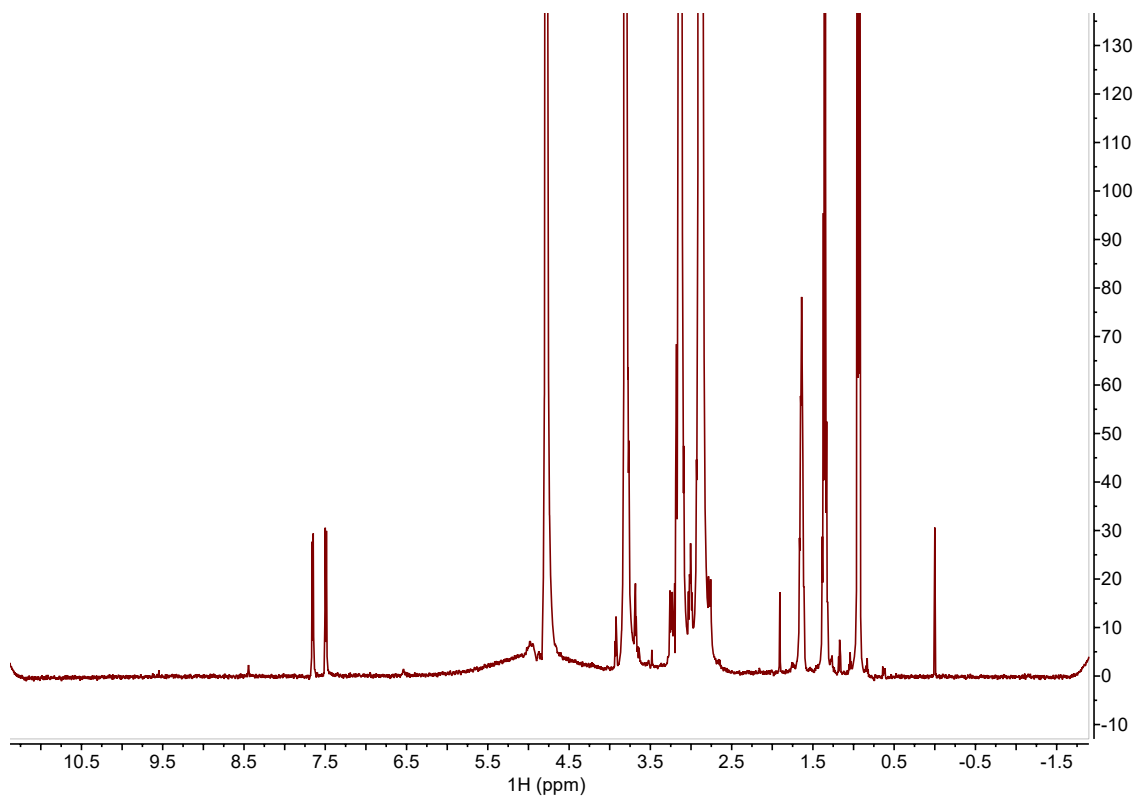


Figure S44. Proton 1D CPMG NMR spectrum of 0.4 mM C30 collected with a spin-lock time of 150 ms at 298K.

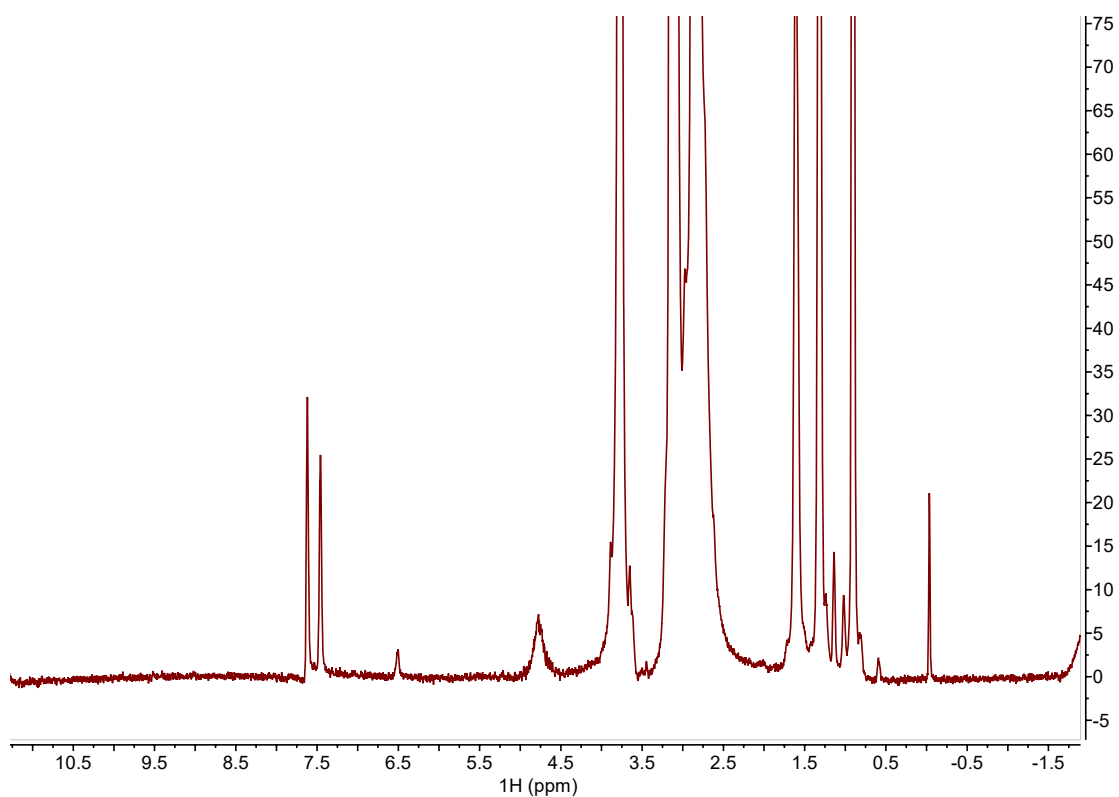


Figure S45. Proton 1D CPMG NMR spectrum of 0.4 mM C30 with the addition of 0.5 mM Mn²⁺ collected with a spin-lock time of 20 ms at 298K.

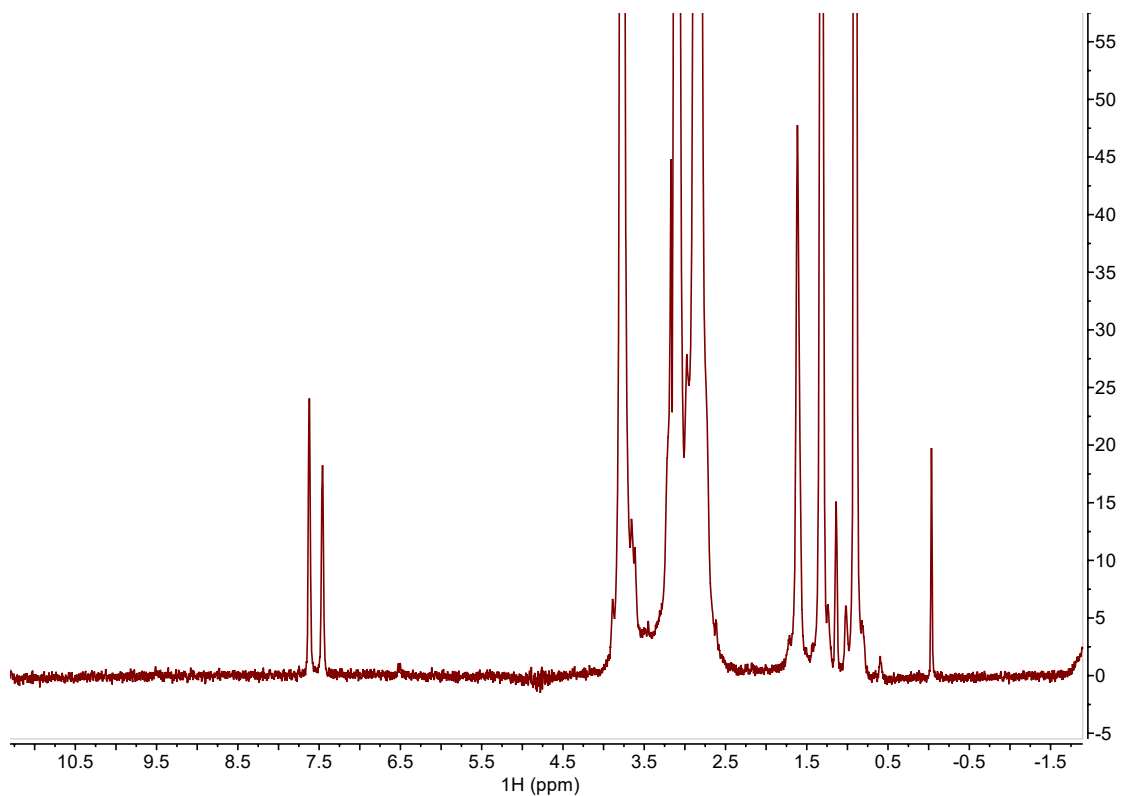


Figure S46. Proton 1D CPMG NMR spectrum of 0.4 mM C30 with the addition of 0.5 mM Mn^{2+} collected with a spin-lock time of 50 ms at 298K.

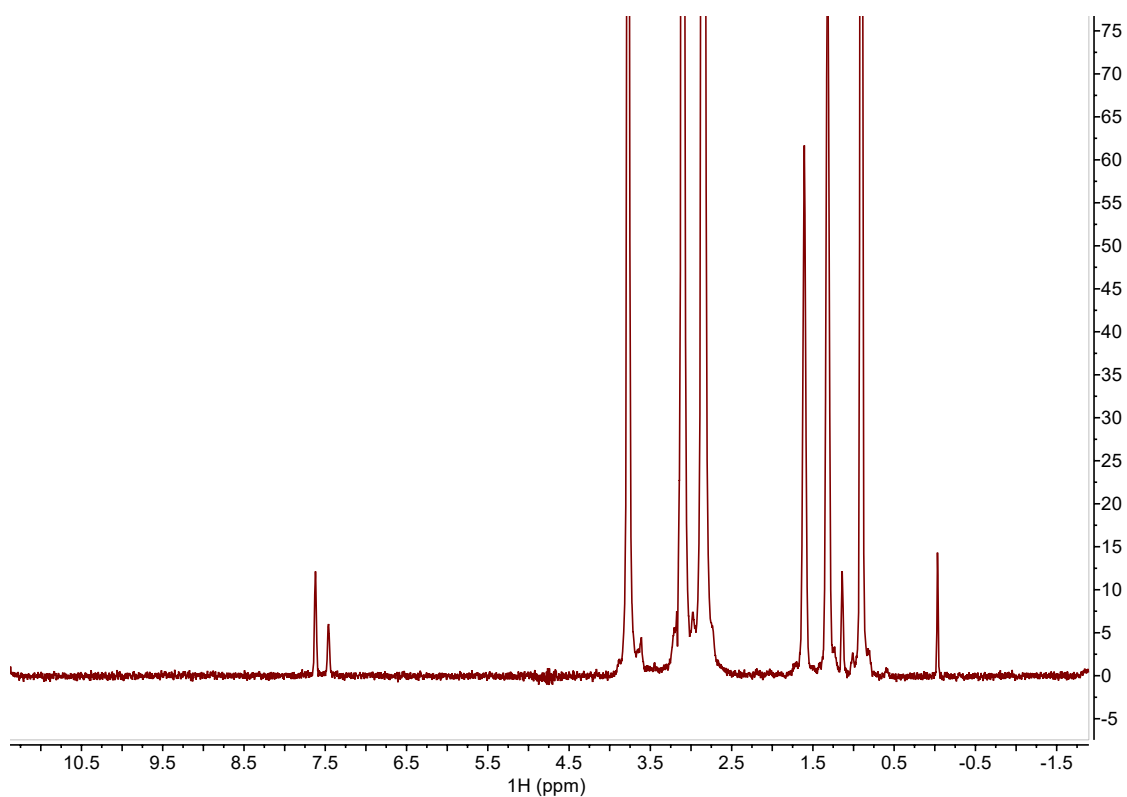


Figure S47. Proton 1D CPMG NMR spectrum of 0.4 mM C30 with the addition of 0.5 mM Mn^{2+} collected with a spin-lock time of 150 ms at 298K.

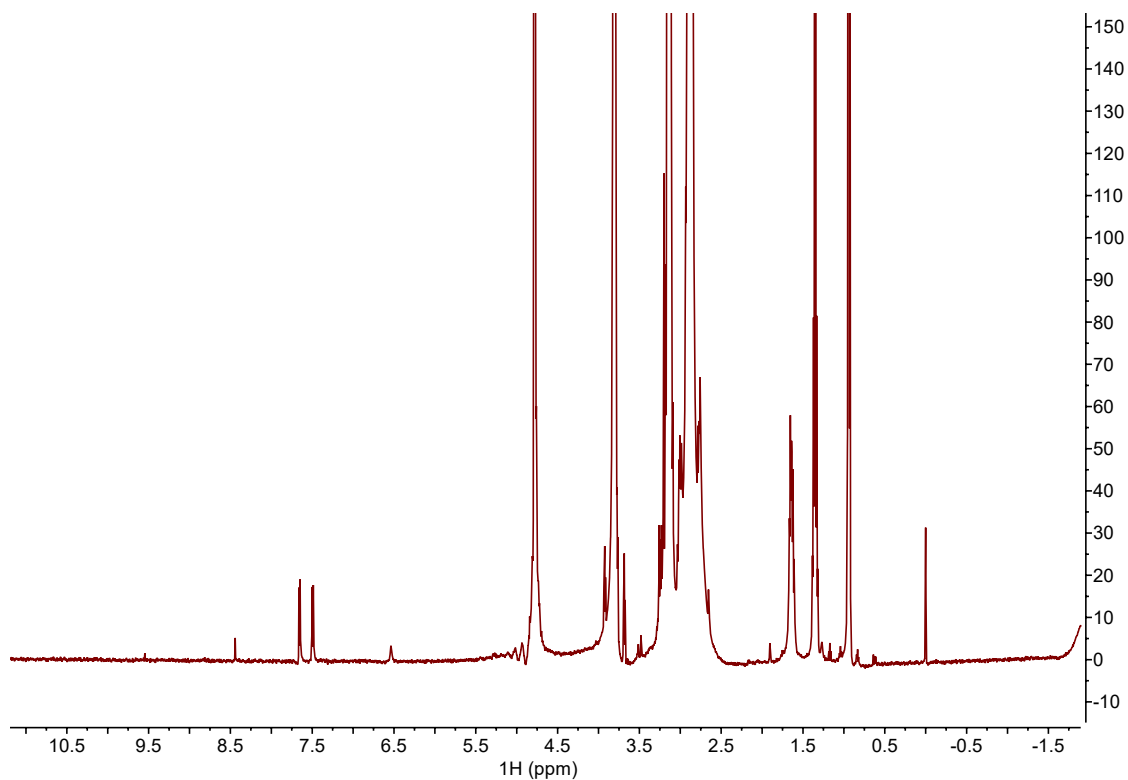


Figure S48. Proton 1D CPMG NMR spectrum of 0.2 mM C30 in the presence of *E. coli* lipid vesicles collected with a spin-lock time of 20 ms at 298K.

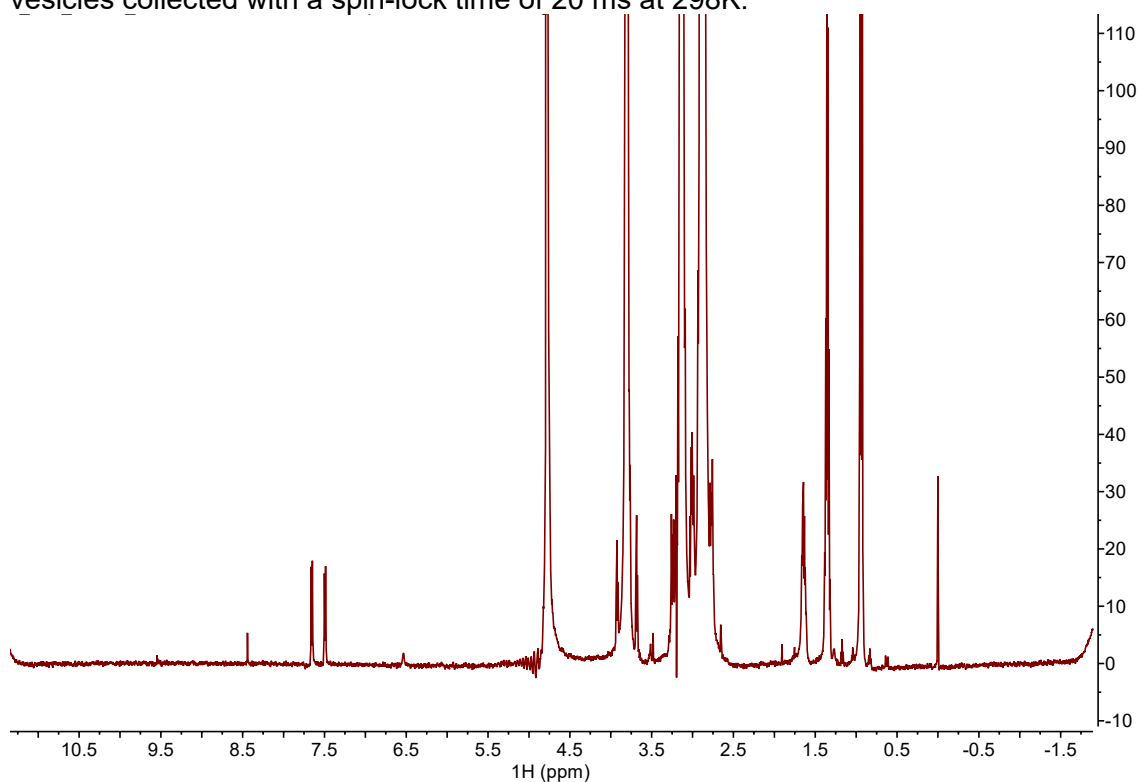


Figure S49. Proton 1D CPMG NMR spectrum of 0.2 mM C30 in the presence of *E. coli* lipid vesicles collected with a spin-lock time of 50 ms at 298K.

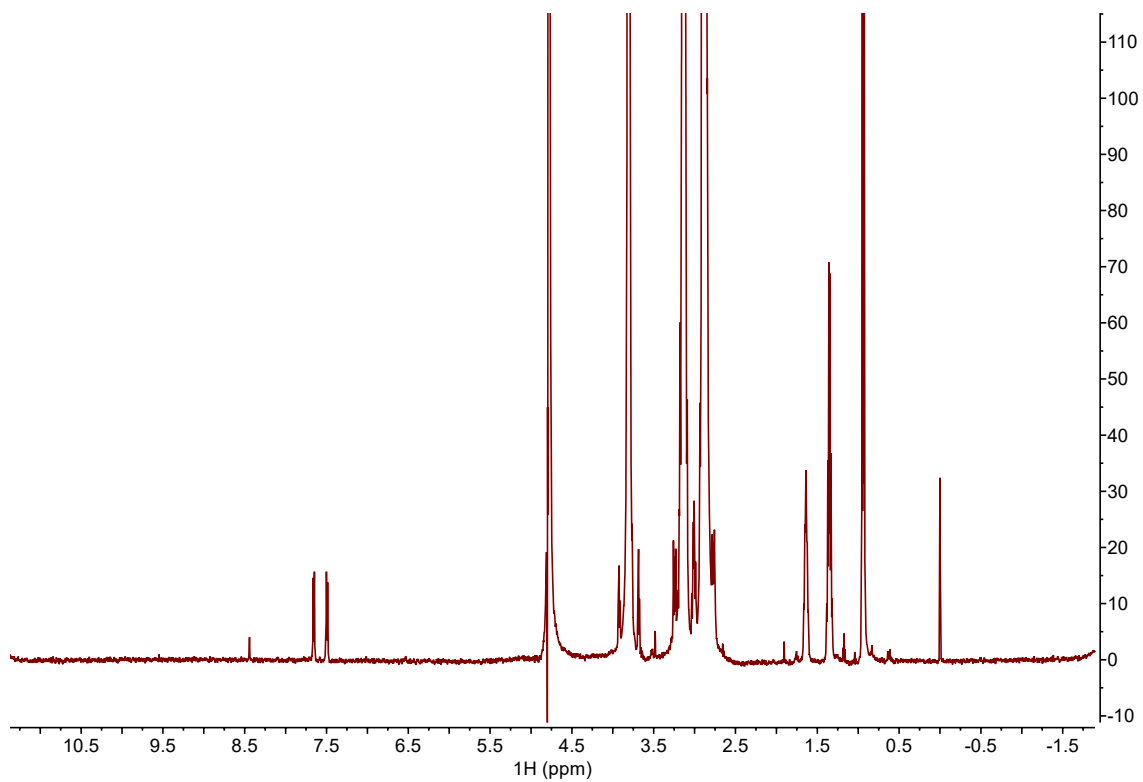


Figure S50. Proton 1D CPMG NMR spectrum of 0.2 mM C30 in the presence of *E. coli* lipid vesicles collected with a spin-lock time of 150 ms at 298K.

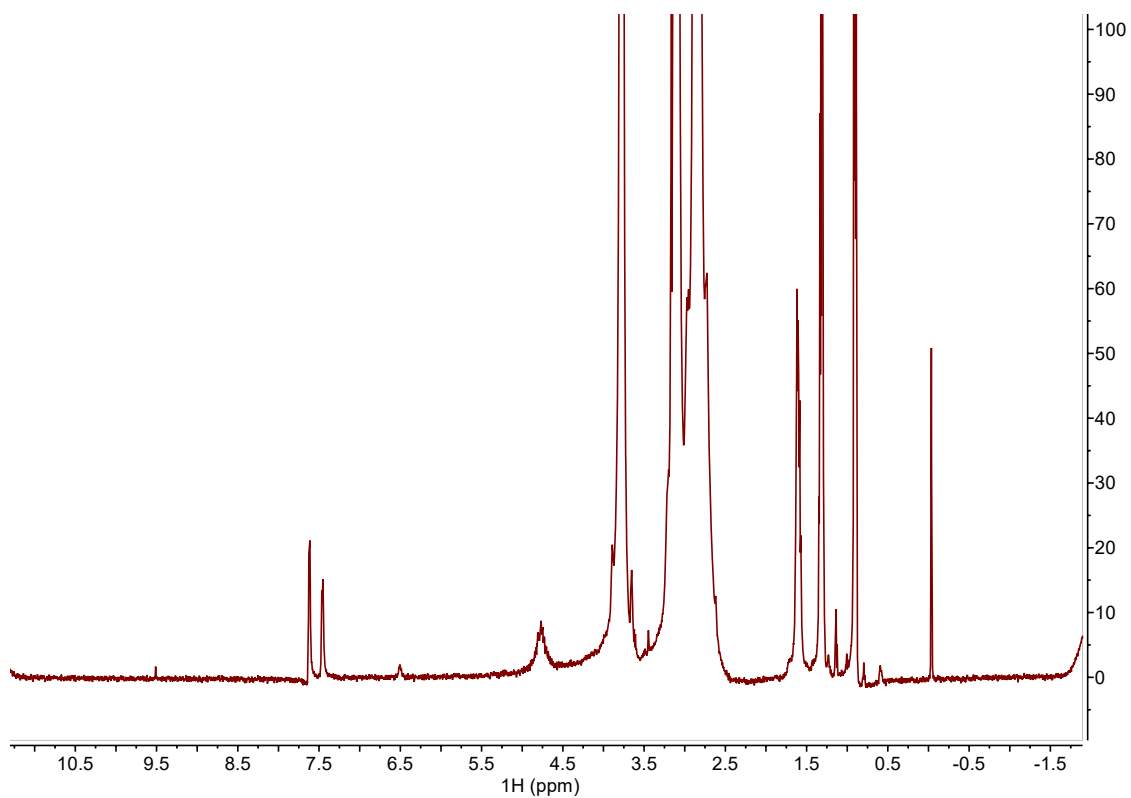


Figure S51. Proton 1D CPMG NMR spectrum of 0.2 mM C30 in the presence of *E. coli* lipid vesicles with the addition of 0.5 mM Mn^{2+} collected with a spin-lock time of 20 ms at 298K.

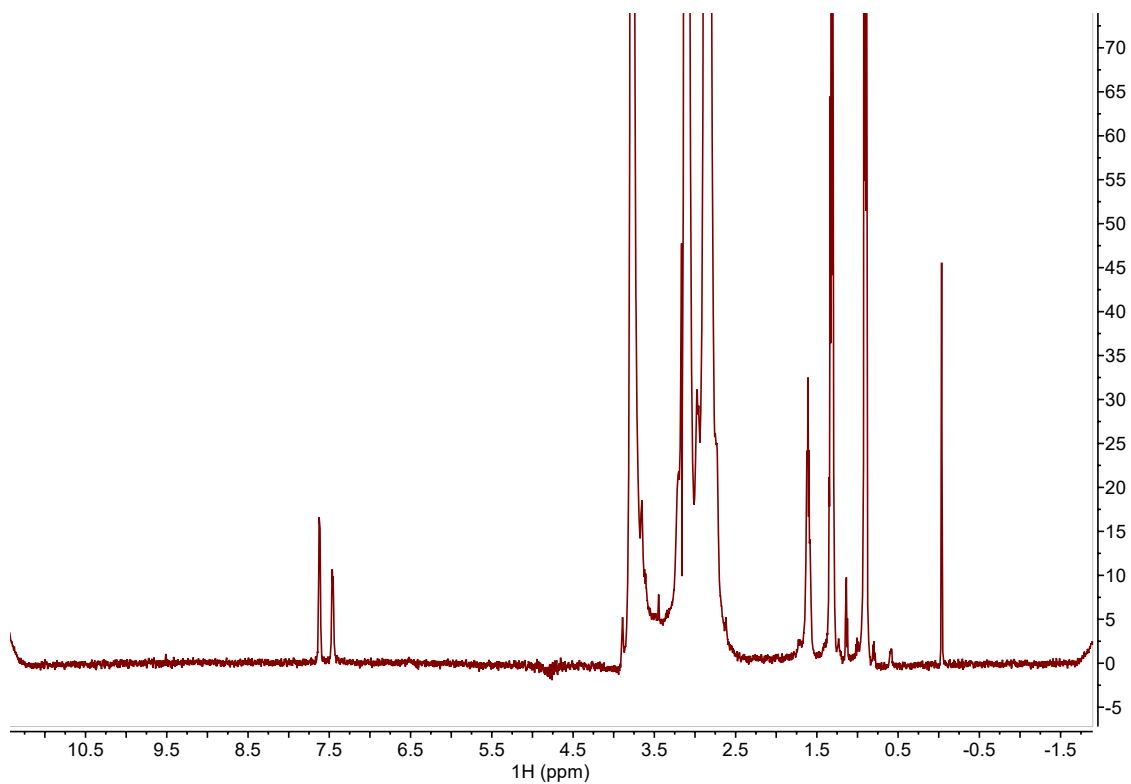


Figure S52. Proton 1D CPMG NMR spectrum of 0.2 mM C30 in the presence of *E. coli* lipid vesicles with the addition of 0.5 mM Mn^{2+} collected with a spin-lock time of 50 ms at 298K.

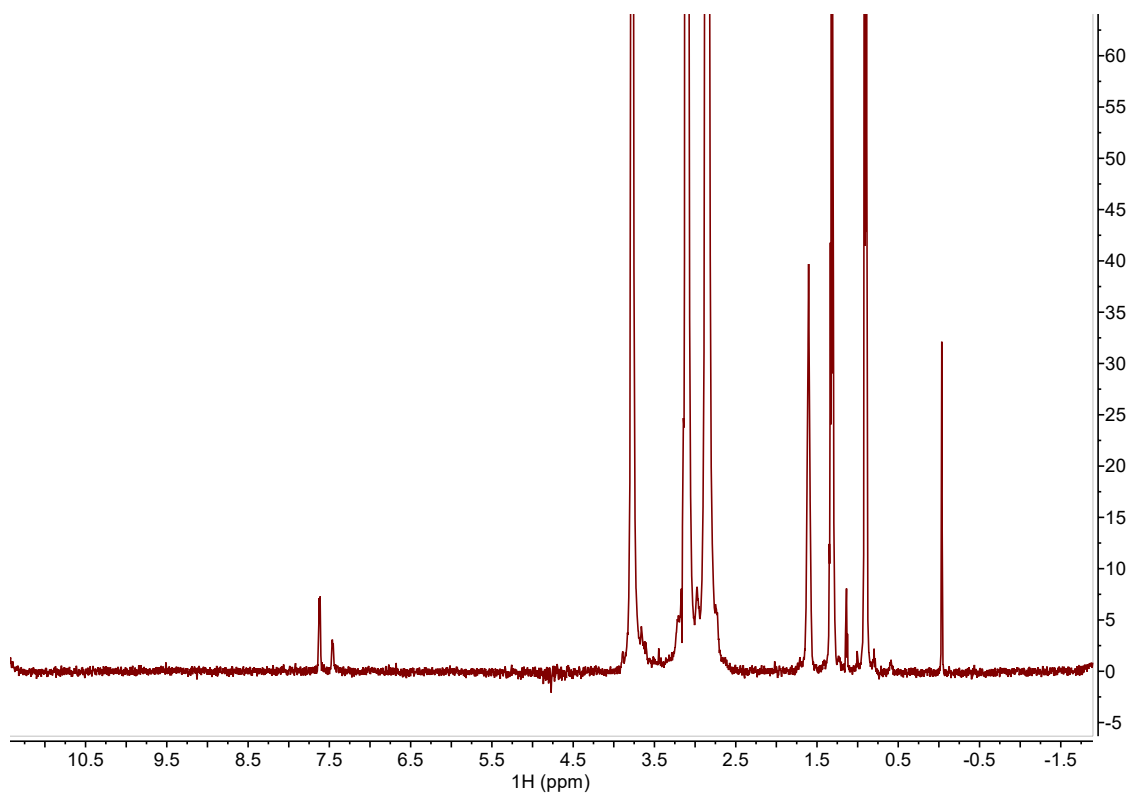


Figure S53. Proton 1D CPMG NMR spectrum of 0.2 mM C30 in the presence of *E. coli* lipid vesicles with the addition of 0.5 mM Mn^{2+} collected with a spin-lock time of 150 ms at 298K.

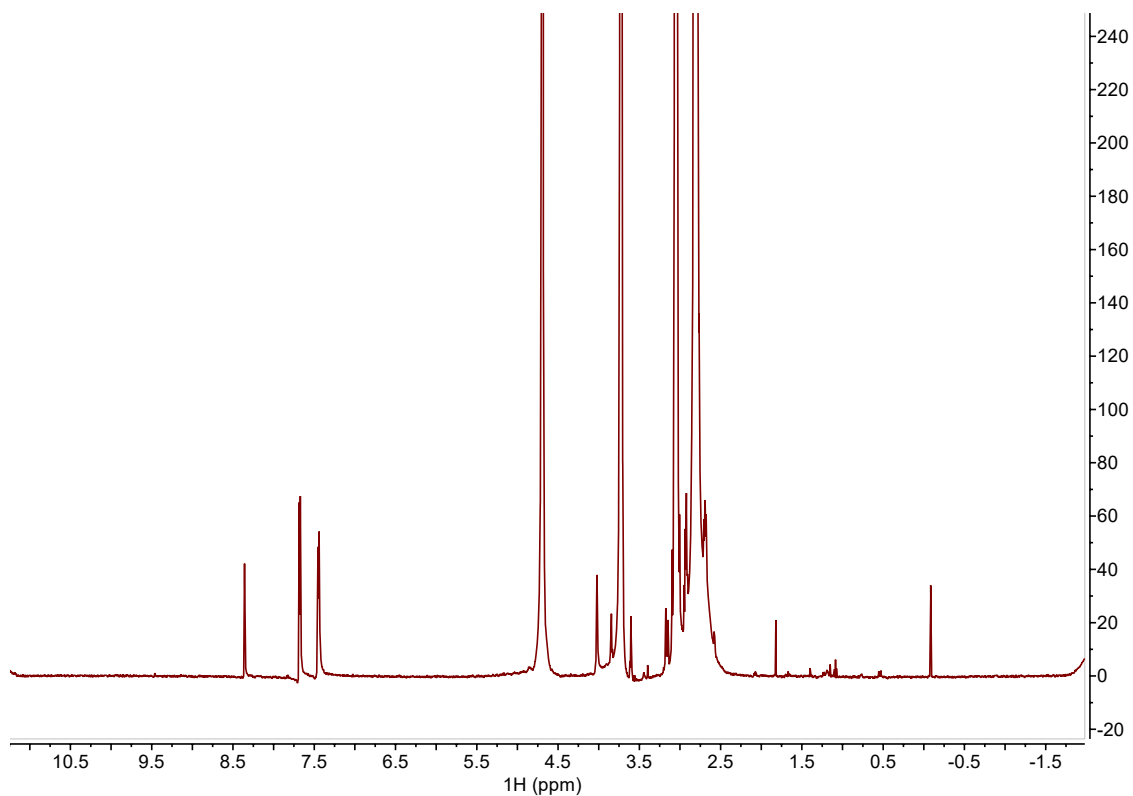


Figure S54. Proton 1D CPMG NMR spectrum of 0.4 mM C32 collected with a spin-lock time of 20 ms at 298K.

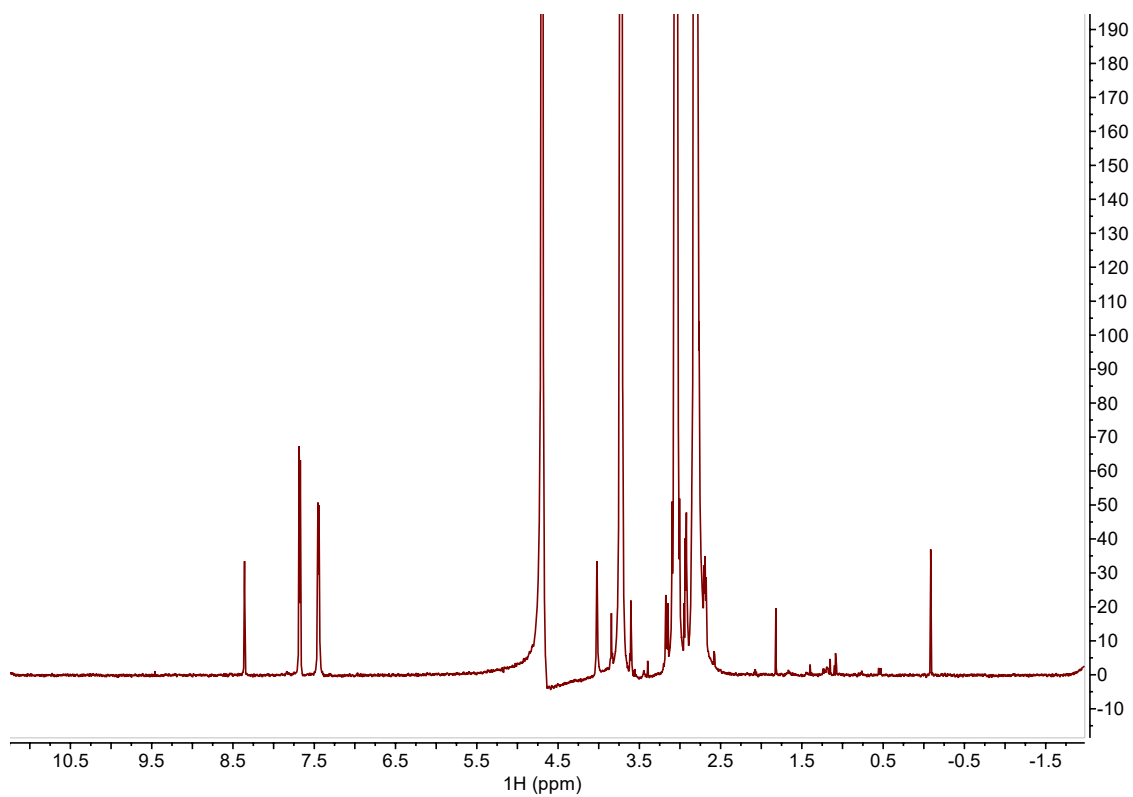


Figure S55. Proton 1D CPMG NMR spectrum of 0.4 mM C32 collected with a spin-lock time of 50 ms at 298K.

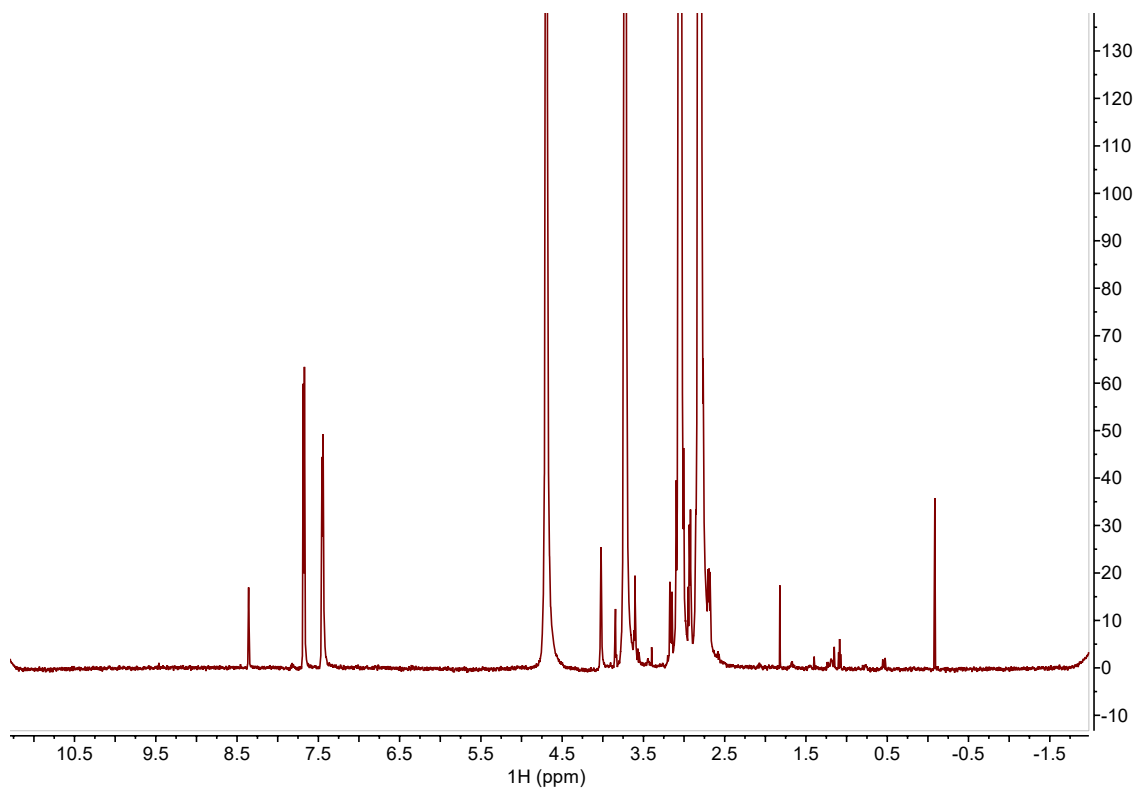


Figure S56. Proton 1D CPMG NMR spectrum of 0.4 mM C32 collected with a spin-lock time of 150 ms at 298K.

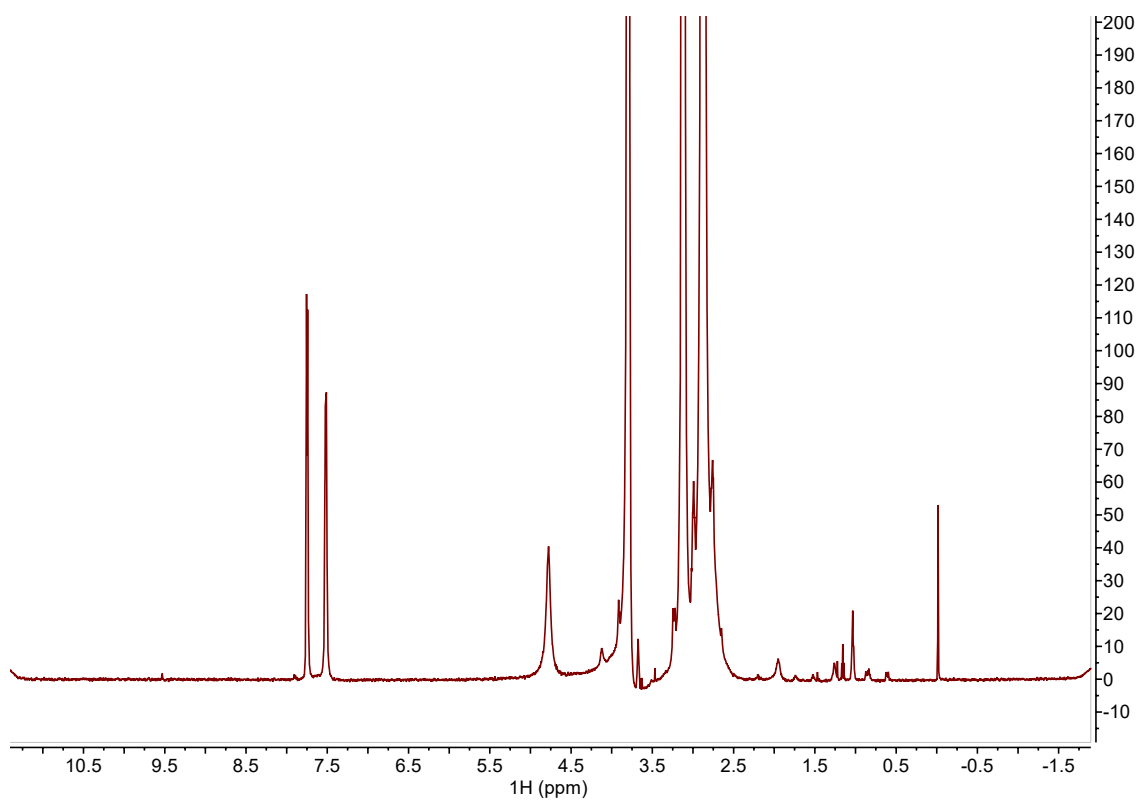


Figure S57. Proton 1D CPMG NMR spectrum of 0.4 mM C32 with the addition of 0.5 mM Mn²⁺ collected with a spin-lock time of 20 ms at 298K.

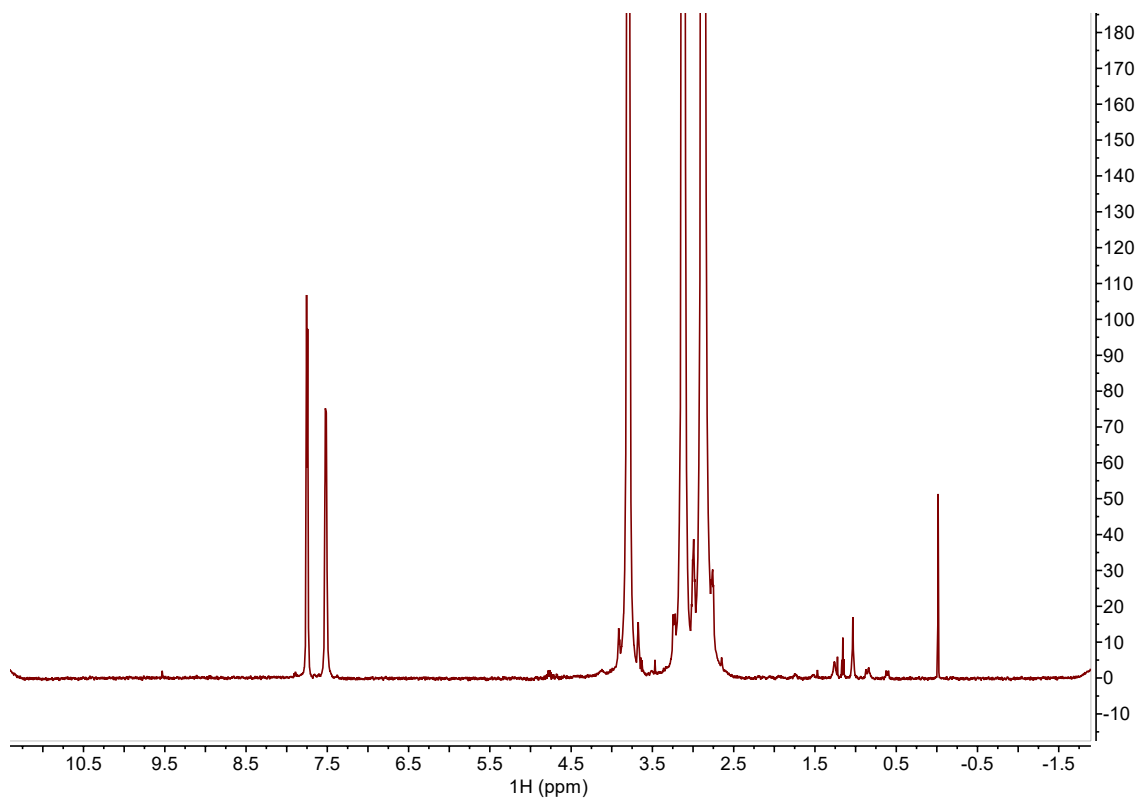


Figure S58. Proton 1D CPMG NMR spectrum of 0.4 mM C32 with the addition of 0.5 mM Mn^{2+} collected with a spin-lock time of 50 ms at 298K.

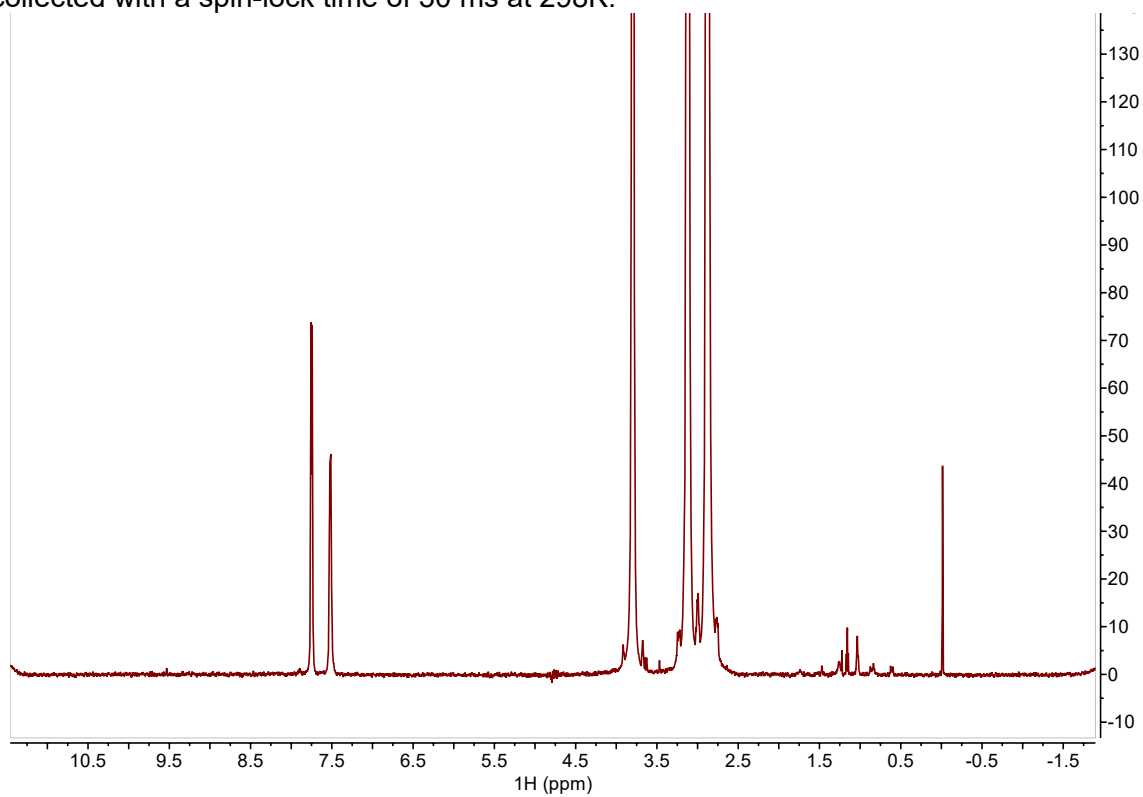


Figure S59. Proton 1D CPMG NMR spectrum of 0.4 mM C32 with the addition of 0.5 mM Mn^{2+} collected with a spin-lock time of 150 ms at 298K.

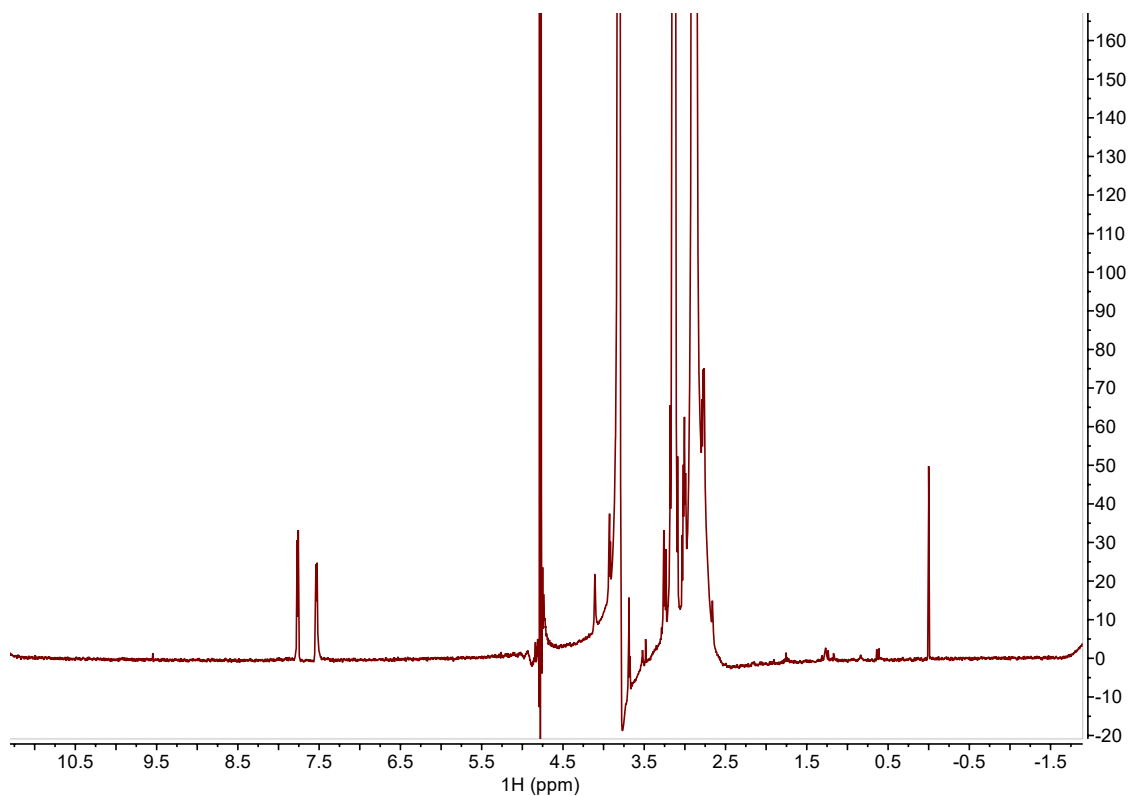


Figure S60. Proton 1D CPMG NMR spectrum of 0.2 mM C32 in the presence of *E. coli* lipid vesicles collected with a spin-lock time of 20 ms at 298K.

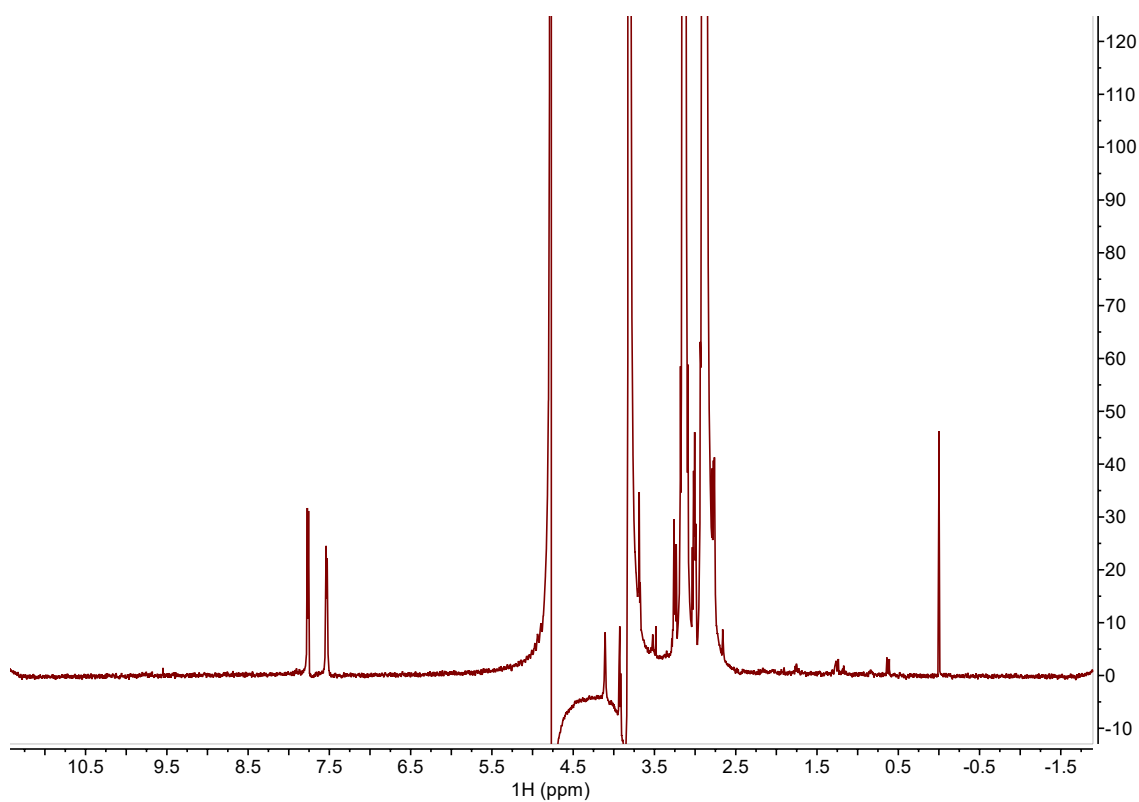


Figure S61. Proton 1D CPMG NMR spectrum of 0.2 mM C32 in the presence of *E. coli* lipid vesicles collected with a spin-lock time of 50 ms at 298K.

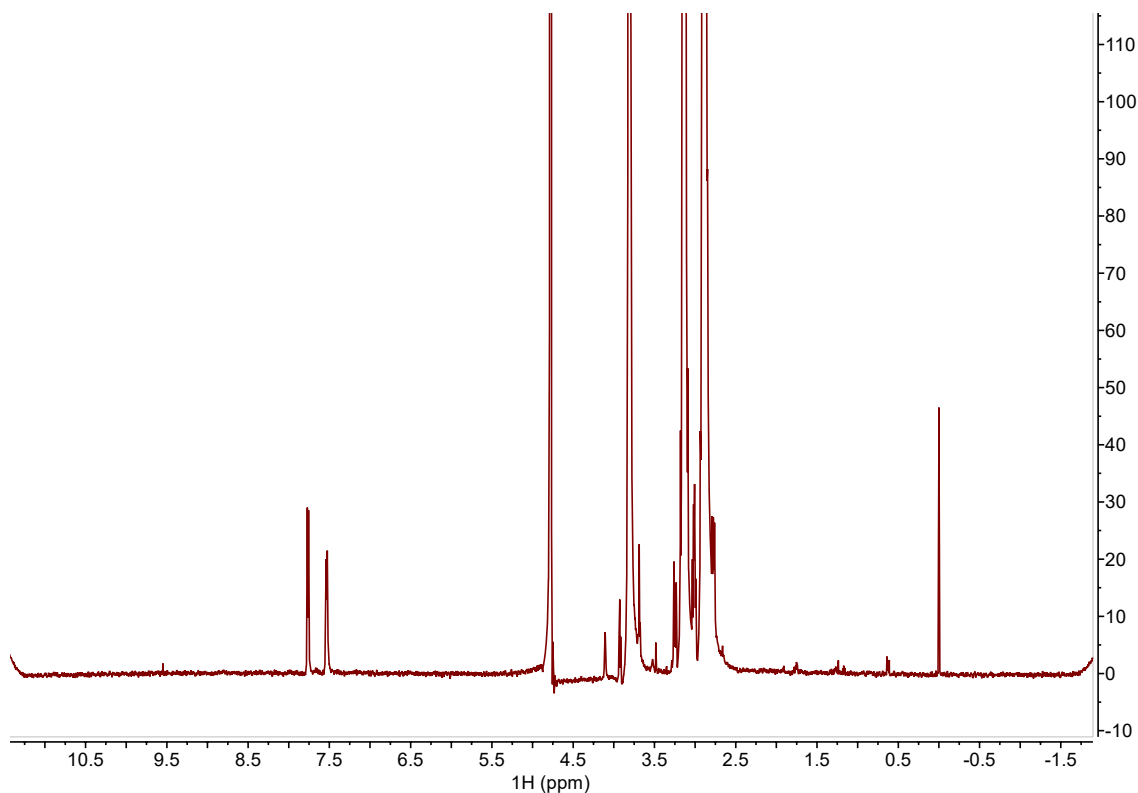


Figure S62. Proton 1D CPMG NMR spectrum of 0.2 mM C32 in the presence of *E. coli* lipid vesicles collected with a spin-lock time of 150 ms at 298K.

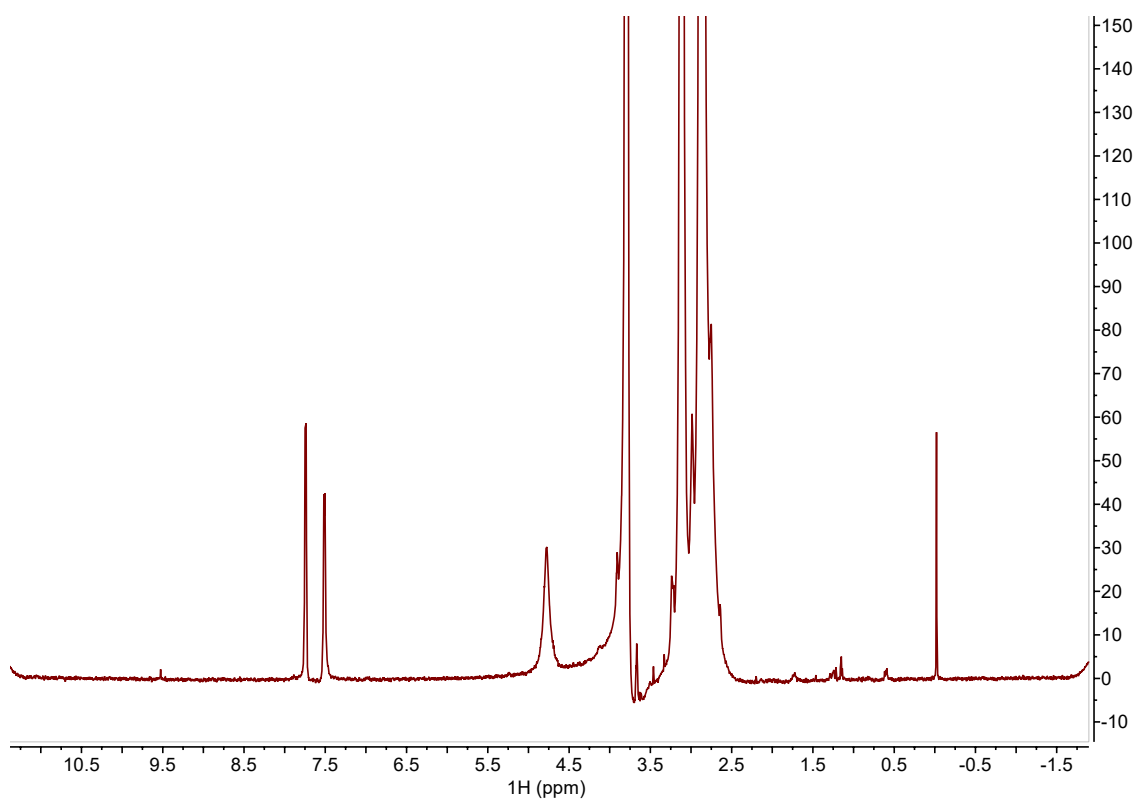


Figure S63. Proton 1D CPMG NMR spectrum of 0.2 mM C32 in the presence of *E. coli* lipid vesicles with the addition of 0.5 mM Mn^{2+} collected with a spin-lock time of 20 ms at 298K.

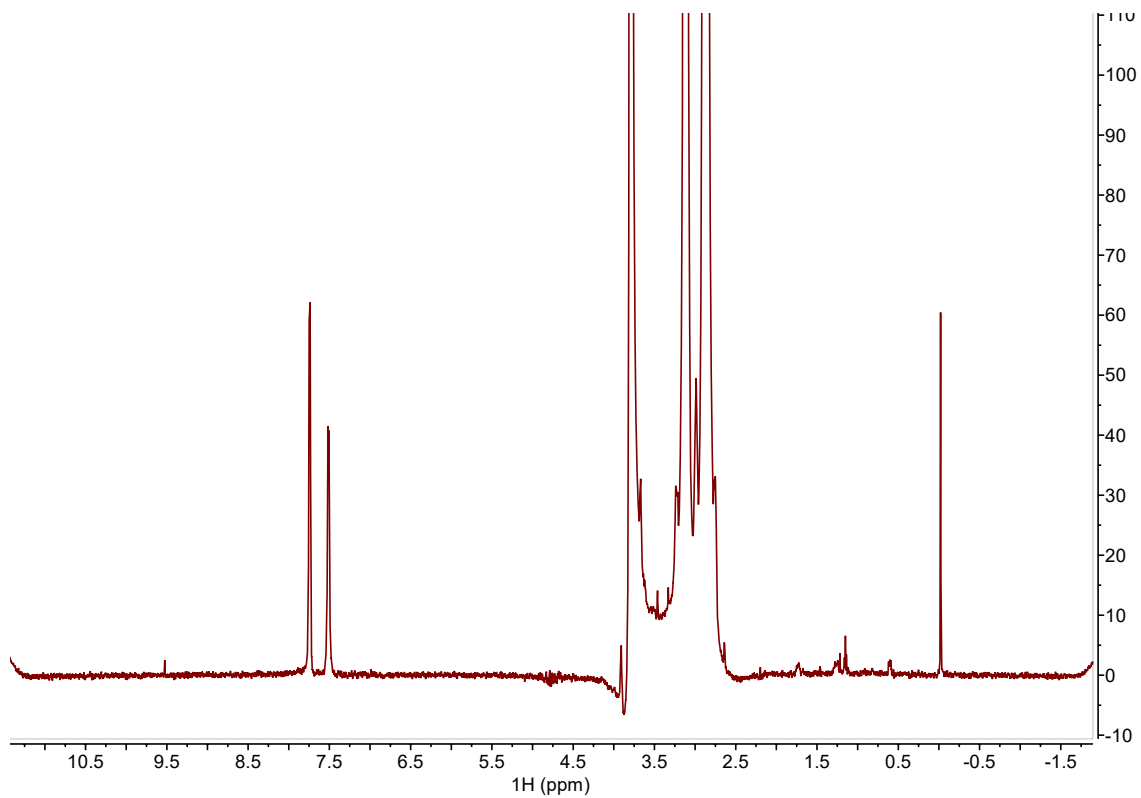


Figure S64. Proton 1D CPMG NMR spectrum of 0.2 mM C32 in the presence of *E. coli* lipid vesicles with the addition of 0.5 mM Mn^{2+} collected with a spin-lock time of 50 ms at 298K.

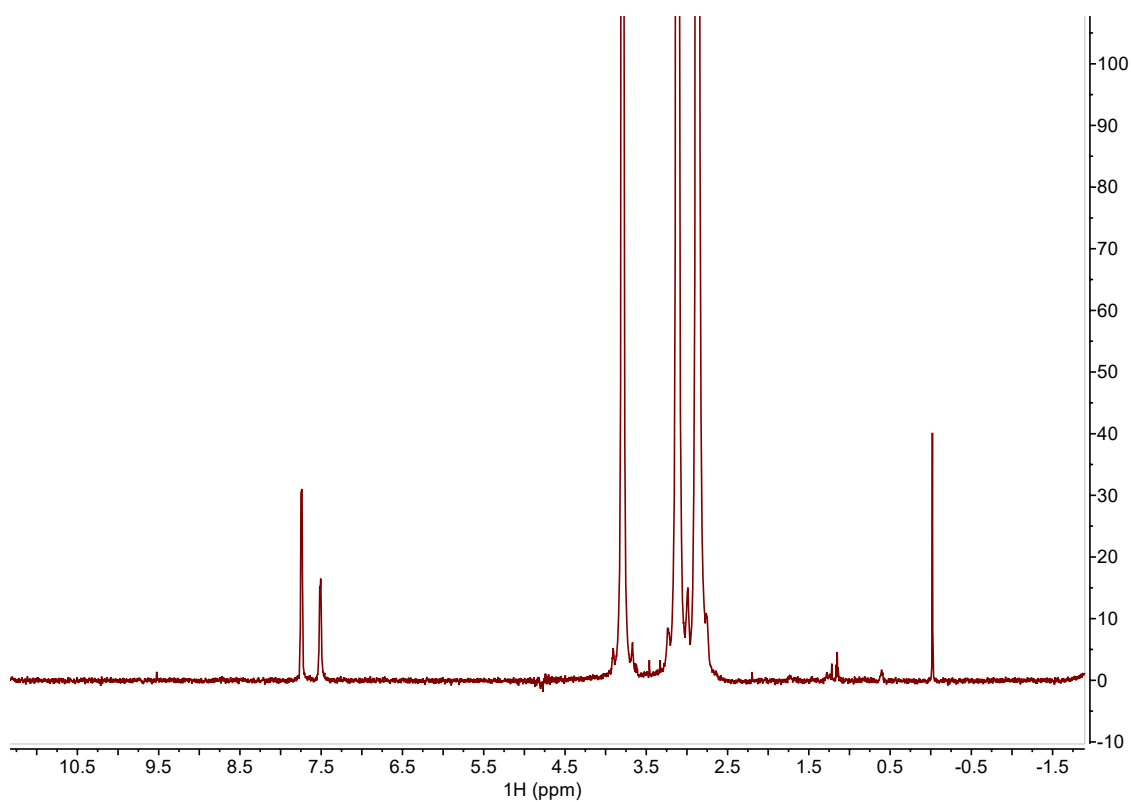


Figure S65. Proton 1D CPMG NMR spectrum of 0.2 mM C32 in the presence of *E. coli* lipid vesicles with the addition of 0.5 mM Mn^{2+} collected with a spin-lock time of 150 ms at 298K.

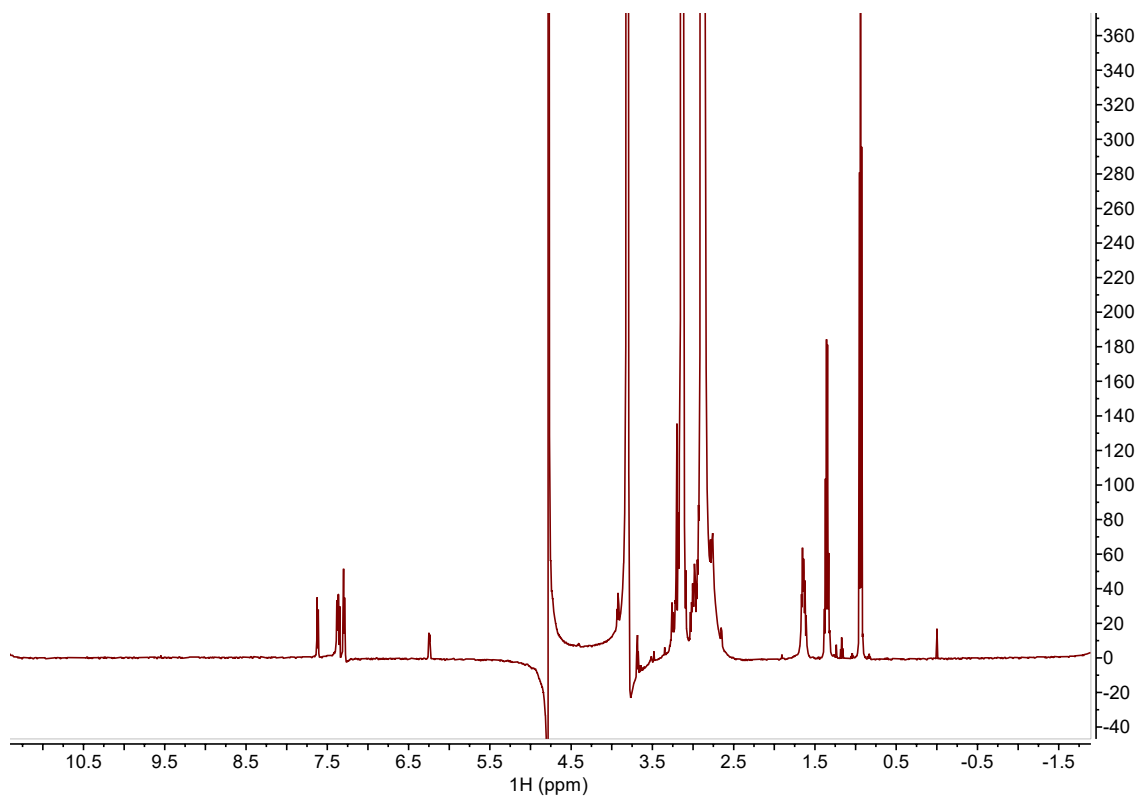


Figure S66. Proton 1D CPMG NMR spectrum of 0.4 mM C57 collected with a spin-lock time of 20 ms at 298K.

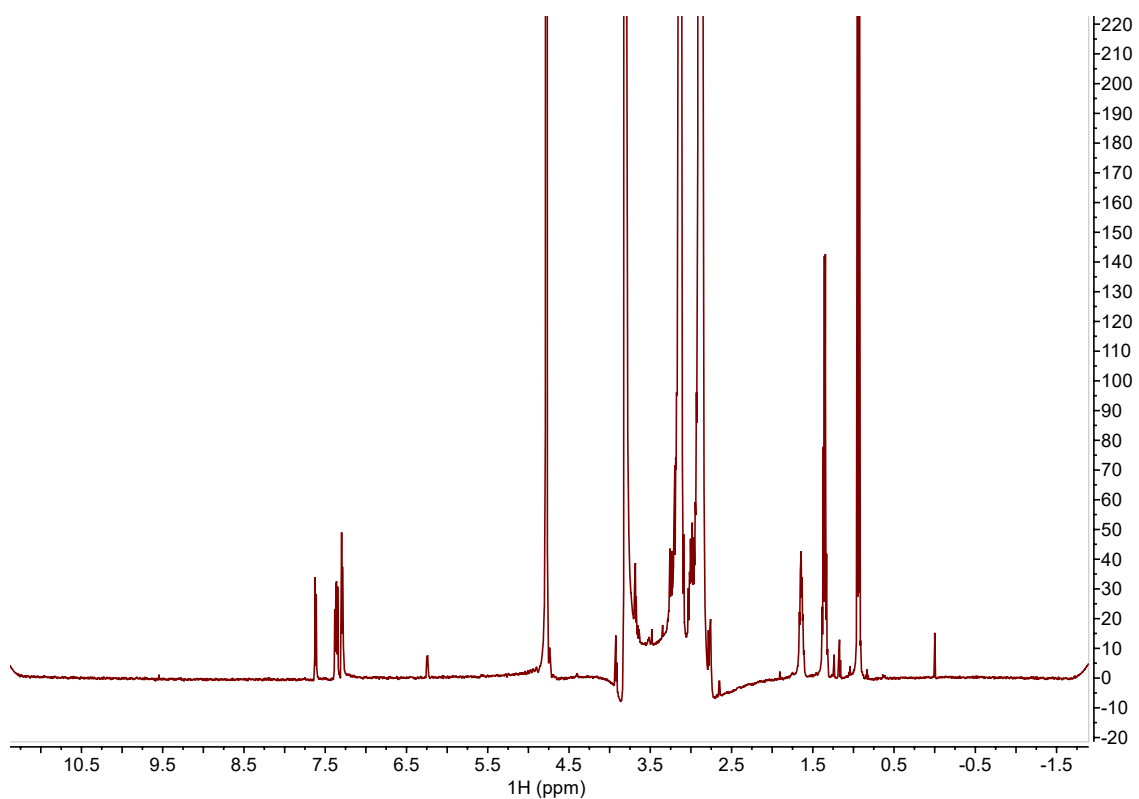


Figure S67. Proton 1D CPMG NMR spectrum of 0.4 mM C57 collected with a spin-lock time of 50 ms at 298K.

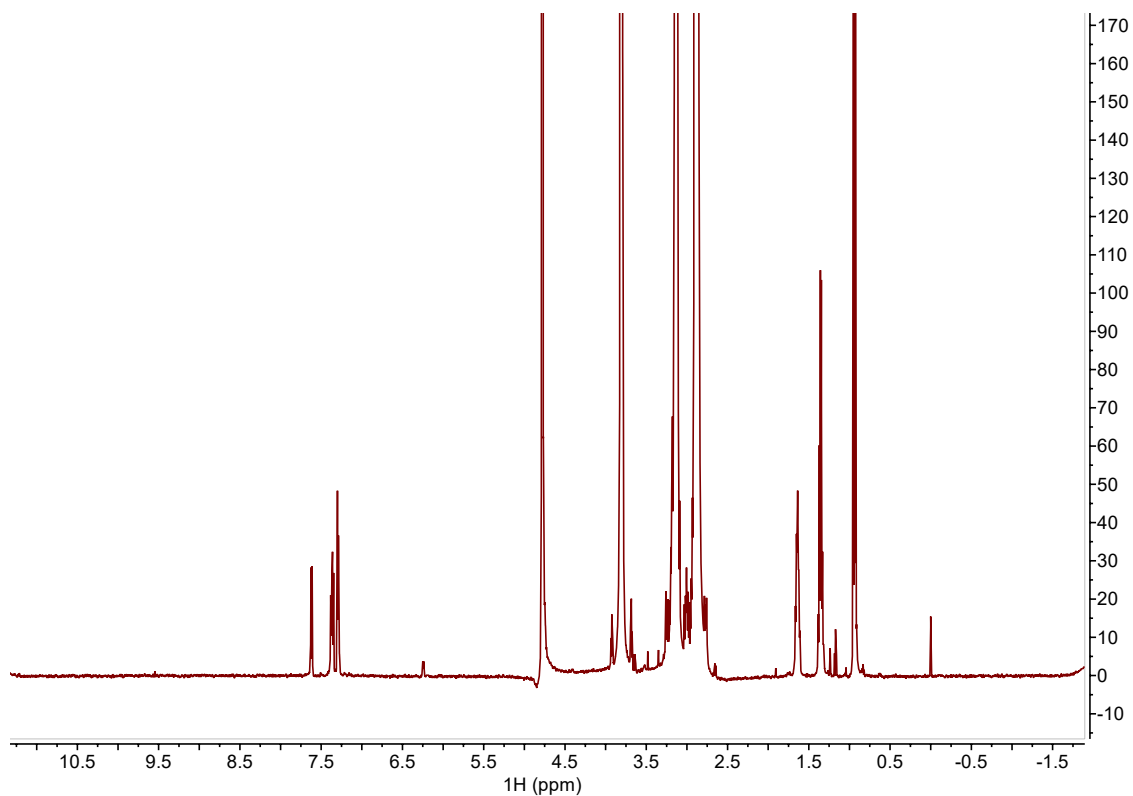


Figure S68. Proton 1D CPMG NMR spectrum of 0.4 mM C57 collected with a spin-lock time of 150 ms at 298K.

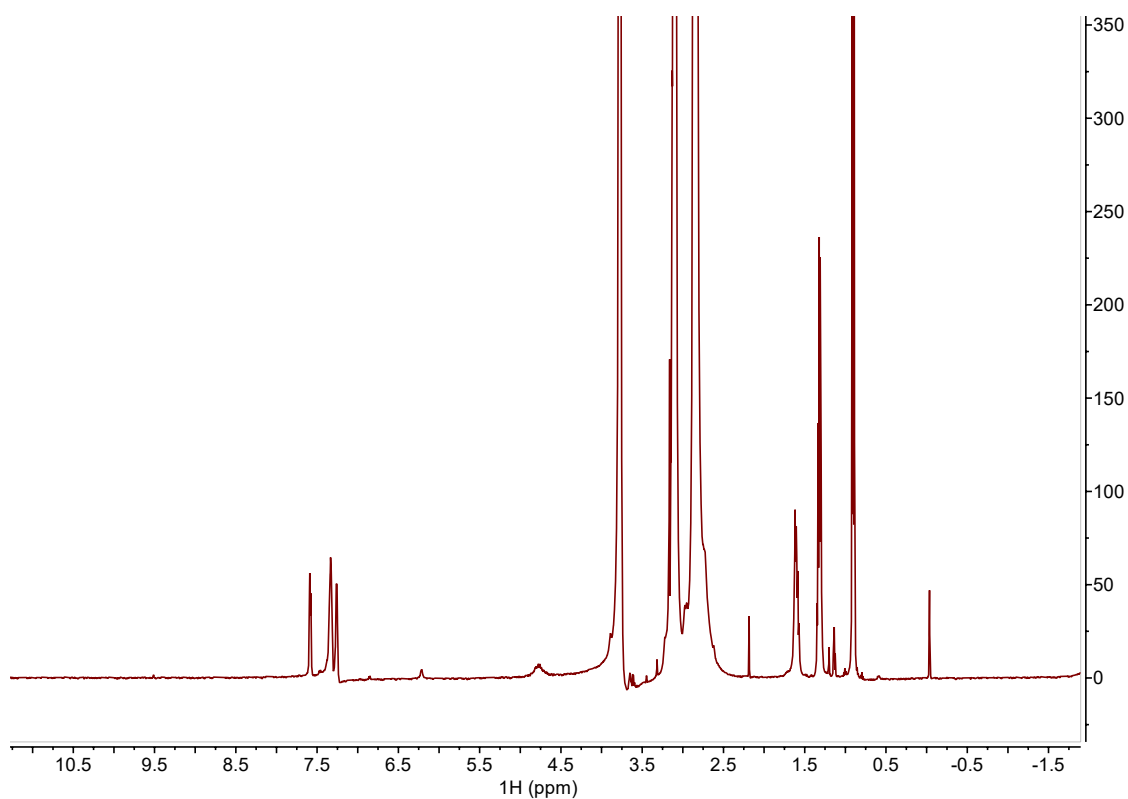


Figure S69. Proton 1D CPMG NMR spectrum of 0.4 mM C57 with the addition of 0.5 mM Mn²⁺ collected with a spin-lock time of 20 ms at 298K.

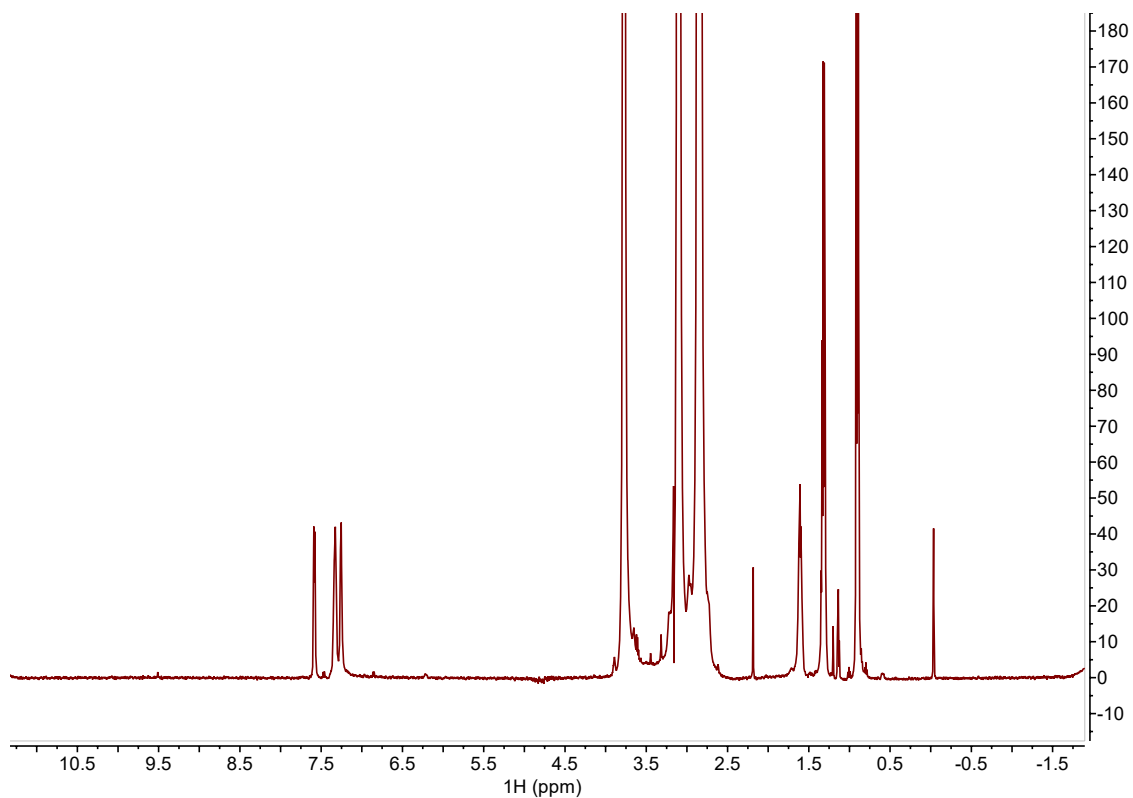


Figure S70. Proton 1D CPMG NMR spectrum of 0.4 mM C57 with the addition of 0.5 mM Mn^{2+} collected with a spin-lock time of 50 ms at 298K.

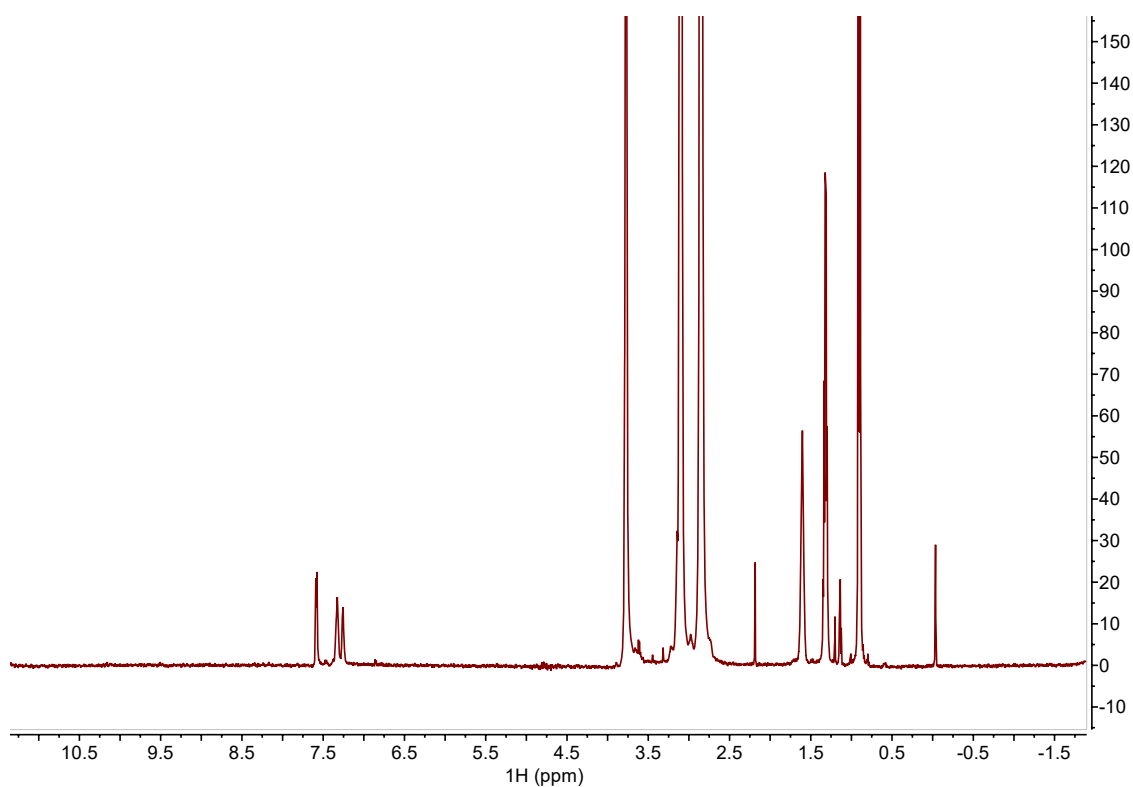


Figure S71. Proton 1D CPMG NMR spectrum of 0.4 mM C57 with the addition of 0.5 mM Mn^{2+} collected with a spin-lock time of 150 ms at 298K.

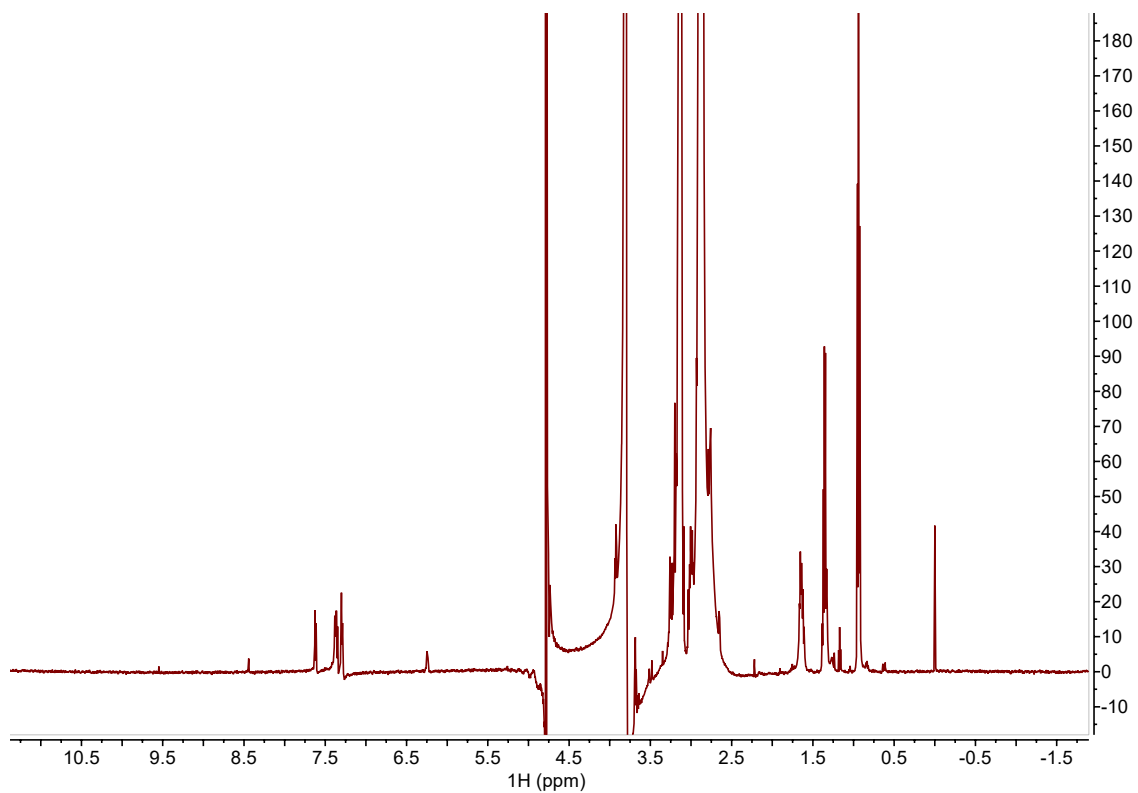


Figure S72. Proton 1D CPMG NMR spectrum of 0.2 mM C57 in the presence of *E. coli* lipid vesicles collected with a spin-lock time of 20 ms at 298K.

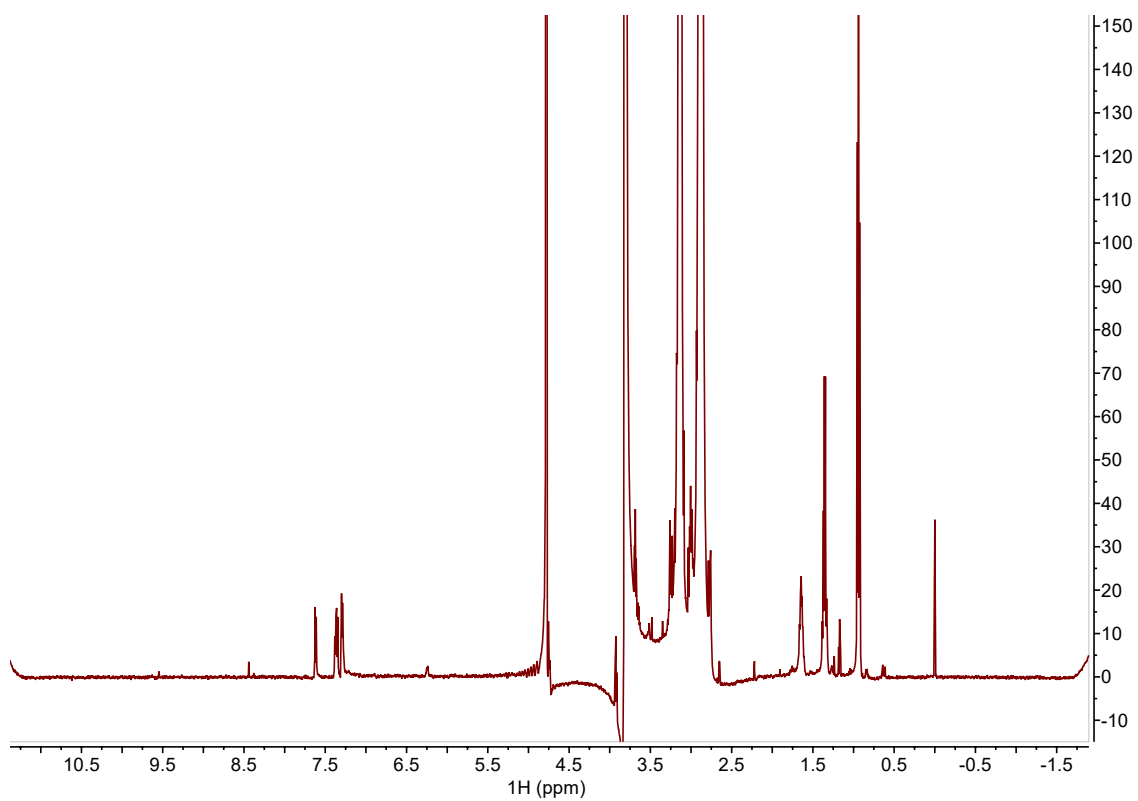


Figure S73. Proton 1D CPMG NMR spectrum of 0.2 mM C57 in the presence of *E. coli* lipid vesicles collected with a spin-lock time of 50 ms at 298K.

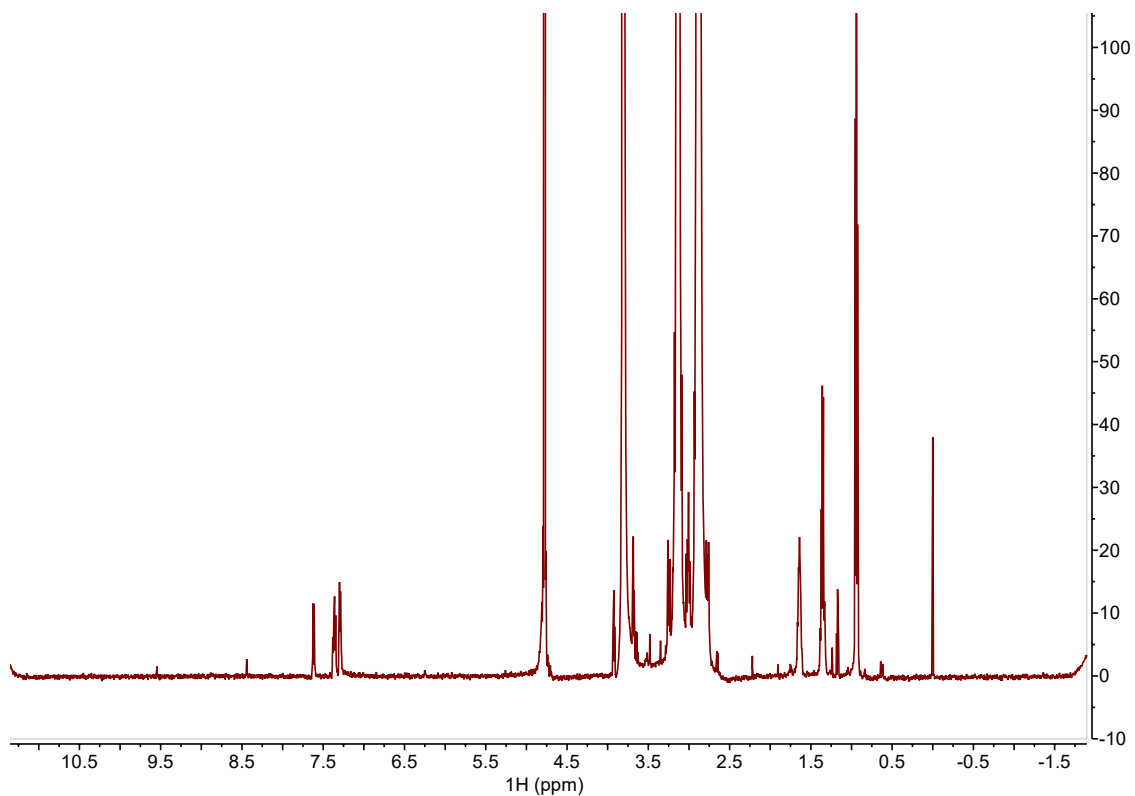


Figure S74. Proton 1D CPMG NMR spectrum of 0.2 mM C57 in the presence of *E. coli* lipid vesicles collected with a spin-lock time of 150 ms at 298K.

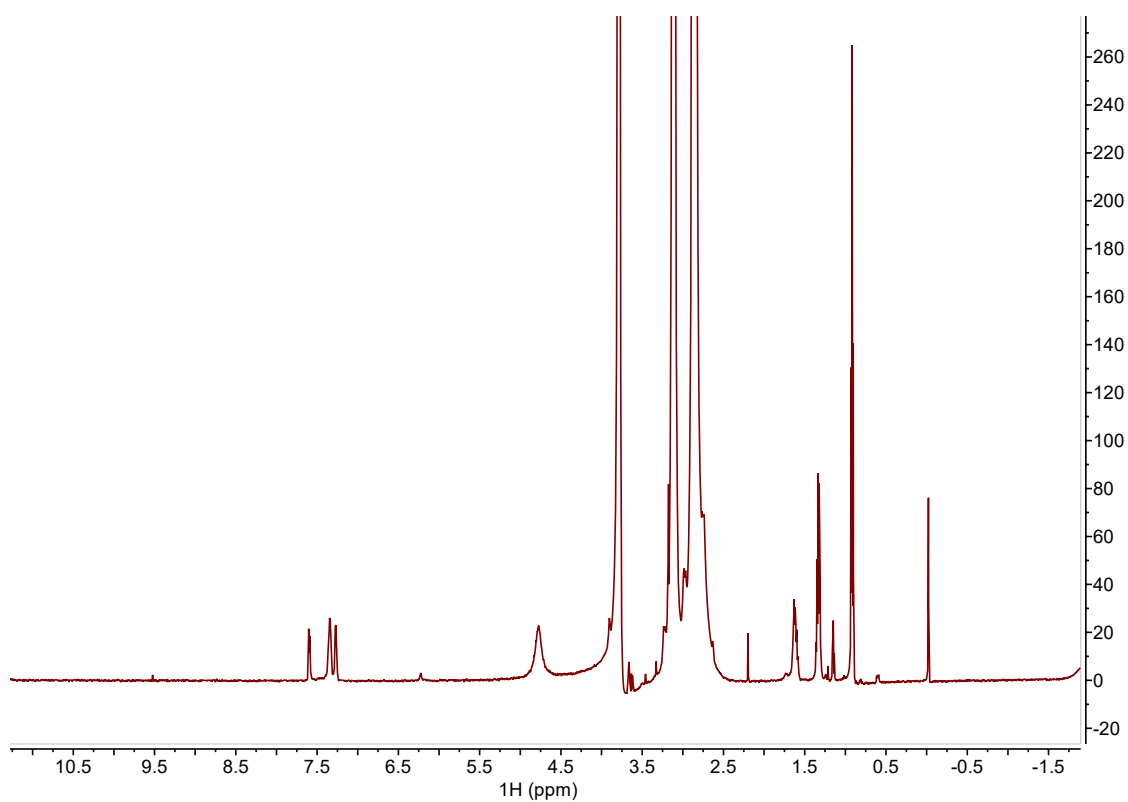


Figure S75. Proton 1D CPMG NMR spectrum of 0.2 mM C57 in the presence of *E. coli* lipid vesicles with the addition of 0.5 mM Mn²⁺ collected with a spin-lock time of 20 ms at 298K.

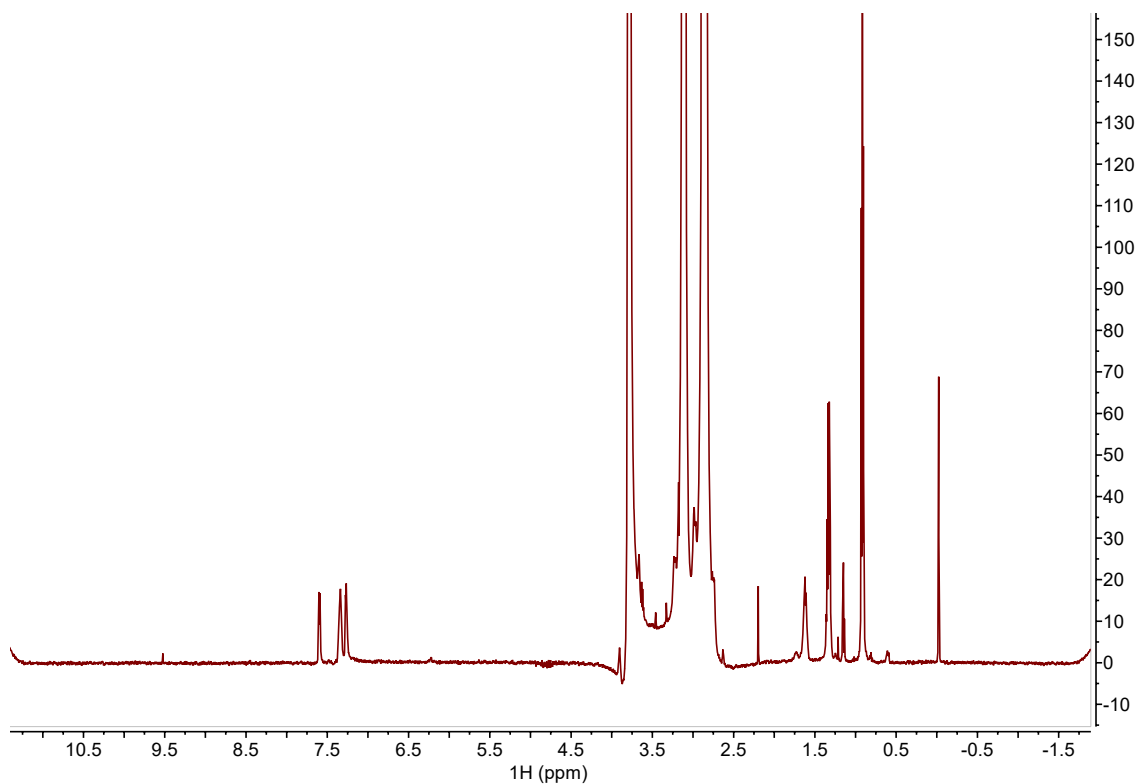


Figure S76. Proton 1D CPMG NMR spectrum of 0.2 mM C57 in the presence of *E. coli* lipid vesicles with the addition of 0.5 mM Mn^{2+} collected with a spin-lock time of 50 ms at 298K.

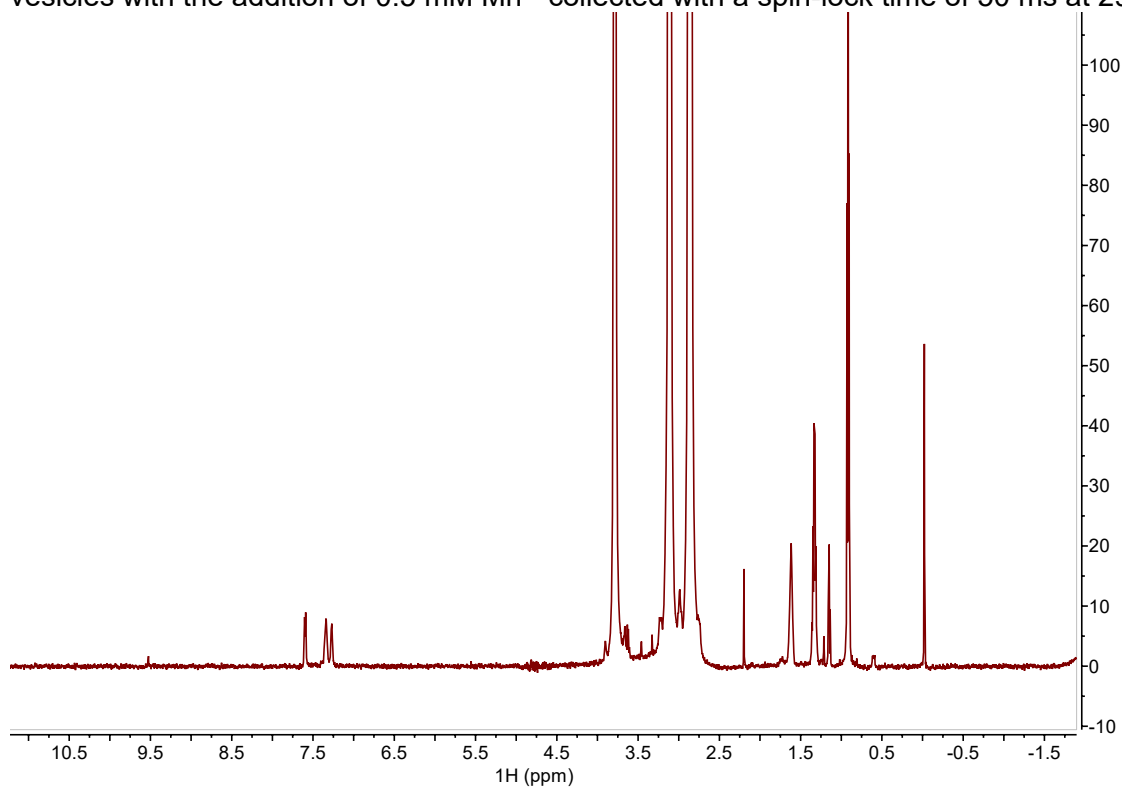


Figure S77. Proton 1D CPMG NMR spectrum of 0.2 mM C57 in the presence of *E. coli* lipid vesicles with the addition of 0.5 mM Mn^{2+} collected with a spin-lock time of 150 ms at 298K.

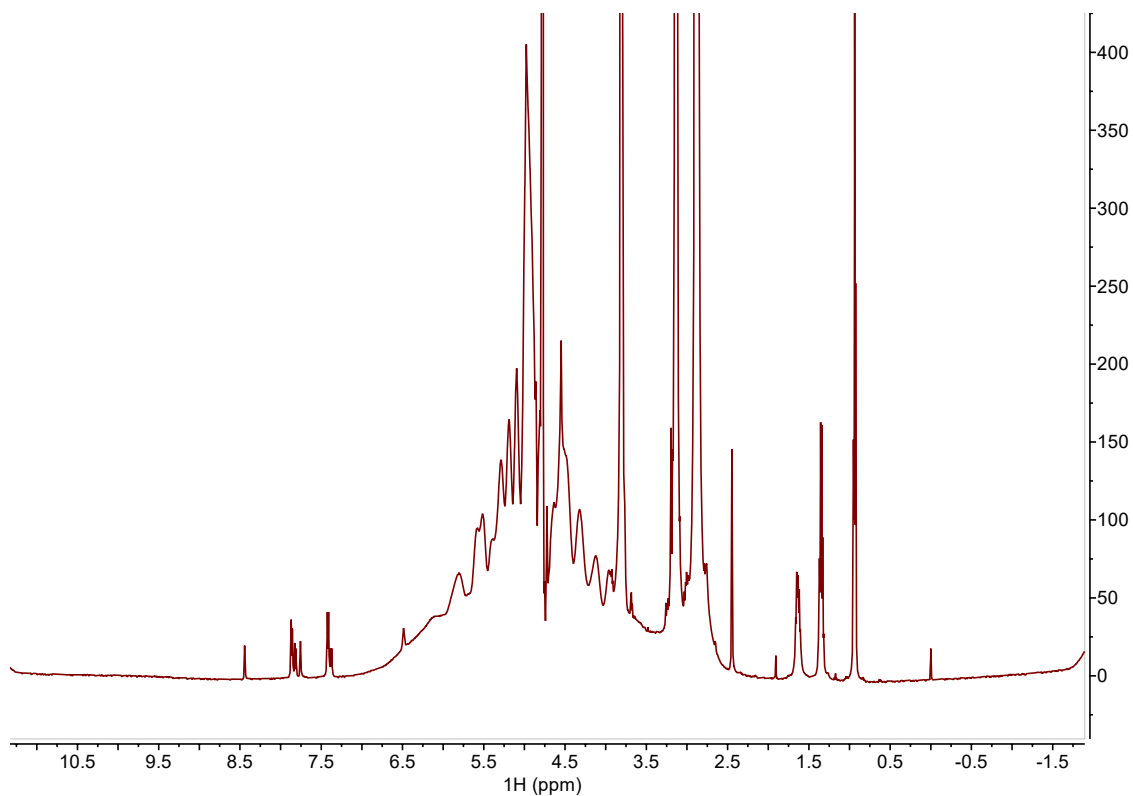


Figure S78. Proton 1D CPMG NMR spectrum of 0.4 mM C60 collected with a spin-lock time of 20 ms at 298K.

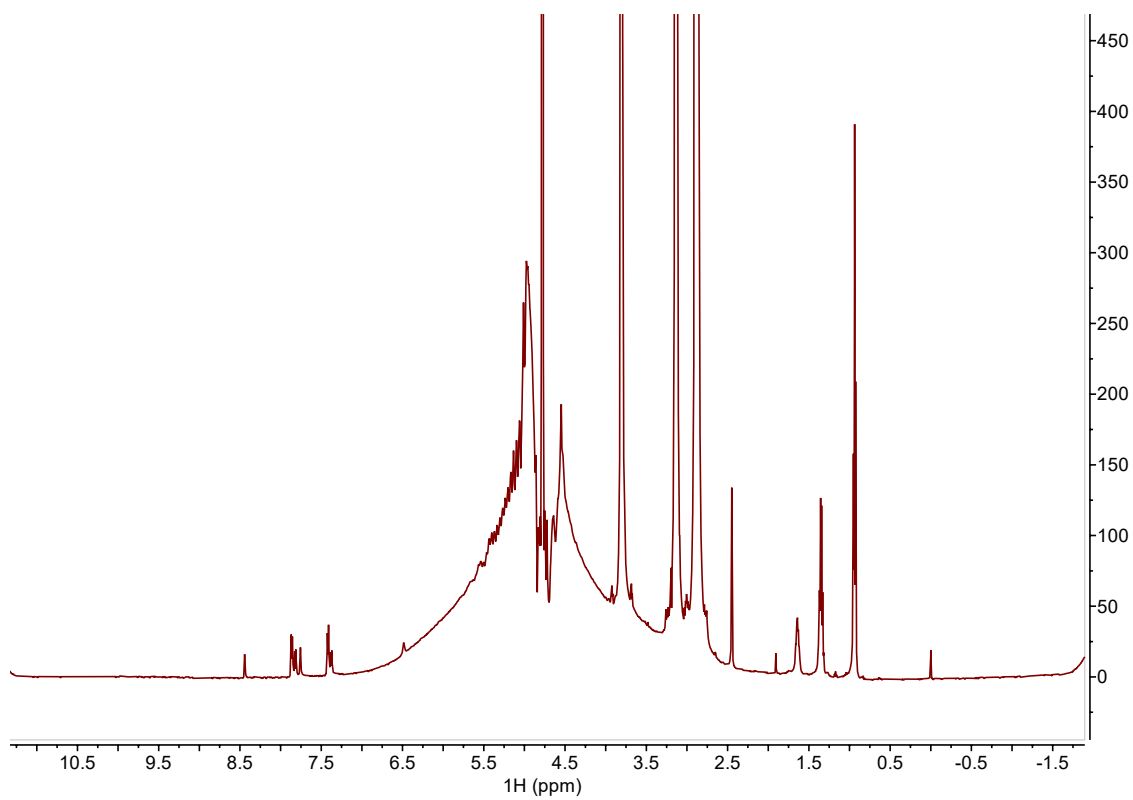


Figure S79. Proton 1D CPMG NMR spectrum of 0.4 mM C60 collected with a spin-lock time of 50 ms at 298K.

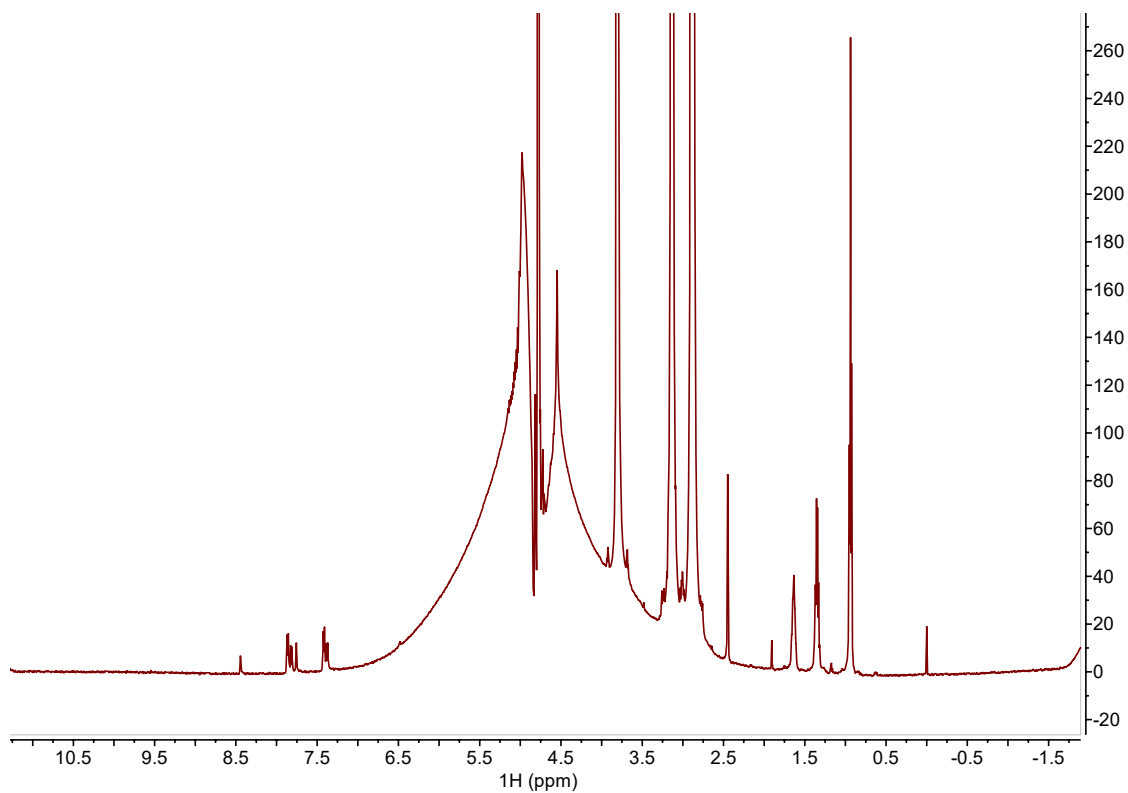


Figure S80. Proton 1D CPMG NMR spectrum of 0.4 mM C60 collected with a spin-lock time of 150 ms at 298K.

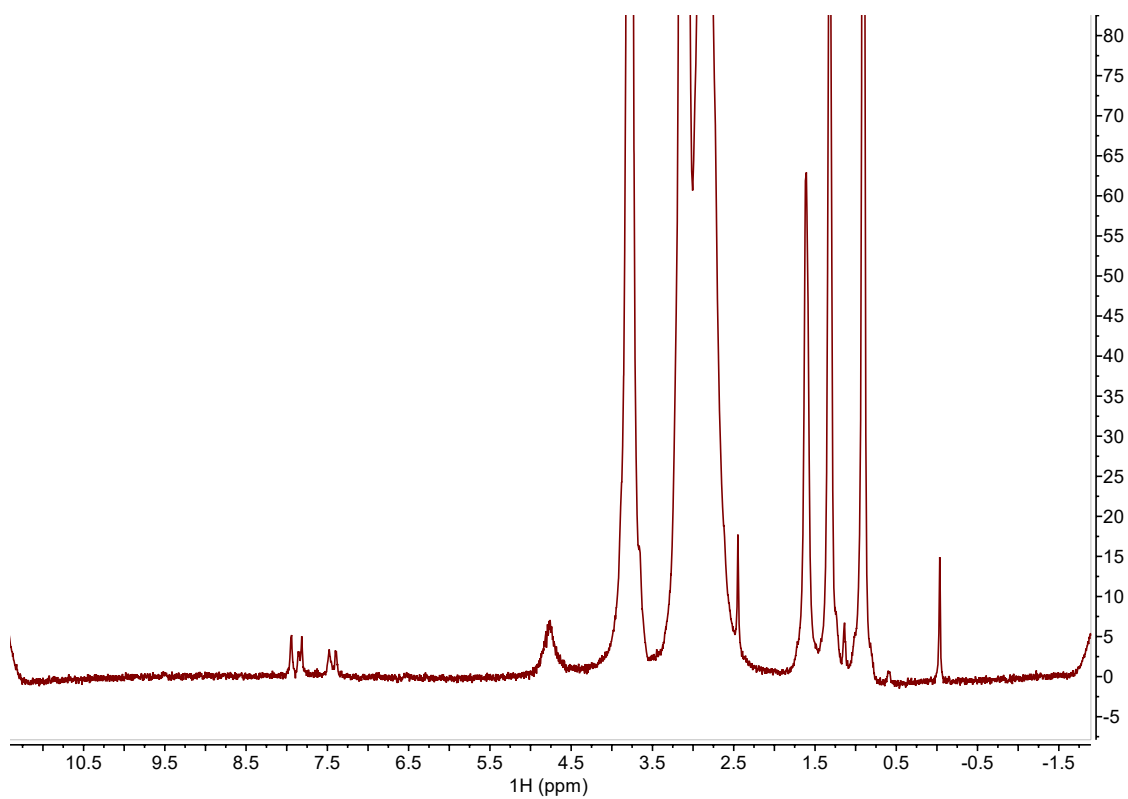


Figure S81. Proton 1D CPMG NMR spectrum of 0.4 mM C60 with the addition of 0.5 mM Mn²⁺ collected with a spin-lock time of 20 ms at 298K.

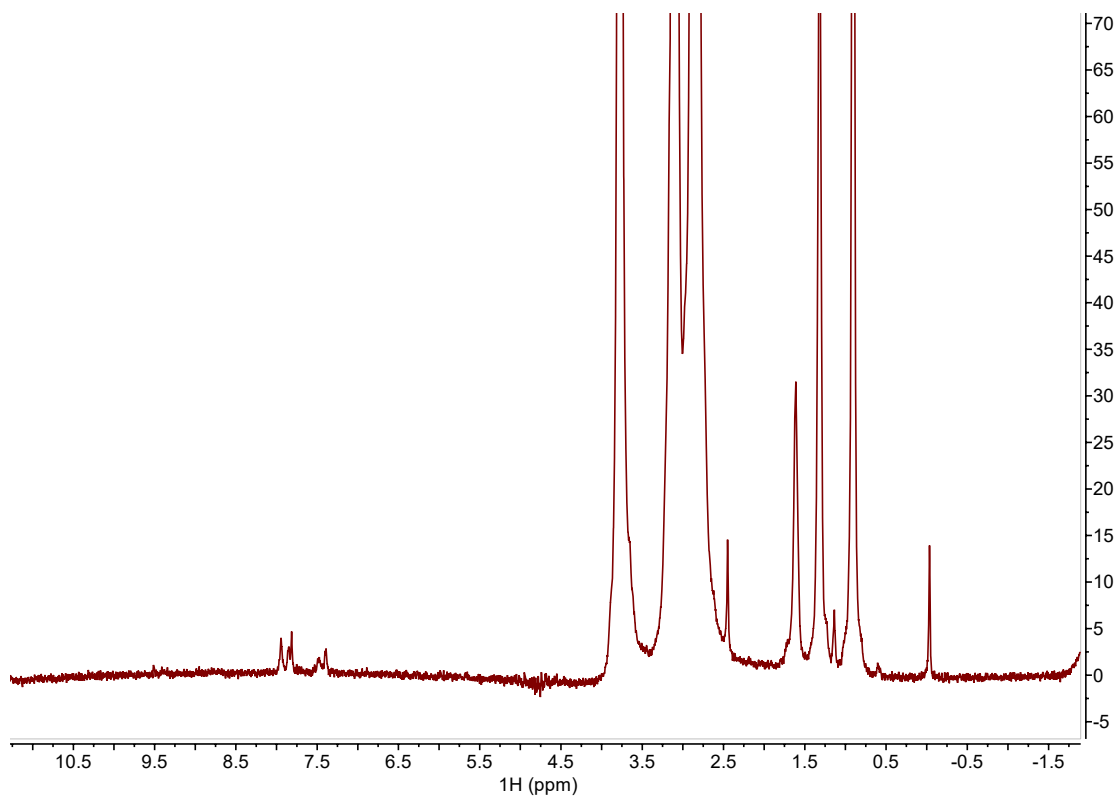


Figure S82. Proton 1D CPMG NMR spectrum of 0.4 mM C60 with the addition of 0.5 mM Mn²⁺ collected with a spin-lock time of 50 ms at 298K.

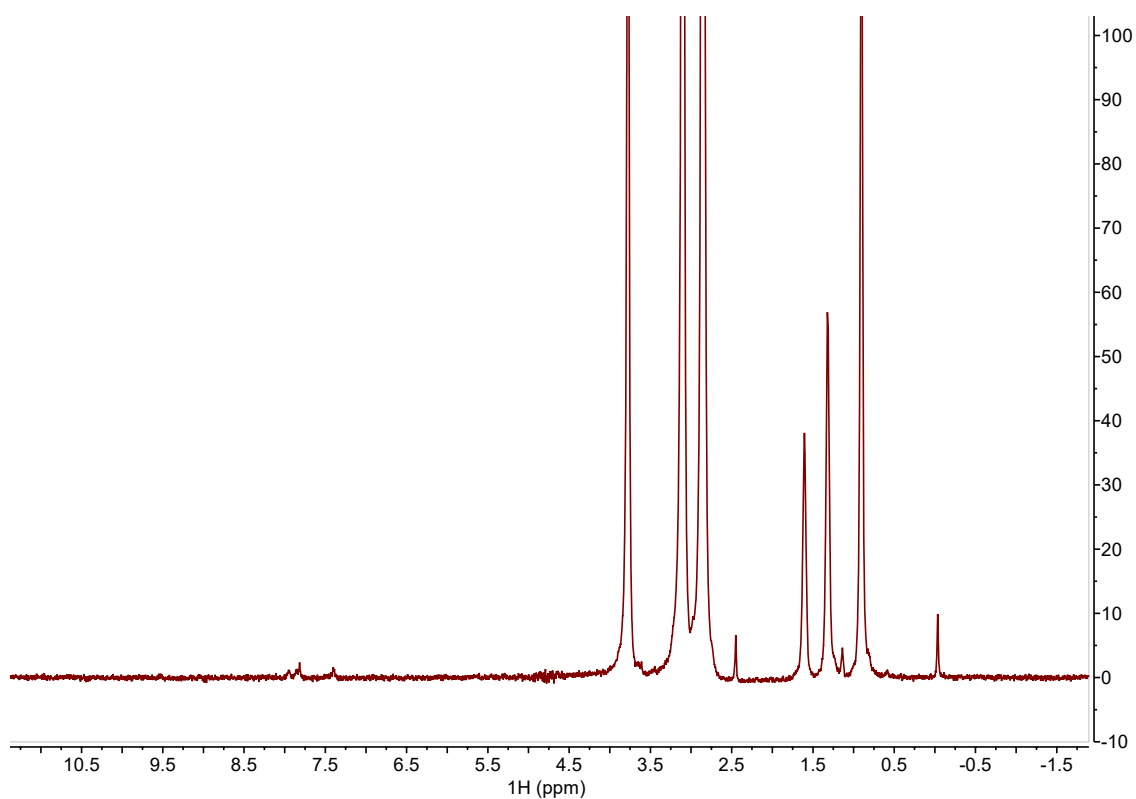


Figure S83. Proton 1D CPMG NMR spectrum of 0.4 mM C60 with the addition of 0.5 mM Mn²⁺ collected with a spin-lock time of 150 ms at 298K.

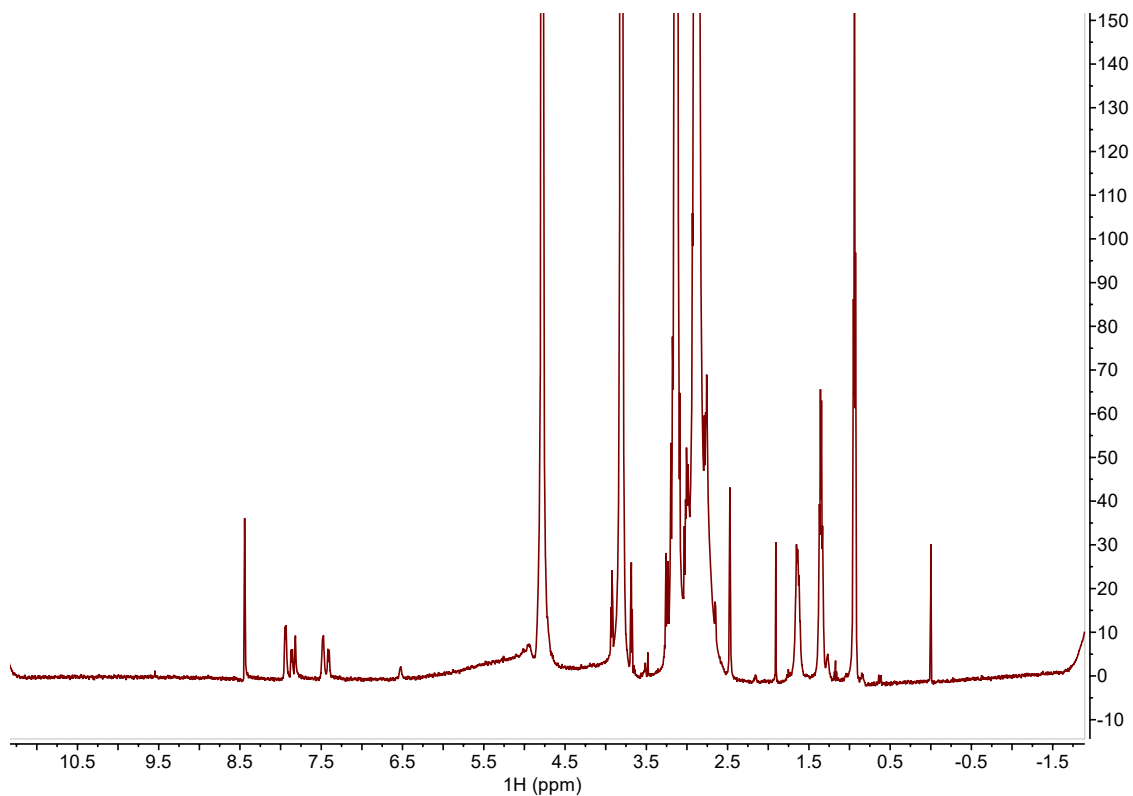


Figure S84. Proton 1D CPMG NMR spectrum of 0.2 mM C60 in the presence of *E. coli* lipid vesicles collected with a spin-lock time of 20 ms at 298K.

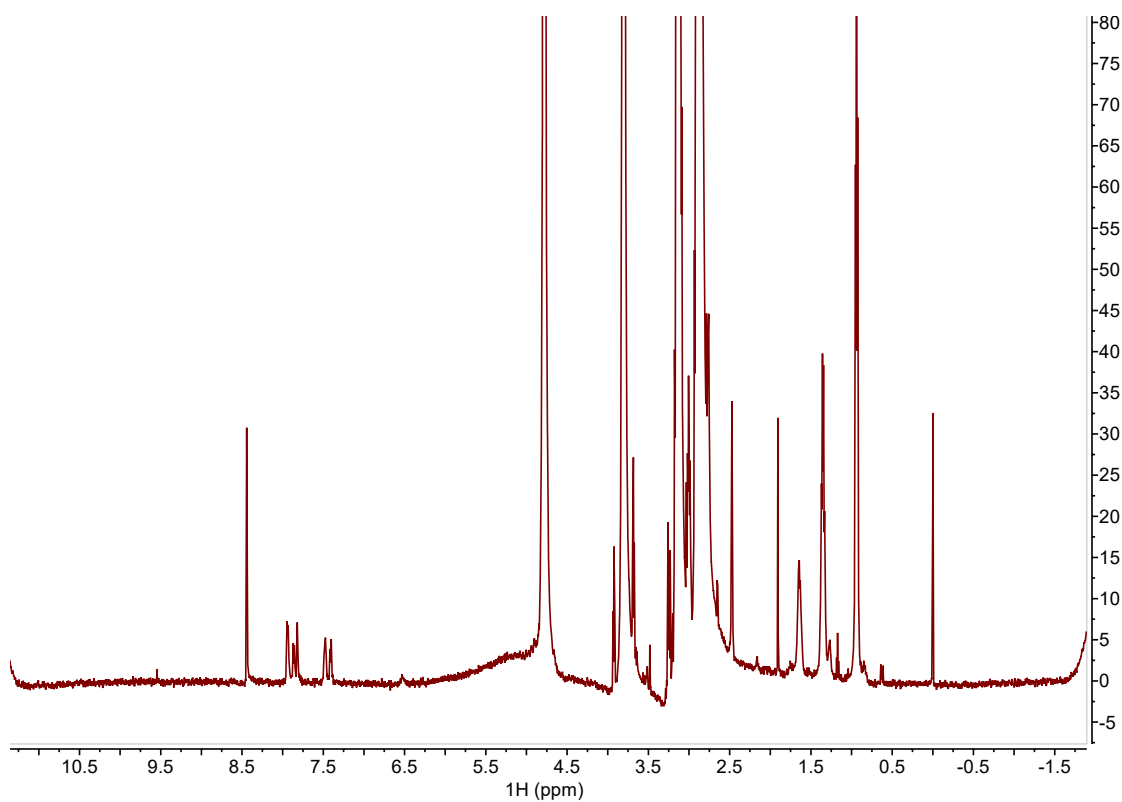


Figure S85. Proton 1D CPMG NMR spectrum of 0.2 mM C60 in the presence of *E. coli* lipid vesicles collected with a spin-lock time of 50 ms at 298K.

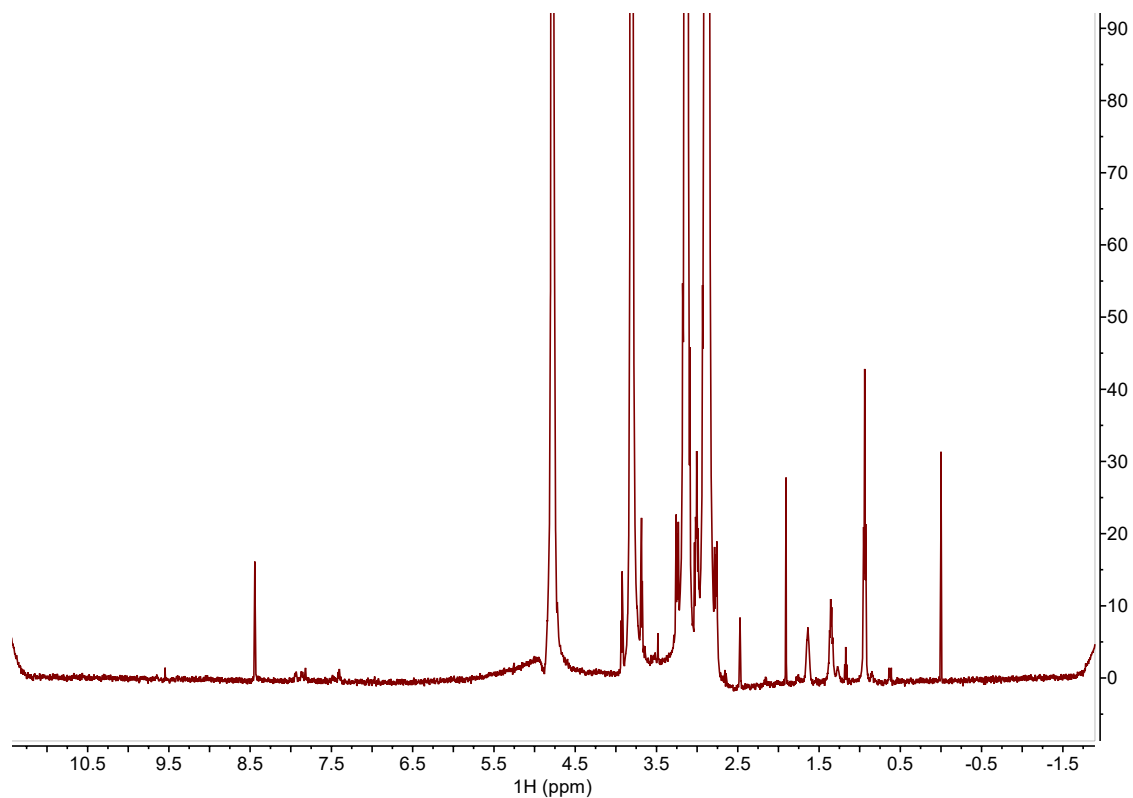


Figure S86. Proton 1D CPMG NMR spectrum of 0.2 mM C60 in the presence of *E. coli* lipid vesicles collected with a spin-lock time of 150 ms at 298K.

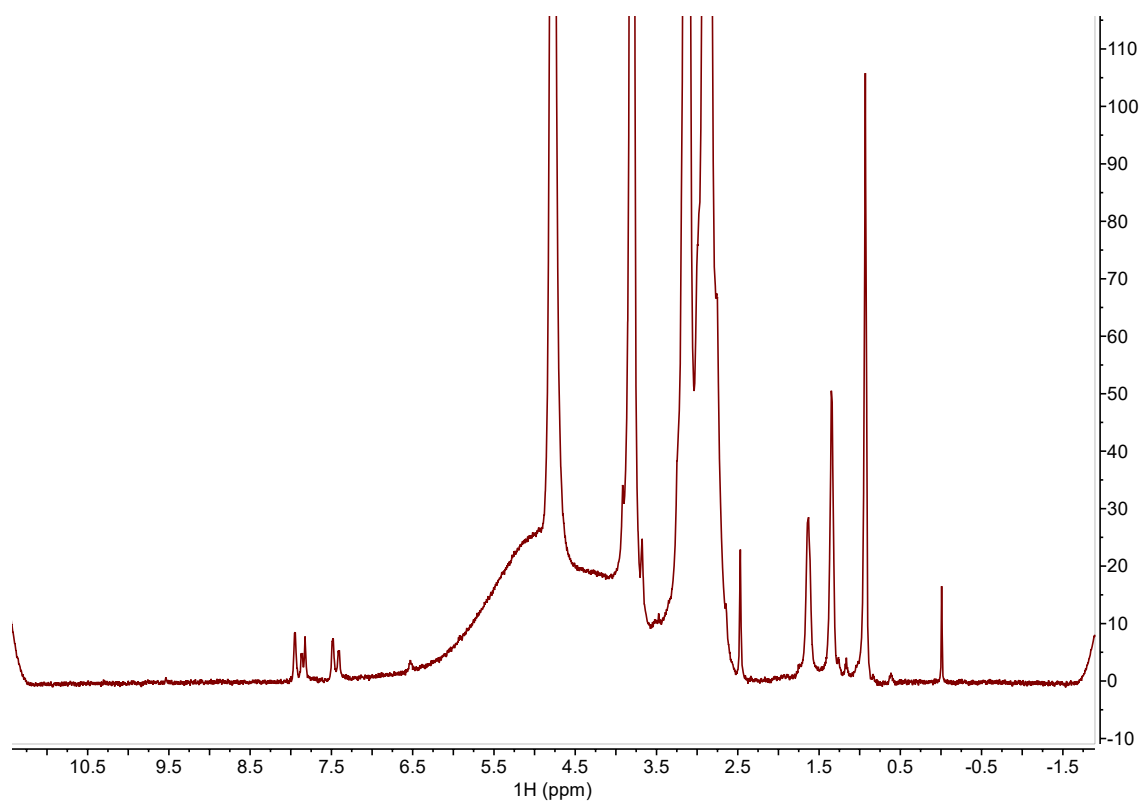


Figure S87. Proton 1D CPMG NMR spectrum of 0.2 mM C60 in the presence of *E. coli* lipid vesicles with the addition of 0.5 mM Mn^{2+} collected with a spin-lock time of 20 ms at 298K.

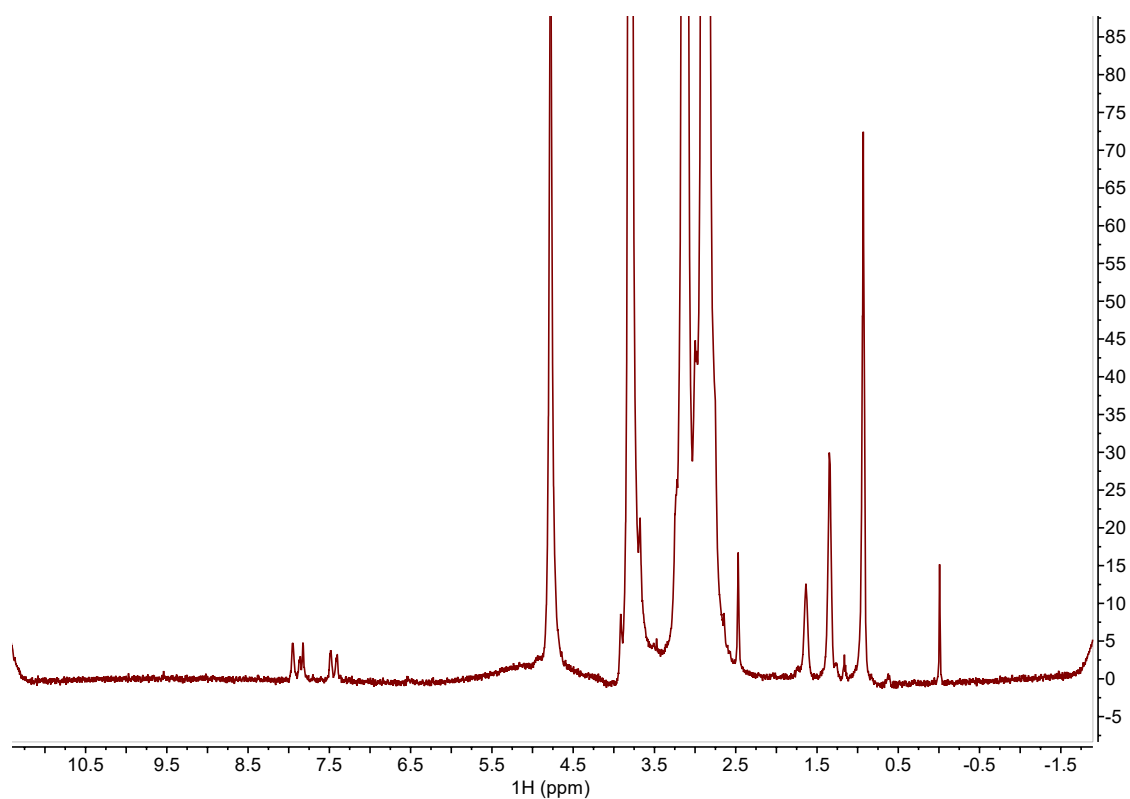


Figure S88. Proton 1D CPMG NMR spectrum of 0.2 mM C60 in the presence of *E. coli* lipid vesicles with the addition of 0.5 mM Mn^{2+} collected with a spin-lock time of 50 ms at 298K.

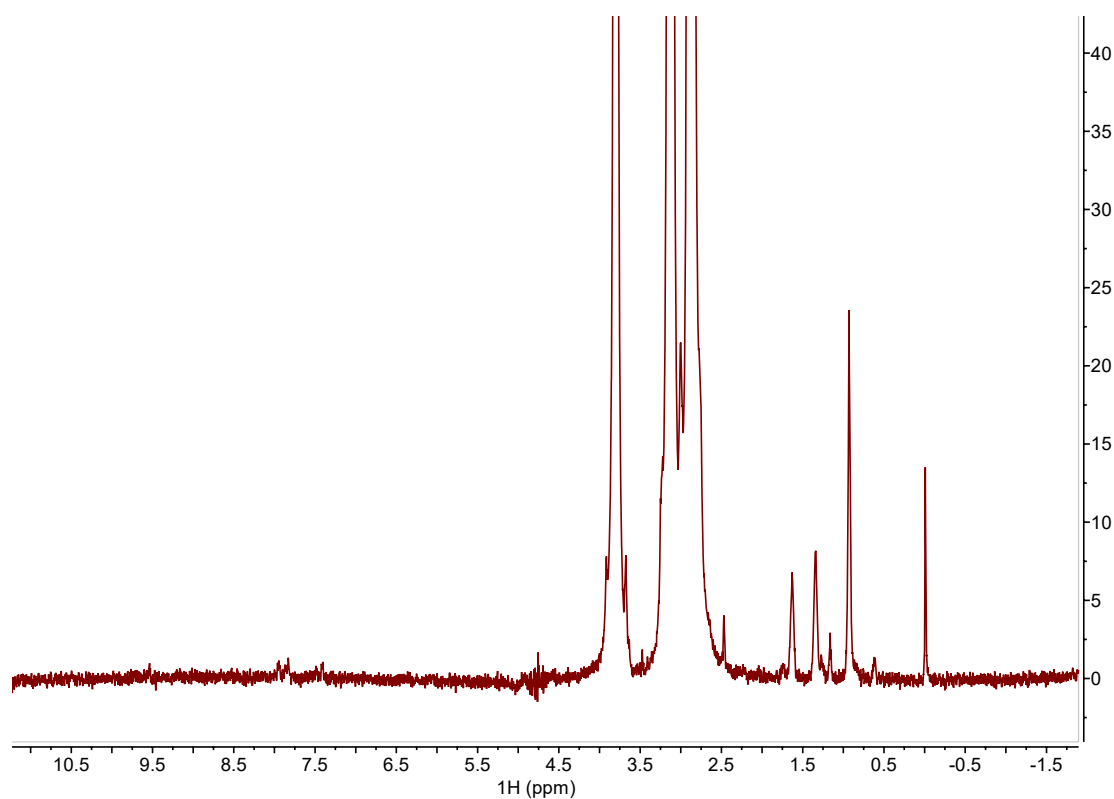


Figure S89. Proton 1D CPMG NMR spectrum of 0.2 mM C60 in the presence of *E. coli* lipid vesicles with the addition of 0.5 mM Mn^{2+} collected with a spin-lock time of 150 ms at 298K.

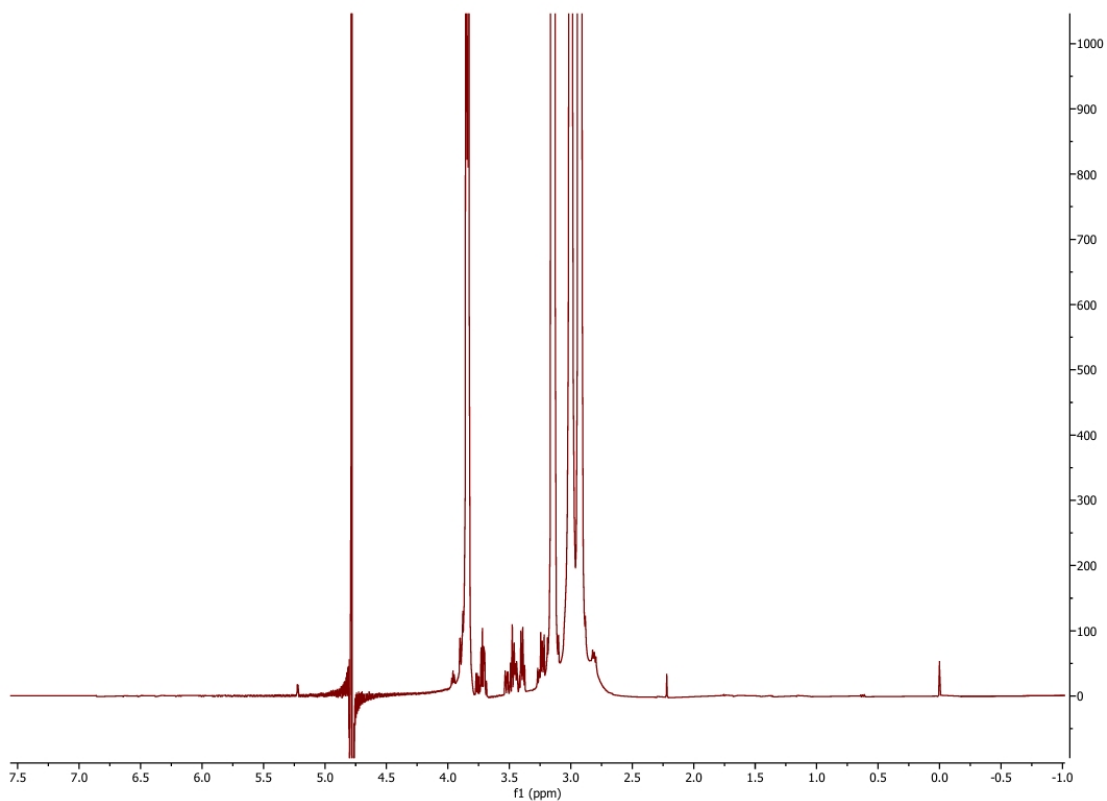


Figure S90. Proton 1D CPMG NMR spectrum of 0.5 mM Glucose collected with a spin-lock time of 20 ms at 298K.

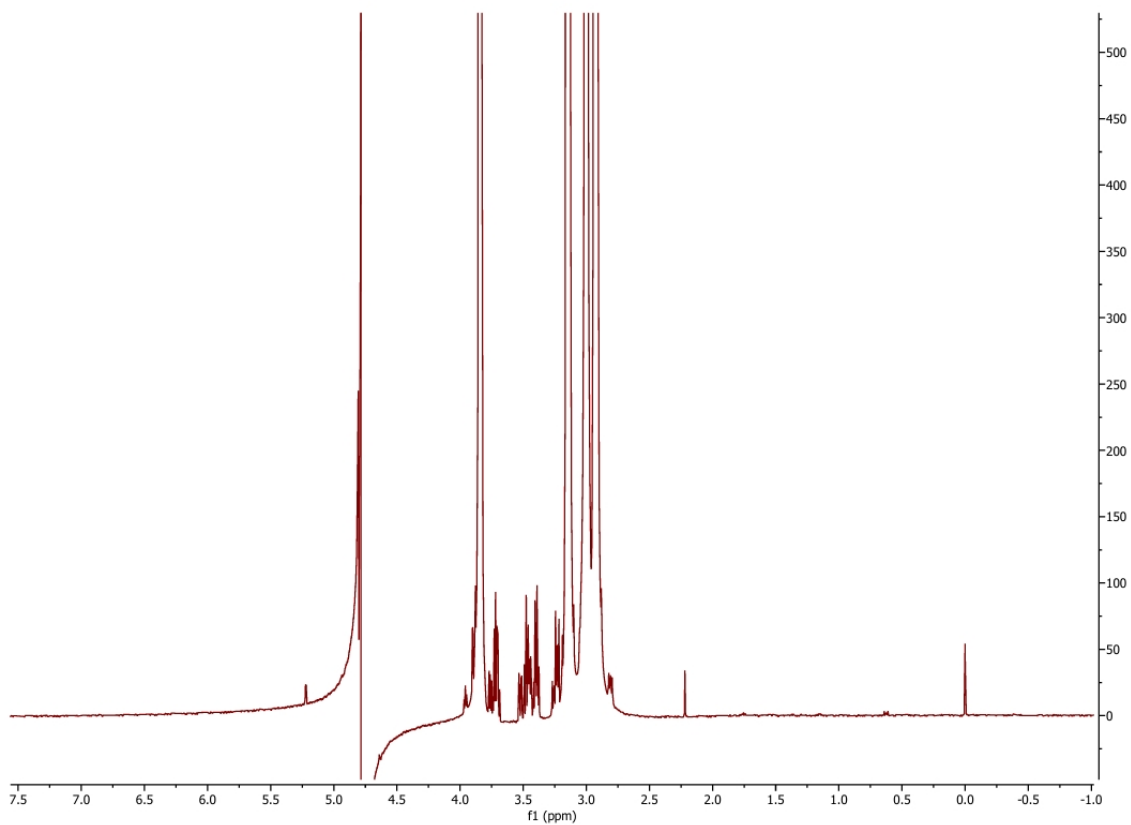


Figure S91. Proton 1D CPMG NMR spectrum of 0.5 mM Glucose collected with a spin-lock time of 50 ms at 298K.

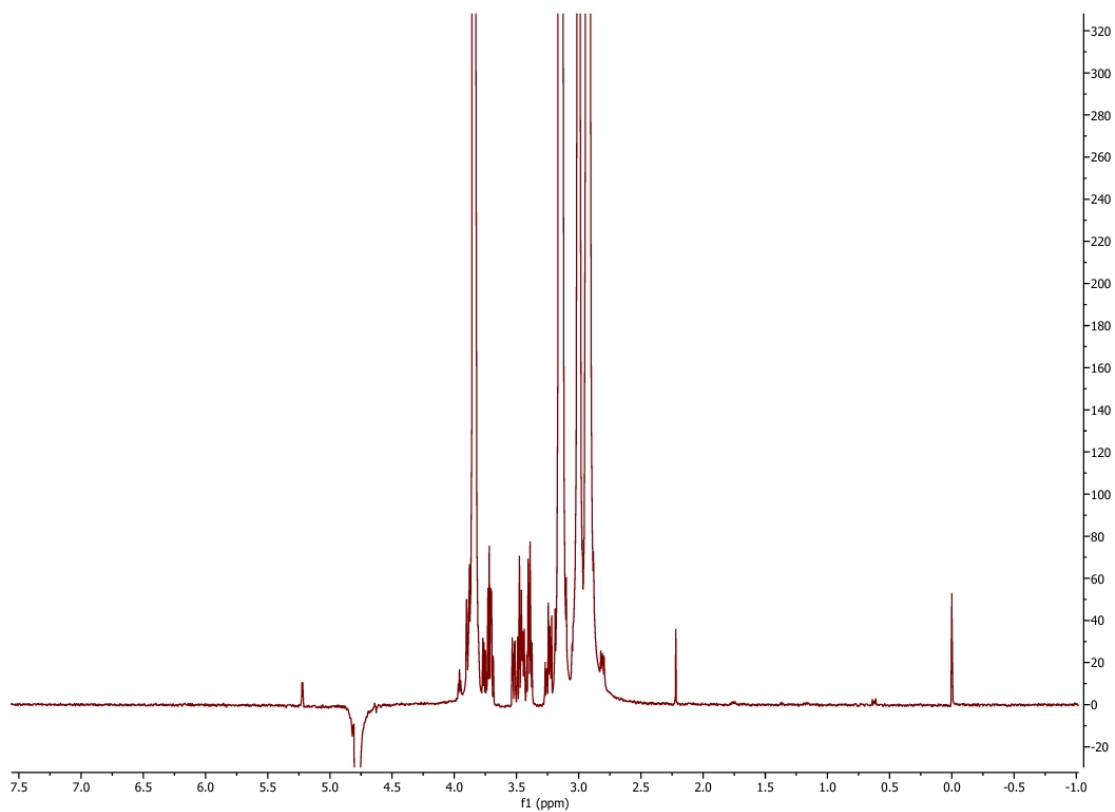


Figure S92. Proton 1D CPMG NMR spectrum of 0.5 mM Glucose collected with a spin-lock time of 150 ms at 298K.

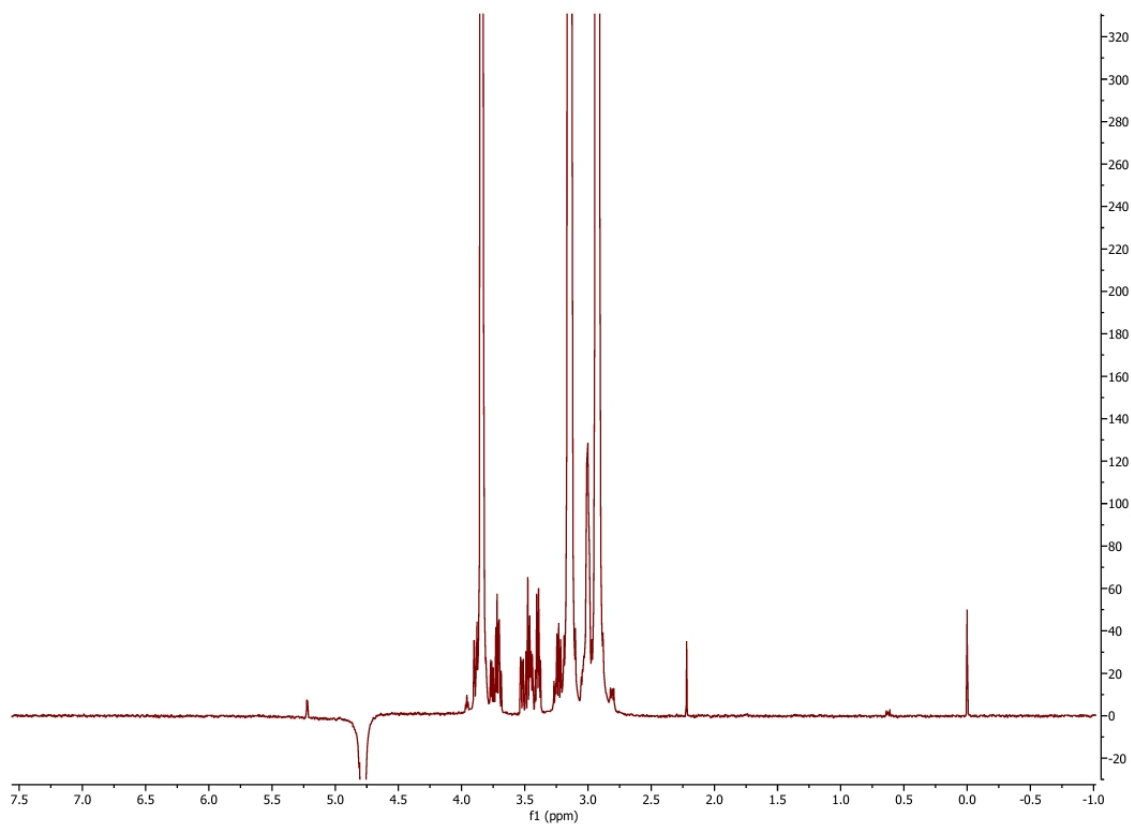


Figure S93. Proton 1D CPMG NMR spectrum of 0.5 mM Glucose collected with a spin-lock time of 300 ms at 298K.

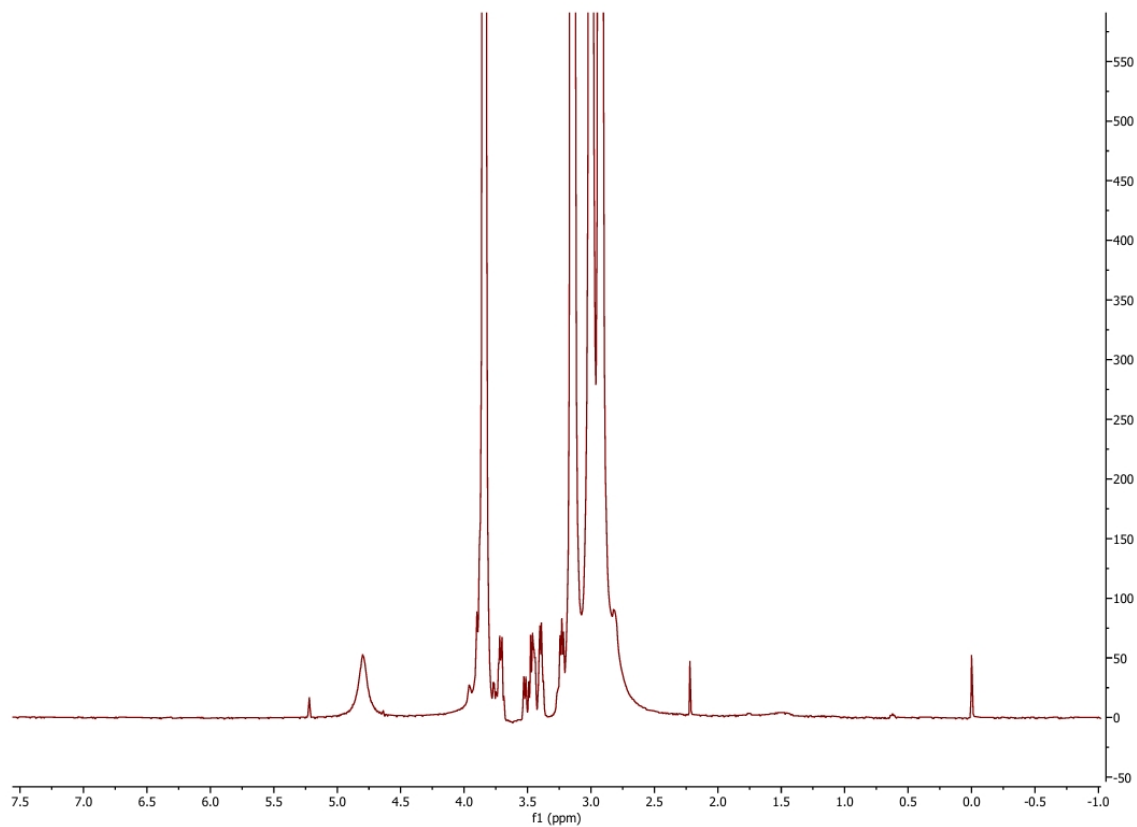


Figure S94. Proton 1D CPMG NMR spectrum of 0.5 mM Glucose with the addition of 0.5mM Mn^{2+} collected with a spin-lock time of 20 ms at 298K.

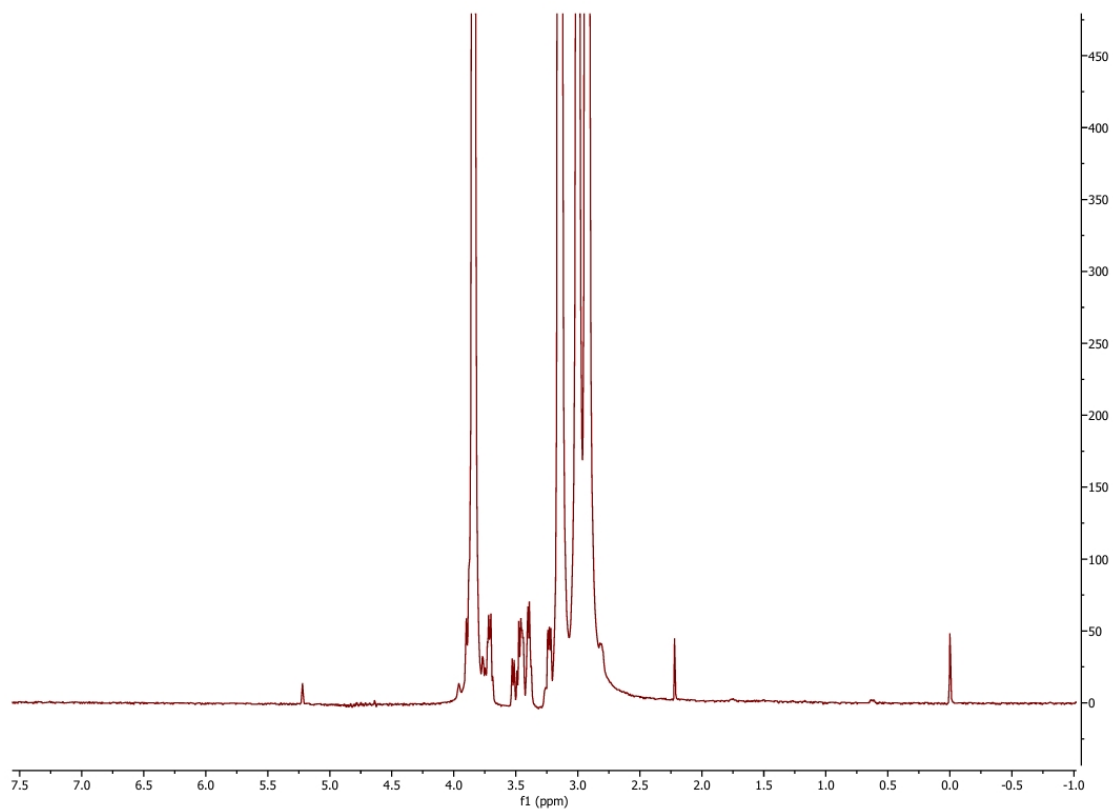


Figure S95. Proton 1D CPMG NMR spectrum of 0.5 mM Glucose with the addition of 0.5mM Mn^{2+} collected with a spin-lock time of 50 ms at 298K.

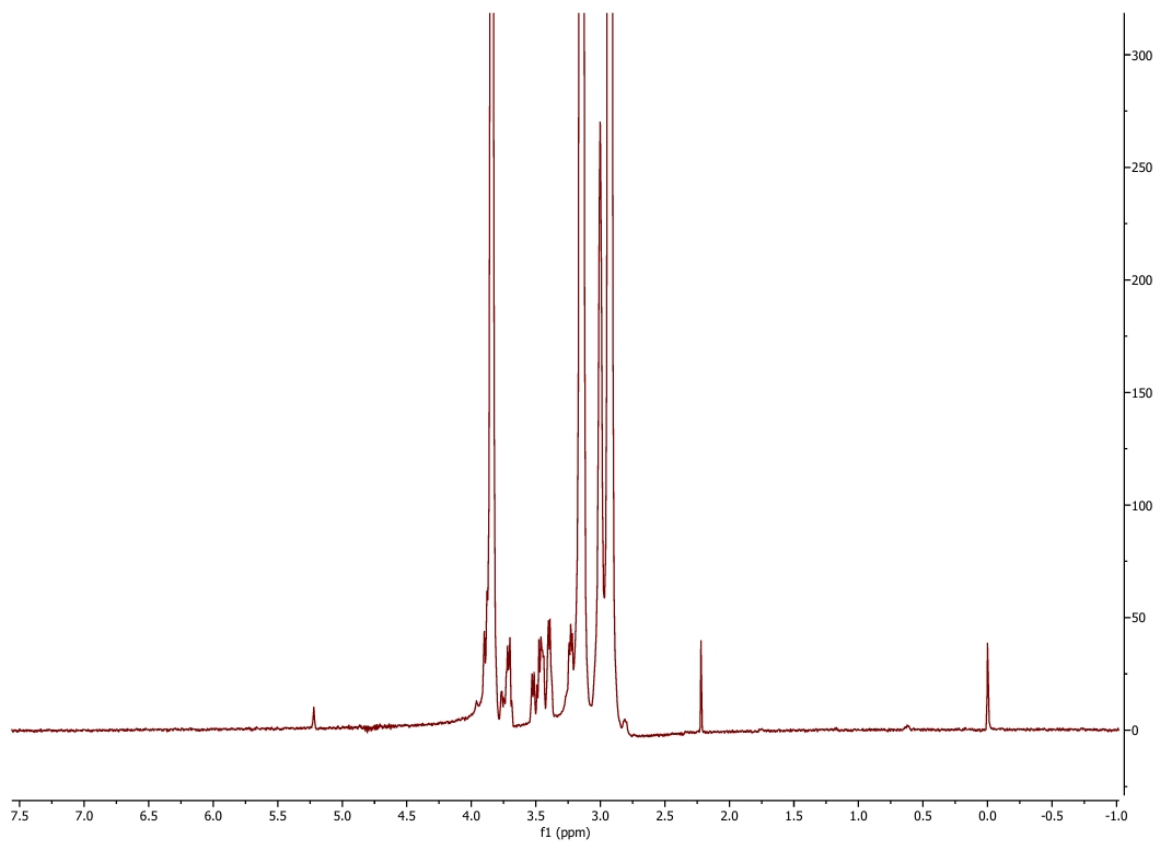


Figure S96. Proton 1D CPMG NMR spectrum of 0.5 mM Glucose with the addition of 0.5mM Mn²⁺ collected with a spin-lock time of 150 ms at 298K.

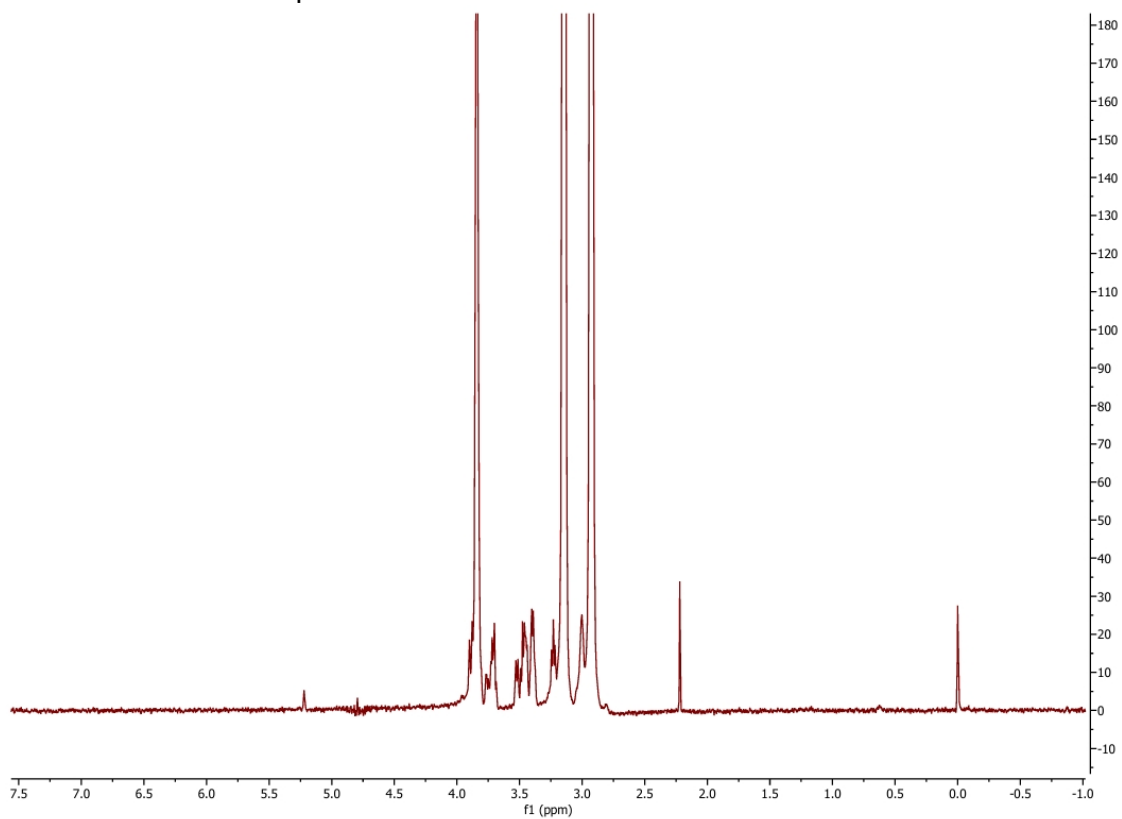


Figure S97. Proton 1D CPMG NMR spectrum of 0.5 mM Glucose with the addition of 0.5mM Mn²⁺ collected with a spin-lock time of 300 ms at 298K.

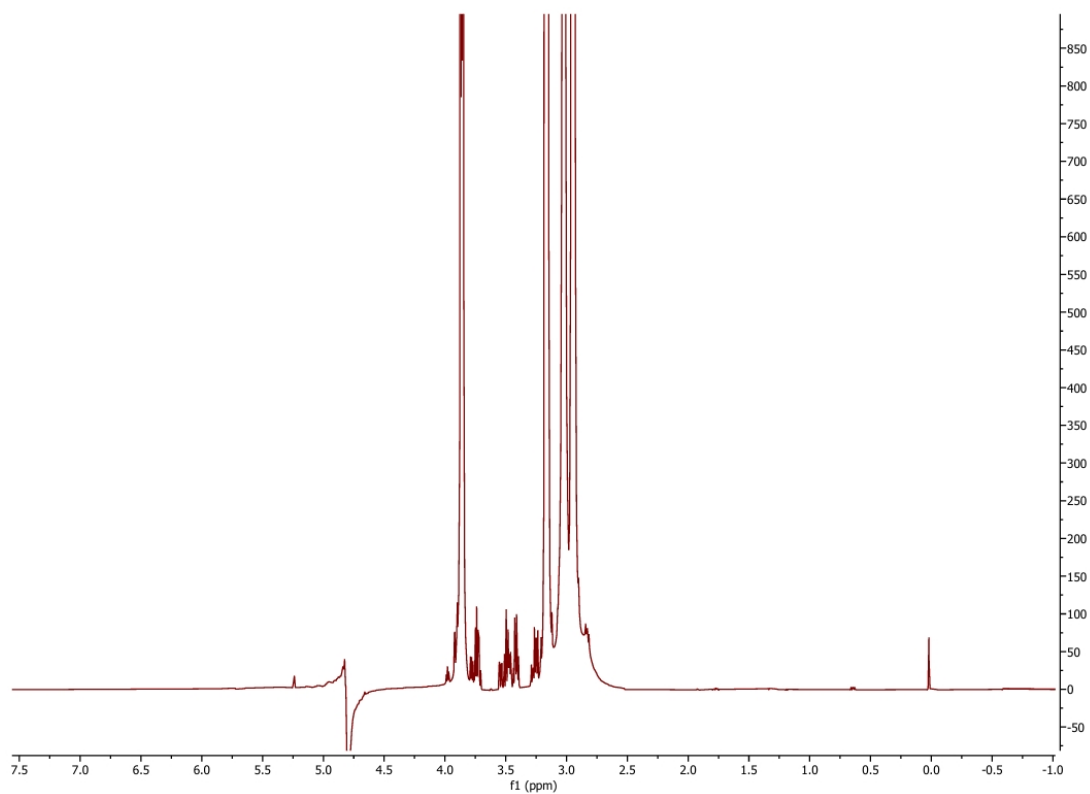


Figure S98. Proton 1D CPMG NMR spectrum of 0.5mM Glucose in the presence of *E. coli* lipid vesicles collected with a spin-lock time of 20 ms at 298K.

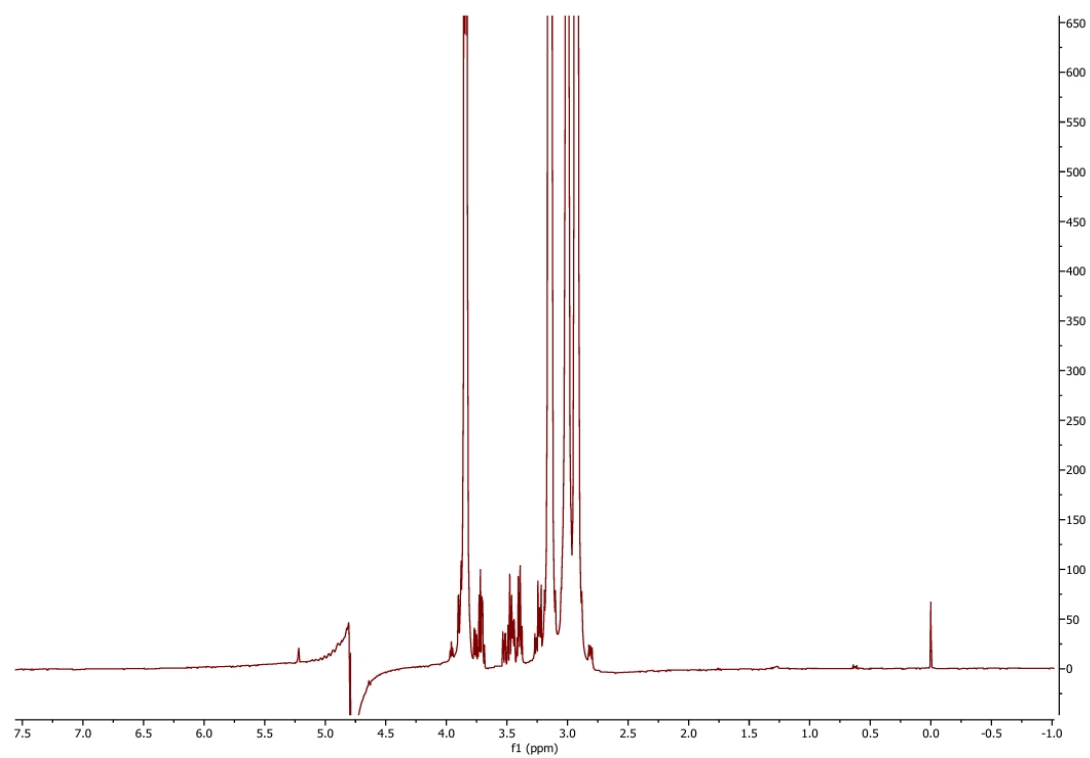


Figure S99. Proton 1D CPMG NMR spectrum of 0.5 mM Glucose in the presence of *E. coli* lipid vesicles collected with a spin-lock time of 50 ms at 298K.

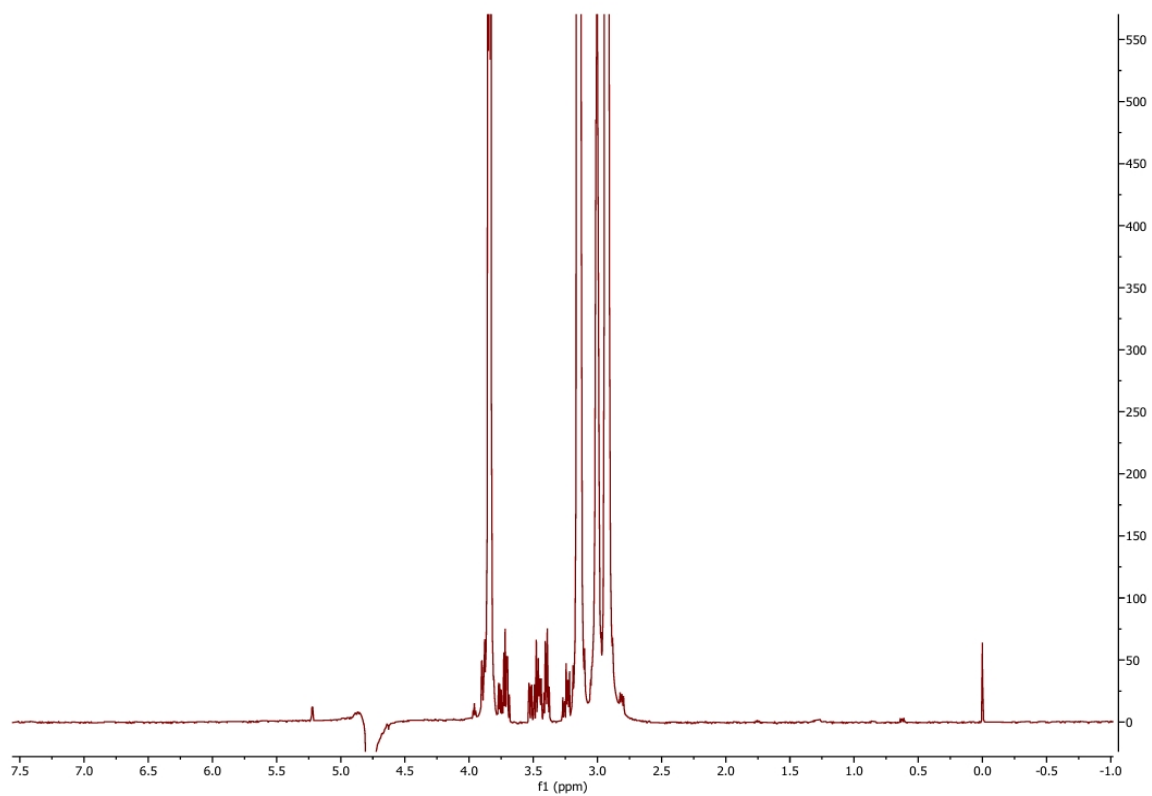


Figure S100. Proton 1D CPMG NMR spectrum of 0.5 mM Glucose in the presence of *E. coli* lipid vesicles collected with a spin-lock time of 150 ms at 298K.

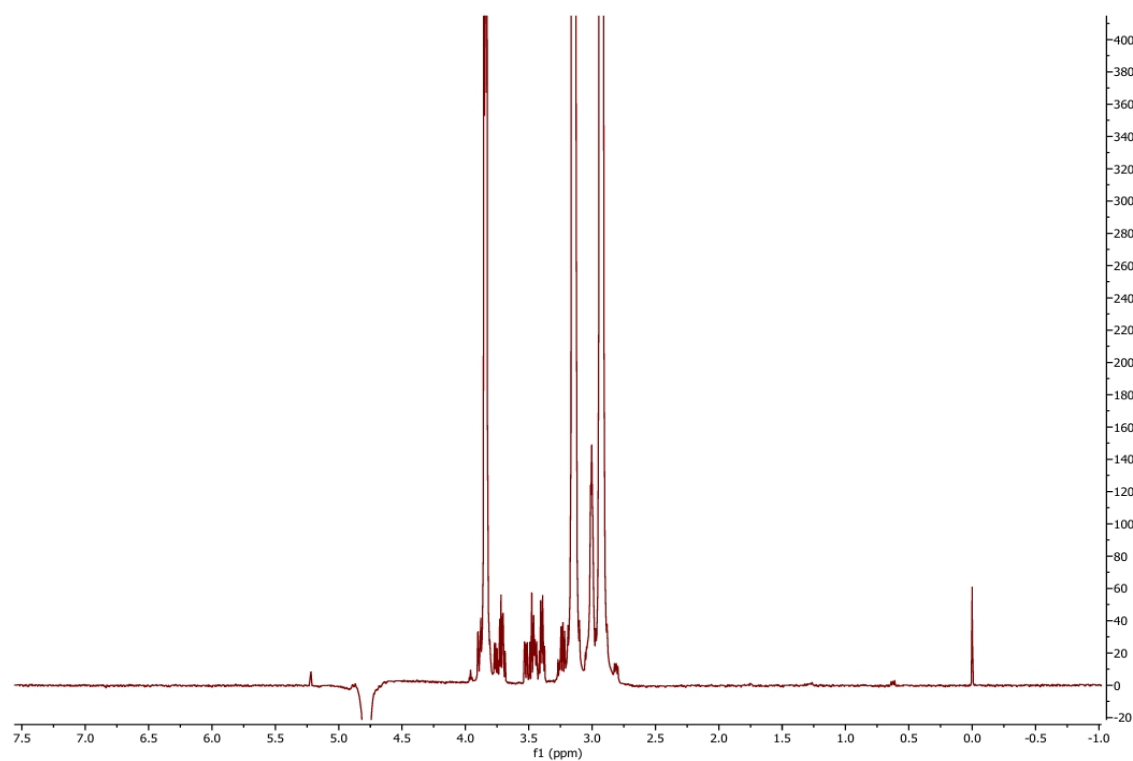


Figure S101. Proton 1D CPMG NMR spectrum of 0.5 mM Glucose in the presence of *E. coli* lipid vesicles collected with a spin-lock time of 300 ms at 298K.

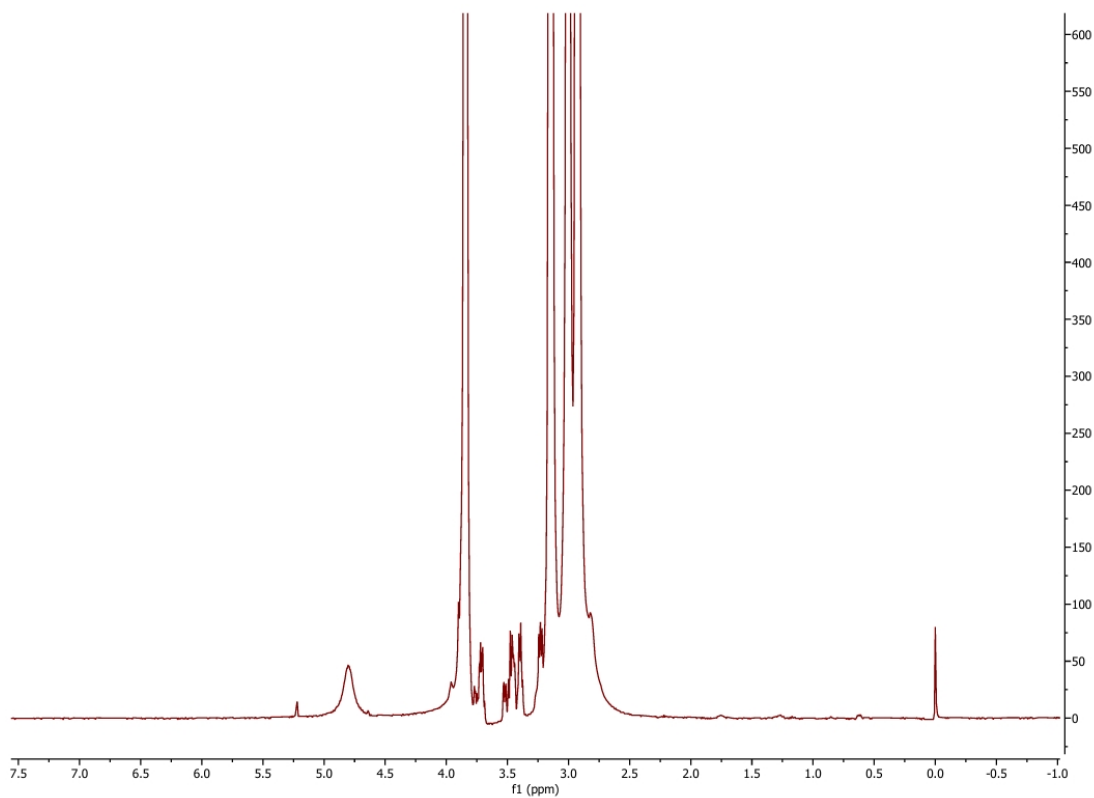


Figure S102. Proton 1D CPMG NMR spectrum of 0.5 mM Glucose in the presence of *E. coli* lipid vesicles with the addition of 0.5mM Mn^{2+} collected with a spin-lock time of 20 ms at 298K.

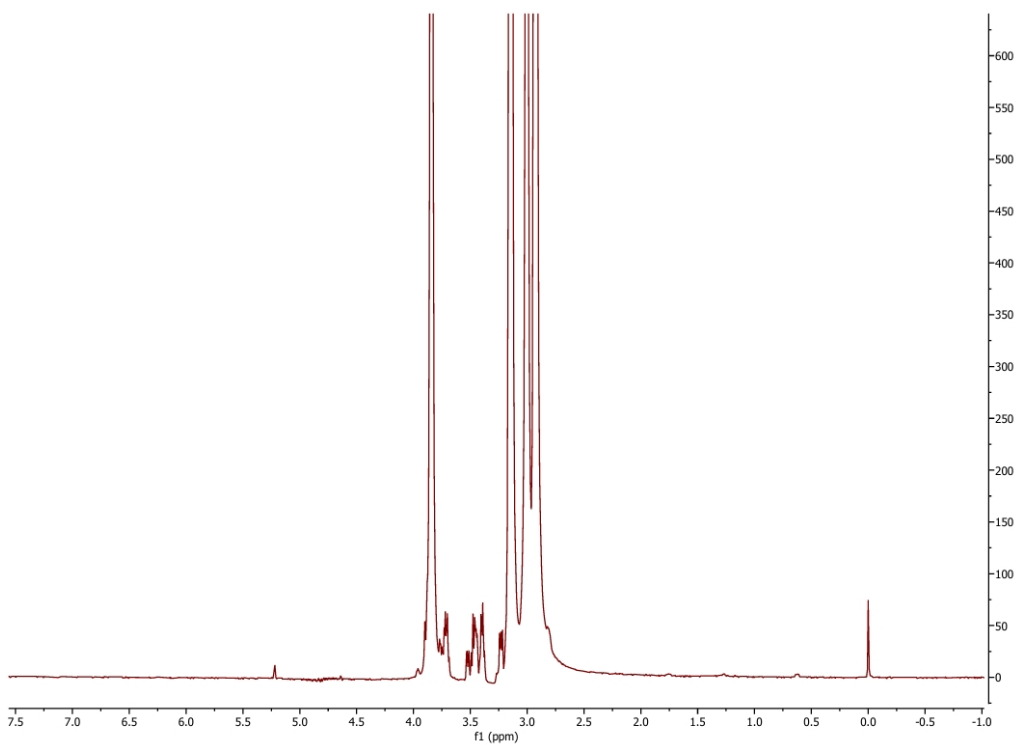


Figure S103. Proton 1D CPMG NMR spectrum of 0.5 mM Glucose in the presence of *E. coli* lipid vesicles with the addition of 0.5 mM Mn^{2+} collected with a spin-lock time of 50 ms at 298K.

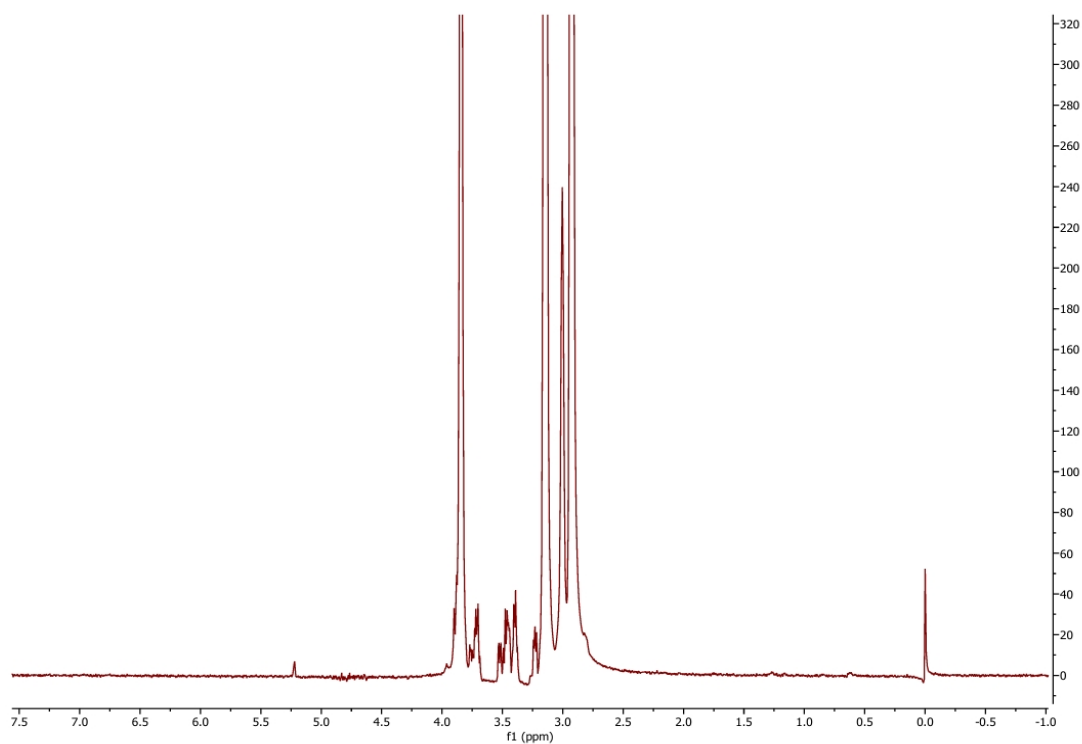


Figure S104. Proton 1D CPMG NMR spectrum of 0.5 mM Glucose in the presence of *E. coli* lipid vesicles with the addition of 0.5 mM Mn^{2+} collected with a spin-lock time of 150 ms at 298K.

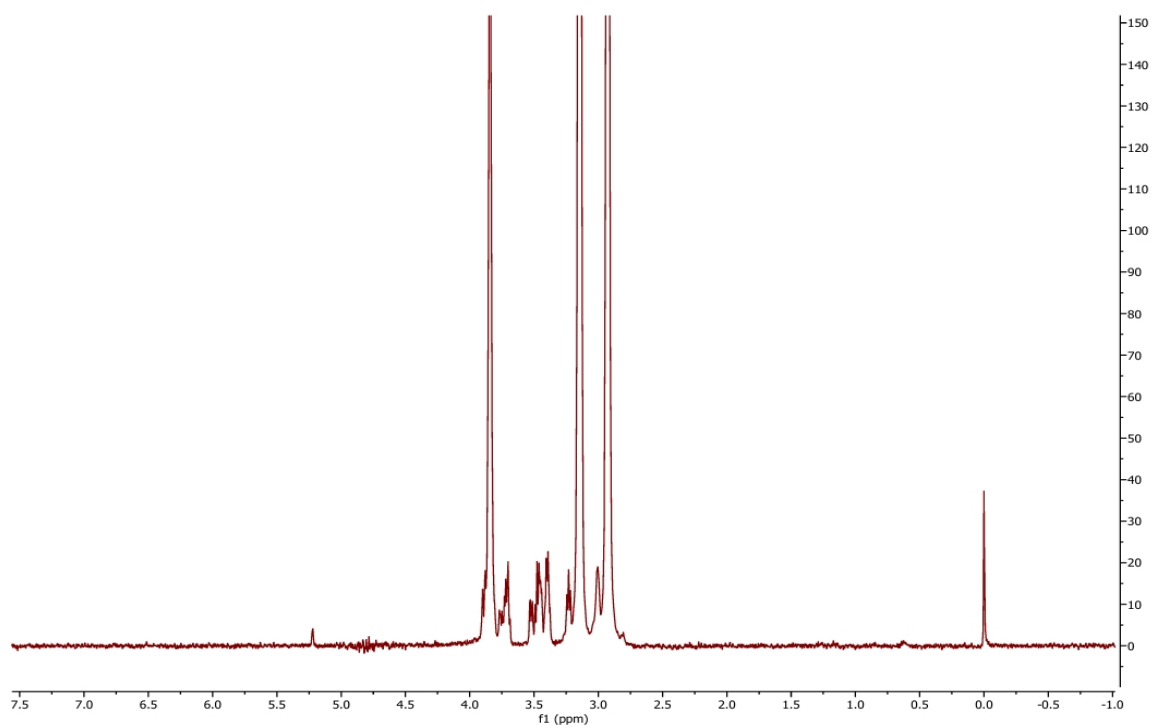


Figure S105. Proton 1D CPMG NMR spectrum of 0.5 mM Glucose in the presence of *E. coli* lipid vesicles with the addition of 0.5 mM Mn^{2+} collected with a spin-lock time of 300 ms at 298K.

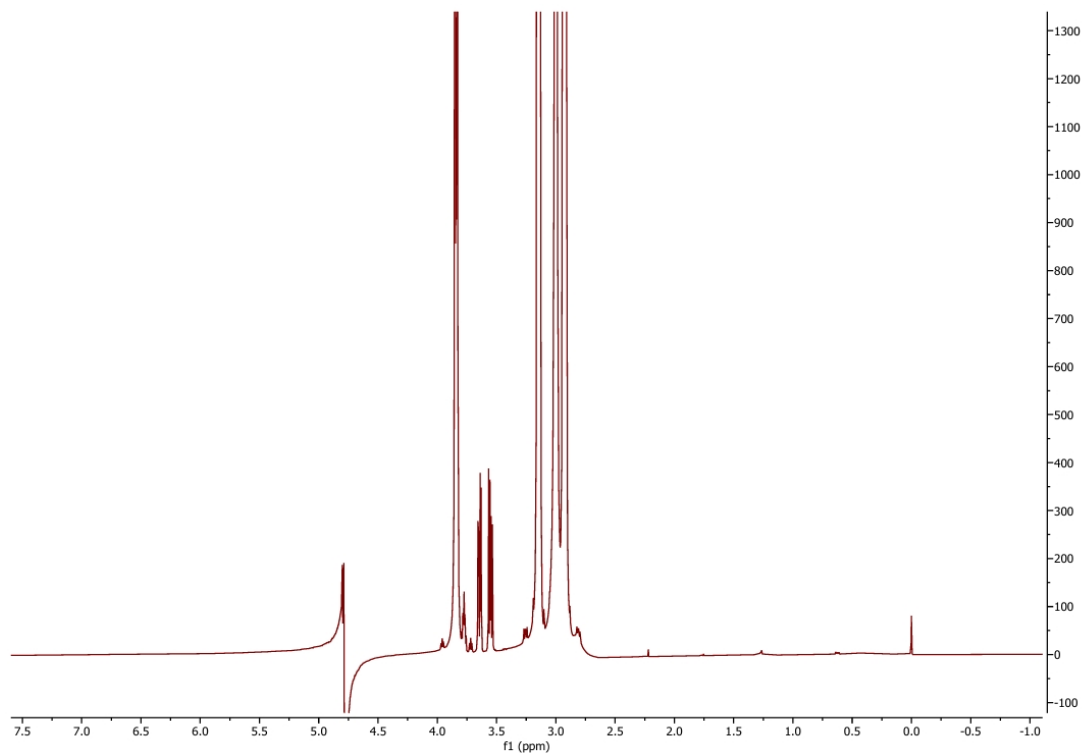


Figure S106. Proton 1D CPMG NMR spectrum of 0.5 mM Glycerol collected with a spin-lock time of 20 ms at 298K.

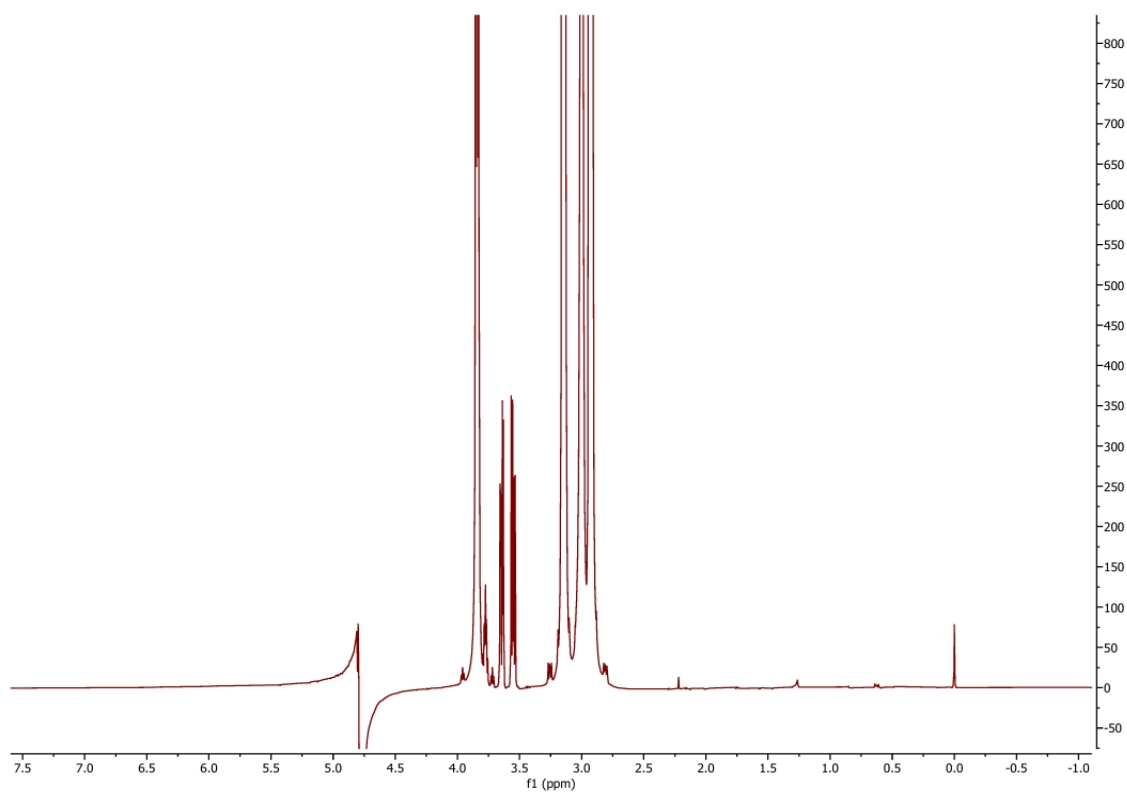


Figure S107. Proton 1D CPMG NMR spectrum of 0.5 mM Glycerol collected with a spin-lock time of 50 ms at 298K.

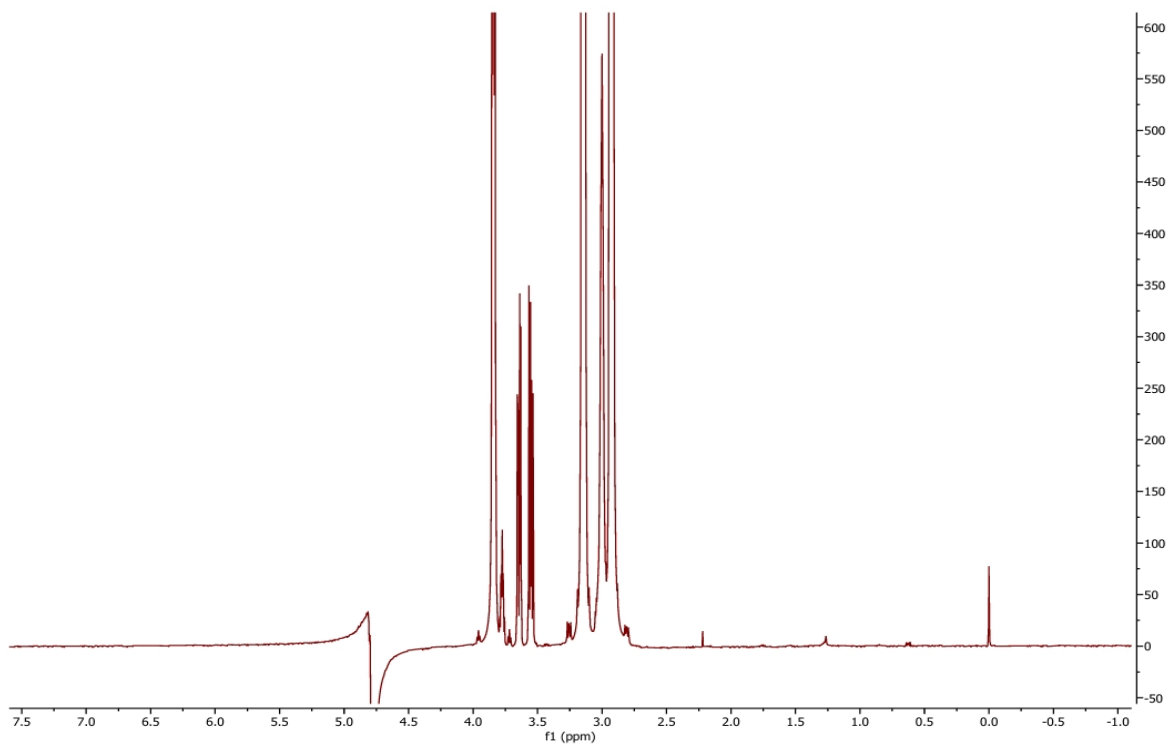


Figure S108. Proton 1D CPMG NMR spectrum of 0.5 mM Glycerol collected with a spin-lock time of 150 ms at 298K.

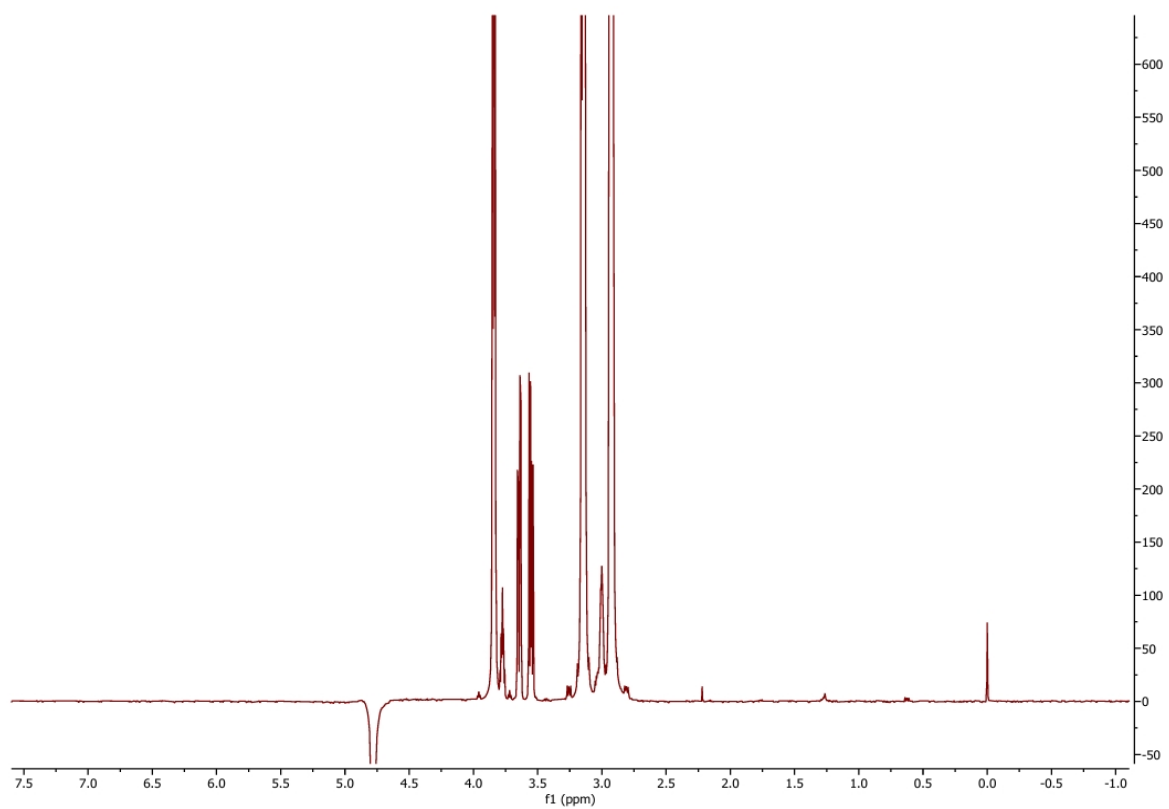


Figure S109. Proton 1D CPMG NMR spectrum of 0.5 mM Glycerol collected with a spin-lock time of 300 ms at 298K.

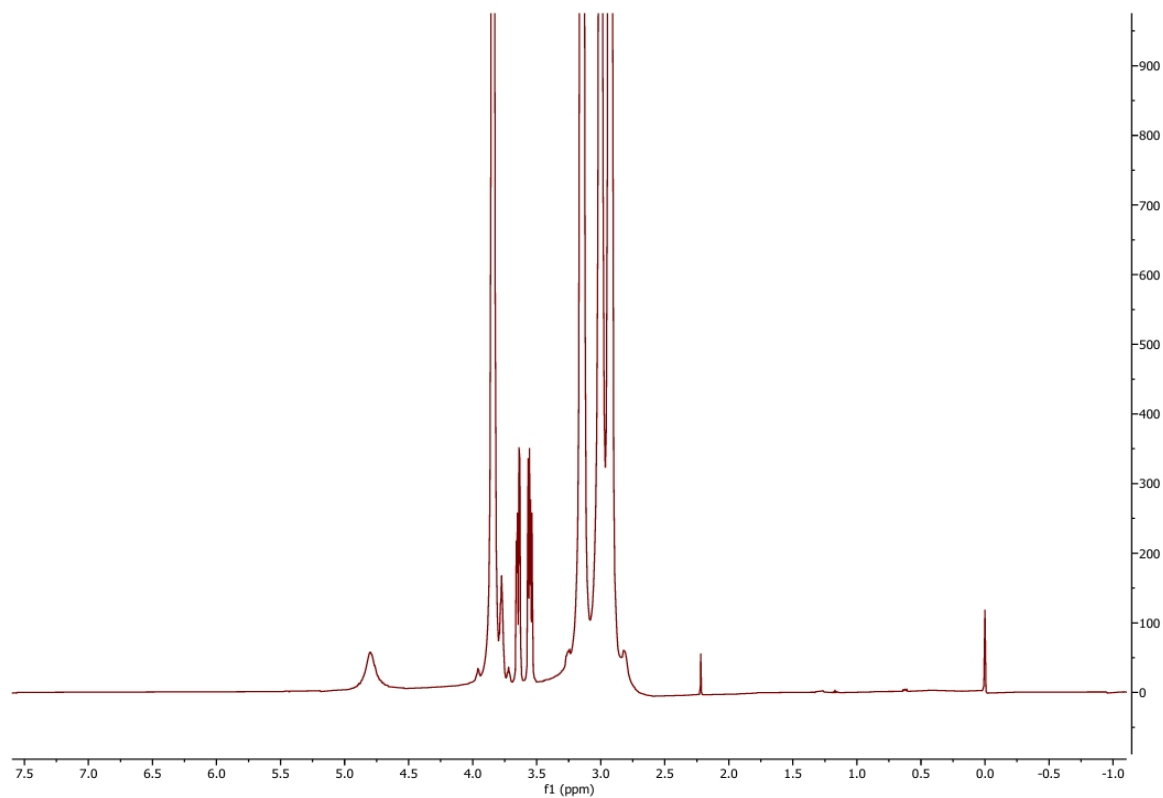


Figure S110. Proton 1D CPMG NMR spectrum of 0.5 mM Glycerol with the addition of 0.5 mM Mn^{2+} collected with a spin-lock time of 20 ms at 298K.

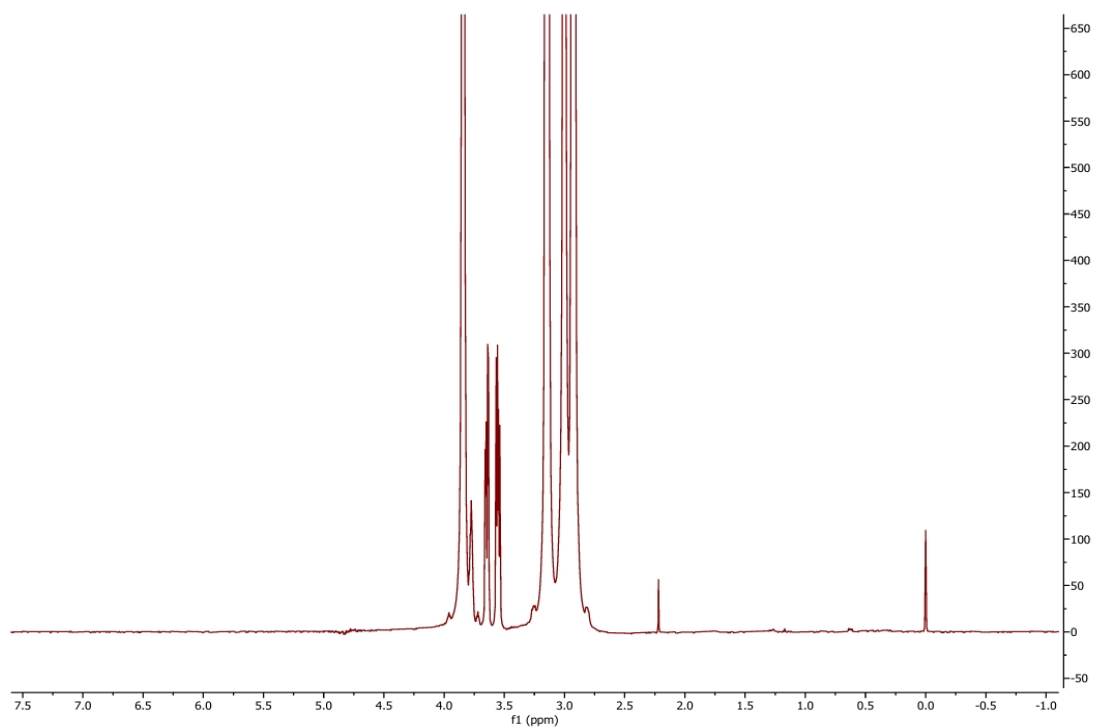


Figure S111. Proton 1D CPMG NMR spectrum of 0.5 mM Glycerol with the addition of 0.5 mM Mn^{2+} collected with a spin-lock time of 50 ms at 298K.

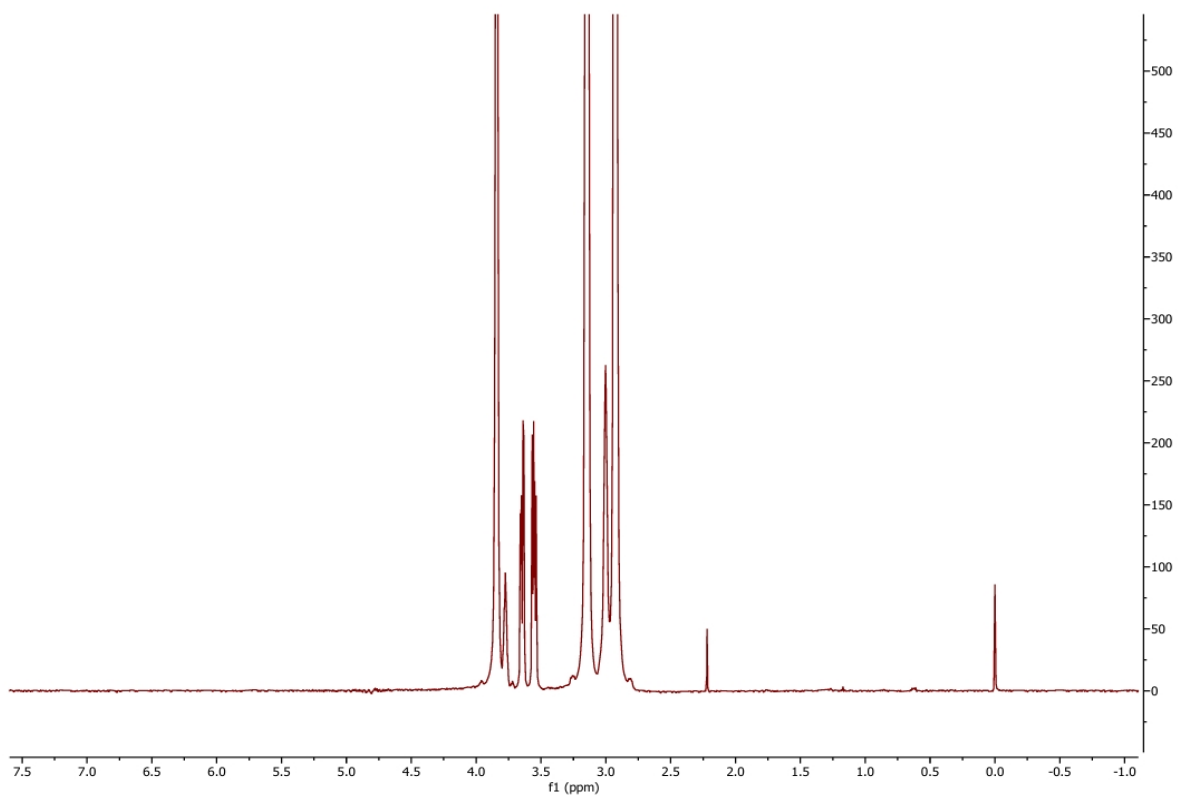


Figure S112. Proton 1D CPMG NMR spectrum of 0.5 mM Glycerol with the addition of 0.5 mM Mn^{2+} collected with a spin-lock time of 150 ms at 298K.

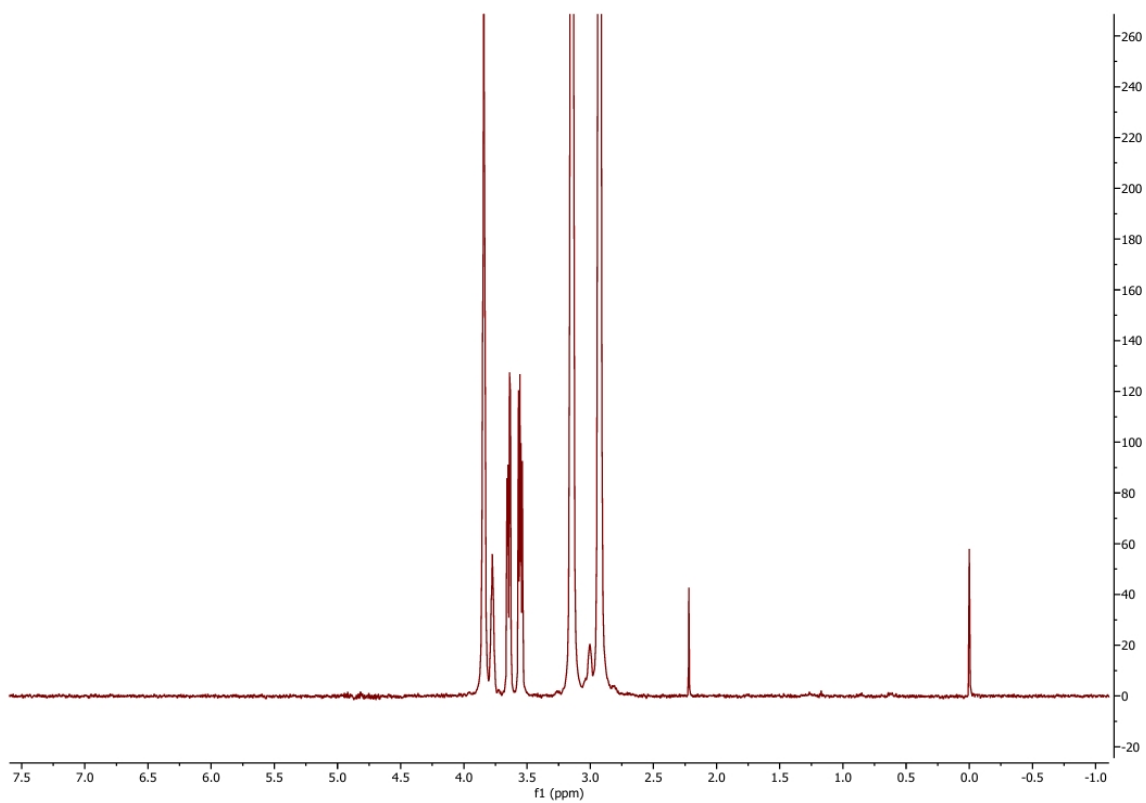


Figure S113. Proton 1D CPMG NMR spectrum of 0.5 mM Glycerol with the addition of 0.5 mM Mn^{2+} collected with a spin-lock time of 300 ms at 298K.

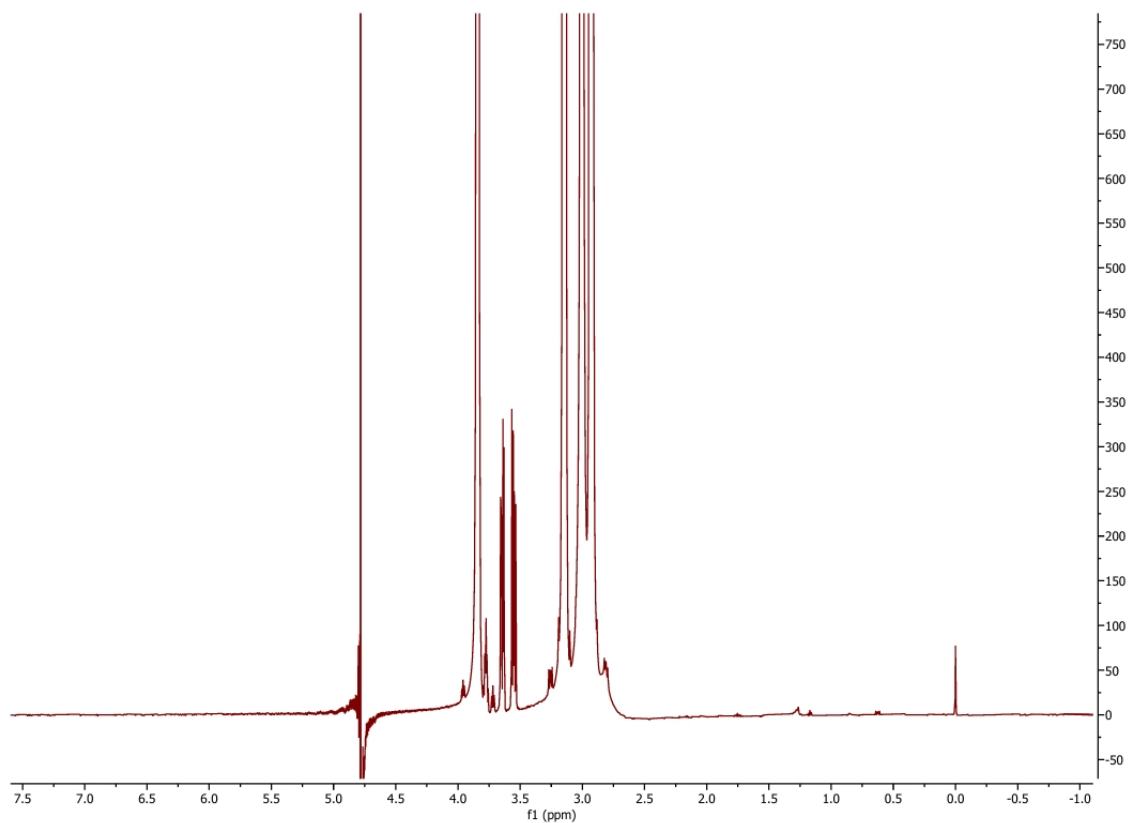


Figure S114. Proton 1D CPMG NMR spectrum of 0.5 mM Glycerol in the presence of *E. coli* lipid vesicles collected with a spin-lock time of 20 ms at 298K.

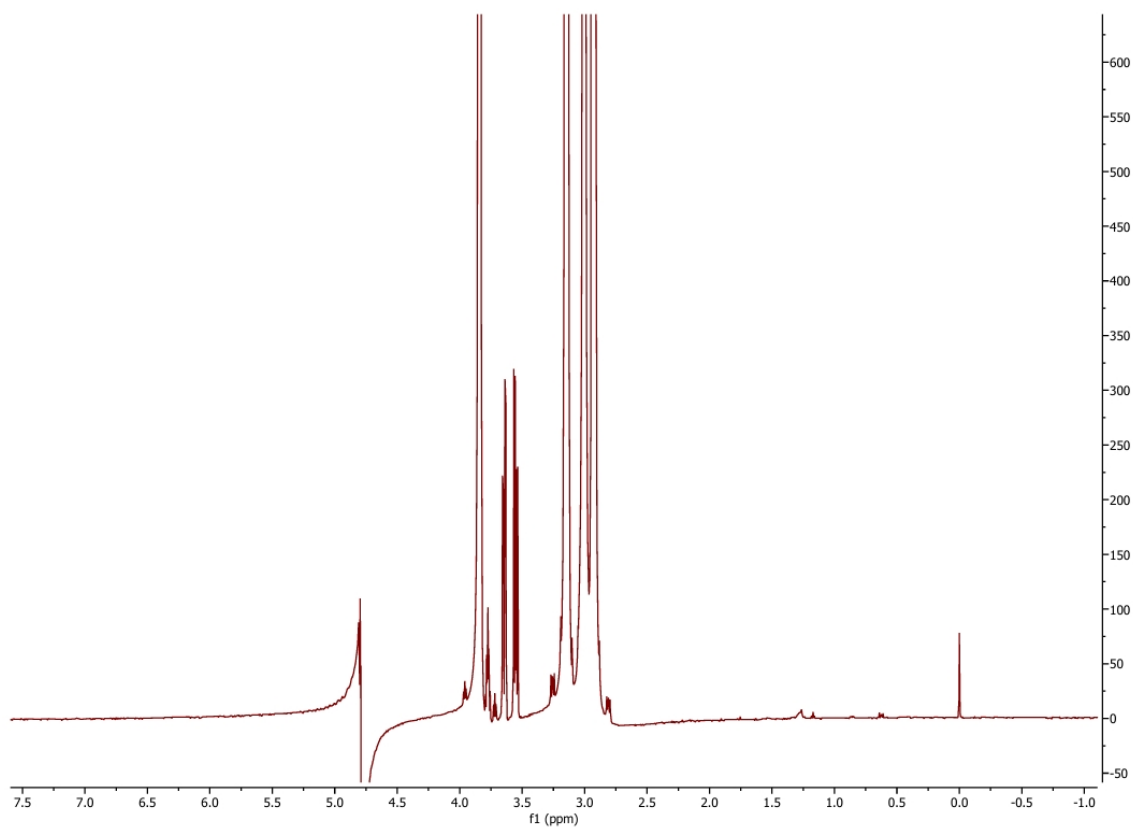


Figure S115. Proton 1D CPMG NMR spectrum of 0.5 mM Glycerol in the presence of *E. coli* lipid vesicles collected with a spin-lock time of 50 ms at 298K.

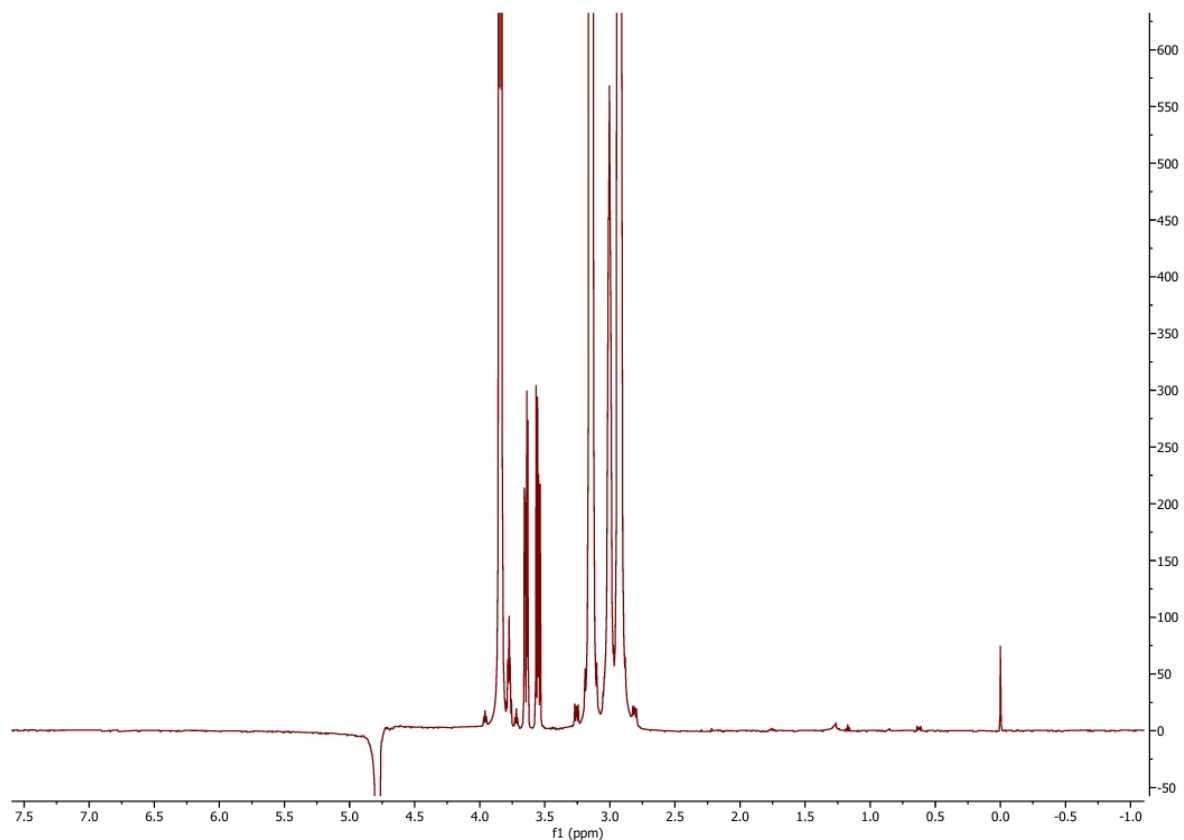


Figure S116. Proton 1D CPMG NMR spectrum of 0.5 mM Glycerol in the presence of *E. coli* lipid vesicles collected with a spin-lock time of 150 ms at 298K.

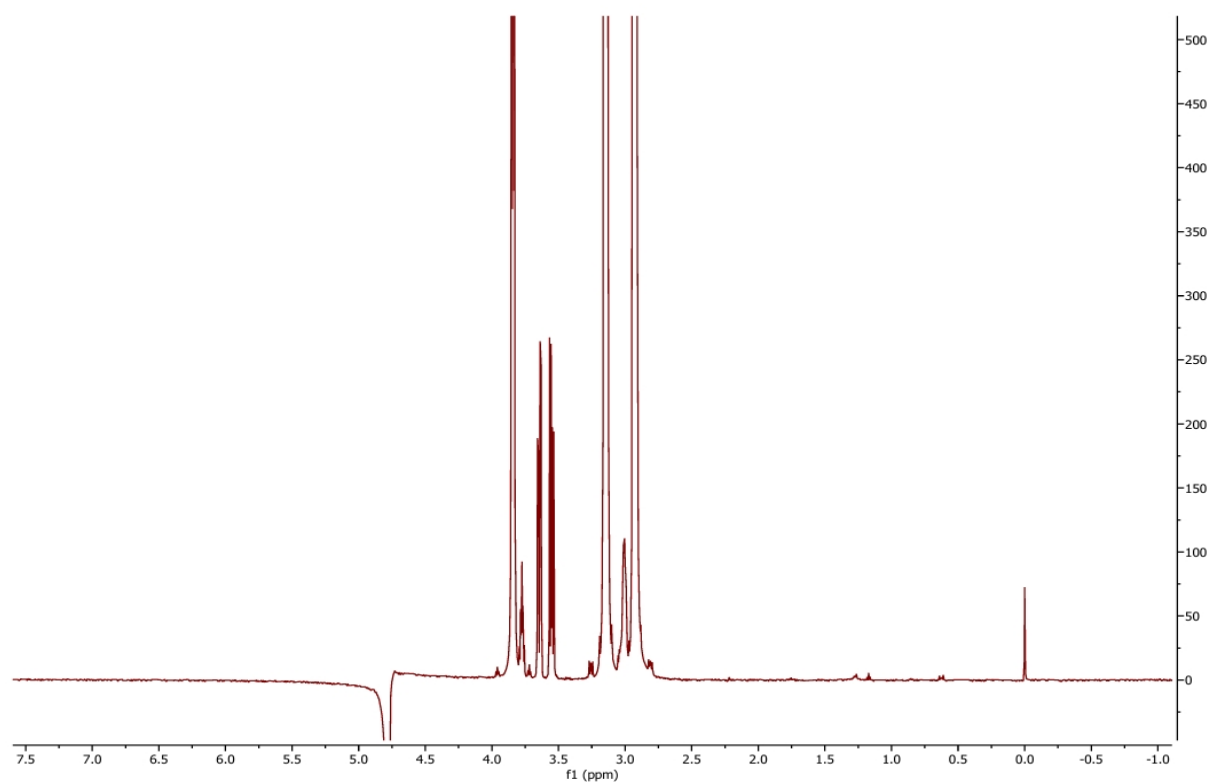


Figure S117. Proton 1D CPMG NMR spectrum of 0.5 mM Glycerol in the presence of *E. coli* lipid vesicles collected with a spin-lock time of 300 ms at 298K.

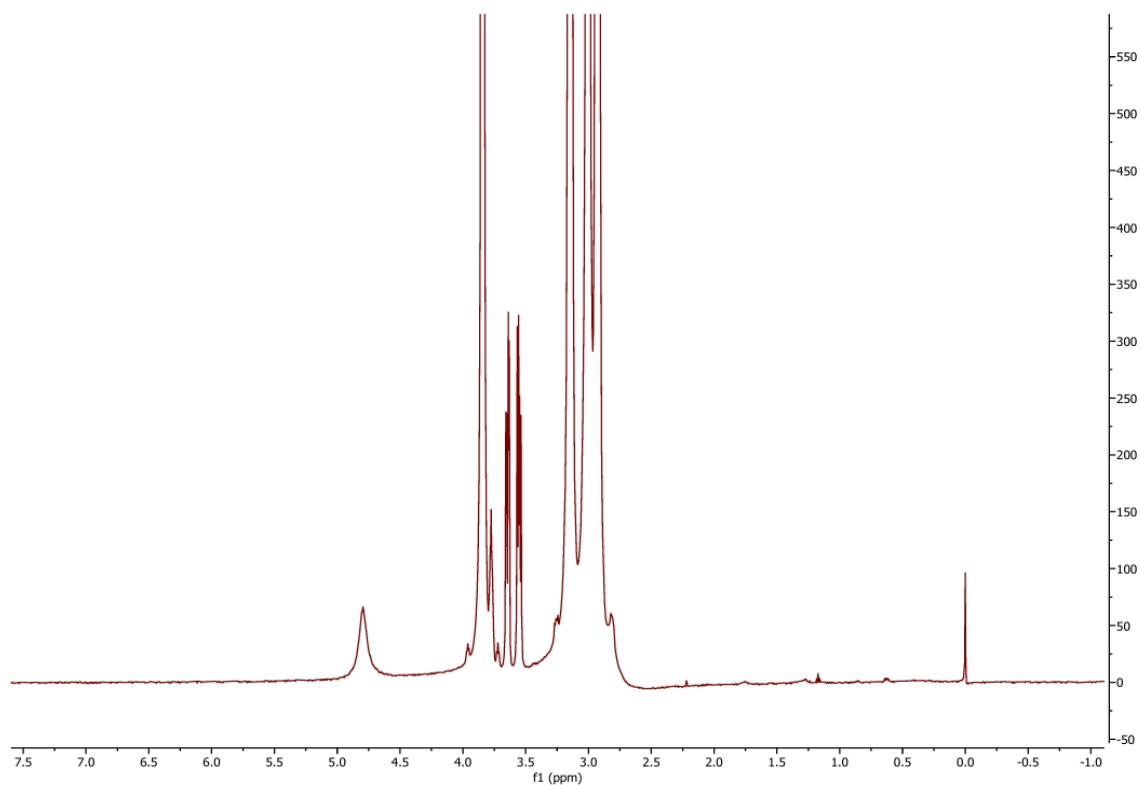


Figure S118. Proton 1D CPMG NMR spectrum of 0.5 mM Glycerol in the presence of *E. coli* lipid vesicles with the addition of 0.5 mM Mn^{2+} collected with a spin-lock time of 20 ms at 298K.

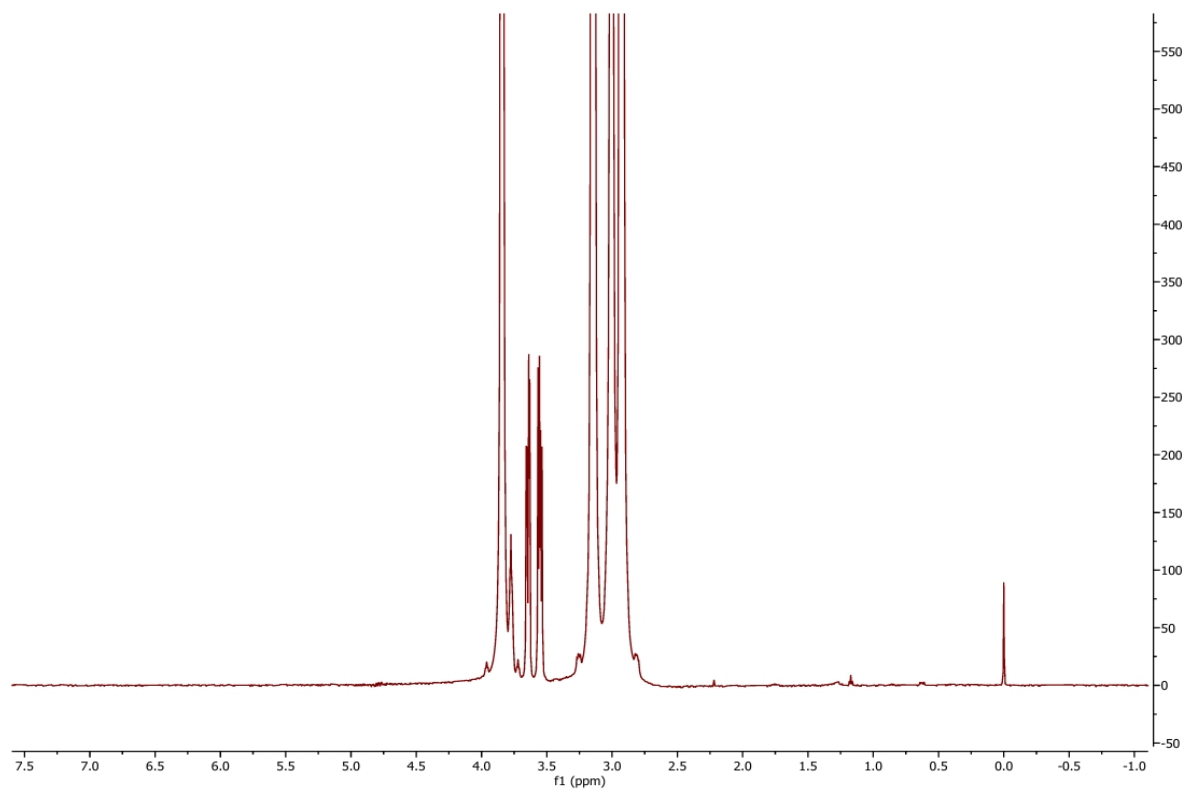


Figure S119. Proton 1D CPMG NMR spectrum of 0.5 mM Glycerol in the presence of *E. coli* lipid vesicles with the addition of 0.5 mM Mn^{2+} collected with a spin-lock time of 50 ms at 298K.

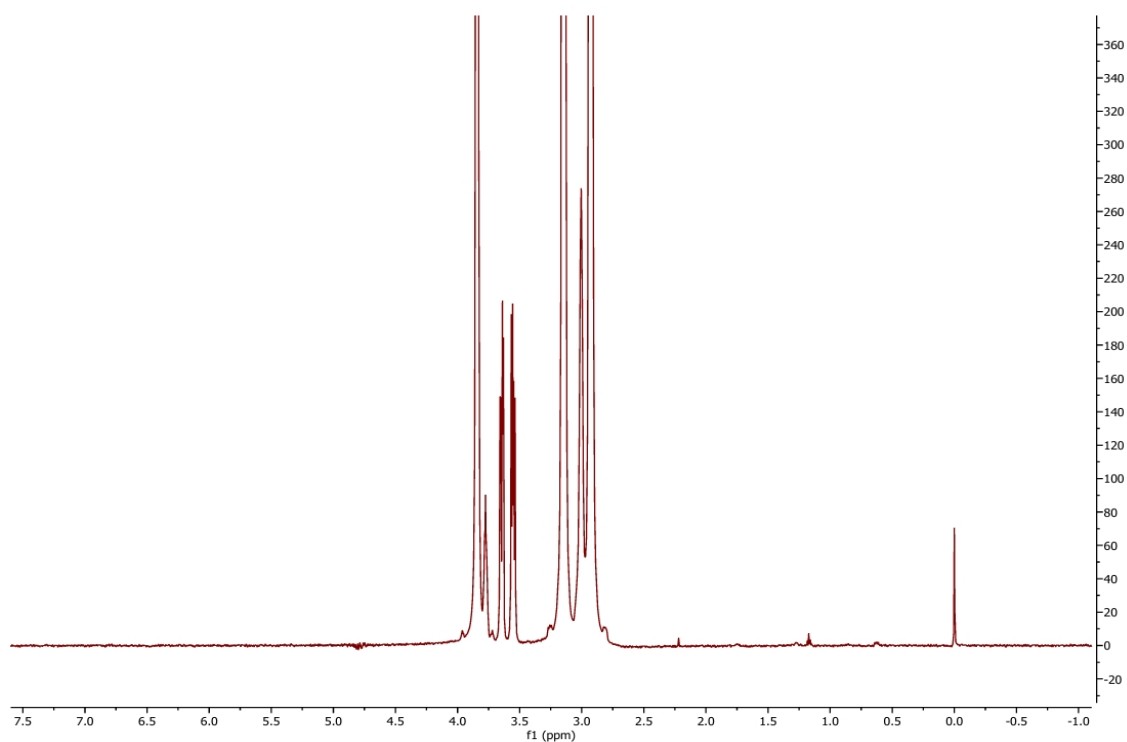


Figure S120. Proton 1D CPMG NMR spectrum of 0.5 mM Glycerol in the presence of *E. coli* lipid vesicles with the addition of 0.5 mM Mn^{2+} collected with a spin-lock time of 150 ms at 298K.

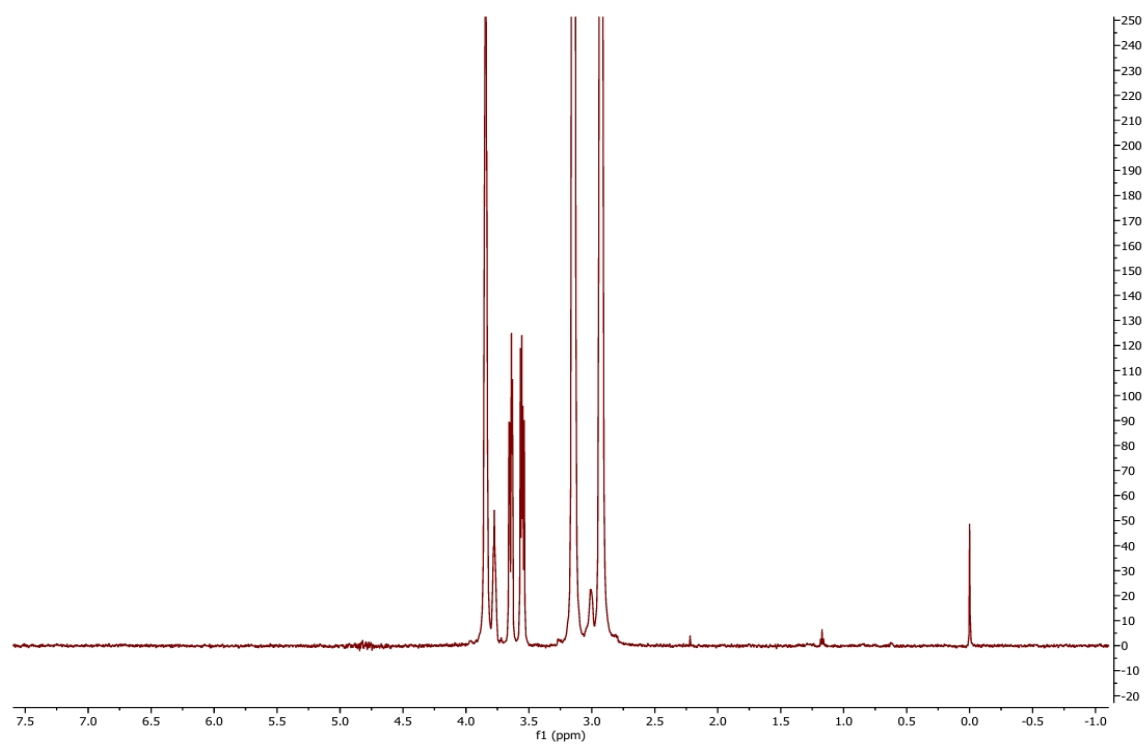


Figure S121. Proton 1D CPMG NMR spectrum of 0.5 mM Glycerol in the presence of *E. coli* lipid vesicles with the addition of 0.5 mM Mn^{2+} collected with a spin-lock time of 300 ms at 298K.

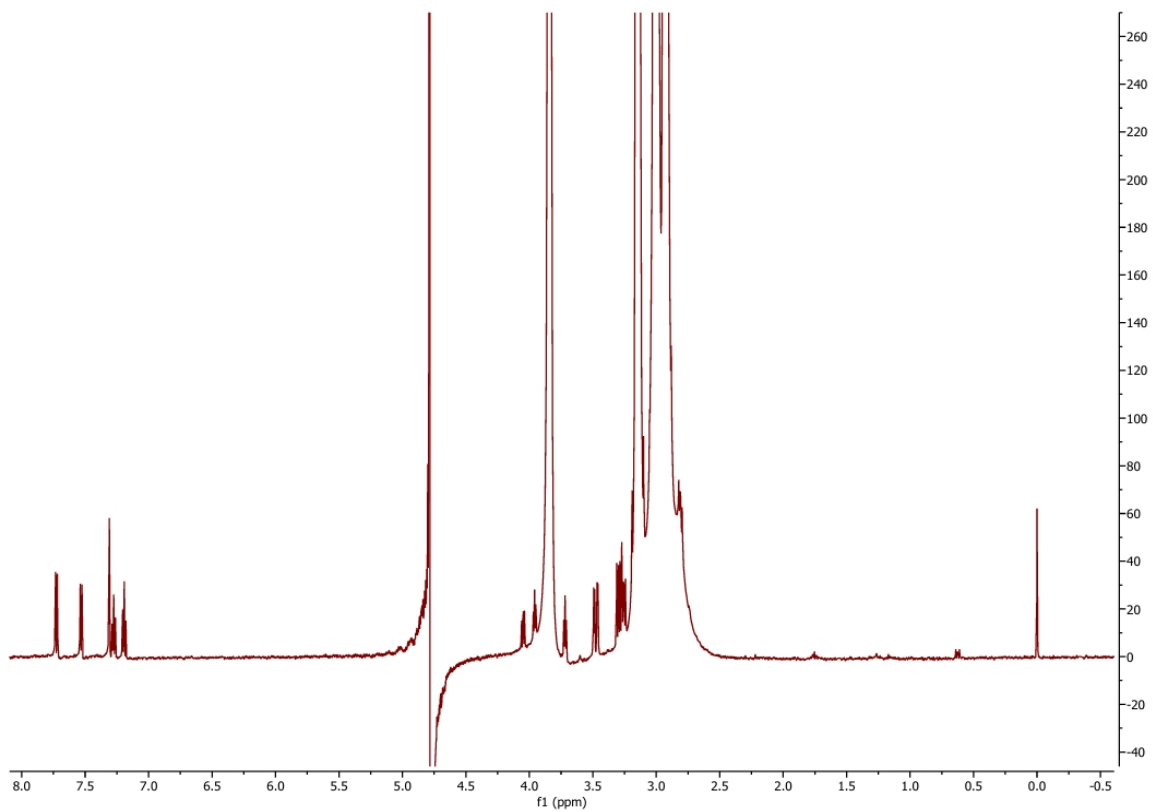


Figure S122. Proton 1D CPMG NMR spectrum of 0.5 mM Tryptophan collected with a spin-lock time of 20 ms at 298K.

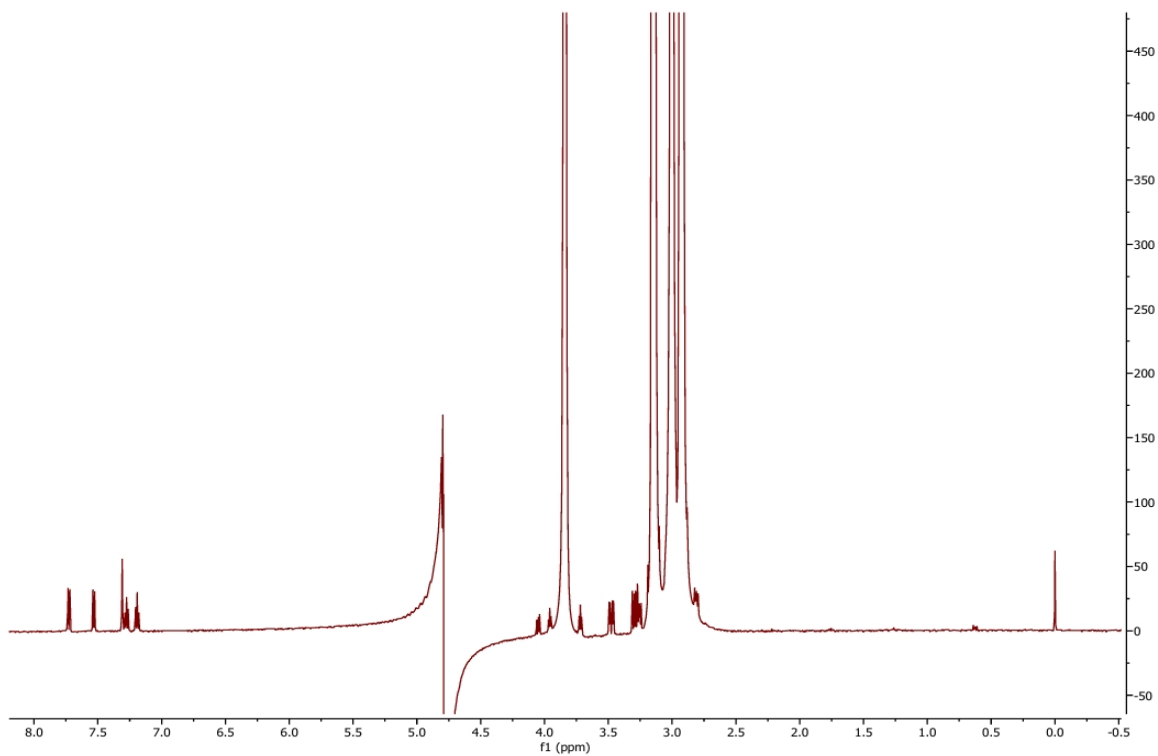


Figure S123. Proton 1D CPMG NMR spectrum of 0.5 mM Tryptophan collected with a spin-lock time of 50 ms at 298K.

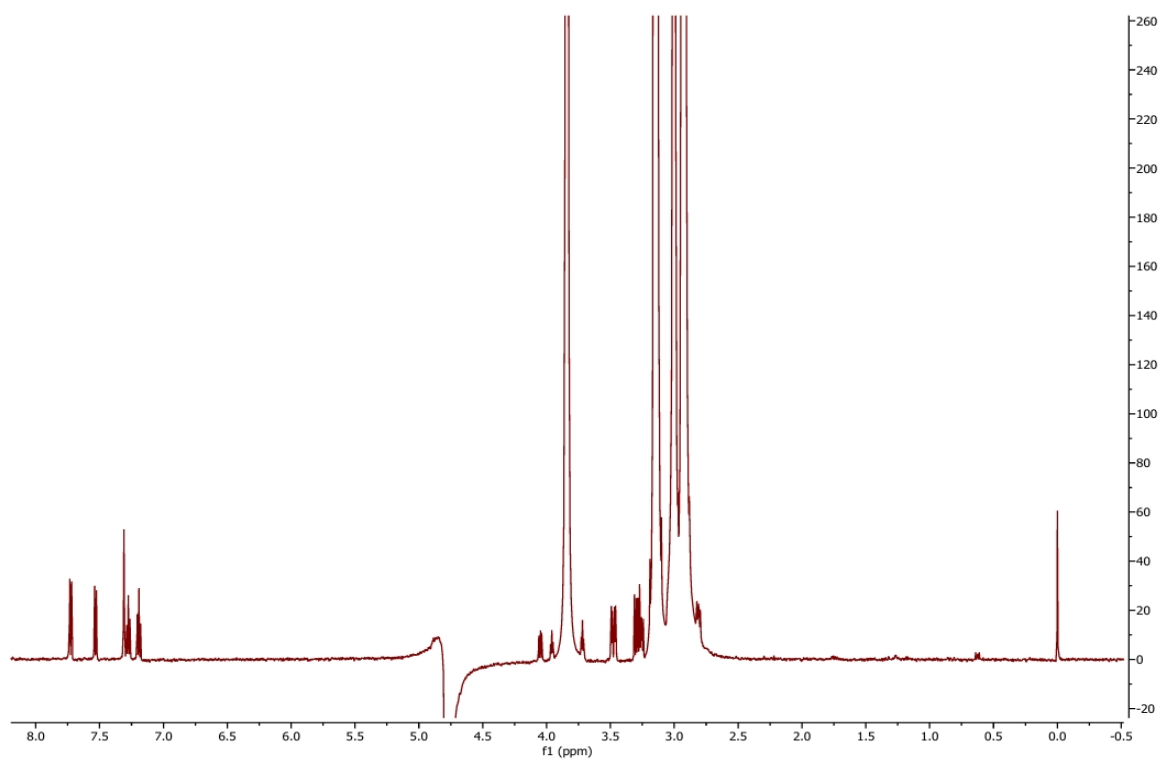


Figure S124. Proton 1D CPMG NMR spectrum of 0.5 mM Tryptophan collected with a spin-lock time of 150 ms at 298K.

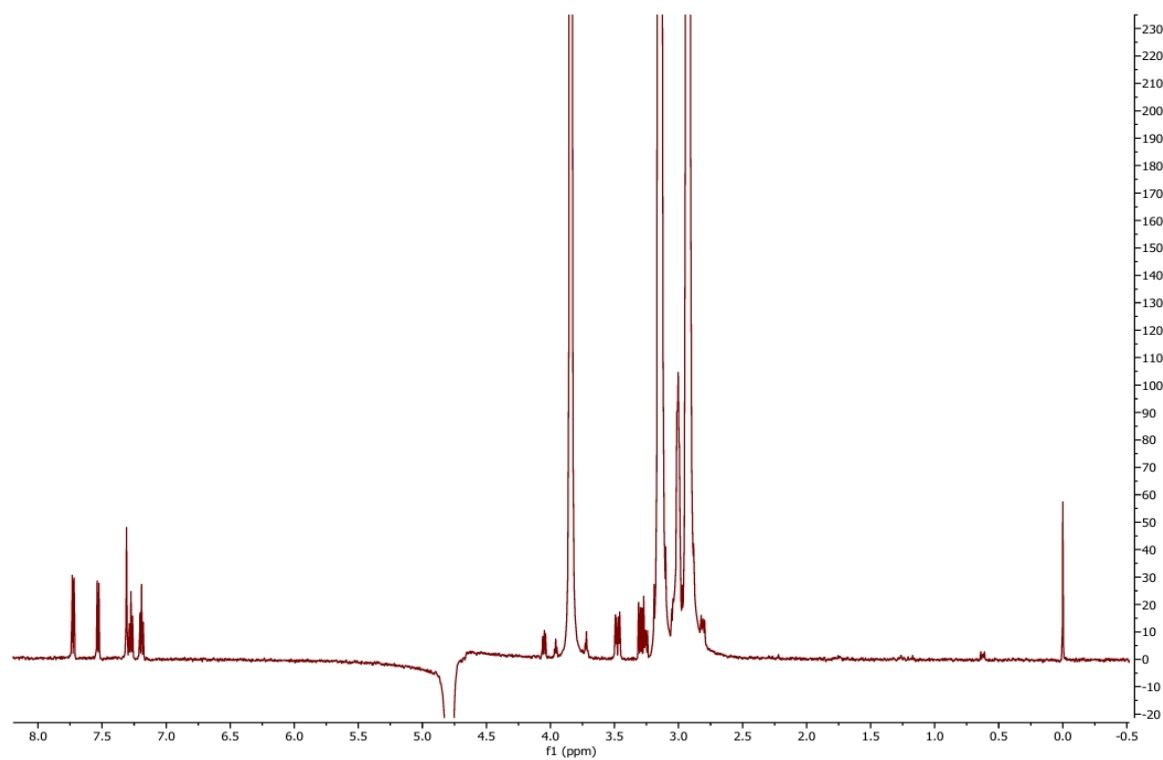


Figure S125. Proton 1D CPMG NMR spectrum of 0.5 mM Tryptophan collected with a spin-lock time of 300 ms at 298K.

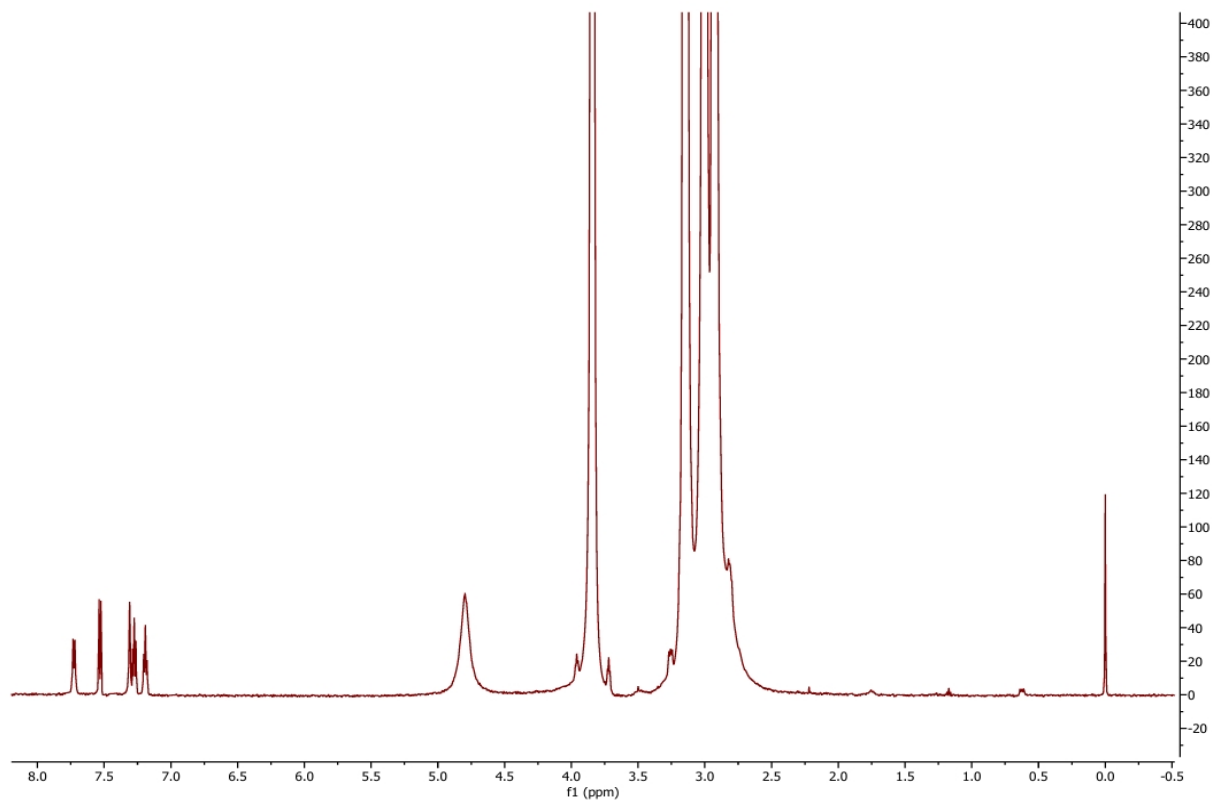


Figure S126. Proton 1D CPMG NMR spectrum of 0.5 mM Tryptophan with the addition of 0.5 mM Mn²⁺ collected with a spin-lock time of 20 ms at 298K.

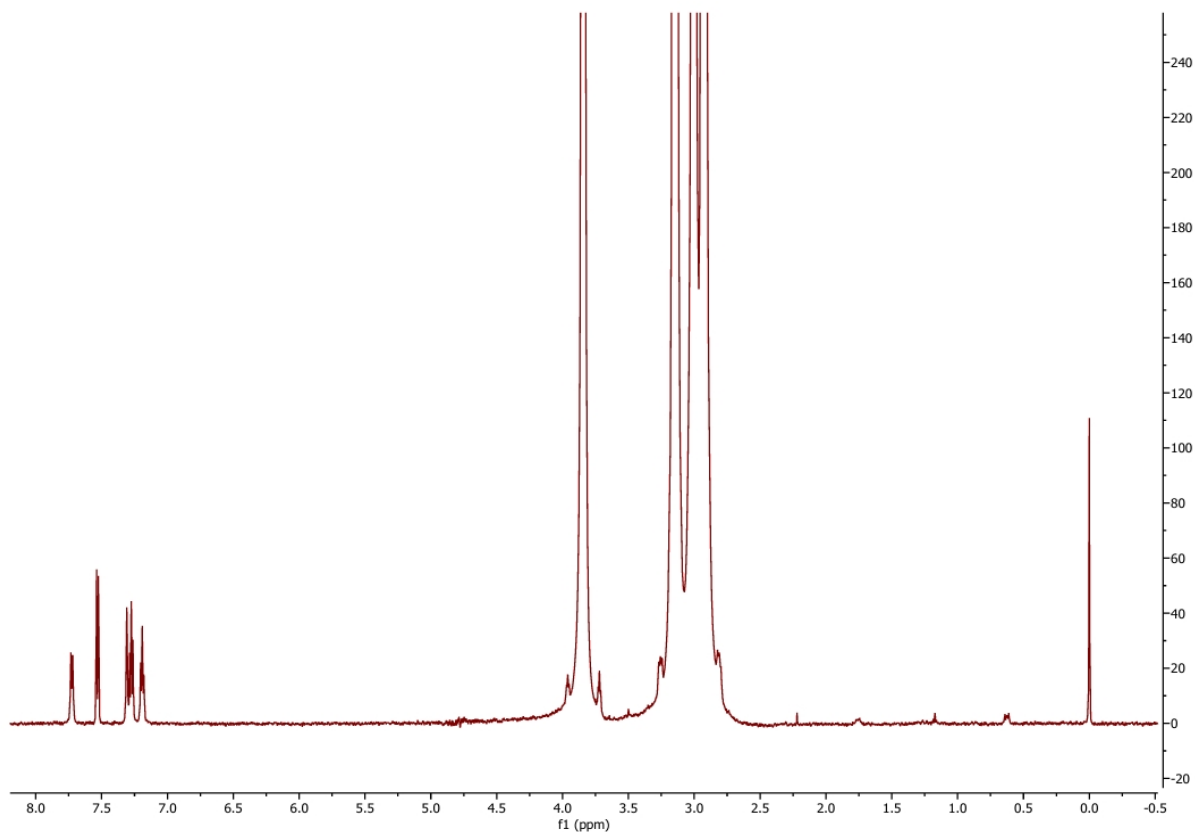


Figure S127. Proton 1D CPMG NMR spectrum of 0.5 mM Tryptophan with the addition of 0.5 mM Mn²⁺ collected with a spin-lock time of 50 ms at 298K.

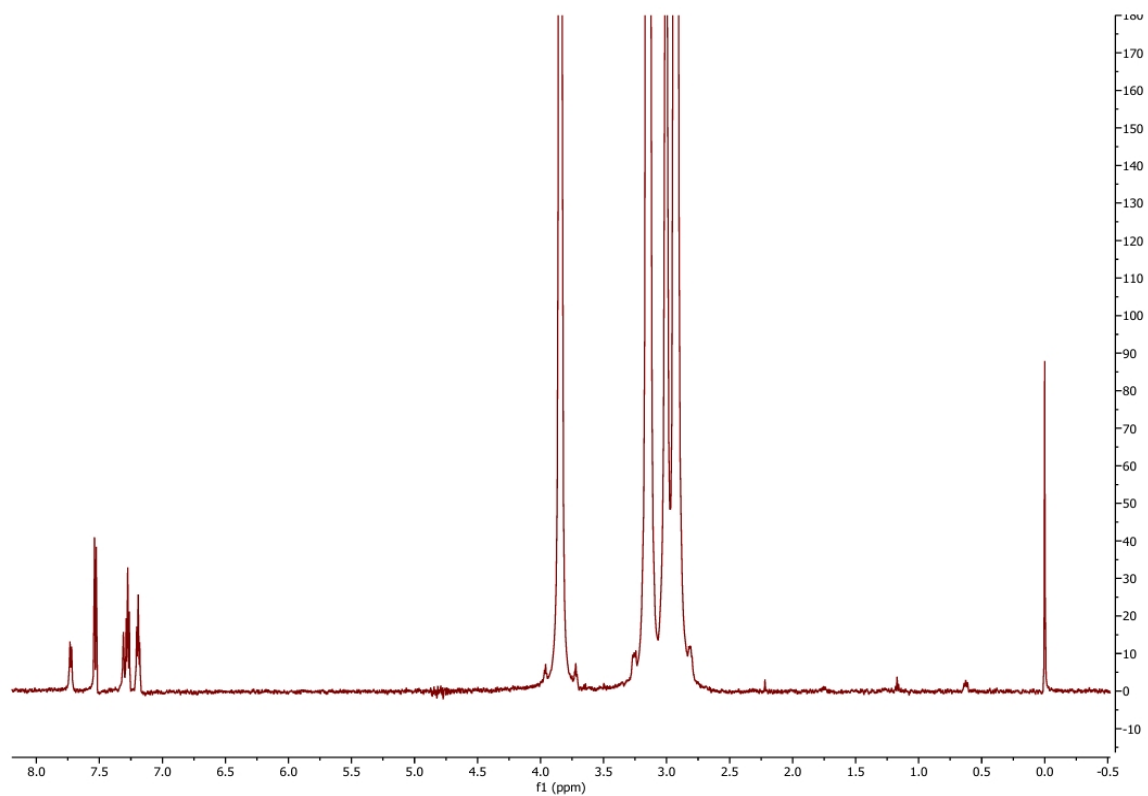


Figure S128. Proton 1D CPMG NMR spectrum of 0.5 mM Tryptophan with the addition of 0.5 mM Mn^{2+} collected with a spin-lock time of 150 ms at 298K.

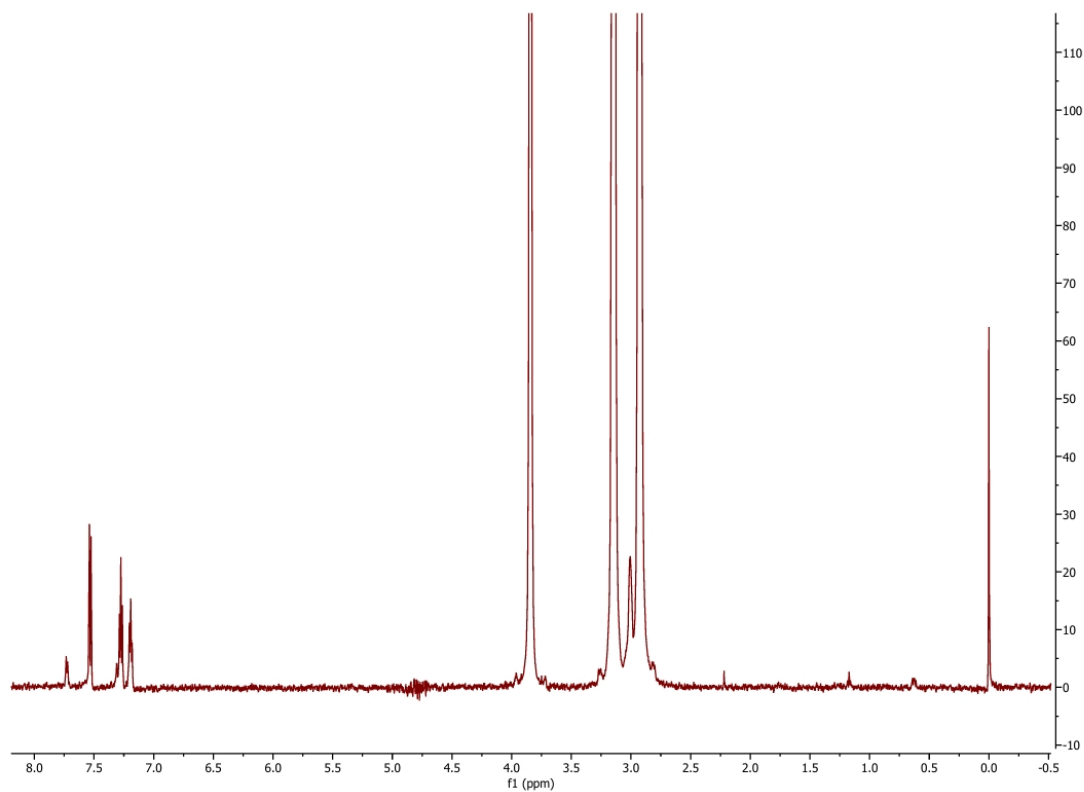


Figure S129. Proton 1D CPMG NMR spectrum of 0.5 mM Tryptophan with the addition of 0.5 mM Mn^{2+} collected with a spin-lock time of 300 ms at 298K.

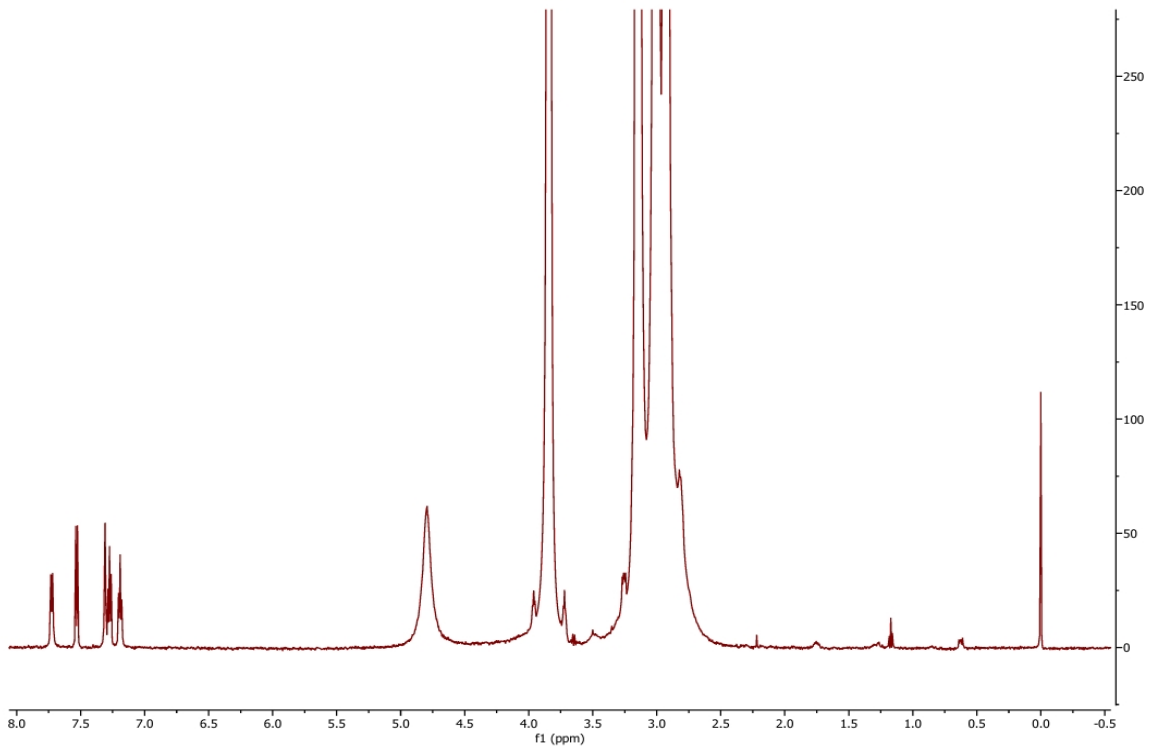


Figure S130. Proton 1D CPMG NMR spectrum of 0.5 mM Tryptophan in the presence of *E. coli* lipid vesicles collected with a spin-lock time of 20 ms at 298K.

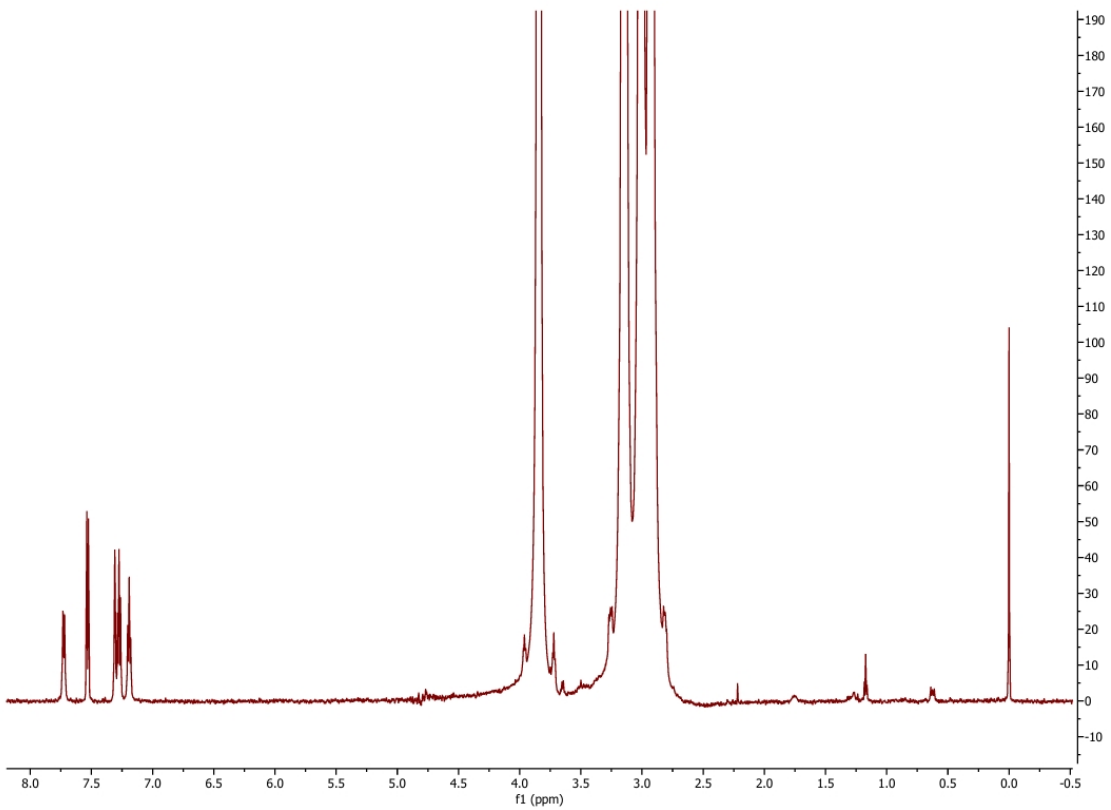


Figure S131. Proton 1D CPMG NMR spectrum of 0.5 mM Tryptophan in the presence of *E. coli* lipid vesicles collected with a spin-lock time of 50 ms at 298K.

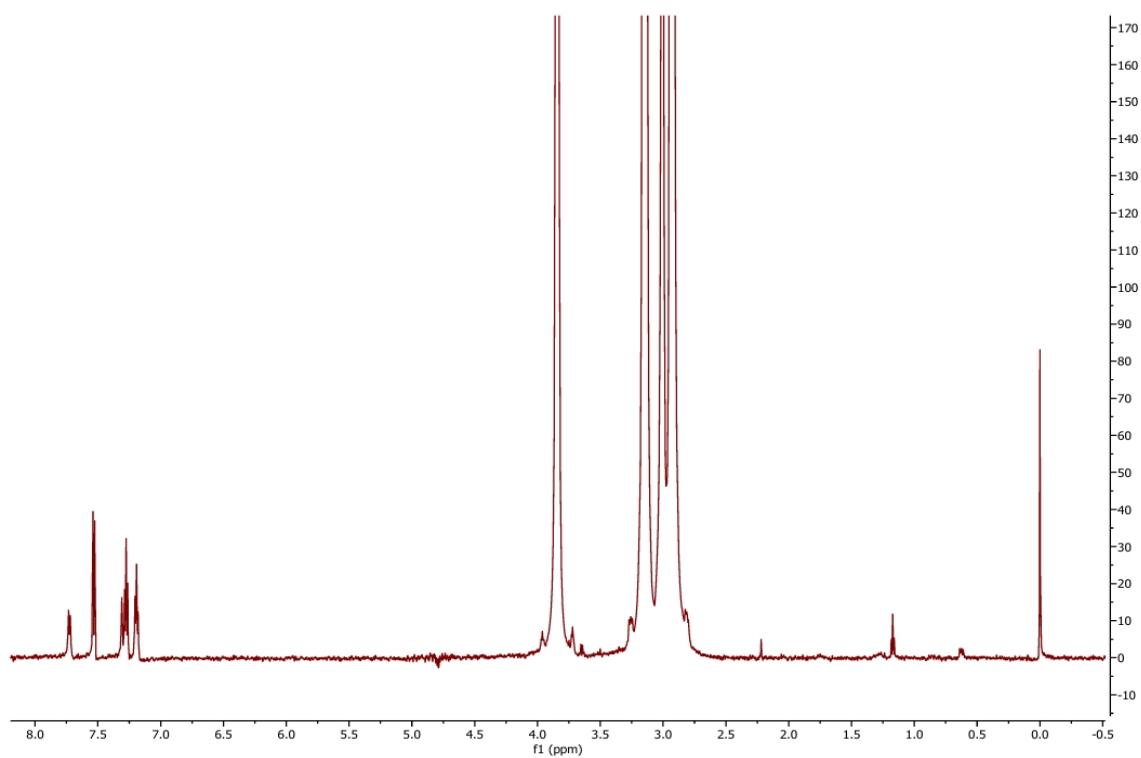


Figure S132. Proton 1D CPMG NMR spectrum of 0.5 mM Tryptophan in the presence of *E. coli* lipid vesicles collected with a spin-lock time of 150 ms at 298K.

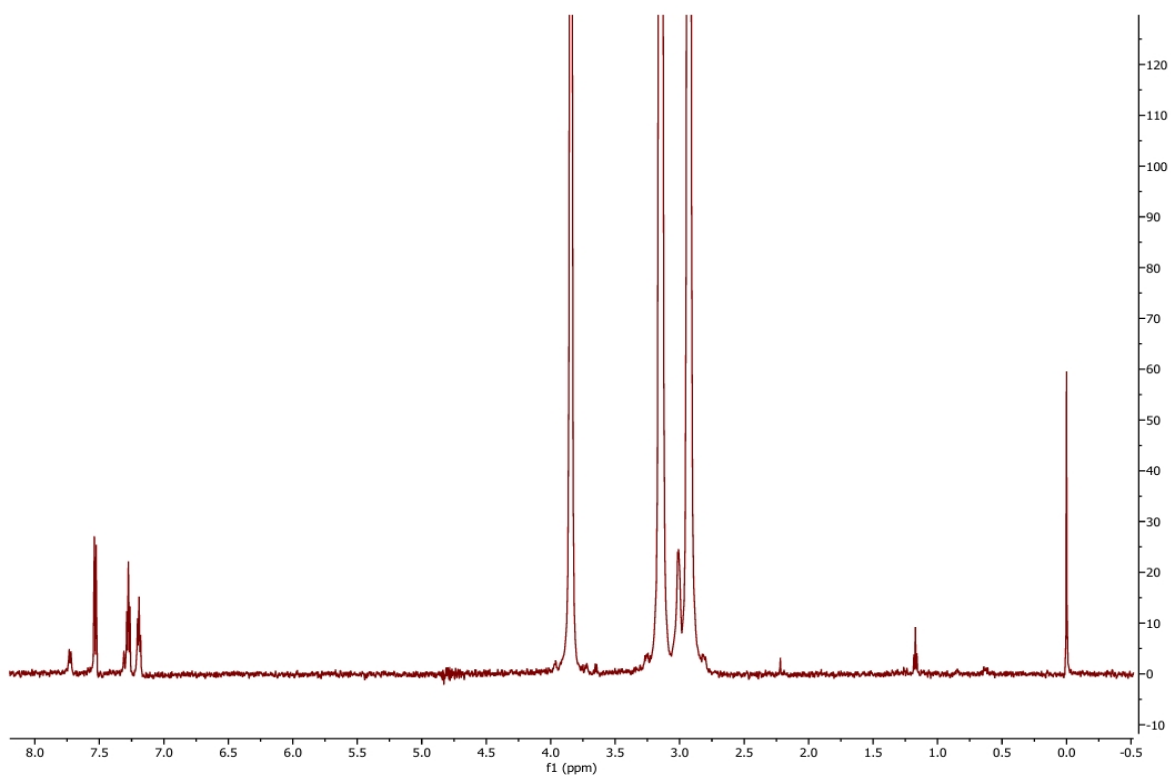


Figure S133. Proton 1D CPMG NMR spectrum of 0.5 mM Tryptophan in the presence of *E. coli* lipid vesicles collected with a spin-lock time of 300 ms at 298K.

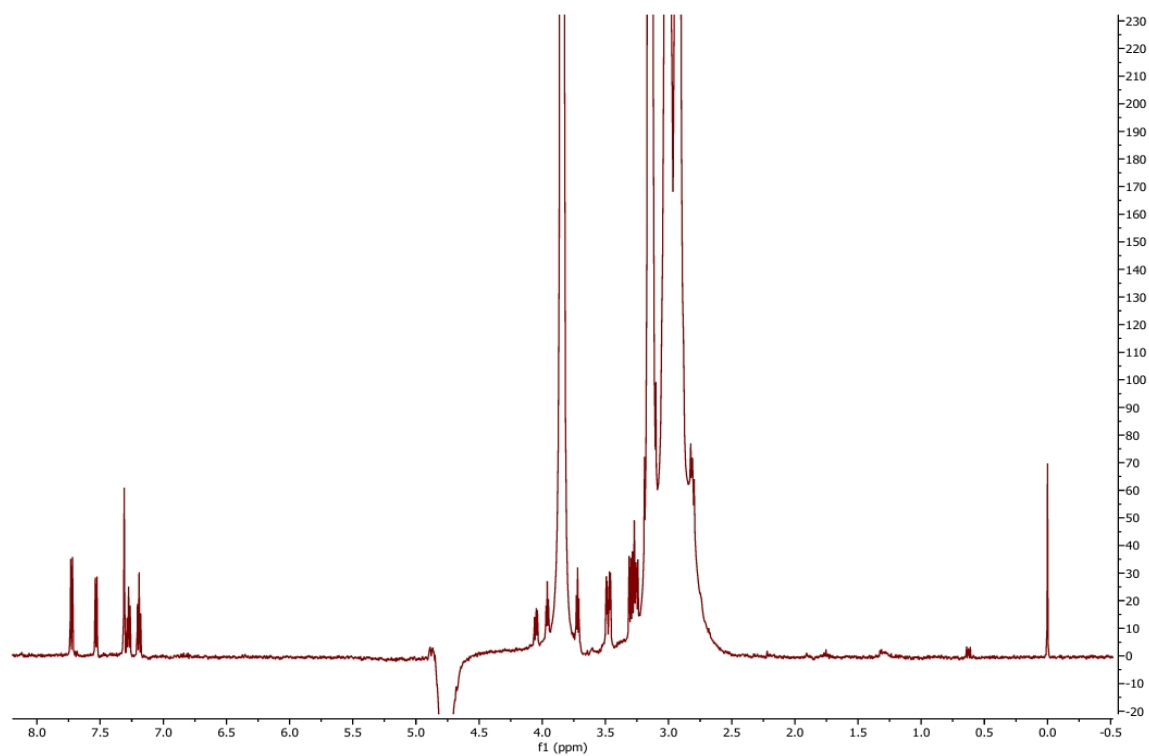


Figure S134. Proton 1D CPMG NMR spectrum of 0.5 mM Tryptophan in the presence of *E. coli* lipid vesicles with the addition of 0.5 mM Mn^{2+} collected with a spin-lock time of 20 ms at 298K.

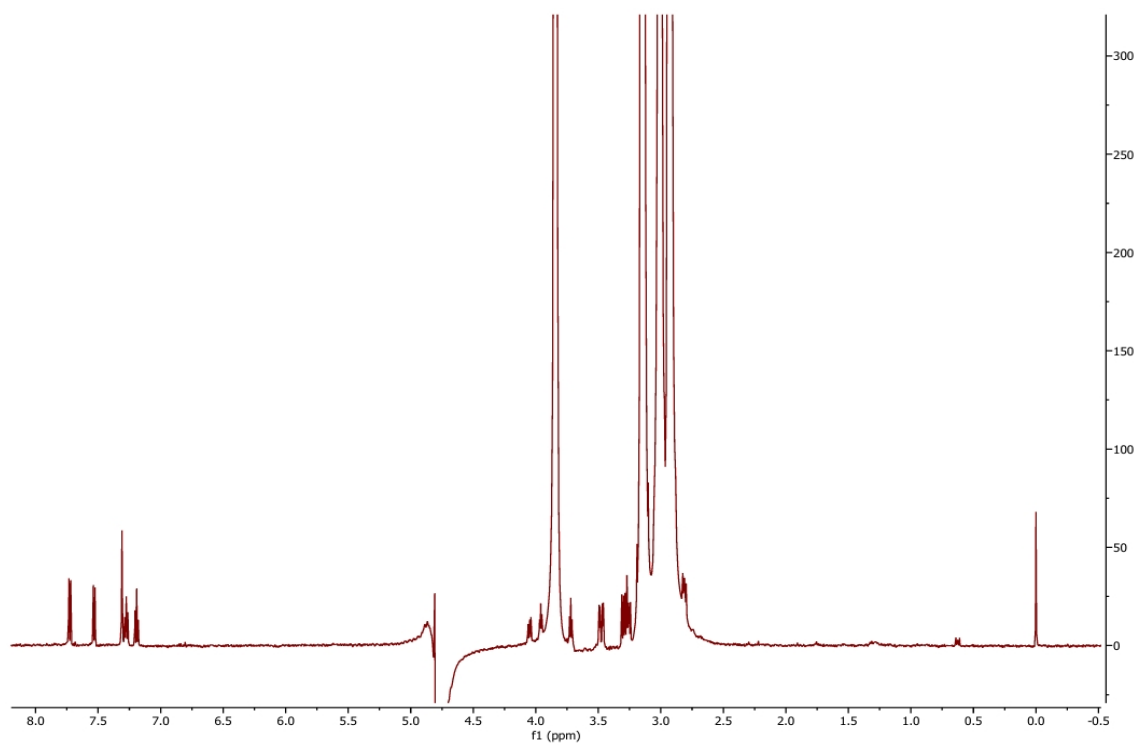


Figure S135. Proton 1D CPMG NMR spectrum of 0.5 mM Tryptophan in the presence of *E. coli* lipid vesicles with the addition of 0.5 mM Mn^{2+} collected with a spin-lock time of 50 ms at 298K.

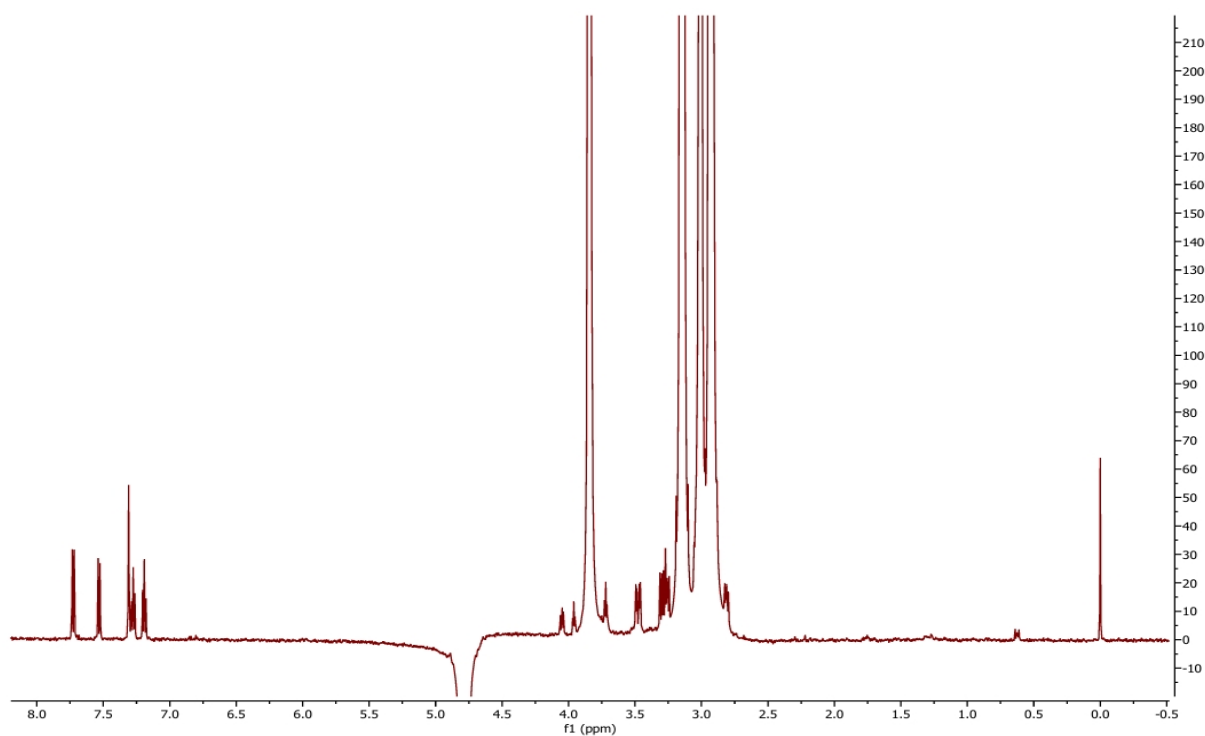


Figure S136. Proton 1D CPMG NMR spectrum of 0.5 mM Tryptophan in the presence of *E. coli* lipid vesicles with the addition of 0.5 mM Mn^{2+} collected with a spin-lock time of 150 ms at 298K.

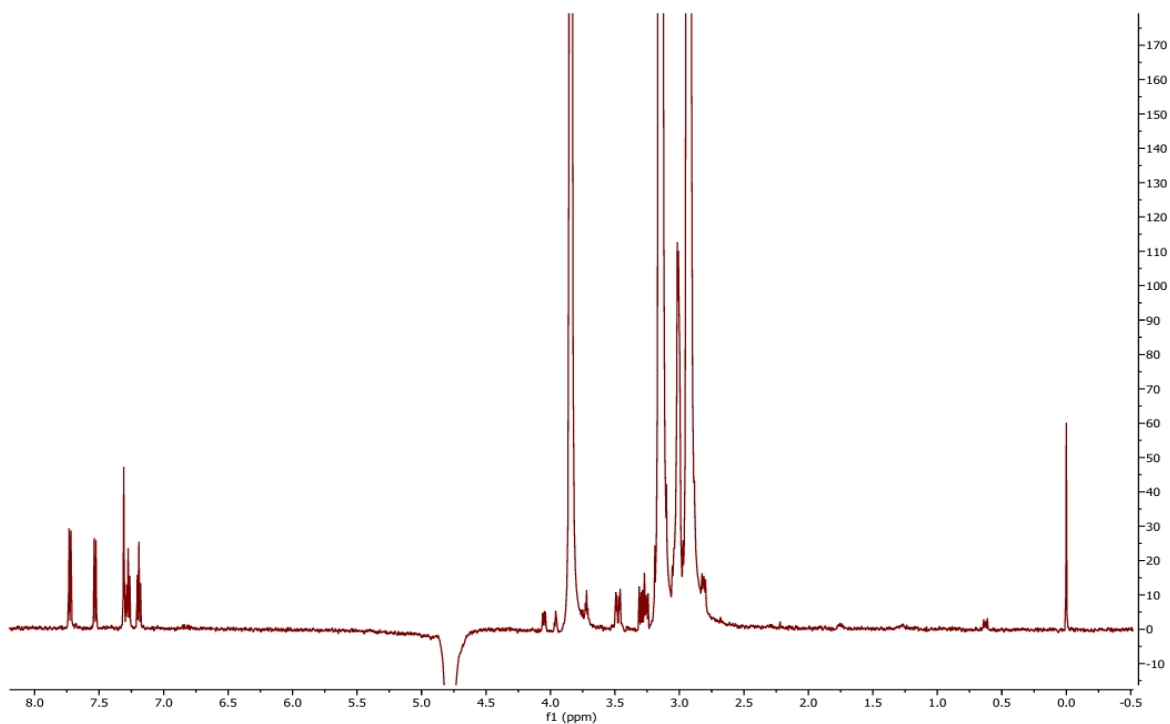


Figure S137. Proton 1D CPMG NMR spectrum of 0.5 mM Tryptophan in the presence of *E. coli* lipid vesicles with the addition of 0.5 mM Mn^{2+} collected with a spin-lock time of 300 ms at 298K.

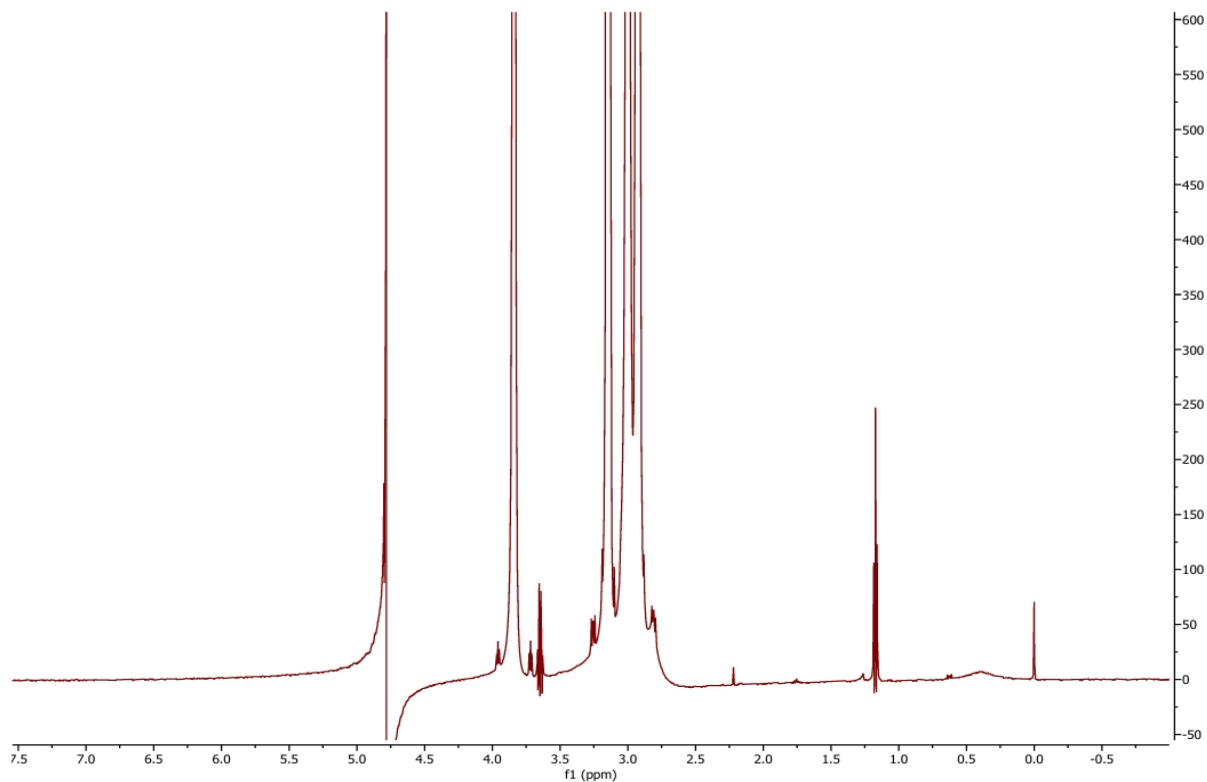


Figure S138. Proton 1D CPMG NMR spectrum of 0.5 mM Ethanol collected with a spin-lock time of 20 ms at 298K.

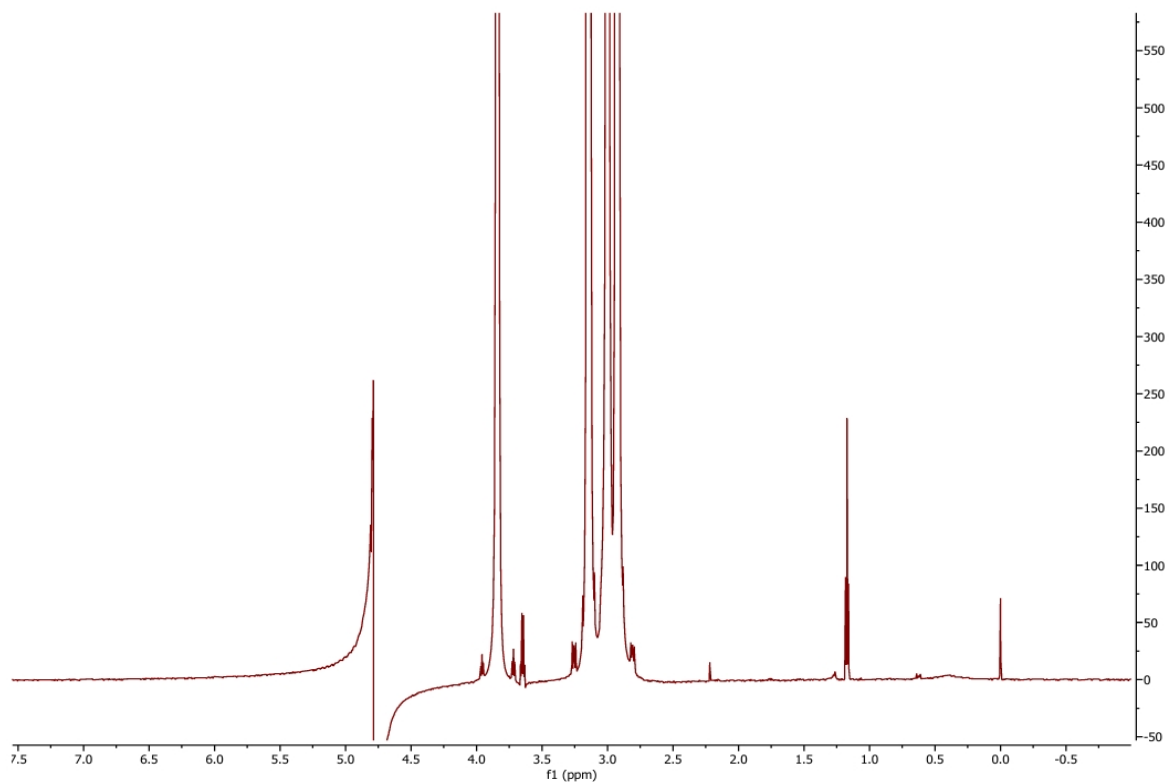


Figure S139. Proton 1D CPMG NMR spectrum of 0.5 mM Ethanol collected with a spin-lock time of 50 ms at 298K.

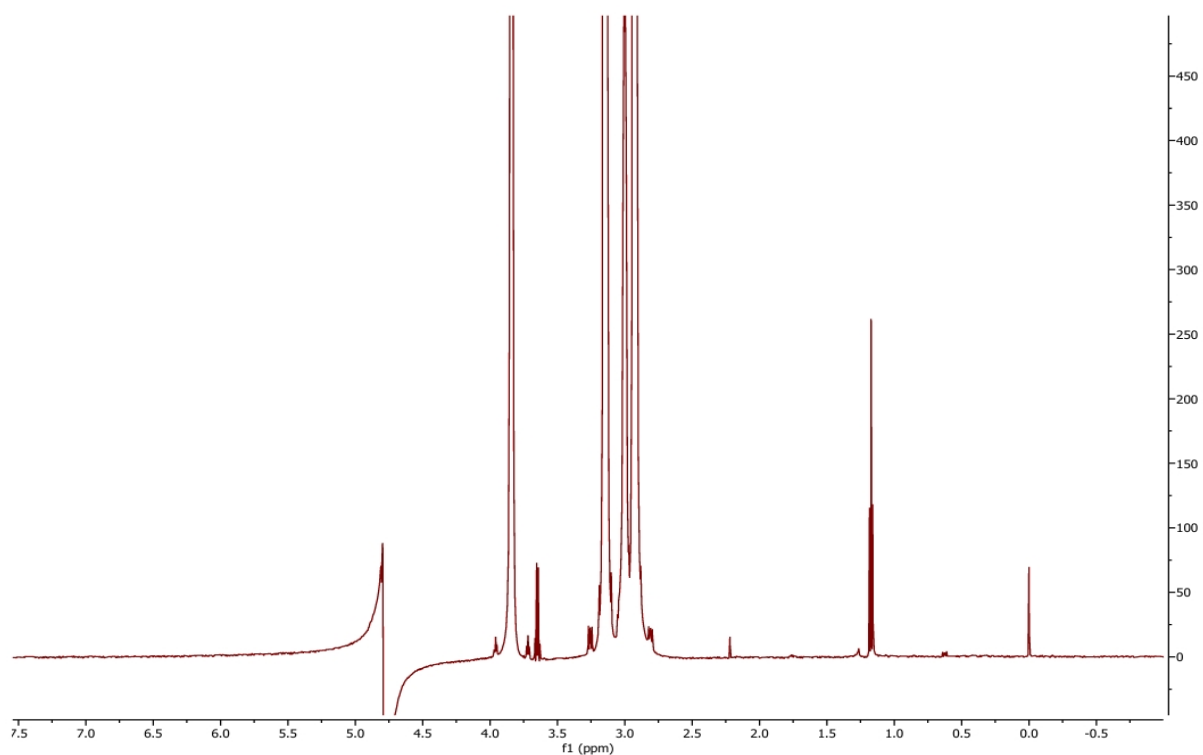


Figure S140. Proton 1D CPMG NMR spectrum of 0.5 mM Ethanol collected with a spin-lock time of 150 ms at 298K.

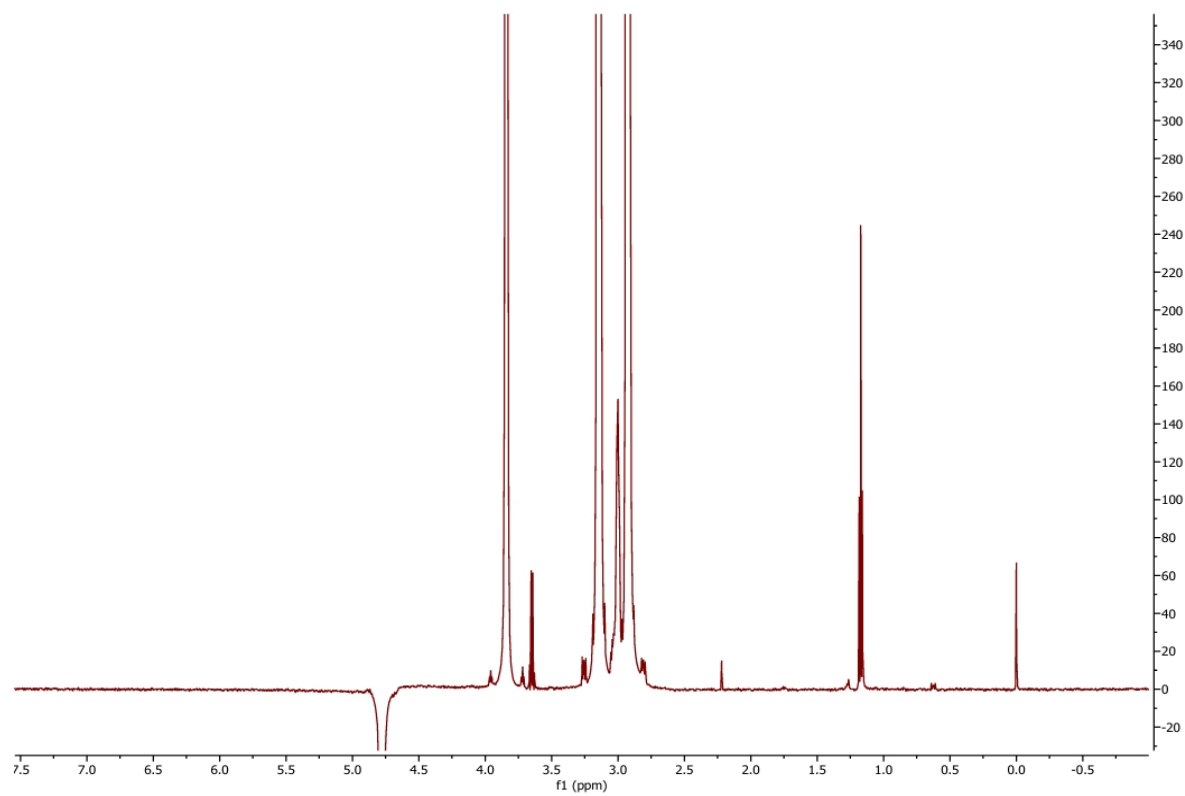


Figure S141. Proton 1D CPMG NMR spectrum of 0.5 mM Ethanol collected with a spin-lock time of 300 ms at 298K.

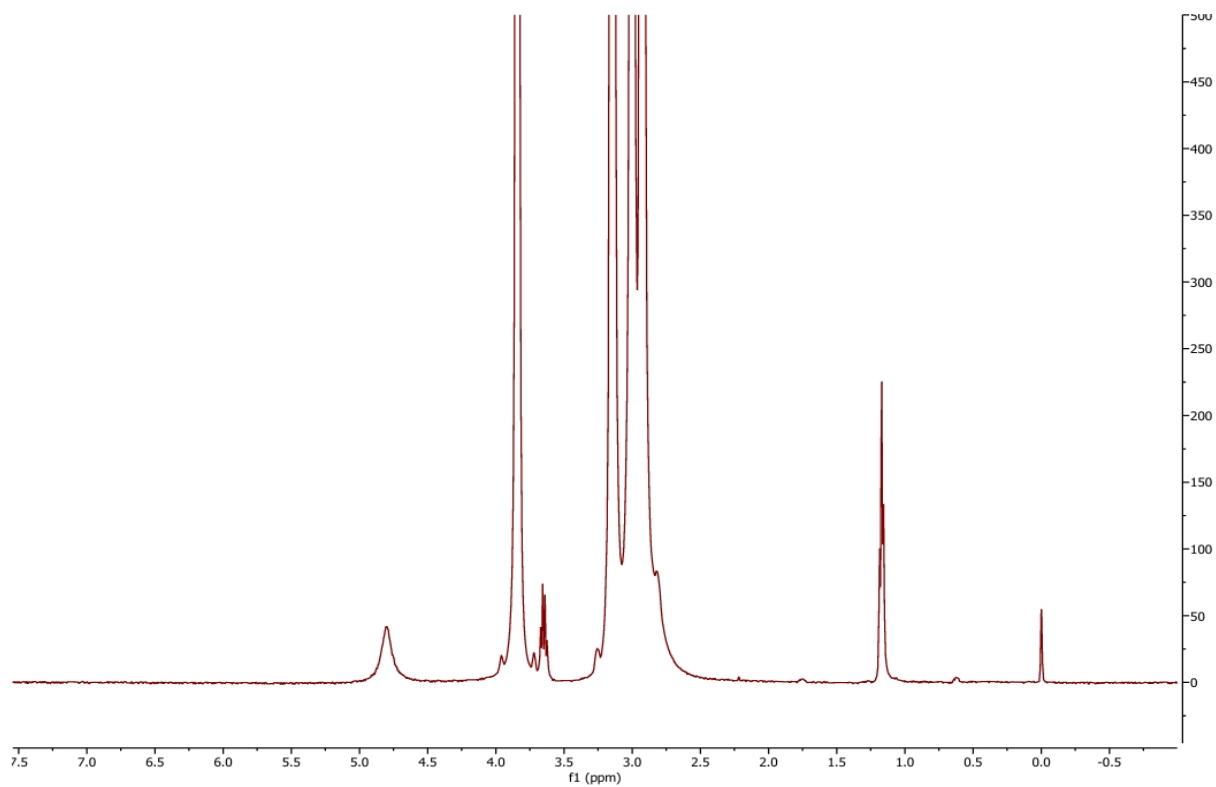


Figure S142. Proton 1D CPMG NMR spectrum of 0.5 mM Ethanol with the addition of 0.5 mM Mn^{2+} collected with a spin-lock time of 20 ms at 298K.

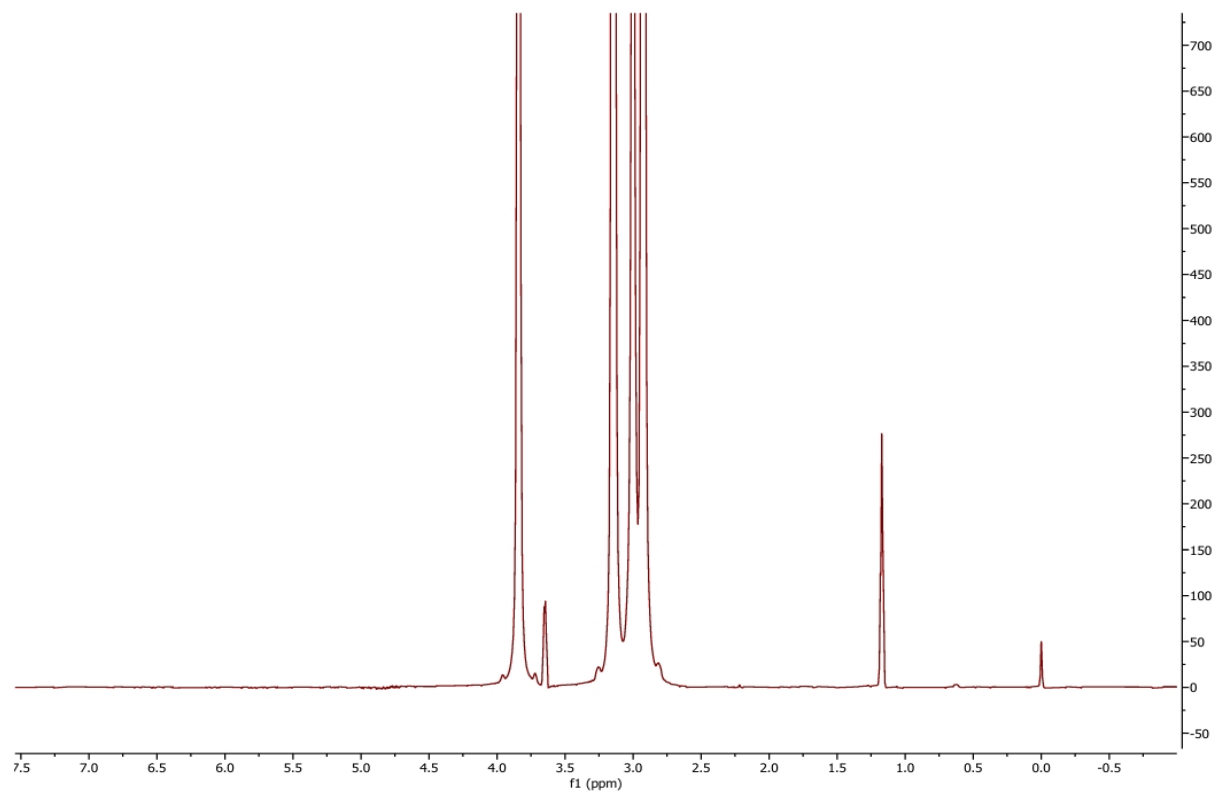


Figure S143. Proton 1D CPMG NMR spectrum of 0.5 mM Ethanol with the addition of 0.5 mM Mn^{2+} collected with a spin-lock time of 50 ms at 298K.

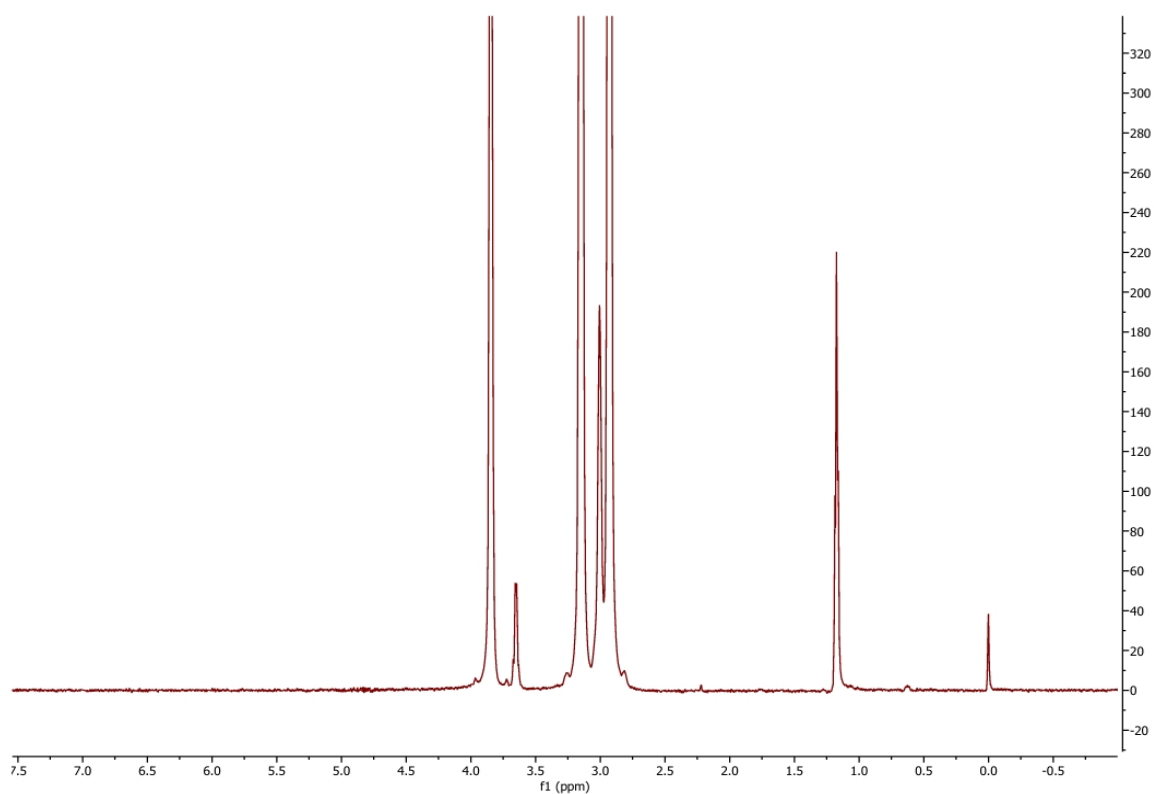


Figure S144. Proton 1D CPMG NMR spectrum of 0.5 mM Ethanol with the addition of 0.5 mM Mn^{2+} collected with a spin-lock time of 150 ms at 298K.

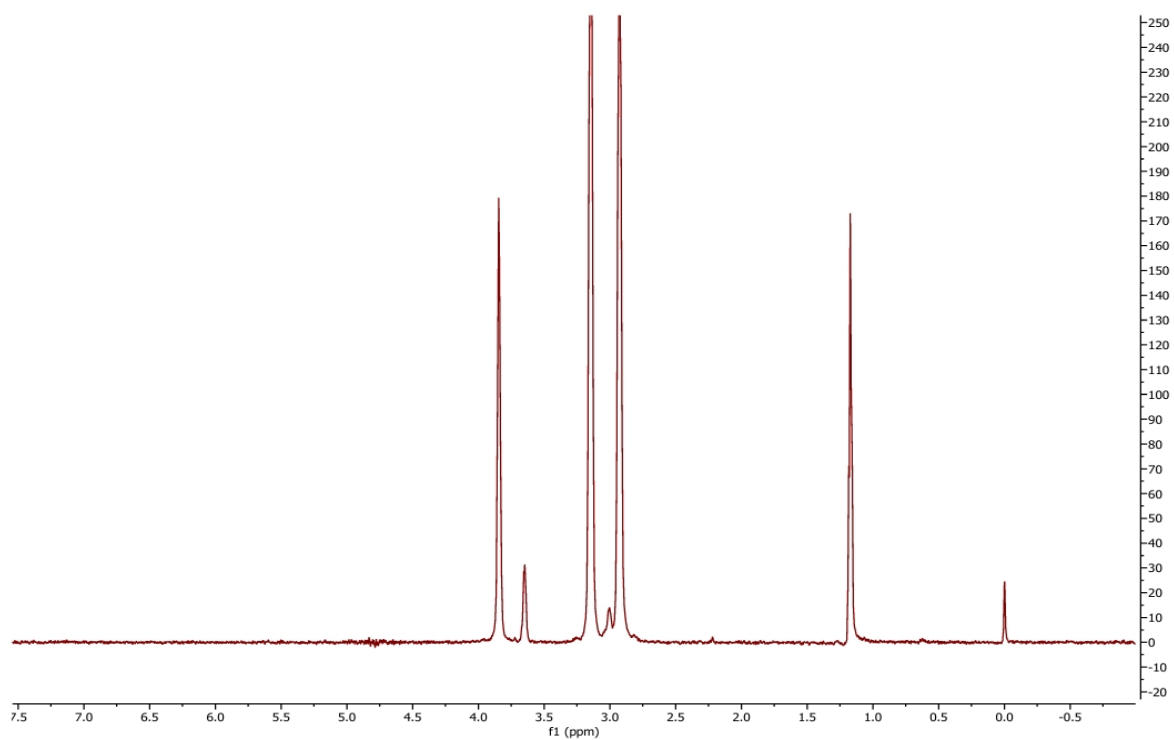


Figure S145. Proton 1D CPMG NMR spectrum of 0.5 mM Ethanol with the addition of 0.5 mM Mn^{2+} collected with a spin-lock time of 300 ms at 298K.

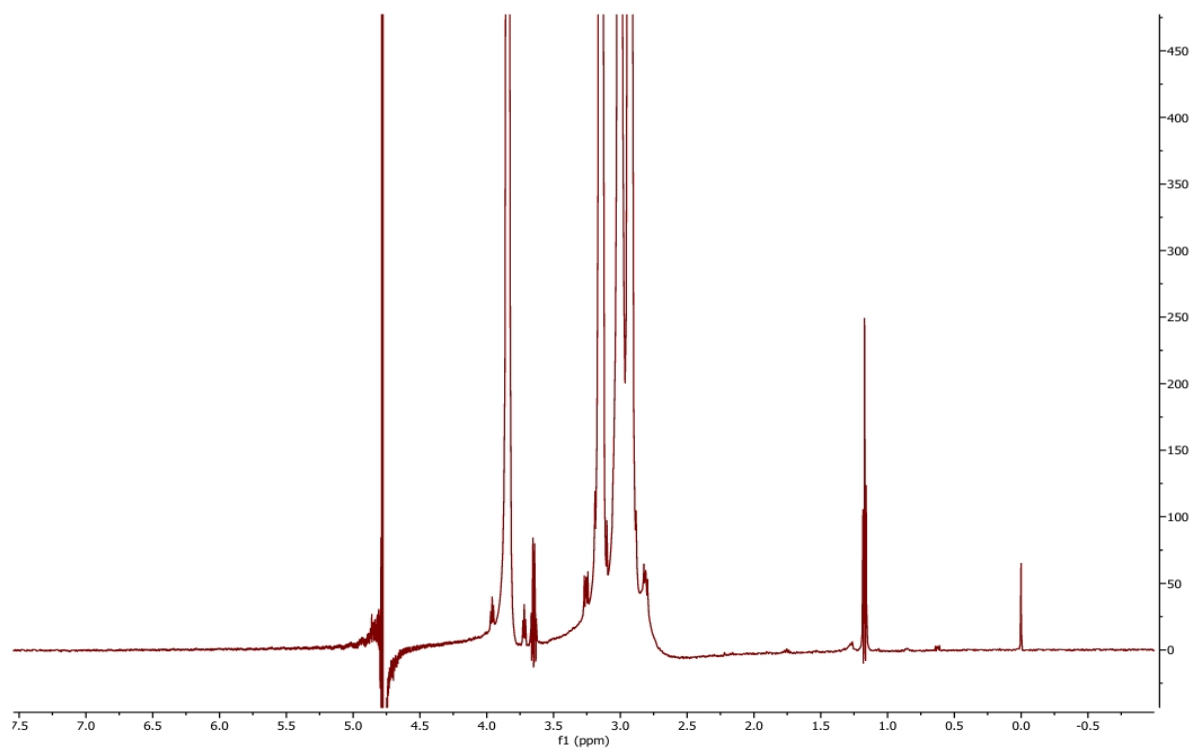


Figure S146. Proton 1D CPMG NMR spectrum of 0.5 mM Ethanol in the presence of *E. coli* lipid vesicles collected with a spin-lock time of 20 ms at 298K.

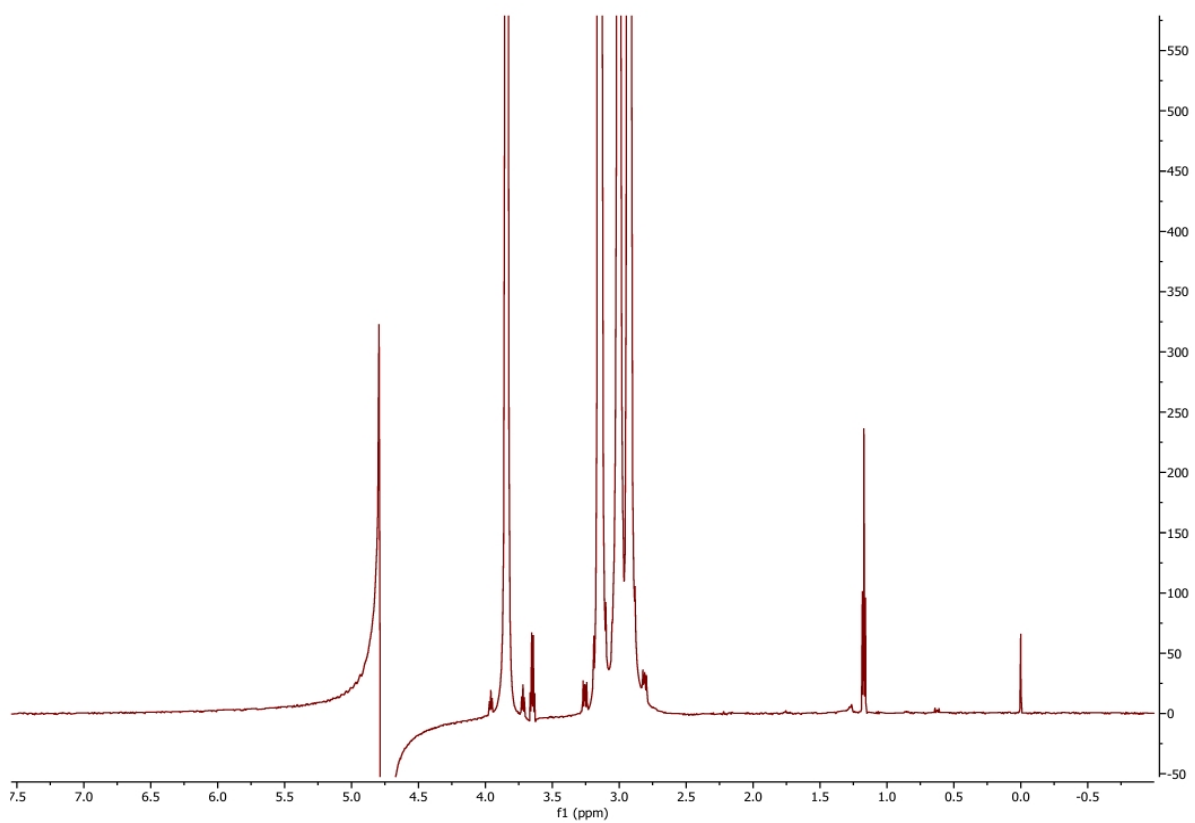


Figure S147. Proton 1D CPMG NMR spectrum of 0.5 mM Ethanol in the presence of *E. coli* lipid vesicles collected with a spin-lock time of 50 ms at 298K.

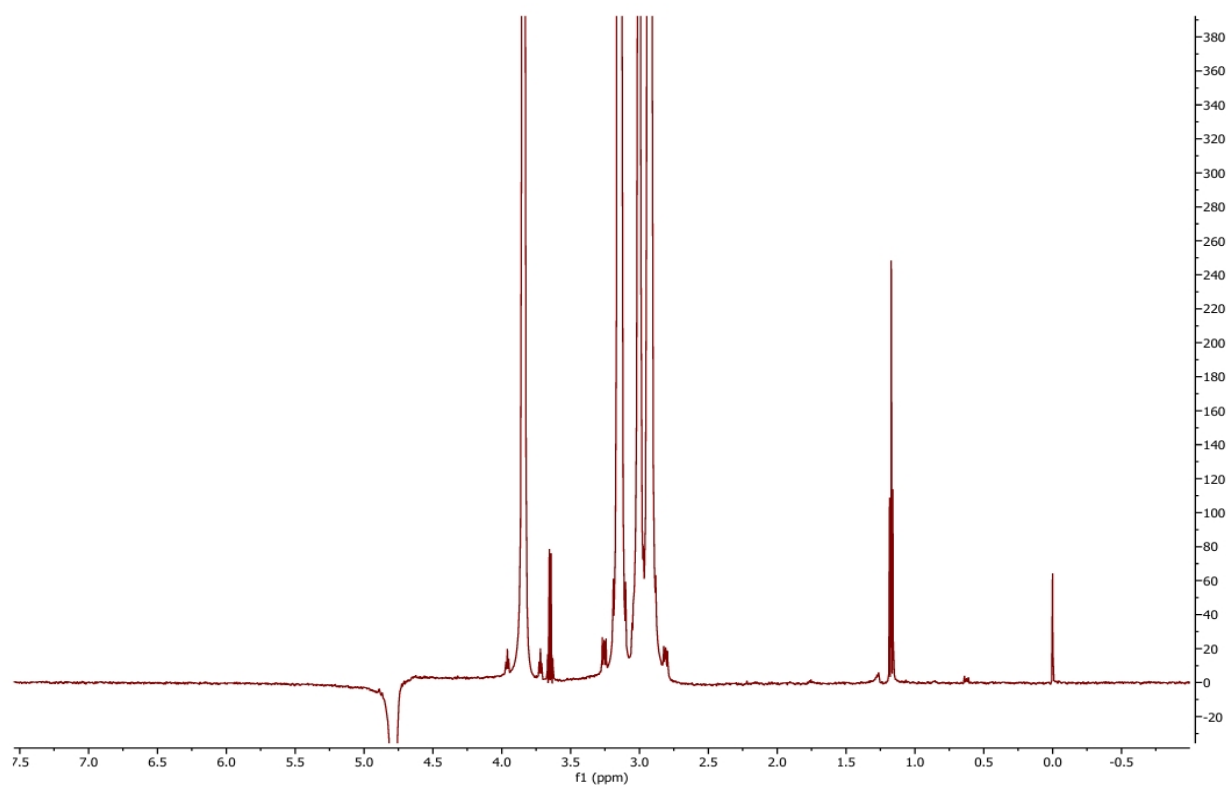


Figure S148. Proton 1D CPMG NMR spectrum of 0.5 mM Ethanol in the presence of *E. coli* lipid vesicles collected with a spin-lock time of 150 ms at 298K.

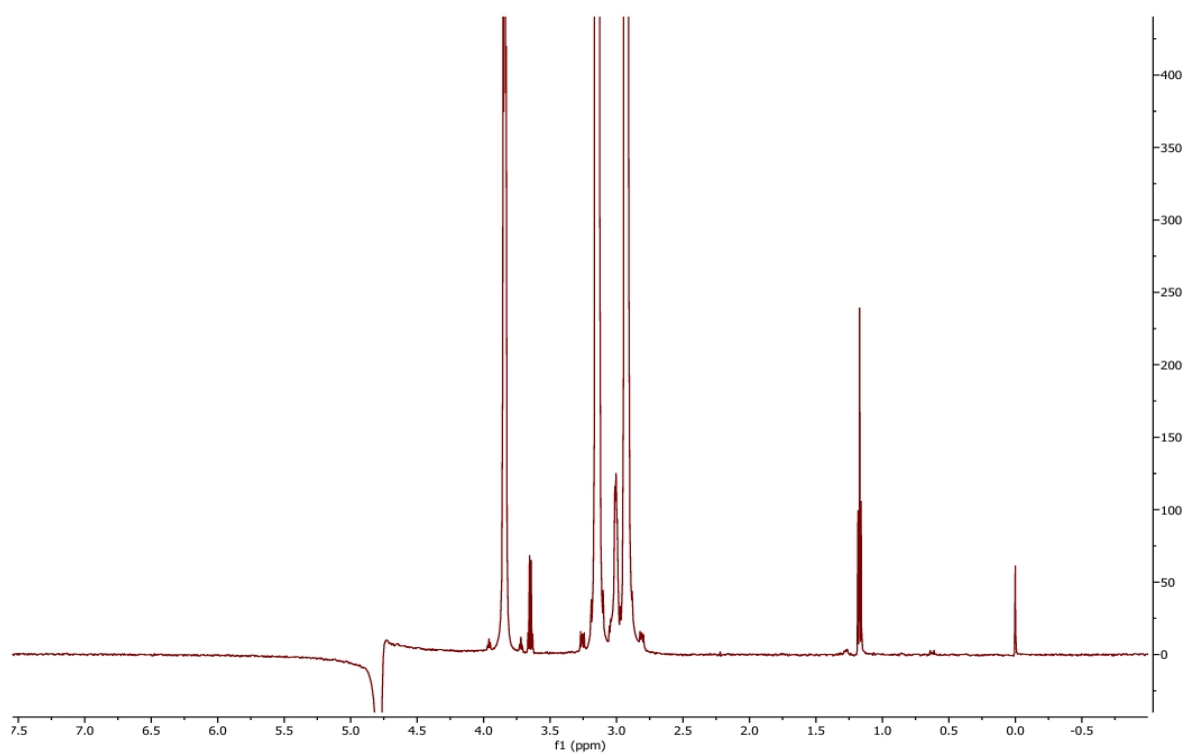


Figure S149. Proton 1D CPMG NMR spectrum of 0.5 mM Ethanol in the presence of *E. coli* lipid vesicles collected with a spin-lock time of 300 ms at 298K.

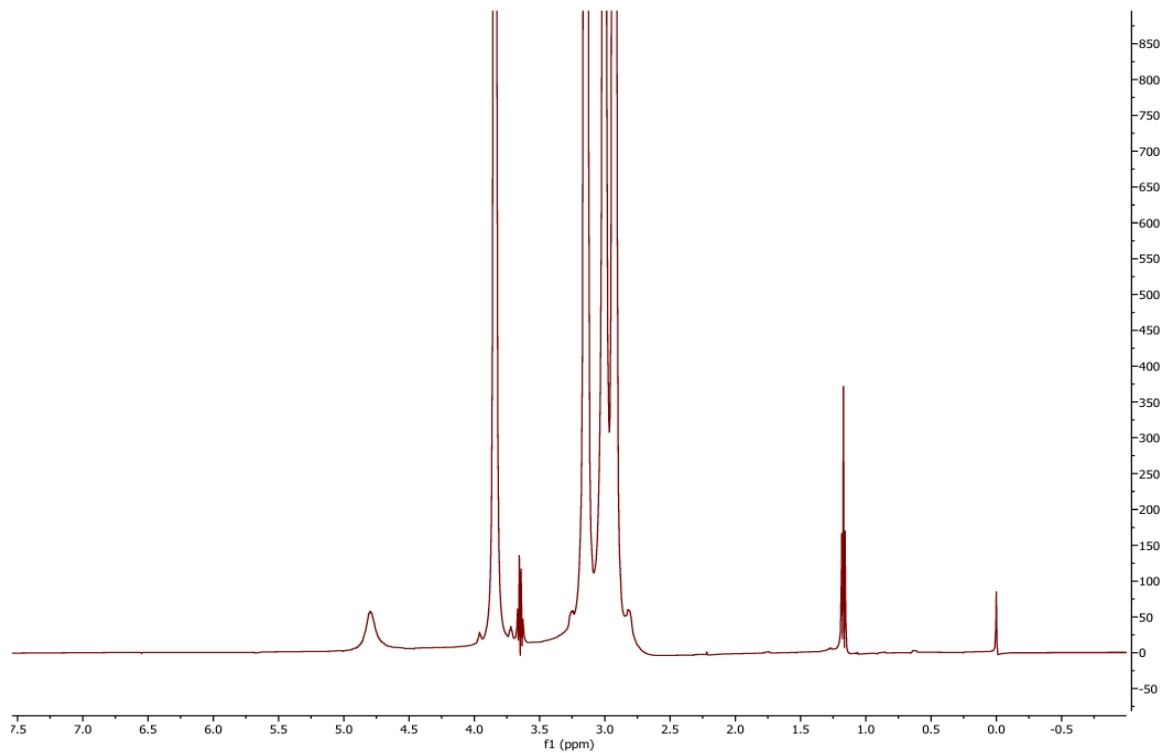


Figure S150. Proton 1D CPMG NMR spectrum of 0.5 mM Ethanol in the presence of *E. coli* lipid vesicles with the addition of 0.5 mM Mn^{2+} collected with a spin-lock time of 20 ms at 298K.

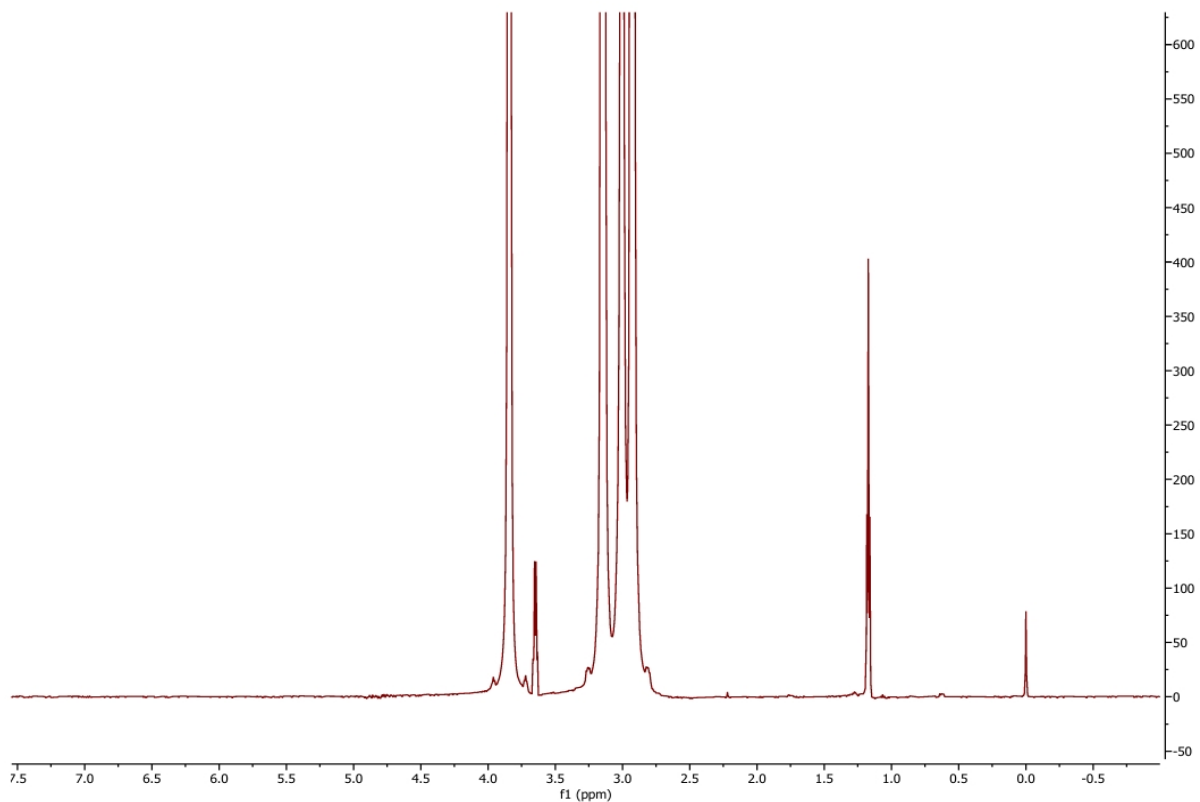


Figure S151. Proton 1D CPMG NMR spectrum of 0.5 mM Ethanol in the presence of *E. coli* lipid vesicles with the addition of 0.5 mM Mn^{2+} collected with a spin-lock time of 50 ms at 298K.

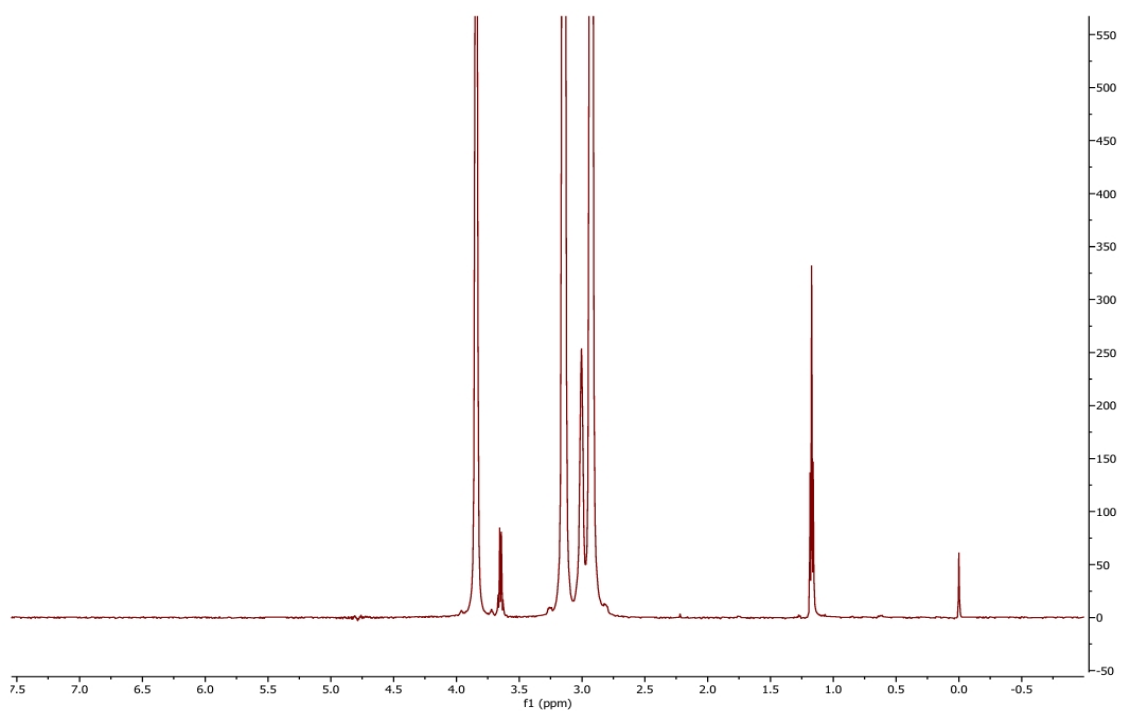


Figure S152. Proton 1D CPMG NMR spectrum of 0.5 mM Ethanol in the presence of *E. coli* lipid vesicles with the addition of 0.5 mM Mn^{2+} collected with a spin-lock time of 150 ms at 298K.

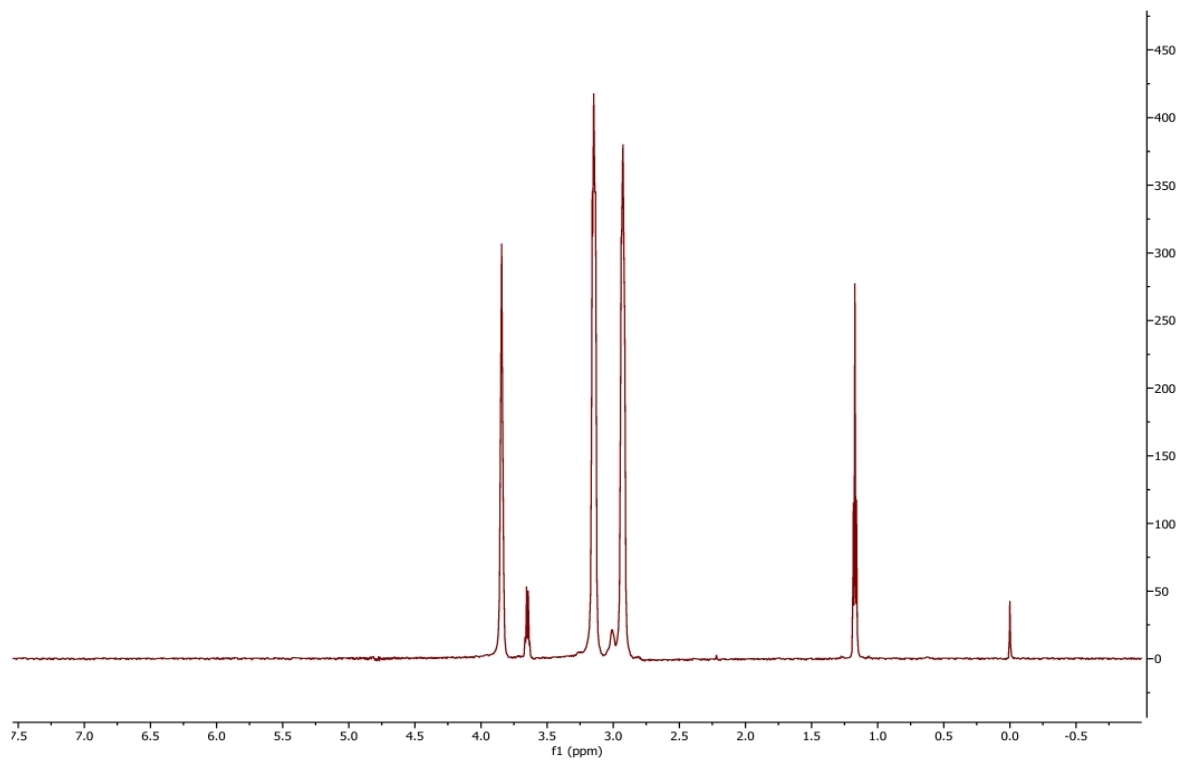


Figure S153. Proton 1D CPMG NMR spectrum of 0.5 mM Ethanol in the presence of *E. coli* lipid vesicles with the addition of 0.5 mM Mn^{2+} collected with a spin-lock time of 300 ms at 298K.

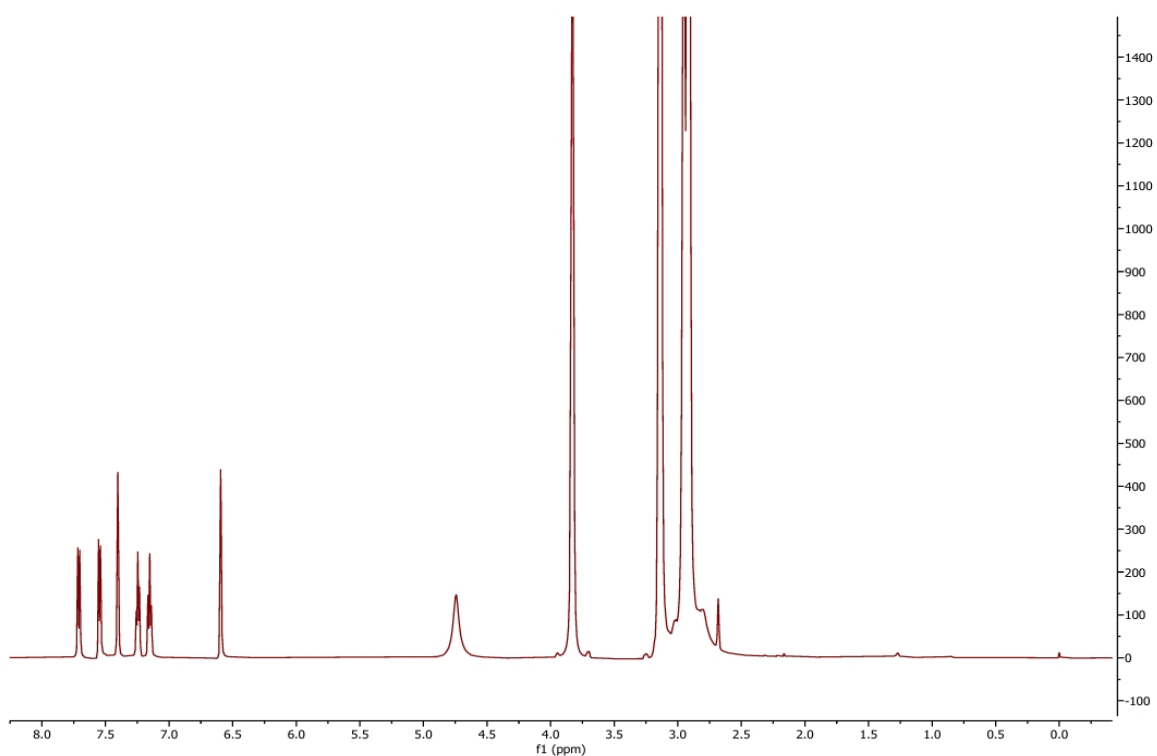


Figure S154. Proton 1D CPMG NMR spectrum of 0.5 mM Indole collected with a spin-lock time of 20 ms at 298K.

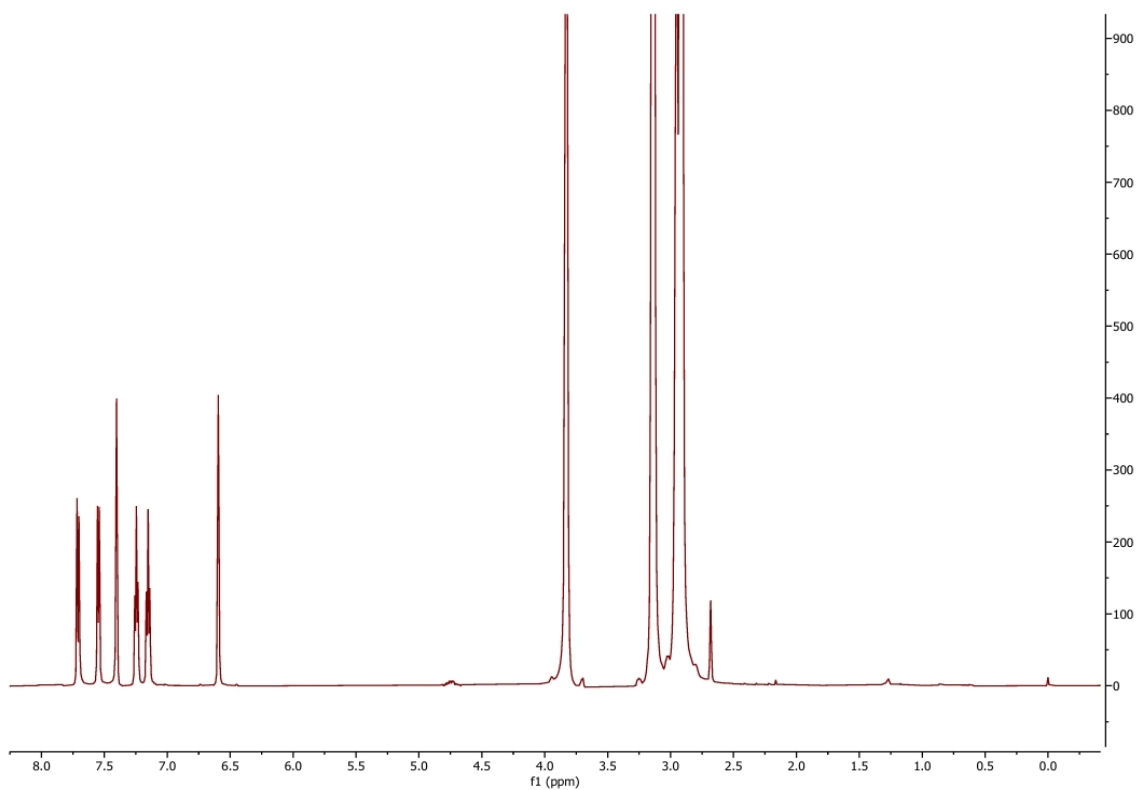


Figure S155. Proton 1D CPMG NMR spectrum of 0.5 mM Indole collected with a spin-lock time of 50 ms at 298K.

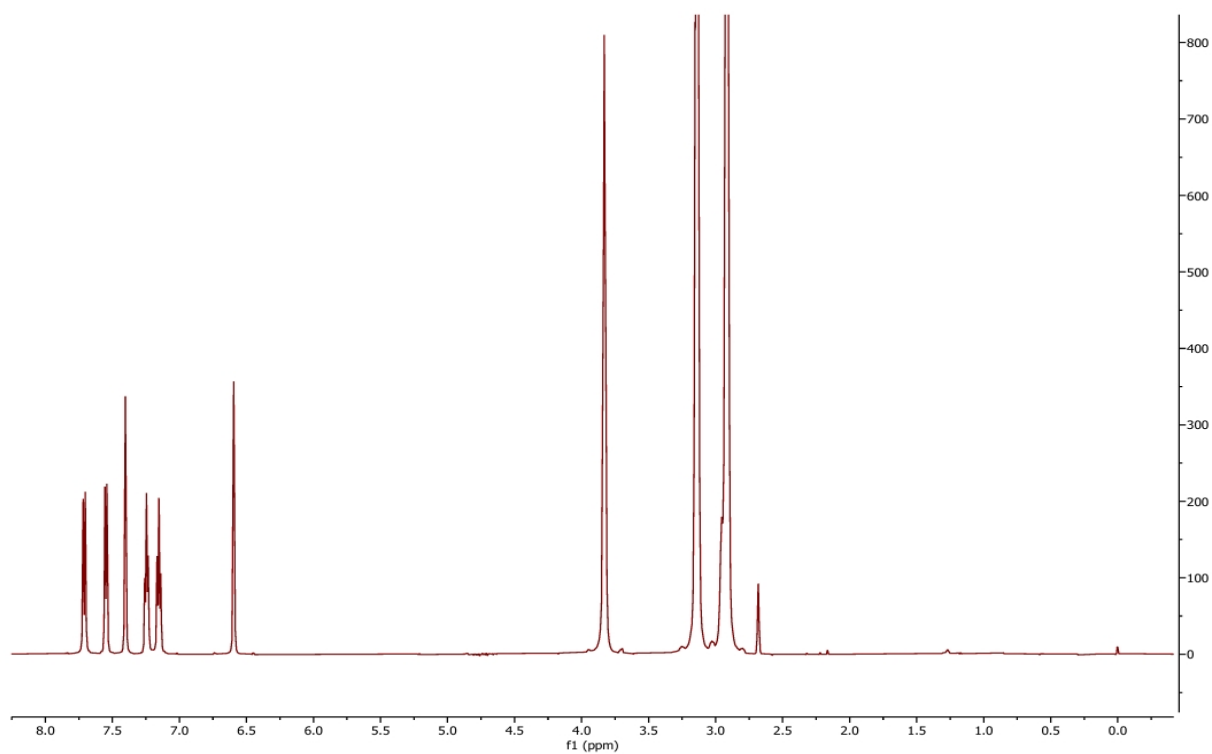


Figure S156. Proton 1D CPMG NMR spectrum of 0.5 mM Indole collected with a spin-lock time of 150 ms at 298K.

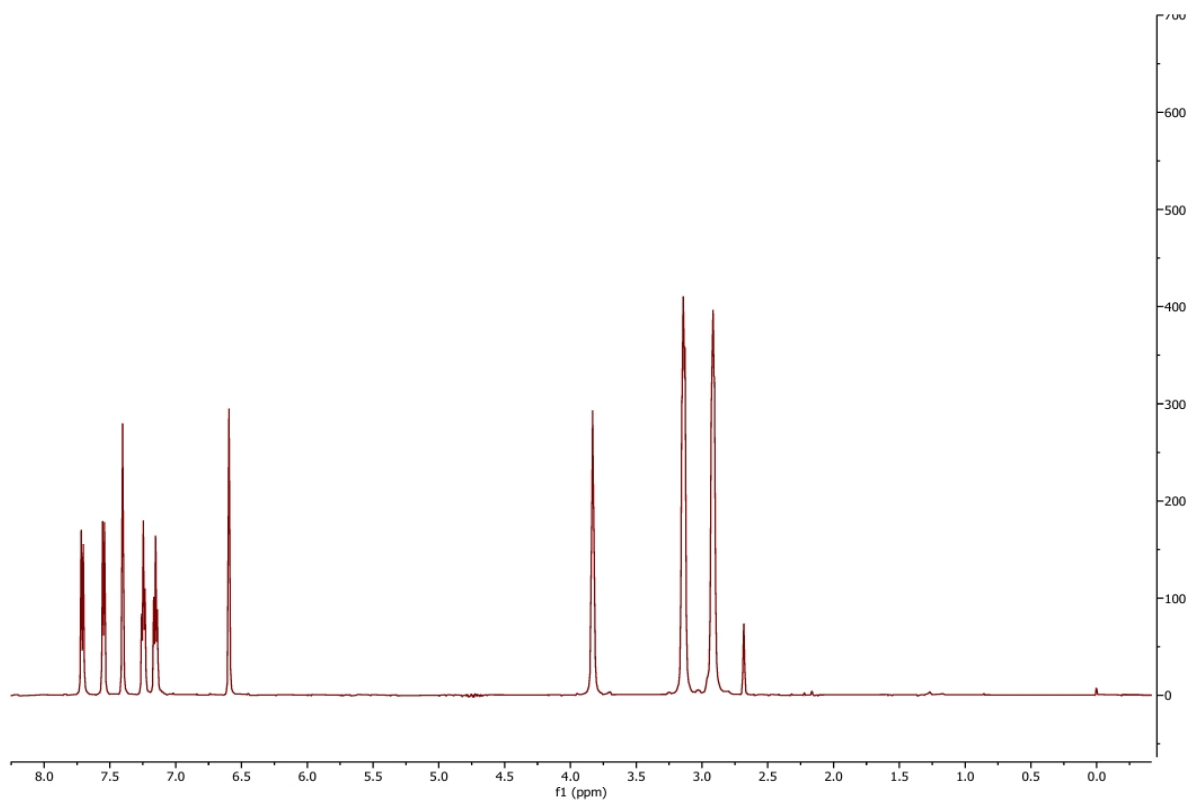


Figure S157. Proton 1D CPMG NMR spectrum of 0.5 mM Indole collected with a spin-lock time of 300 ms at 298K.

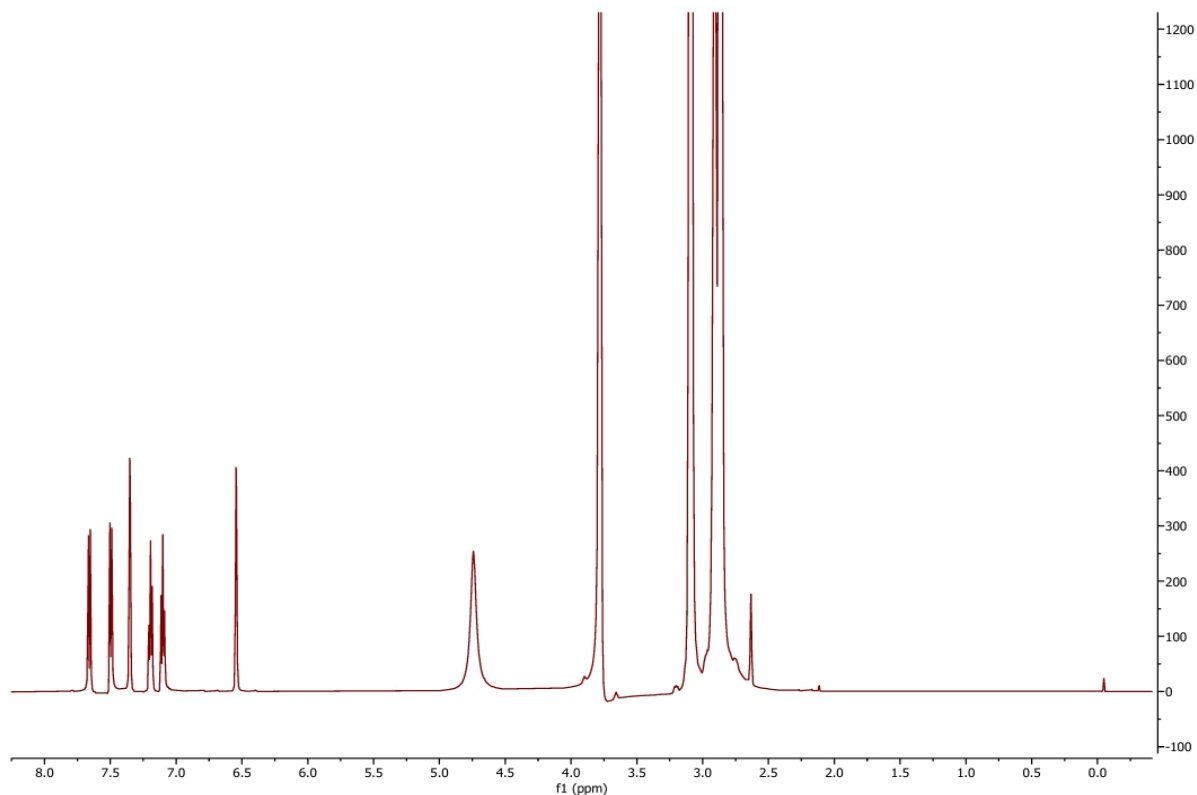


Figure S158. Proton 1D CPMG NMR spectrum of 0.5 mM Indole with the addition of 0.5 mM Mn^{2+} collected with a spin-lock time of 20 ms at 298K.

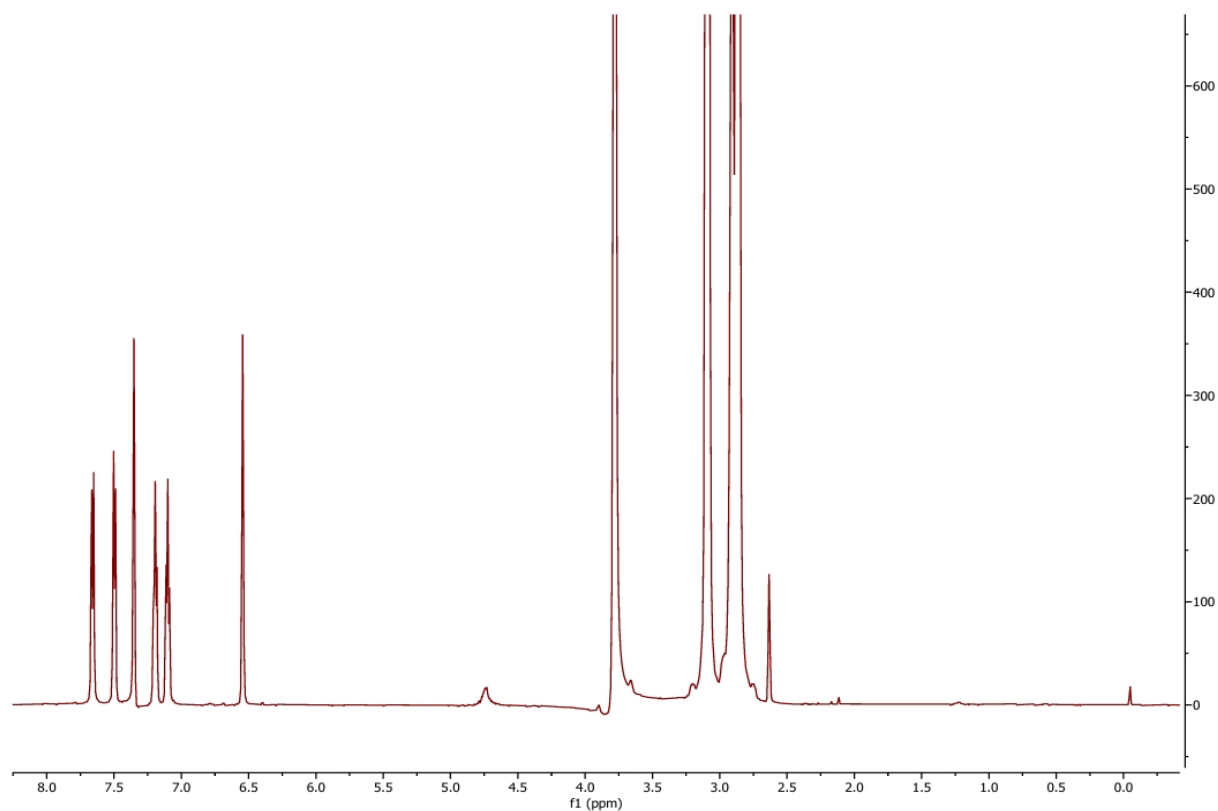


Figure S159. Proton 1D CPMG NMR spectrum of 0.5 mM Indole with the addition of 0.5 mM Mn^{2+} collected with a spin-lock time of 50 ms at 298K.

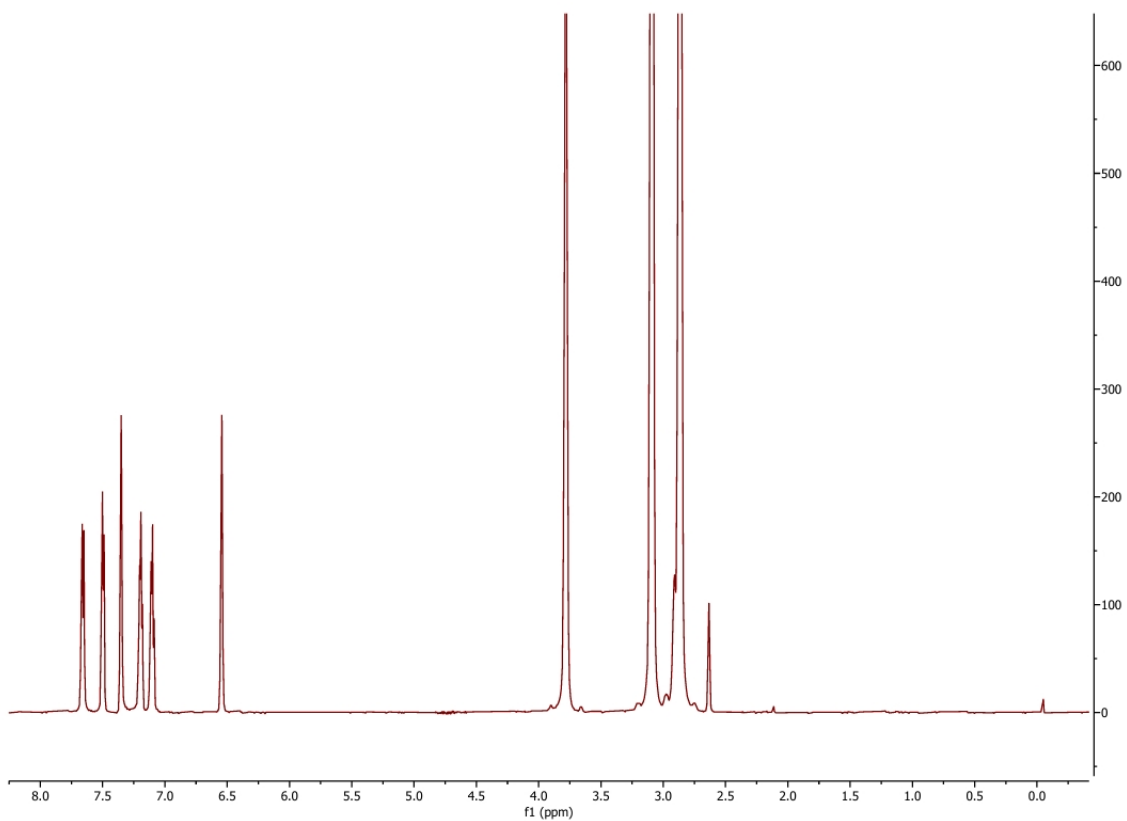


Figure S160. Proton 1D CPMG NMR spectrum of 0.5 mM Indole with the addition of 0.5 mM Mn^{2+} collected with a spin-lock time of 150 ms at 298K.

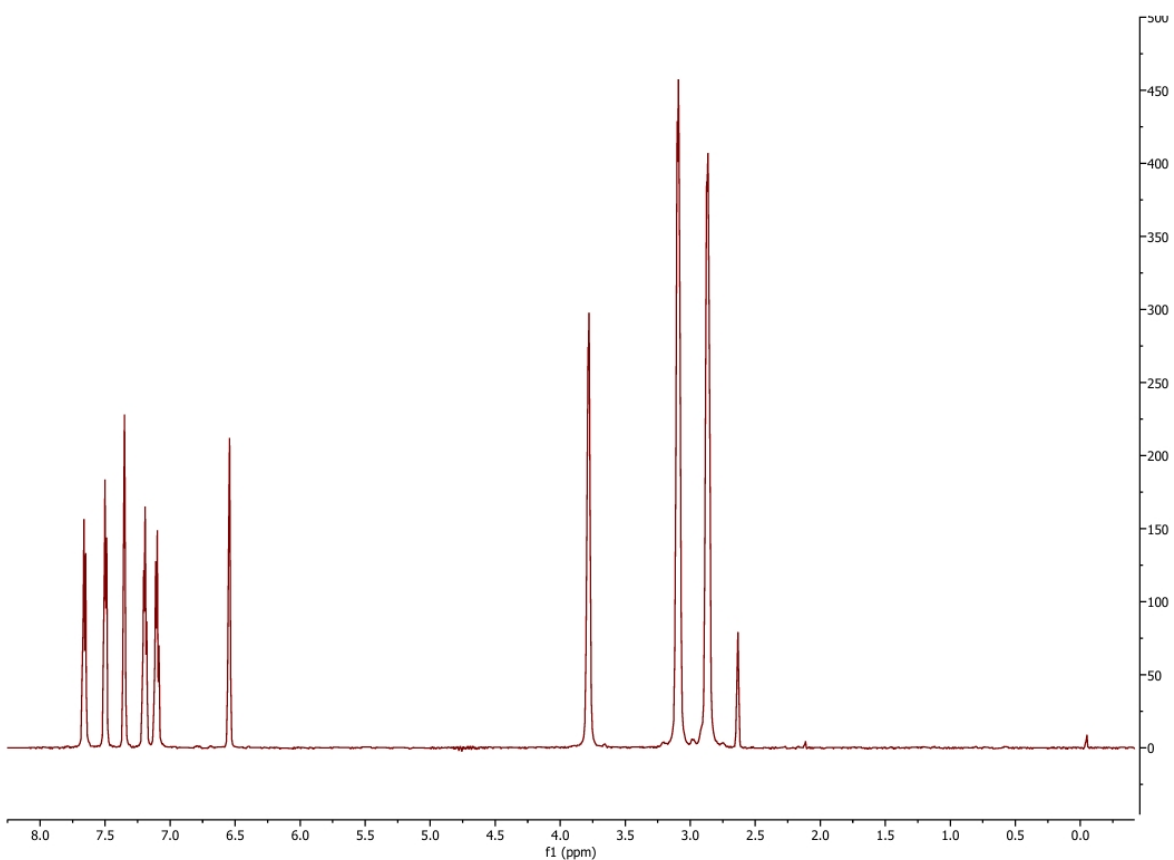


Figure S161. Proton 1D CPMG NMR spectrum of 0.5 mM Indole with the addition of 0.5 mM Mn^{2+} collected with a spin-lock time of 300 ms at 298K.

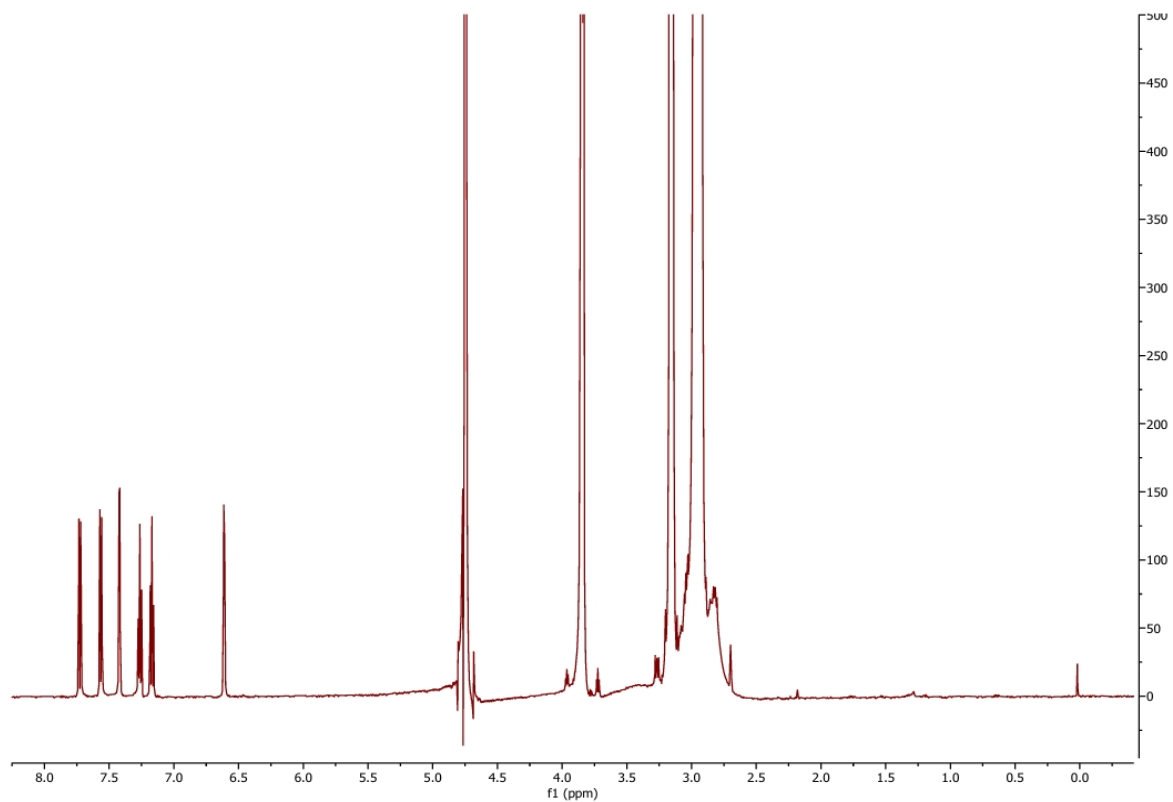


Figure S162. Proton 1D CPMG NMR spectrum of 0.5 mM Indole in the presence of *E. coli* lipid vesicles collected with a spin-lock time of 20 ms at 298K.

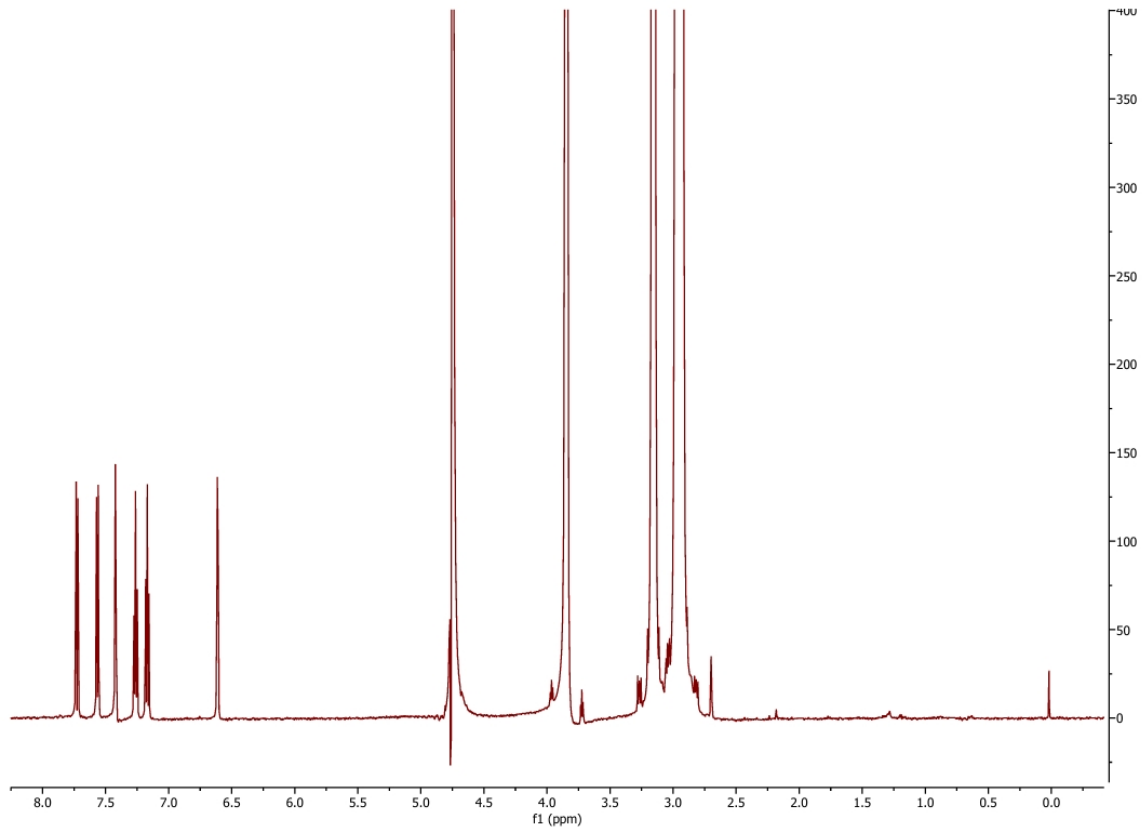


Figure S163. Proton 1D CPMG NMR spectrum of 0.5 mM Indole in the presence of *E. coli* lipid vesicles collected with a spin-lock time of 50 ms at 298K.

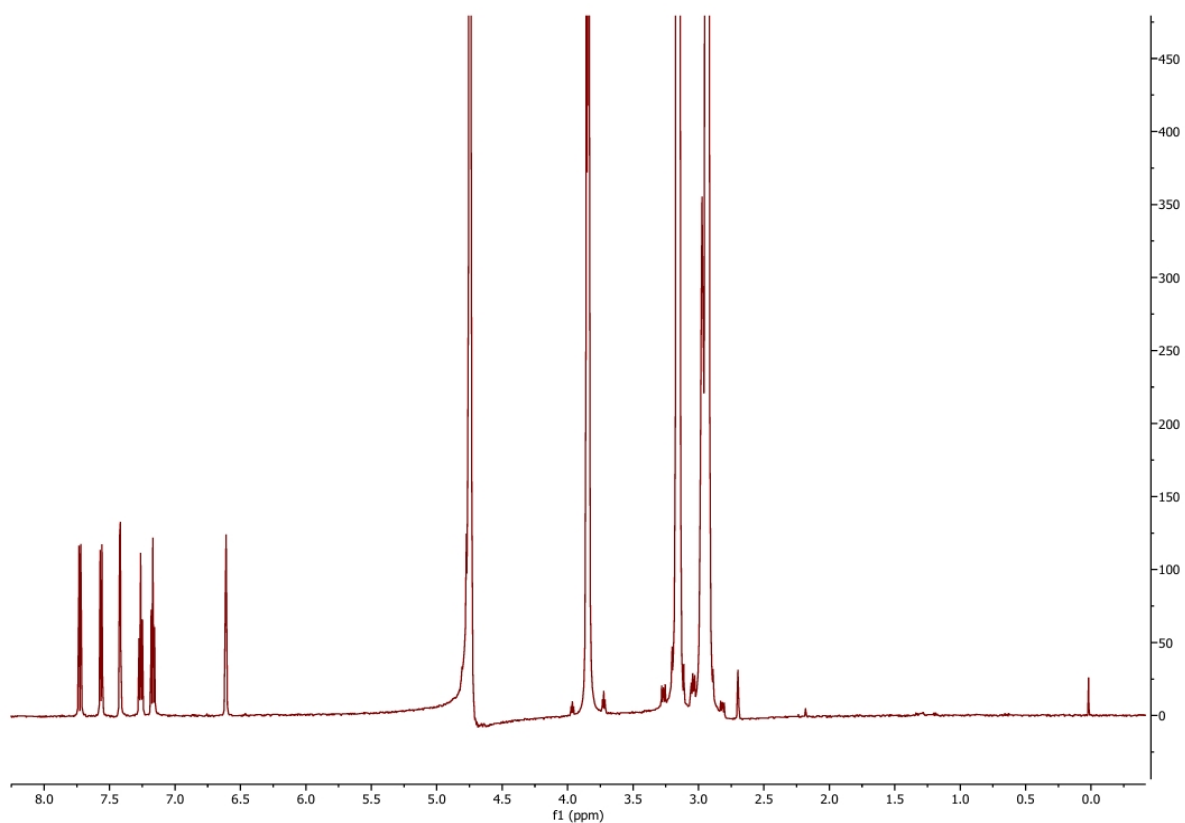


Figure S164. Proton 1D CPMG NMR spectrum of 0.5 mM Indole in the presence of *E. coli* lipid vesicles collected with a spin-lock time of 150 ms at 298K.

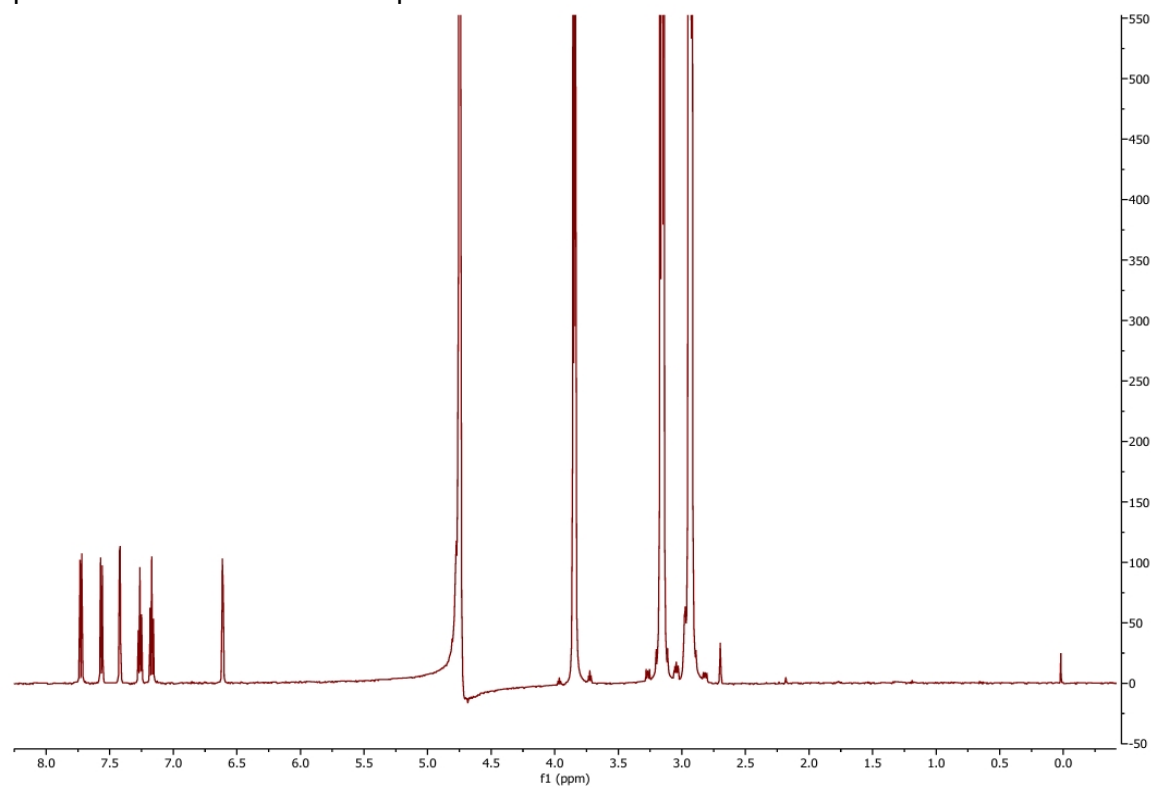


Figure S165. Proton 1D CPMG NMR spectrum of 0.5 mM Indole in the presence of *E. coli* lipid vesicles collected with a spin-lock time of 300 ms at 298K.

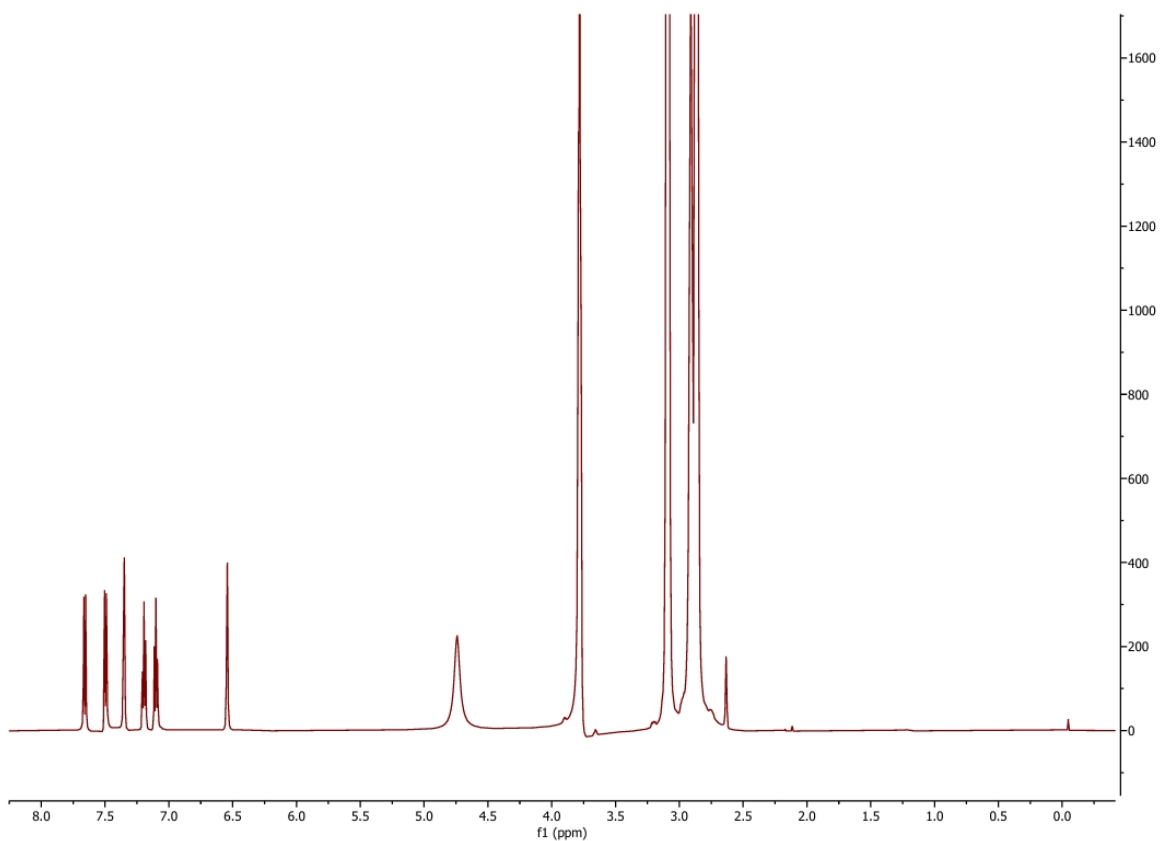


Figure S166. Proton 1D CPMG NMR spectrum of 0.5 mM Indole in the presence of *E. coli* lipid vesicles with the addition of 0.5 mM Mn^{2+} collected with a spin-lock time of 20 ms at 298K.

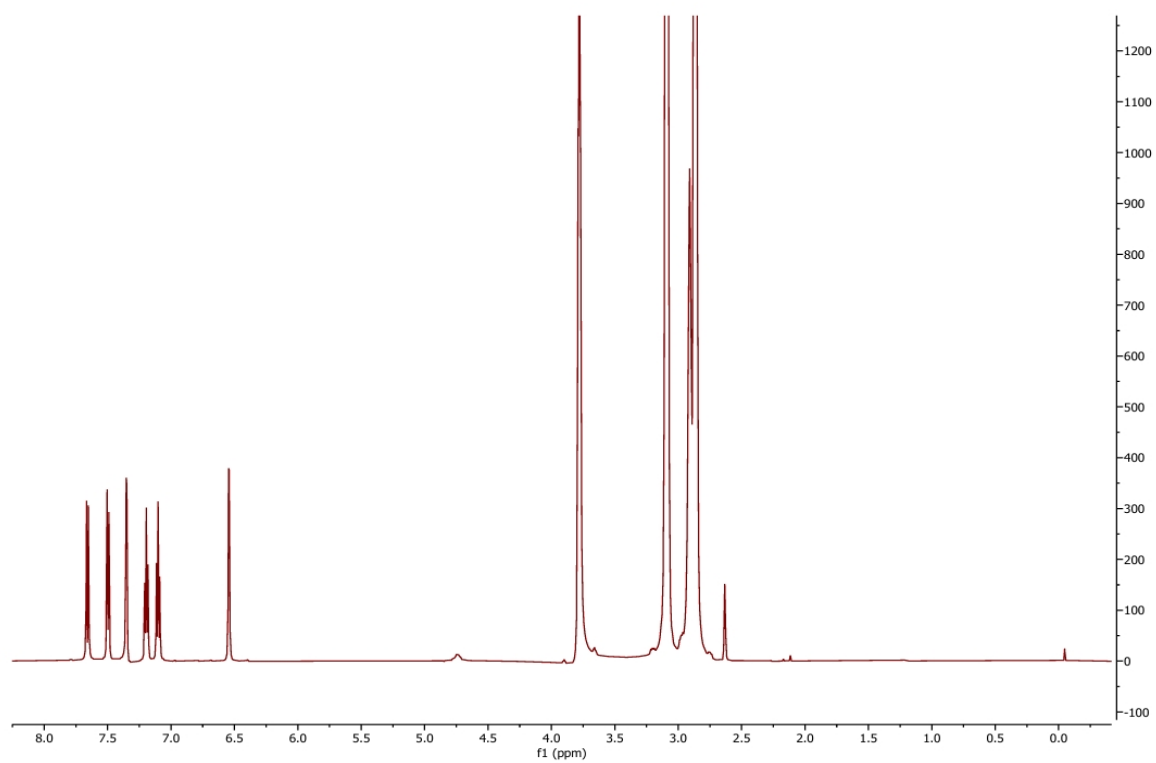


Figure S167. Proton 1D CPMG NMR spectrum of 0.5 mM Indole in the presence of *E. coli* lipid vesicles with the addition of 0.5 mM Mn^{2+} collected with a spin-lock time of 50 ms at 298K.

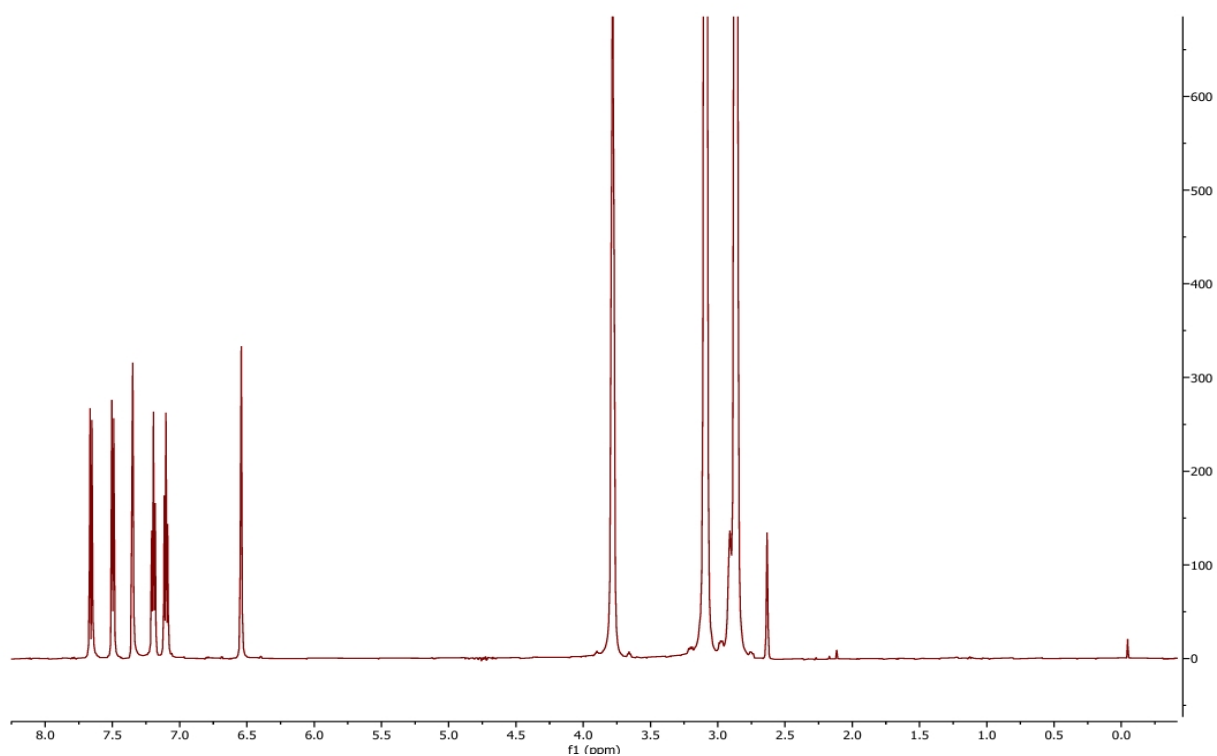


Figure S168. Proton 1D CPMG NMR spectrum of 0.5 mM Indole in the presence of *E. coli* lipid vesicles with the addition of 0.5 mM Mn^{2+} collected with a spin-lock time of 150 ms at 298K.

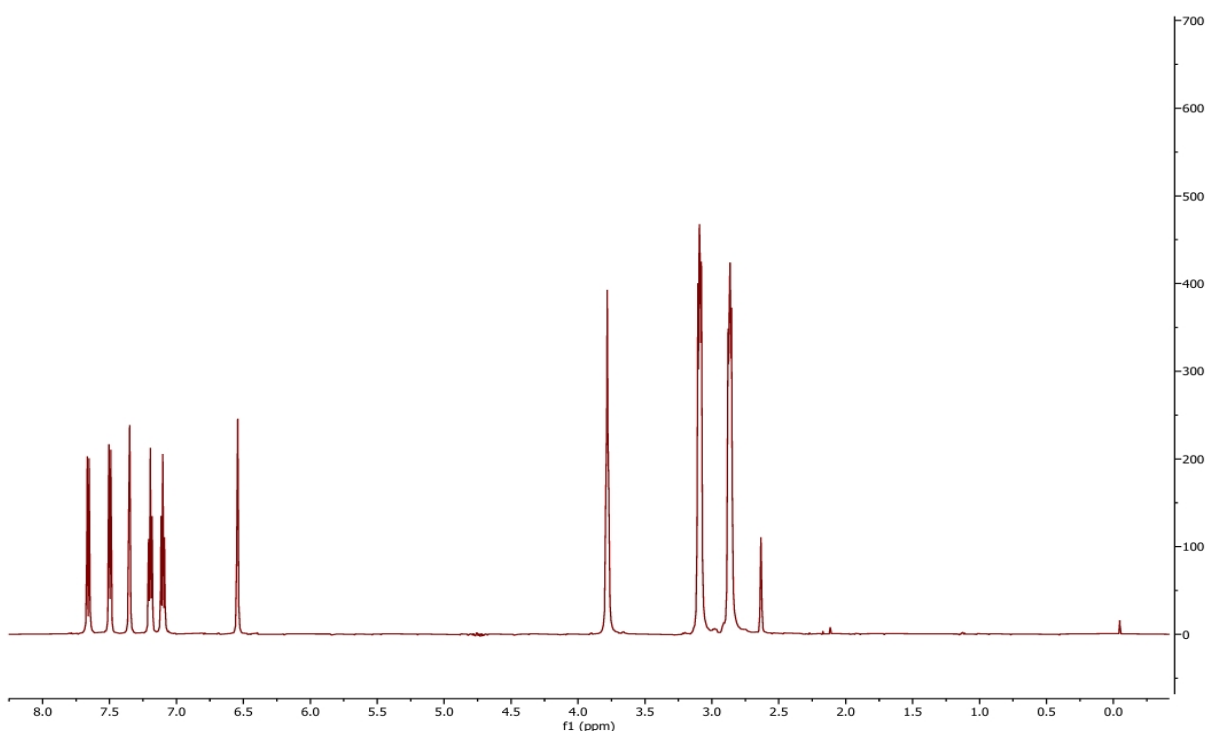


Figure S169. Proton 1D CPMG NMR spectrum of 0.5 mM Indole in the presence of *E. coli* lipid vesicles with the addition of 0.5 mM Mn^{2+} collected with a spin-lock time of 300 ms at 298K.

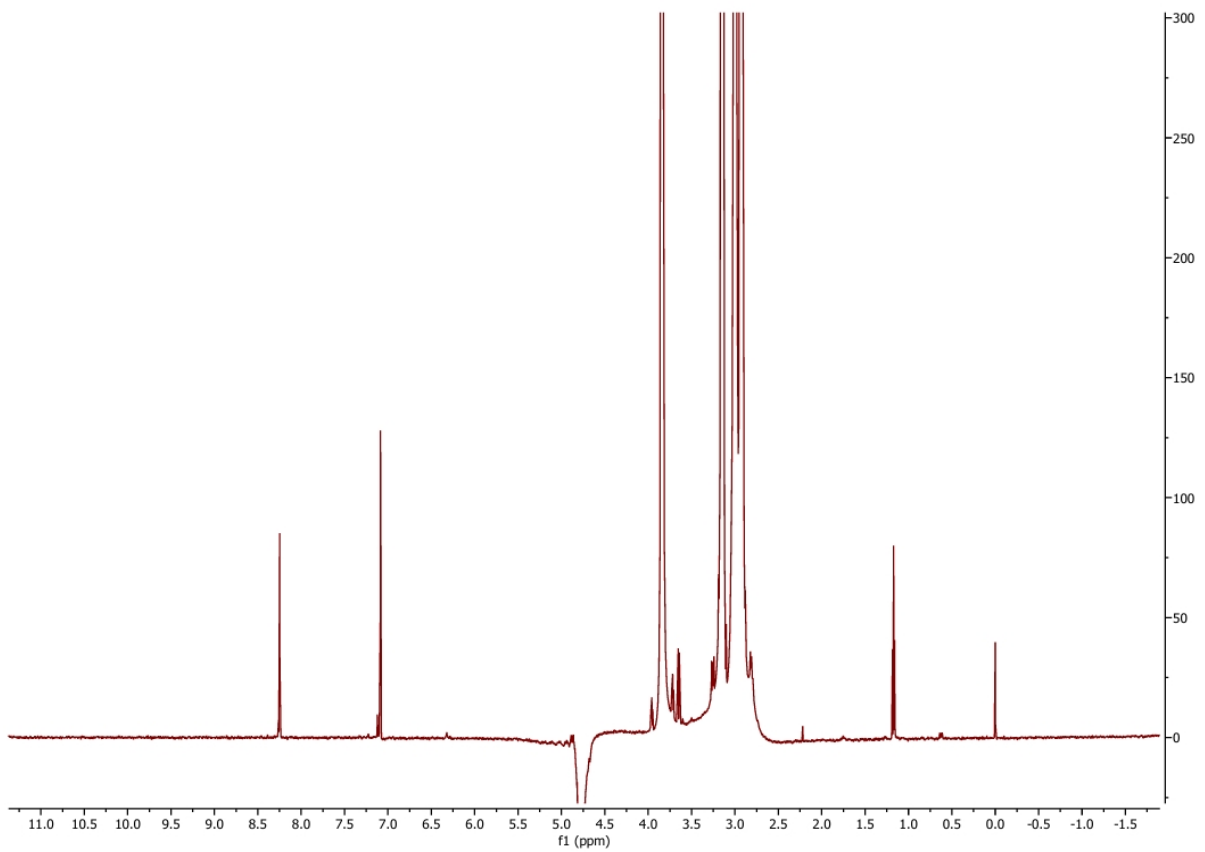


Figure S170. Proton 1D CPMG NMR spectrum of 0.5 mM Hydrochlorothiazide collected with a spin-lock time of 20 ms at 298K.

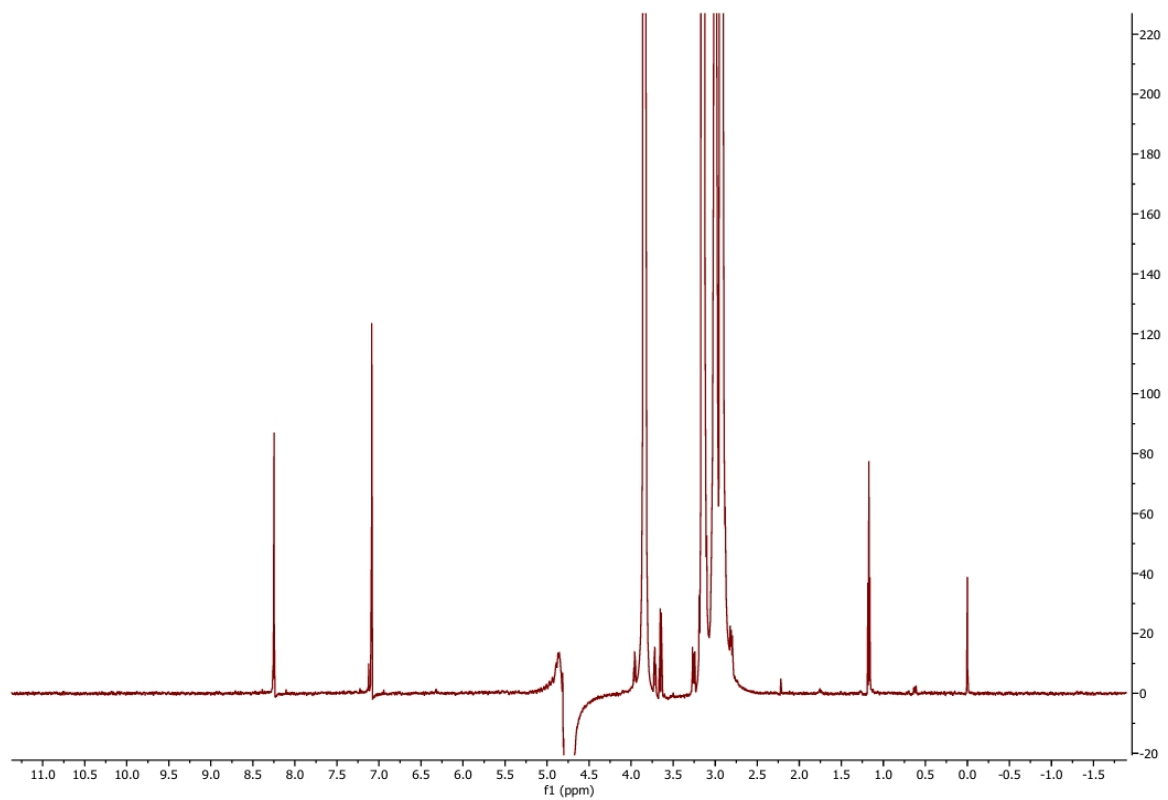


Figure S171. Proton 1D CPMG NMR spectrum of 0.5 mM Hydrochlorothiazide collected with a spin-lock time of 50 ms at 298K.

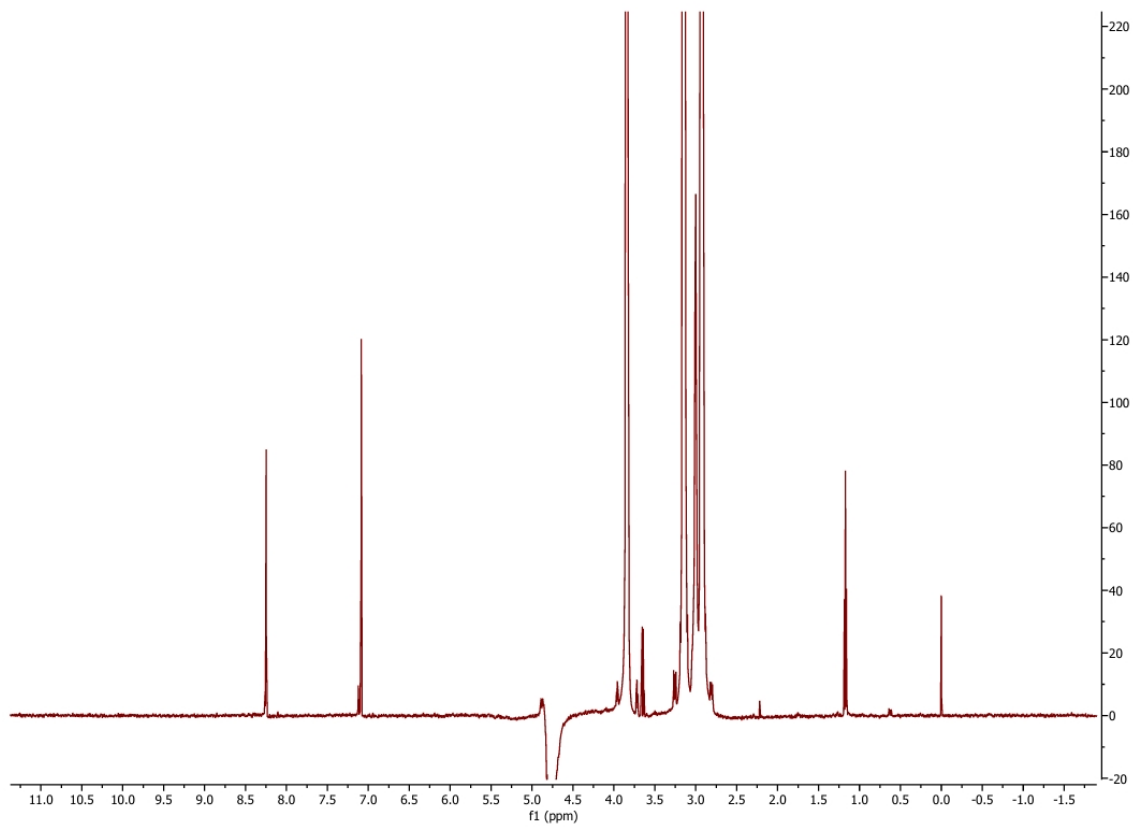


Figure S172. Proton 1D CPMG NMR spectrum of 0.5 mM Hydrochlorothiazide collected with a spin-lock time of 150 ms at 298K.

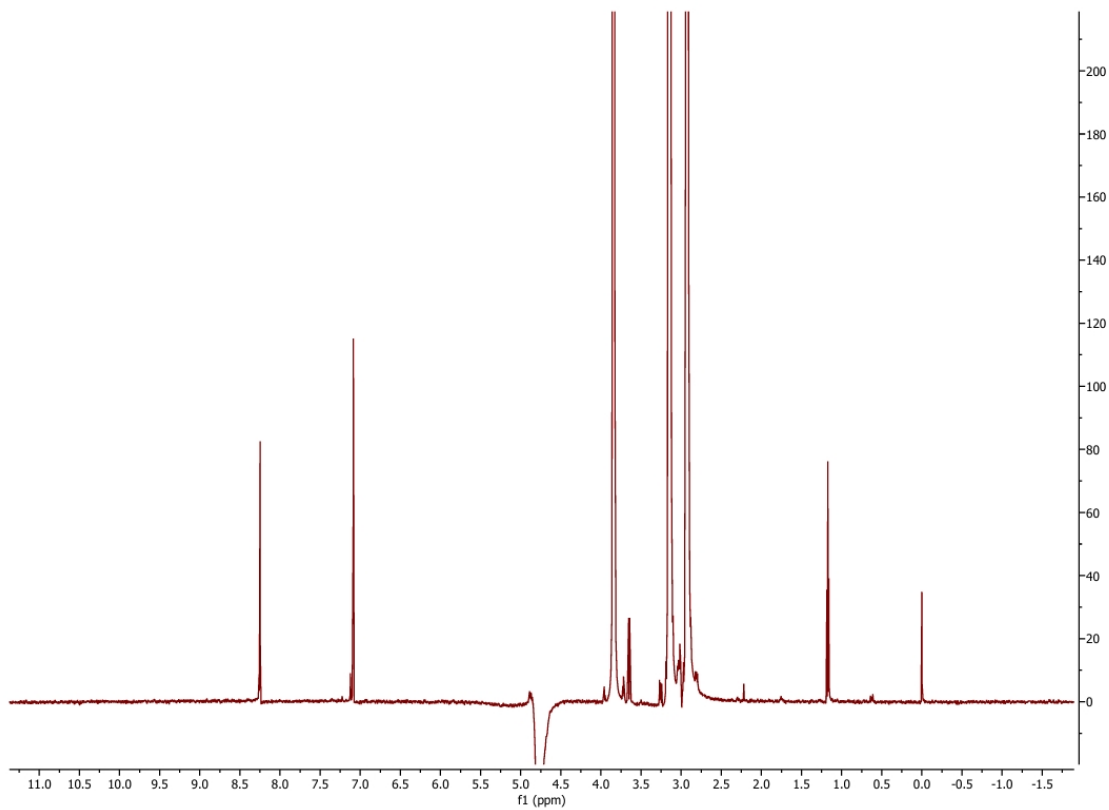


Figure S173. Proton 1D CPMG NMR spectrum of 0.5 mM Hydrochlorothiazide collected with a spin-lock time of 300 ms at 298K.

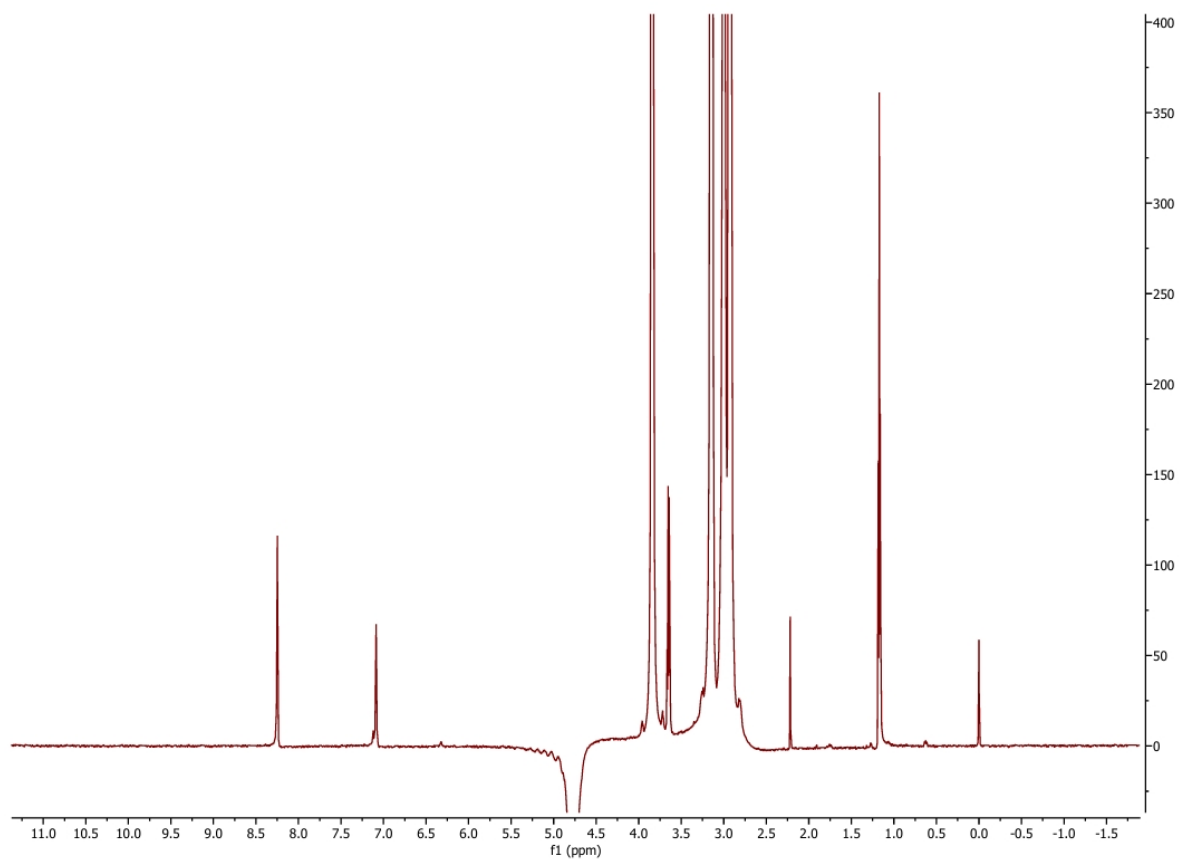


Figure S174. Proton 1D CPMG NMR spectrum of 0.5 mM Hydrochlorothiazide with the addition of 1 mM Gadodiamide collected with a spin-lock time of 20 ms at 298K.

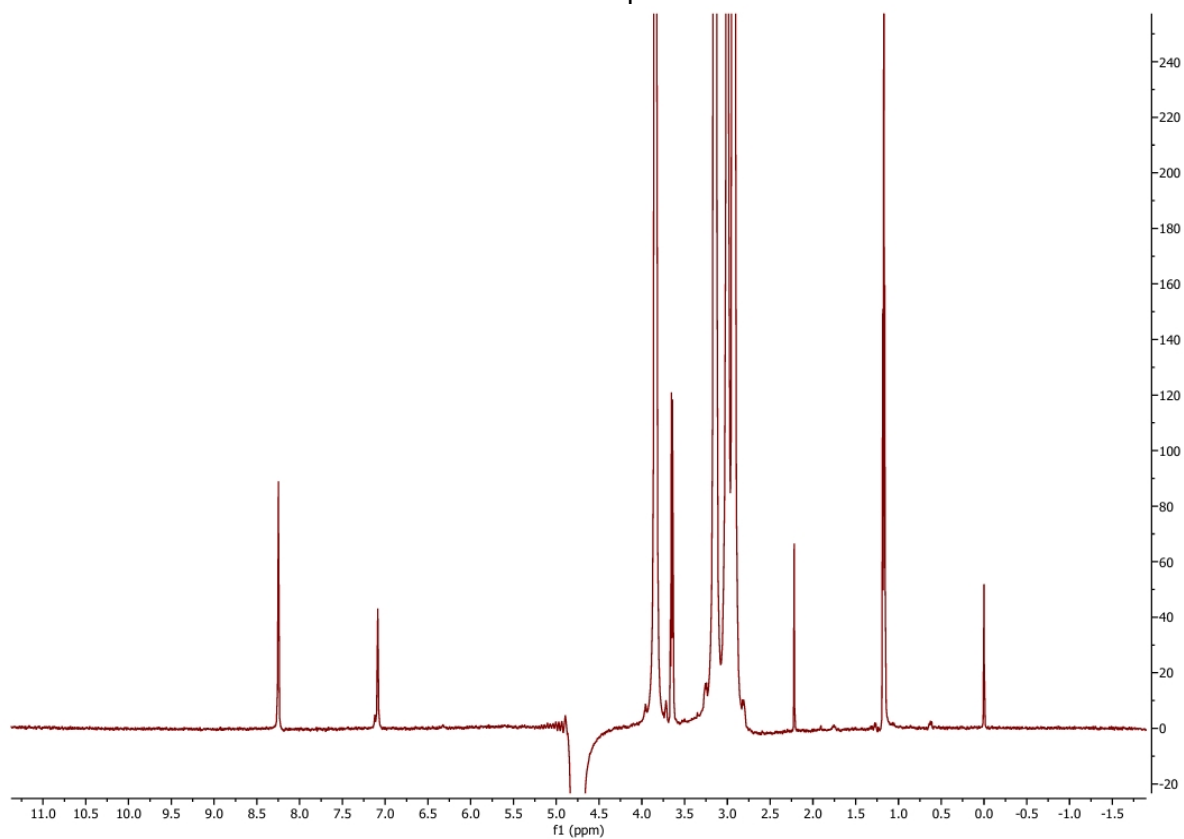


Figure S175. Proton 1D CPMG NMR spectrum of 0.5 mM Hydrochlorothiazide with the addition of 1 mM Gadodiamide collected with a spin-lock time of 50 ms at 298K.

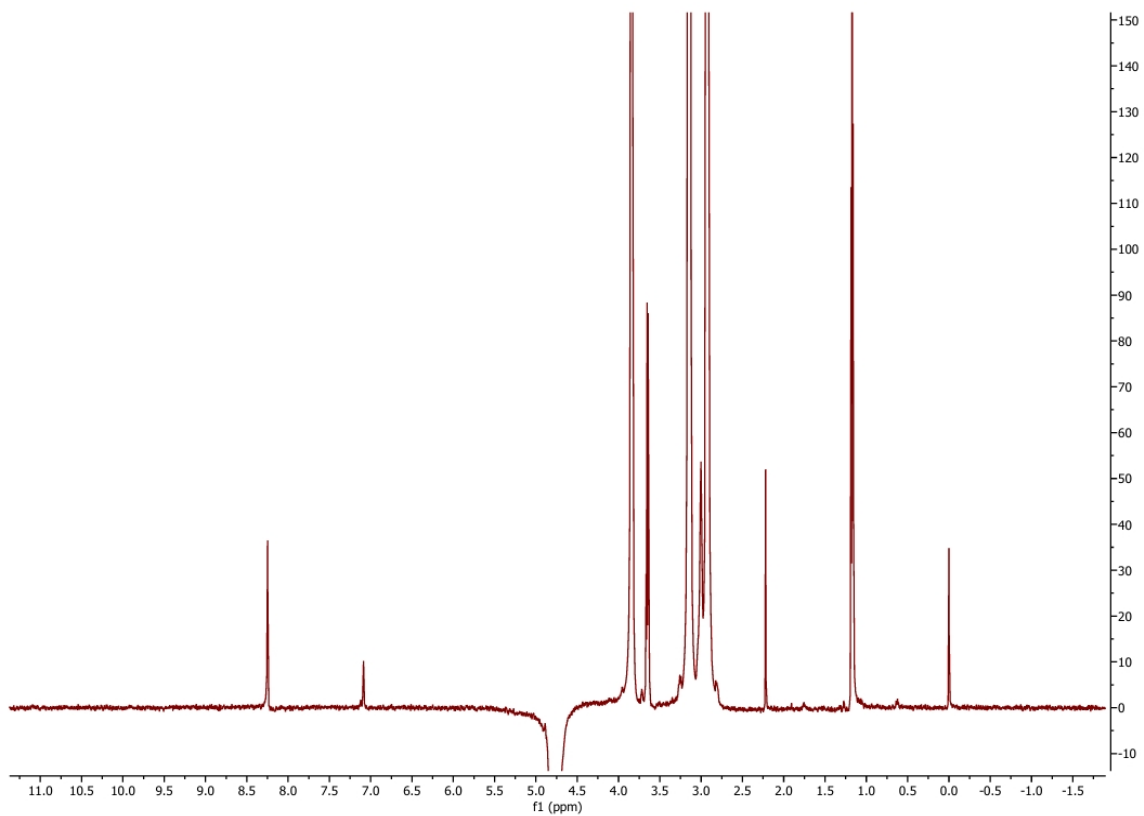


Figure S176. Proton 1D CPMG NMR spectrum of 0.5 mM Hydrochlorothiazide with the addition of 1 mM Gadodiamide collected with a spin-lock time of 150 ms at 298K.

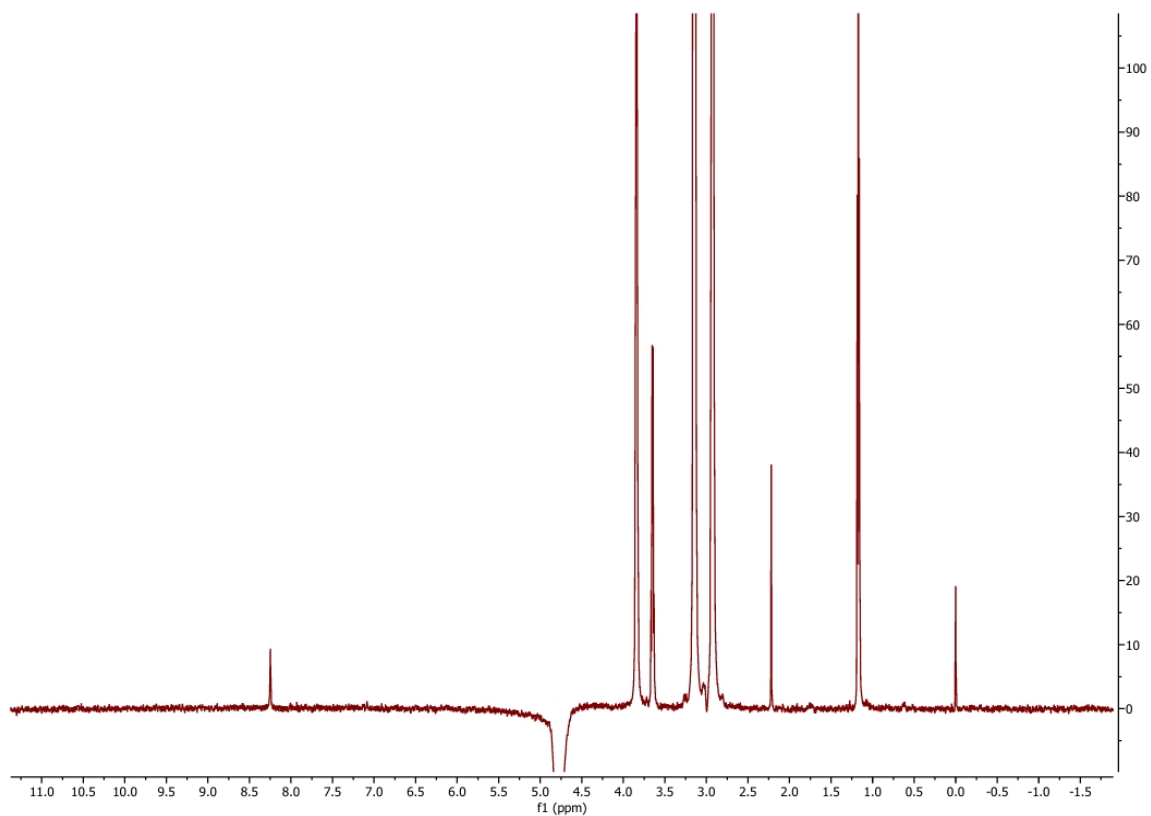


Figure S177. Proton 1D CPMG NMR spectrum of 0.5 mM Hydrochlorothiazide with the addition of 1 mM Gadodiamide collected with a spin-lock time of 300 ms at 298K.

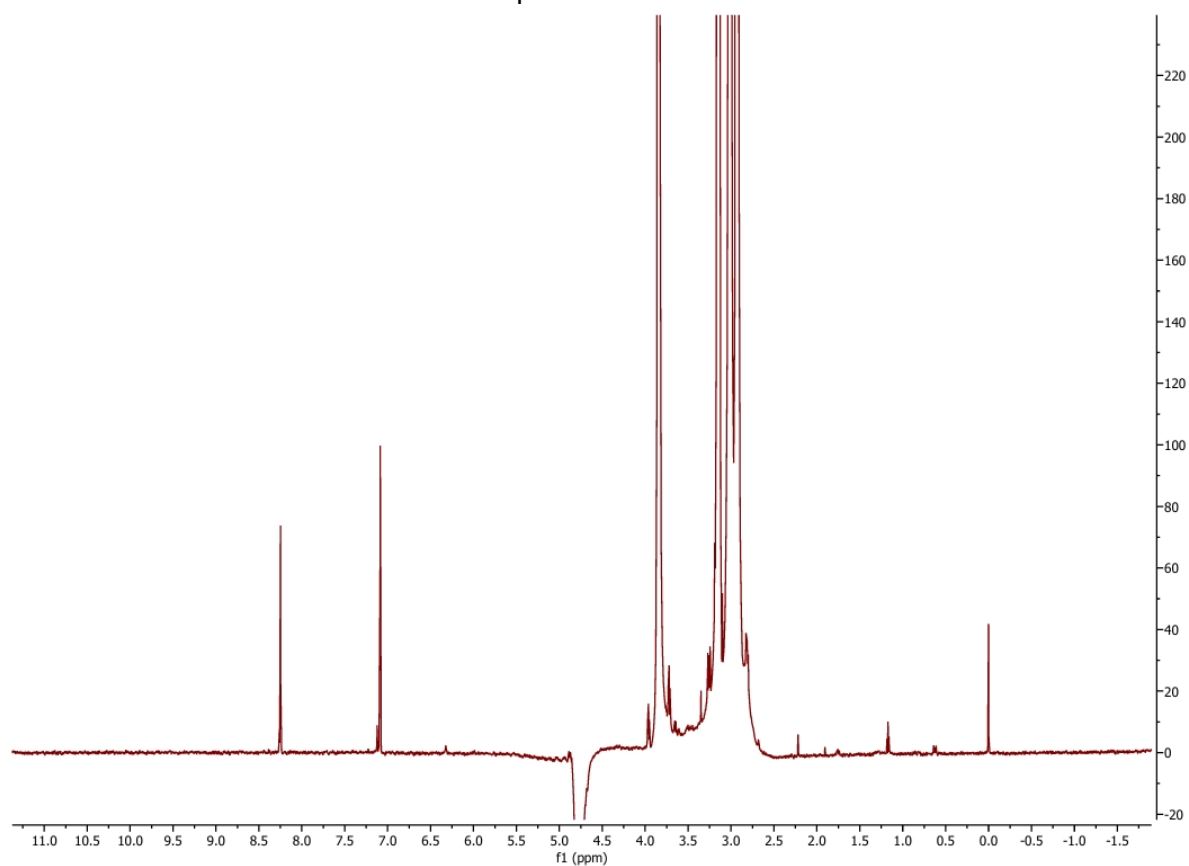


Figure S178. Proton 1D CPMG NMR spectrum of 0.5 mM Hydrochlorothiazide in the presence of *E. coli* lipid vesicles collected with a spin-lock time of 20 ms at 298K.

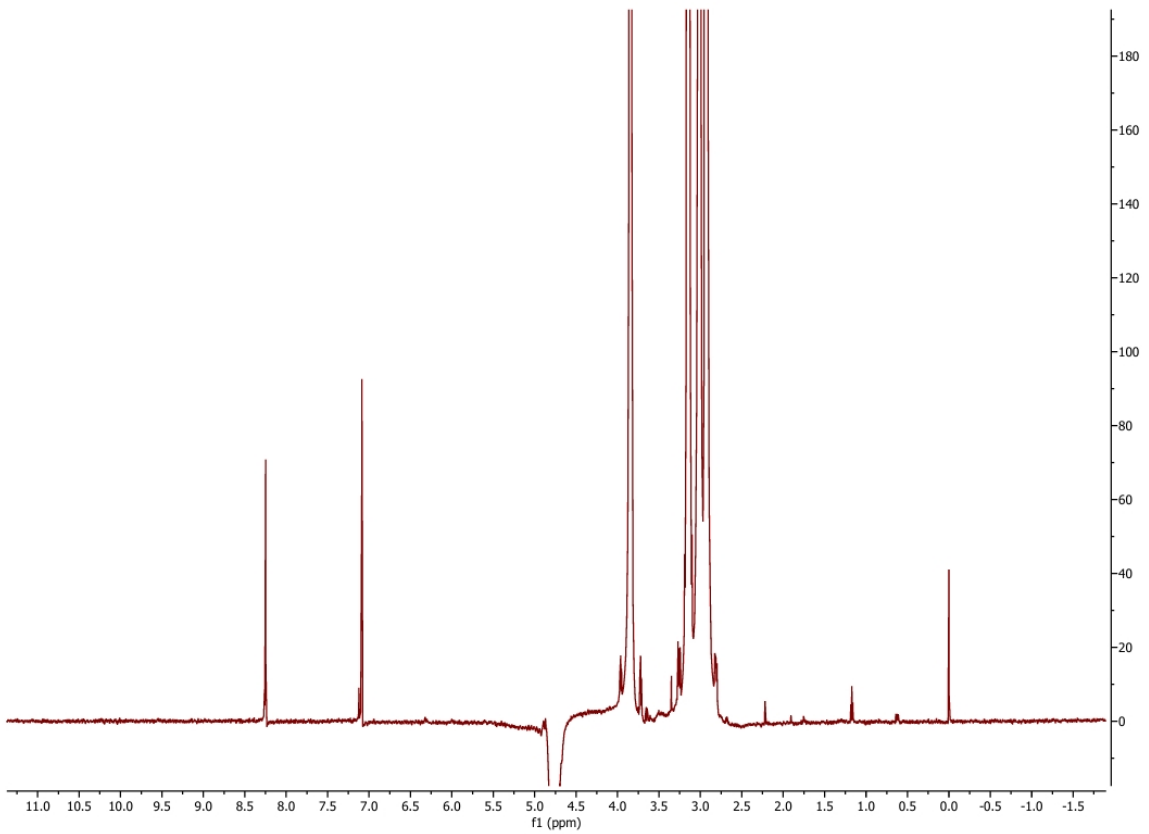


Figure S179. Proton 1D CPMG NMR spectrum of 0.5 mM Hydrochlorothiazide in the presence of *E. coli* lipid vesicles collected with a spin-lock time of 50 ms at 298K.

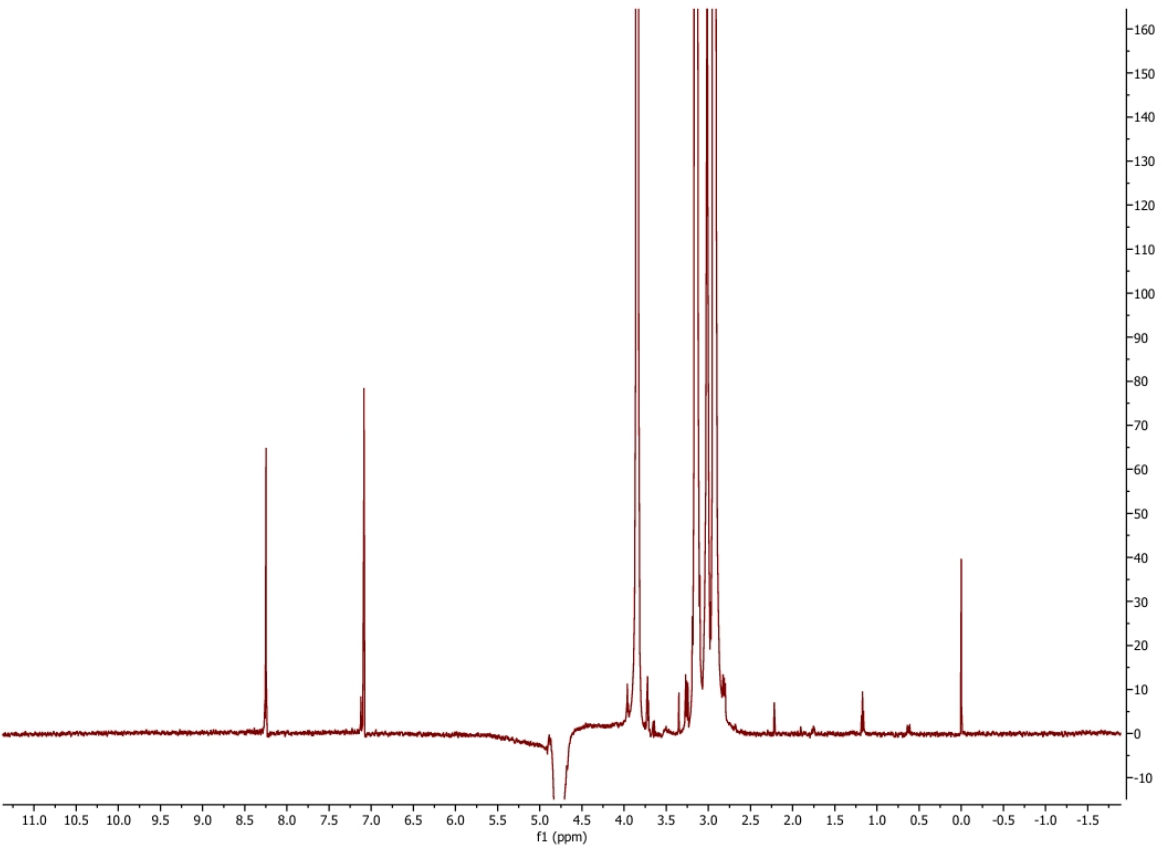
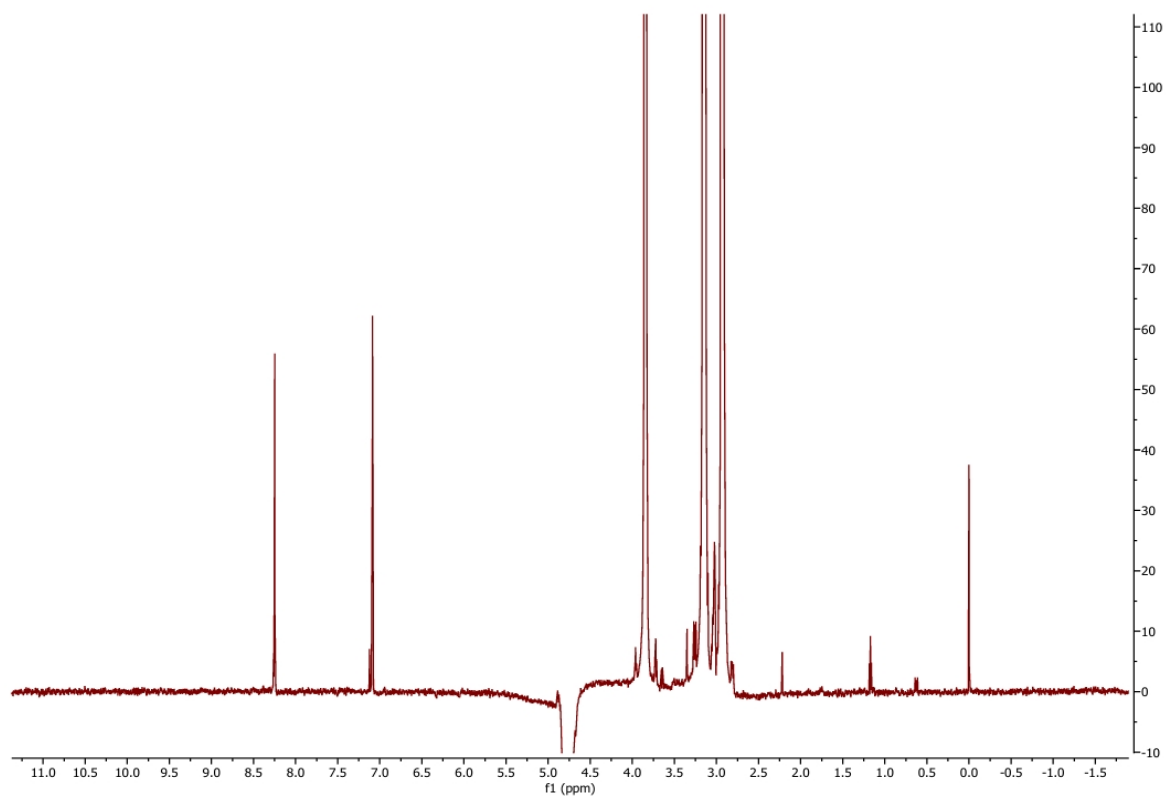


Figure S180. Proton 1D CPMG NMR spectrum of 0.5 mM Hydrochlorothiazide in the presence of *E. coli* lipid vesicles collected with a spin-lock time of 150 ms at 298K.



F

Figure S181. Proton 1D CPMG NMR spectrum of 0.5 mM Hydrochlorothiazide in the presence of *E. coli* lipid vesicles collected with a spin-lock time of 300 ms at 298K.

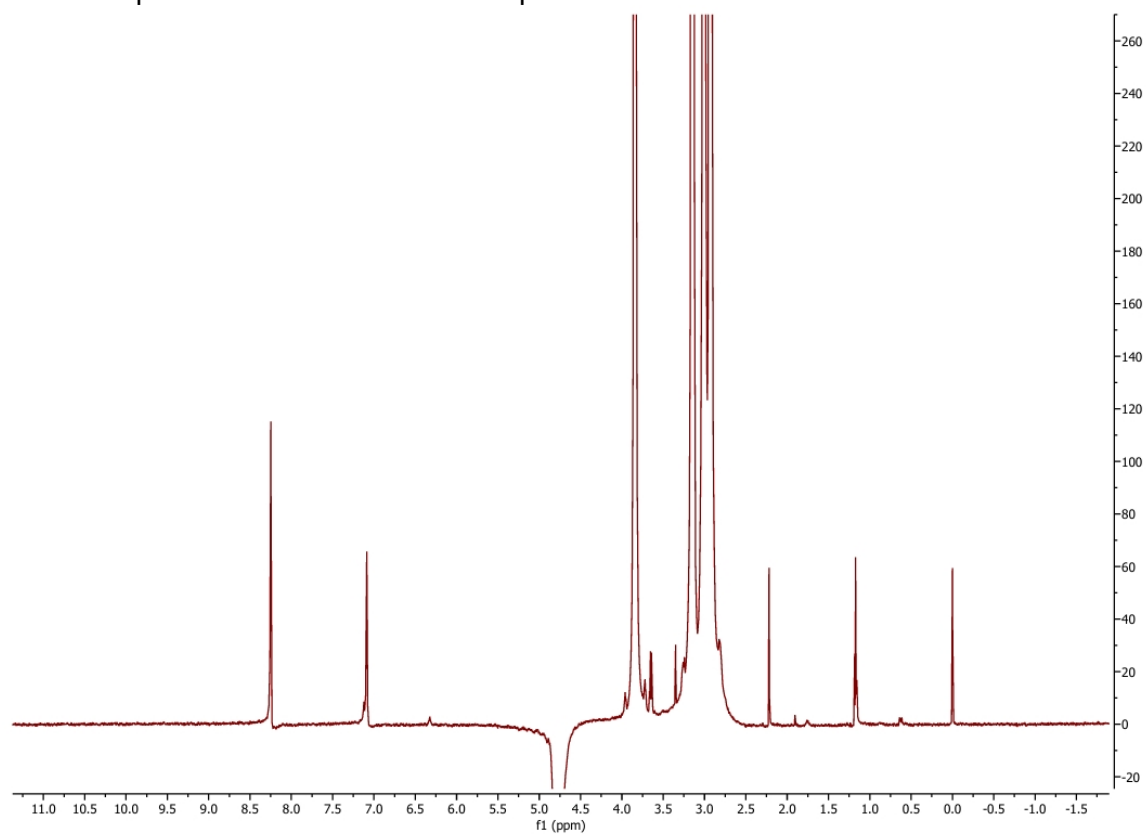


Figure S182. Proton 1D CPMG NMR spectrum of 0.5 mM Hydrochlorothiazide in the presence of *E. coli* lipid vesicles with the addition of 1 mM Gadodiamide collected with a spin-lock time of 20 ms at 298K.

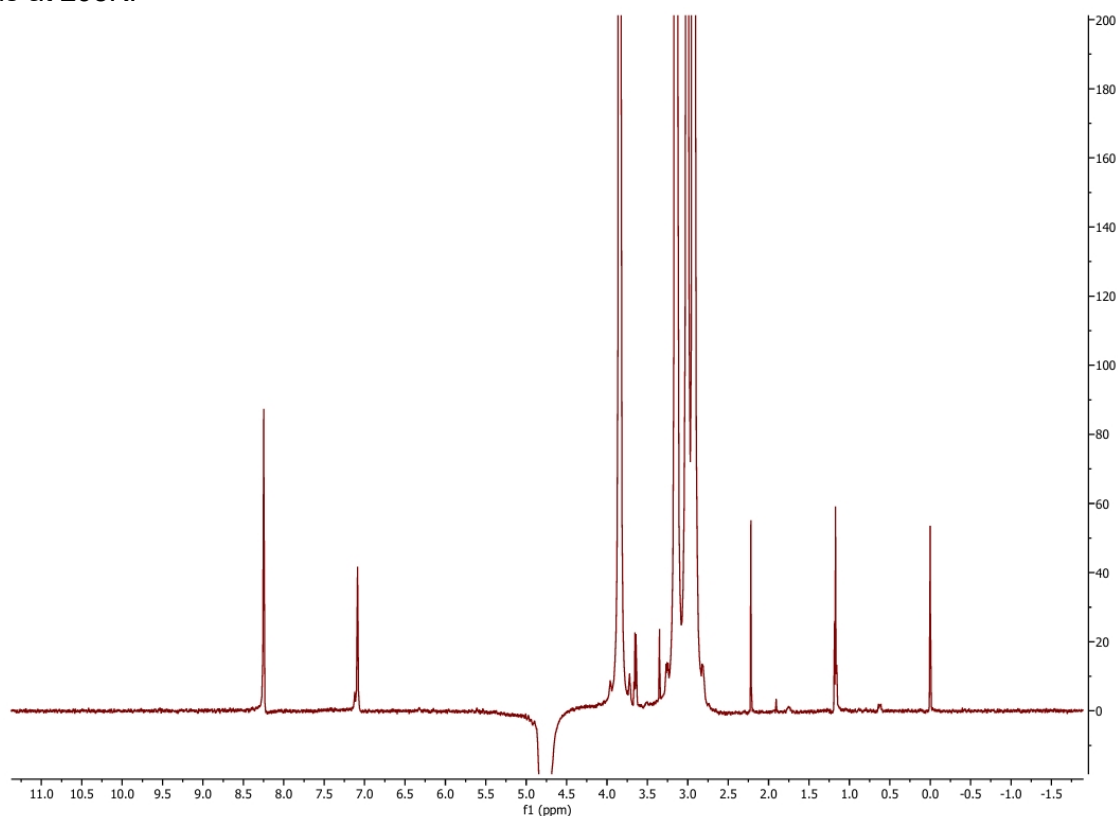


Figure S183. Proton 1D CPMG NMR spectrum of 0.5 mM Hydrochlorothiazide in the presence of *E. coli* lipid vesicles with the addition of 1 mM Gadodiamide collected with a spin-lock time of 50 ms at 298K.

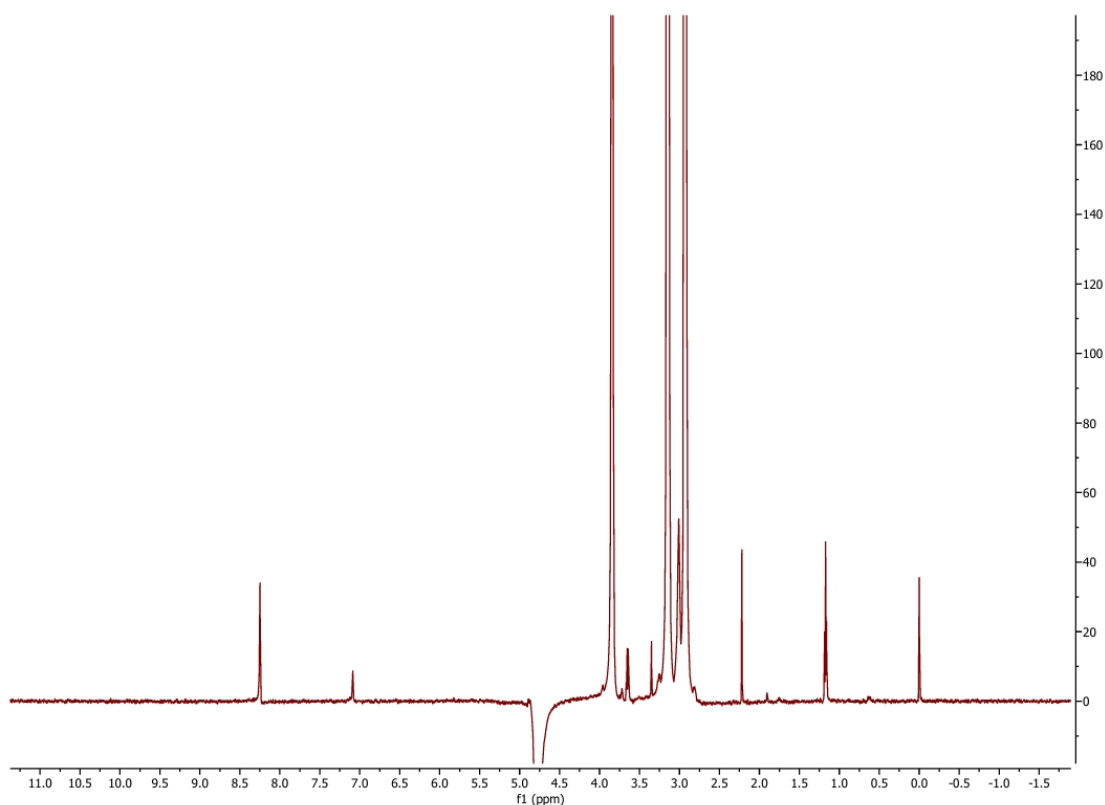


Figure S184. Proton 1D CPMG NMR spectrum of 0.5 mM Hydrochlorothiazide in the presence of *E. coli* lipid vesicles with the addition of 1 mM Gadodiamide collected with a spin-lock time of 150 ms at 298K.

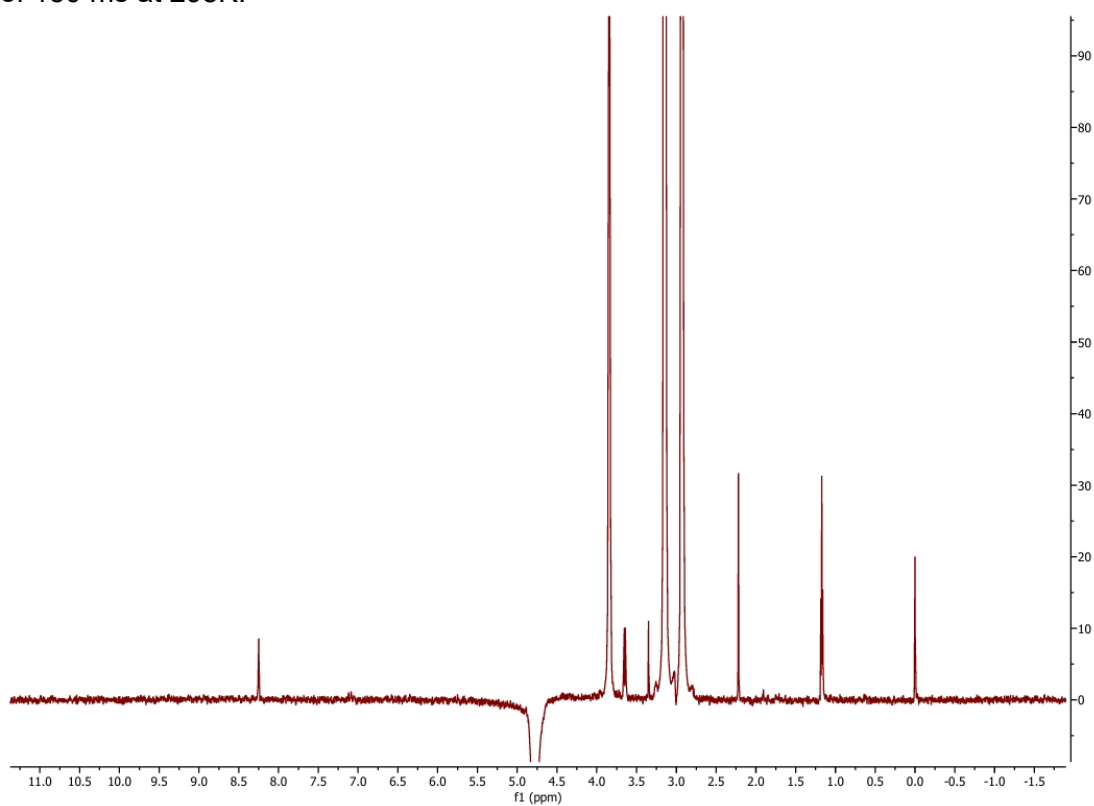


Figure S185. Proton 1D CPMG NMR spectrum of 0.5 mM Hydrochlorothiazide in the presence of *E. coli* lipid vesicles with the addition of 1 mM Gadodiamide collected with a spin-lock time of 300 ms at 298K.

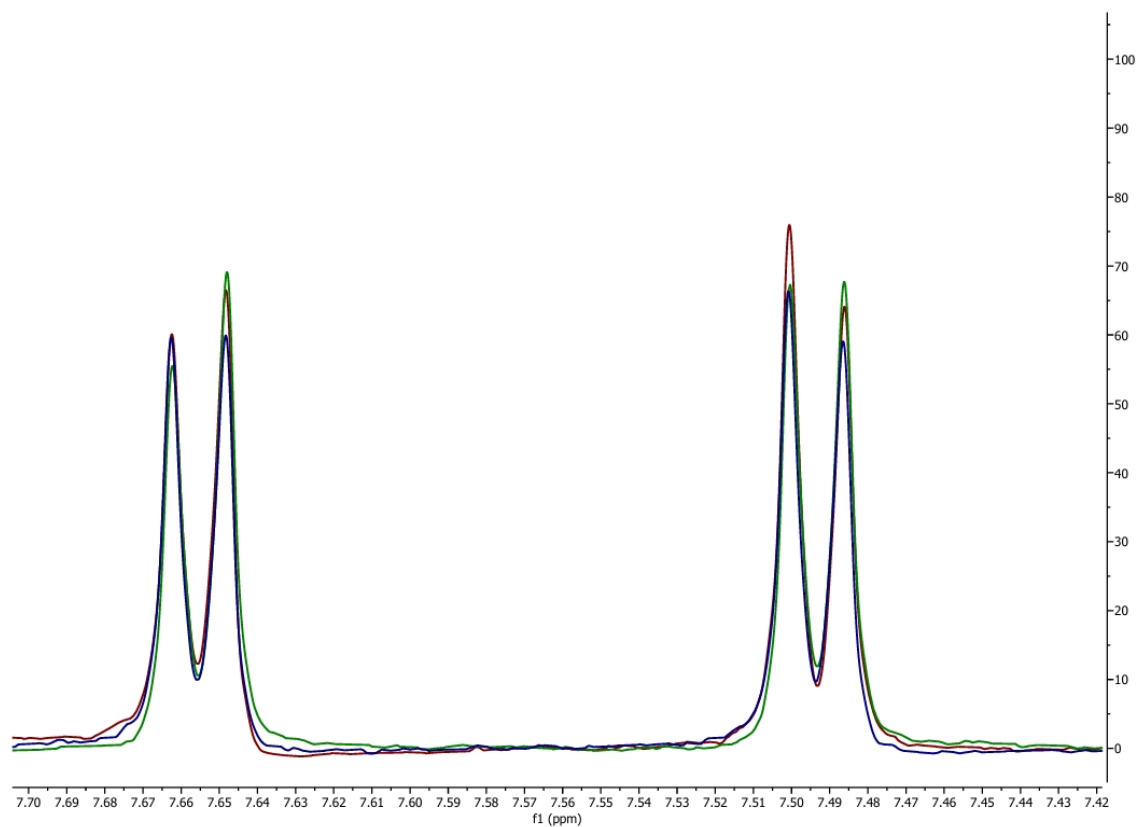


Figure S186. Proton 1D CPMG NMR spectrum of 0.4 mM C29 collected with spin-lock times of 20 (red) 50 (green) and 150 ms (blue) at 298K.

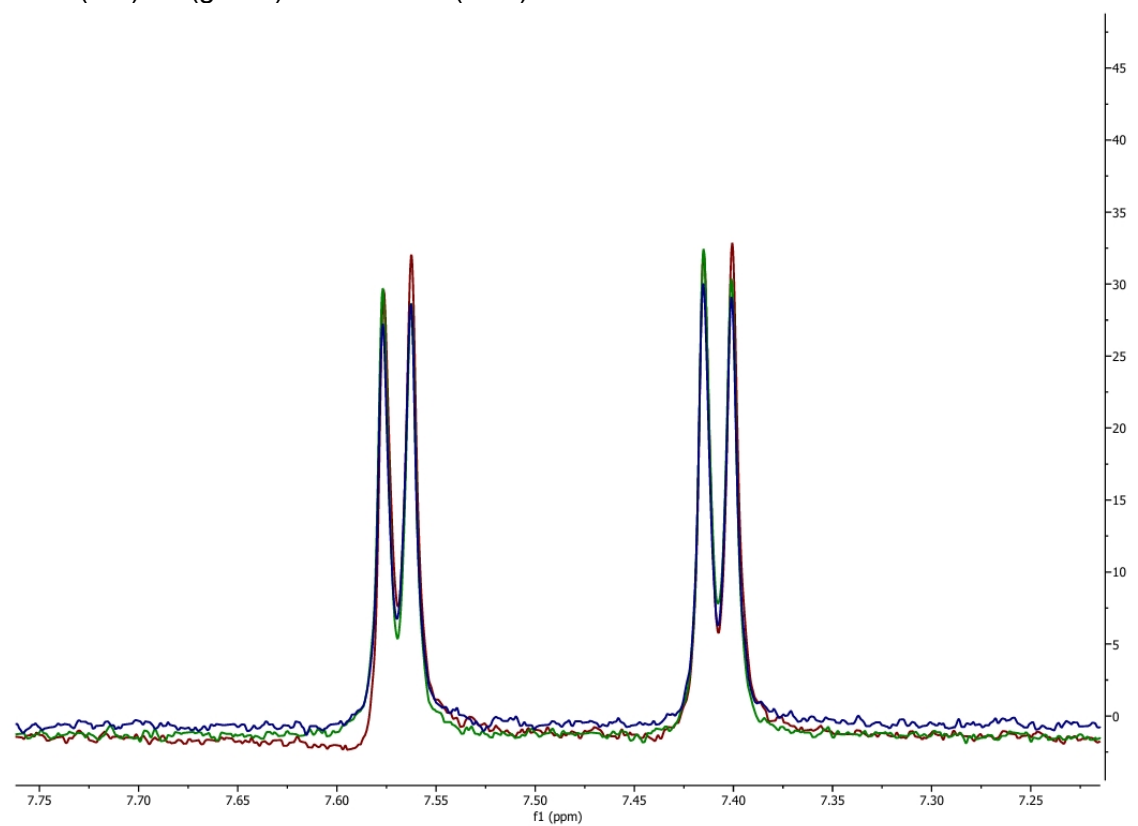


Figure S187. Proton 1D CPMG NMR spectrum of 0.4 mM C30 collected with spin-lock times of 20 (red) 50 (green) and 150 ms (blue) at 298K.

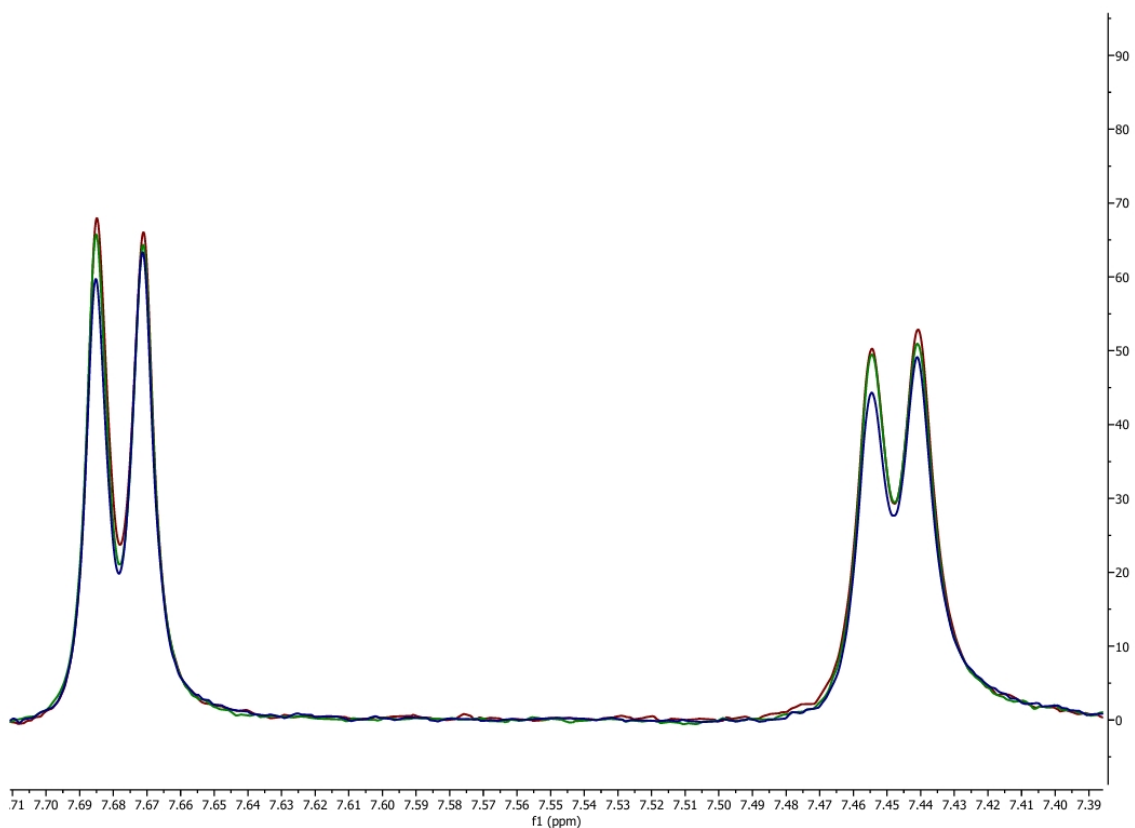


Figure S188. Proton 1D CPMG NMR spectrum of 0.4 mM C32 collected with spin-lock times of 20 (red) 50 (green) and 150 ms (blue) at 298K.

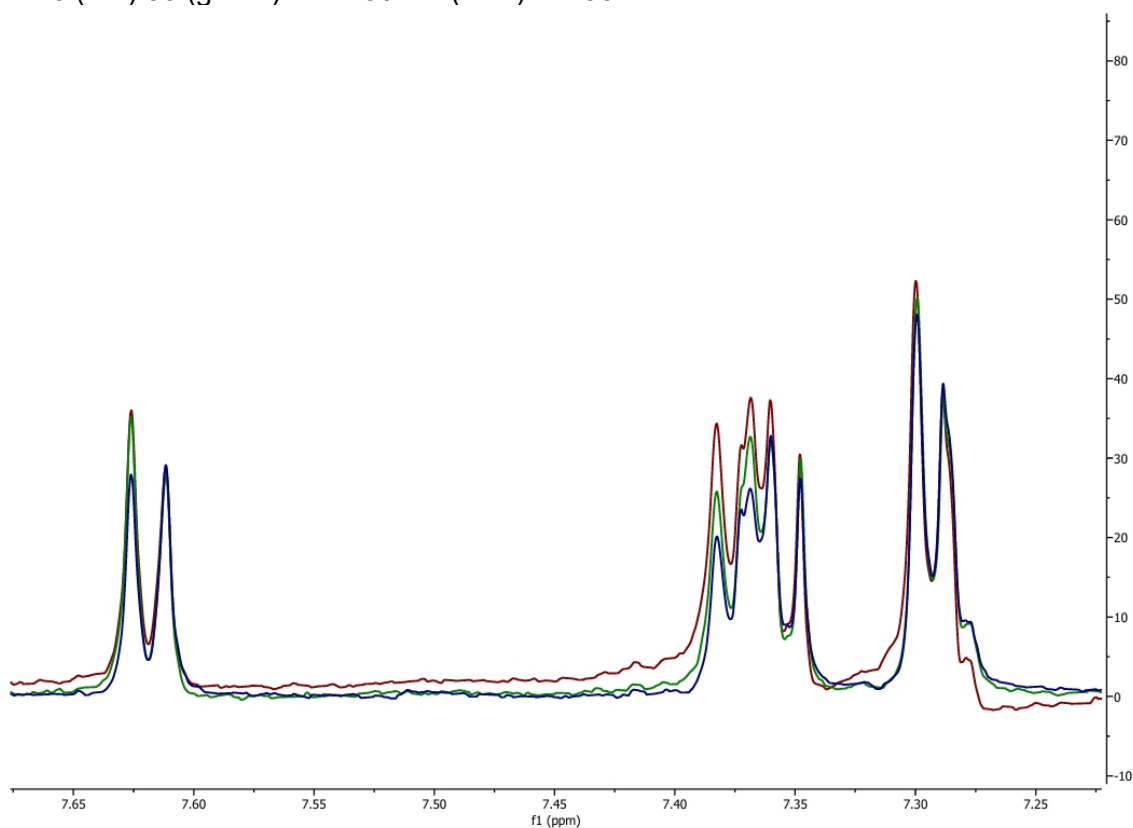


Figure S189. Proton 1D CPMG NMR spectrum of 0.4 mM C57 collected with spin-lock times of 20 (red) 50 (green) and 150 ms (blue) at 298K.

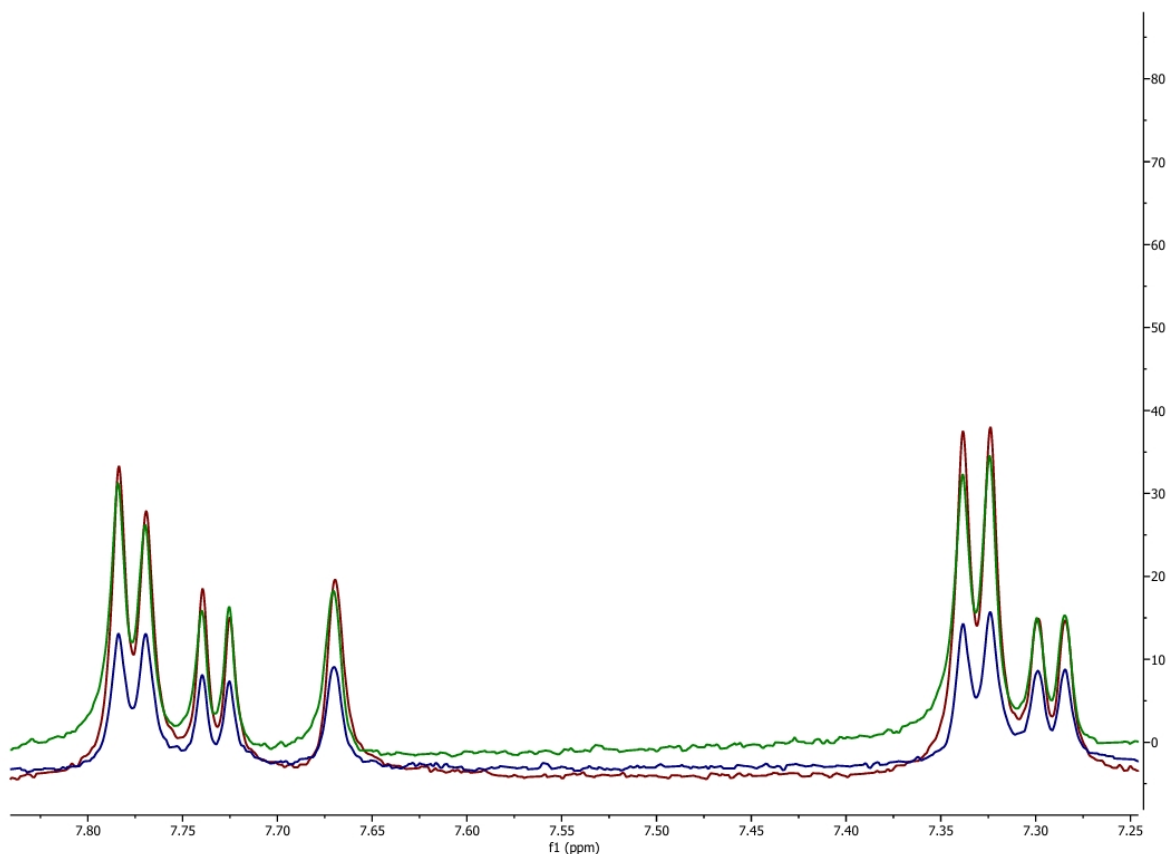


Figure S190. Proton 1D CPMG NMR spectrum of 0.4 mM C60 collected with spin-lock times of 20 (red) 50 (green) and 150 ms (blue) at 298K.

T1 and T2 spin relaxation data for reference compounds

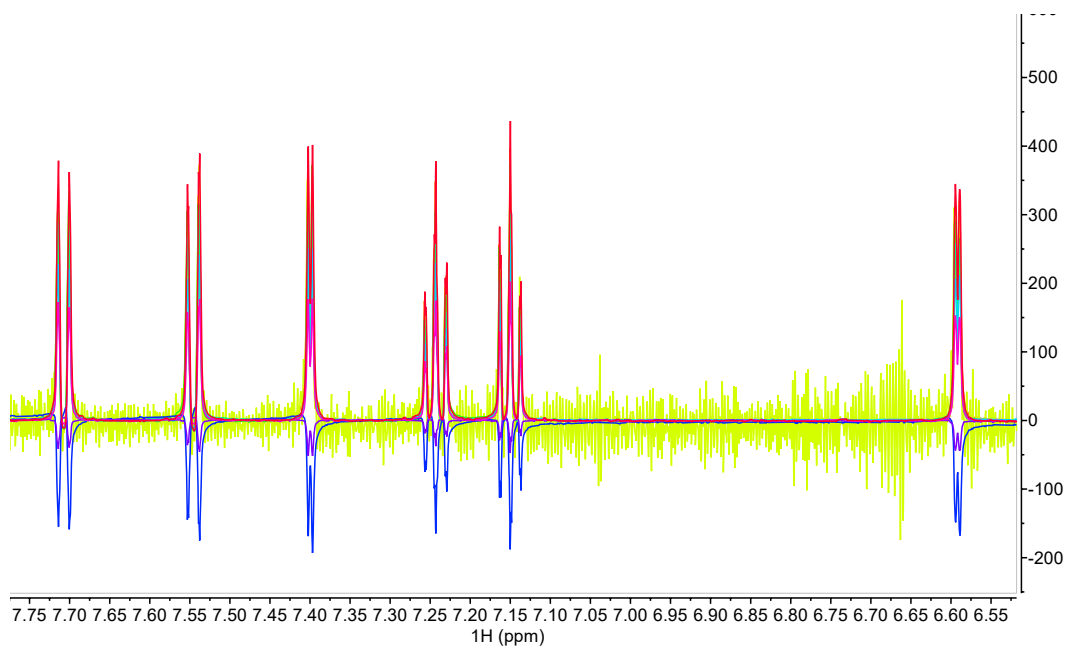


Figure S191. Proton 1D NMR spectrum of 2 mM indole without the addition of 0.5 mM Mn²⁺ collected at 298K at different T1 delays (sec): 0.001 (orange), 0.05 (yellow), 0.1 (light green), 0.25 (dark green), 0.5 (light blue), 0.8 (dark blue), 1.5 (purple), 3 (magenta), and 5 (red).

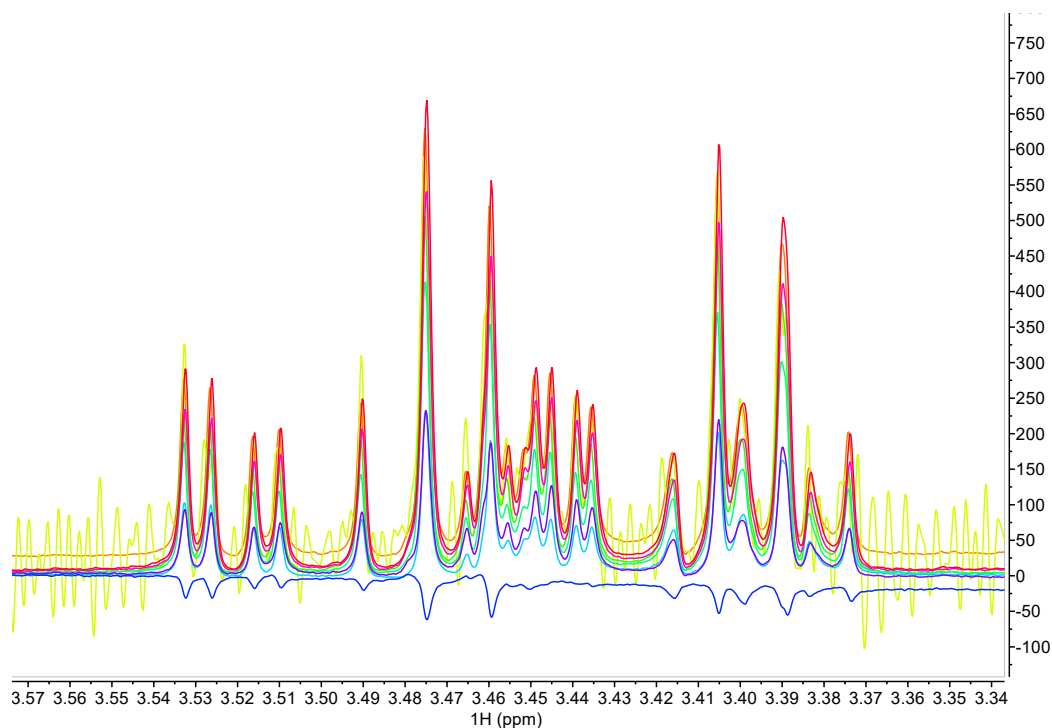


Figure S192. Proton 1D NMR spectrum of 4 mM glucose without the addition of 0.5 mM Mn^{2+} collected at 298K at different T1 delays (sec): 0.001 (orange), 0.05 (yellow), 0.1 (light green), 0.25 (dark green), 0.5 (light blue), 0.8 (dark blue), 1.5 (purple), 3 (magenta), and 5 (red).

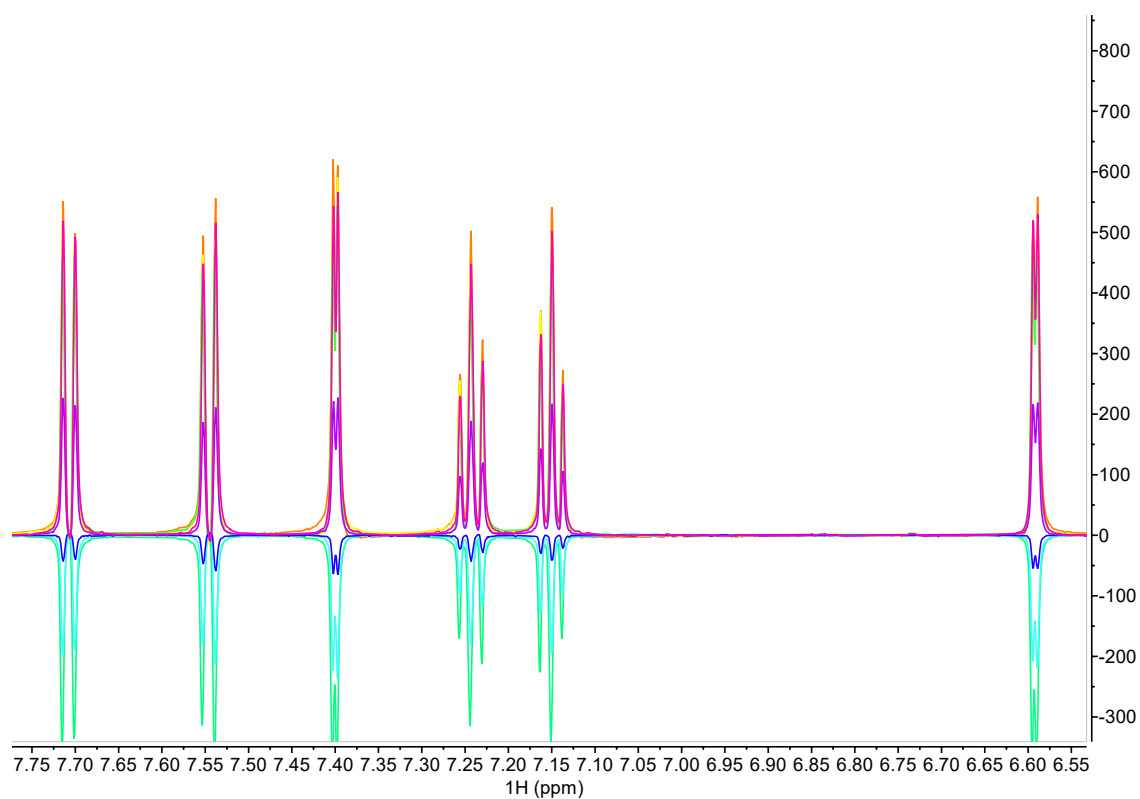


Figure S193. Proton 1D NMR spectrum of 2 mM indole with the addition of 0.5 mM Mn^{2+} collected with at 298K at different T1 delays (sec): 0.001 (orange), 0.05 (yellow), 0.1 (light green), 0.25 (dark green), 0.5 (light blue), 0.8 (dark blue), 1.5 (purple), 3 (magenta), and 5 (red).

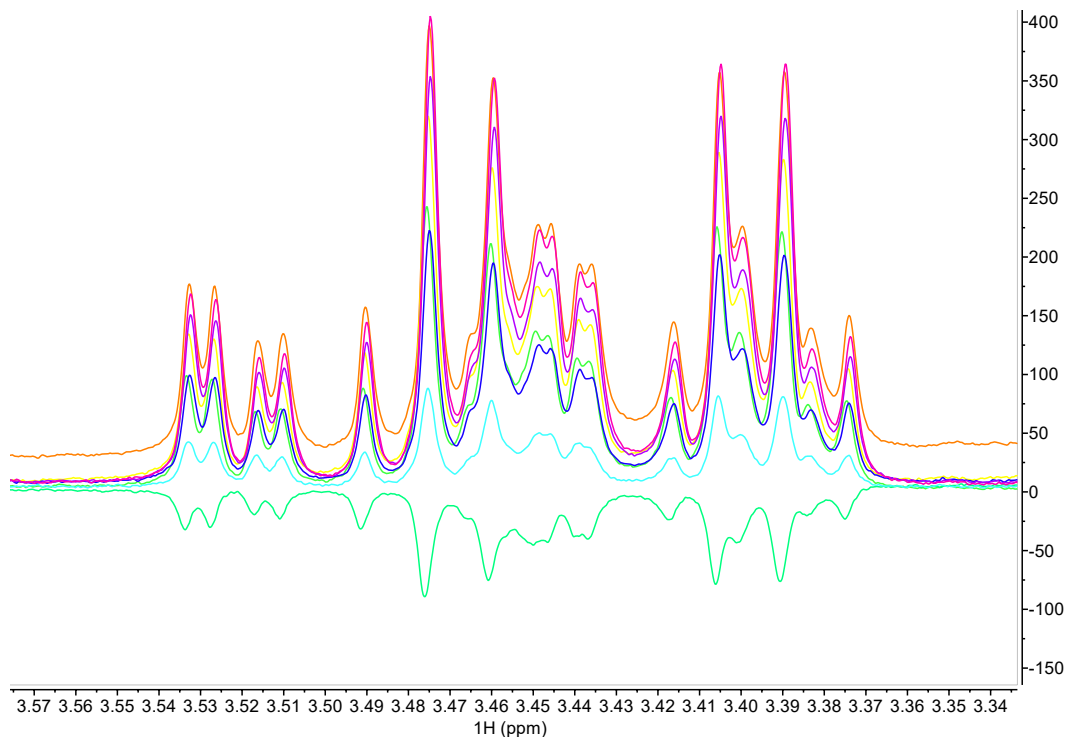


Figure S194. Proton 1D NMR spectrum of 4 mM glucose with the addition of 0.5 mM Mn^{2+} collected with at 298K at different T1 delays (sec): 0.001 (orange), 0.05 (yellow), 0.1 (light green), 0.25 (dark green), 0.5 (light blue), 0.8 (dark blue), 1.5 (purple), 3 (magenta), and 5 (red).

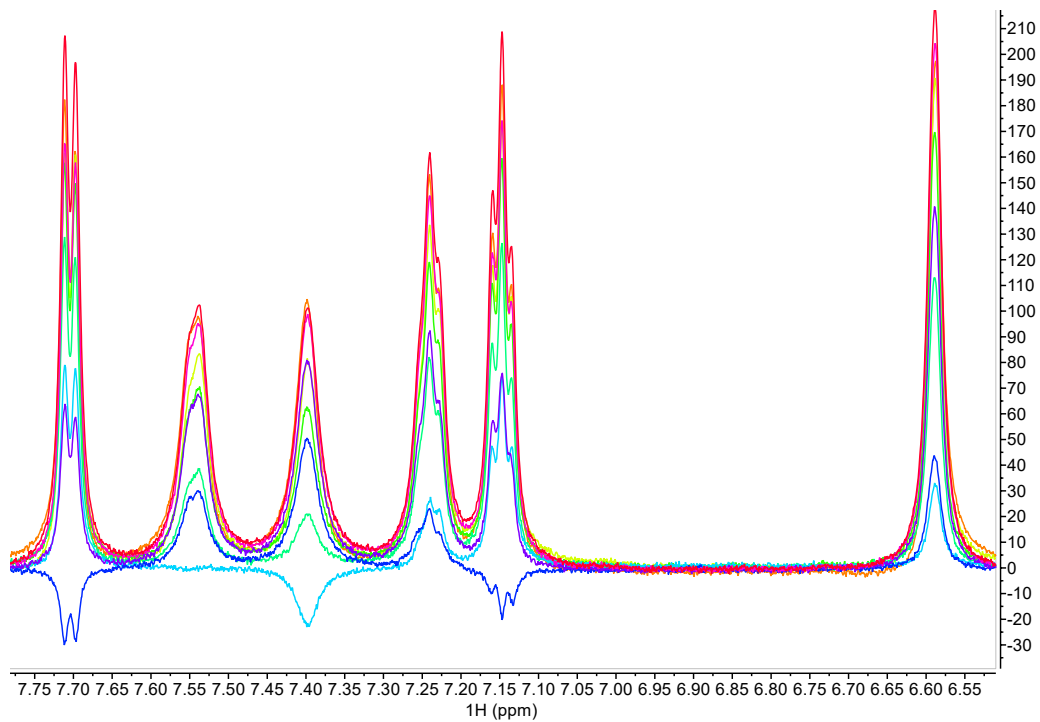


Figure S195. Proton 1D NMR spectrum of 2 mM indole in the presence of *E. coli* lipid vesicles without the addition of 0.5 mM Mn^{2+} collected with at 298K at different T1 delays (sec): 0.001 (orange), 0.05 (yellow), 0.1 (light green), 0.25 (dark green), 0.5 (light blue), 0.8 (dark blue), 1.5 (purple), 3 (magenta), and 5 (red).

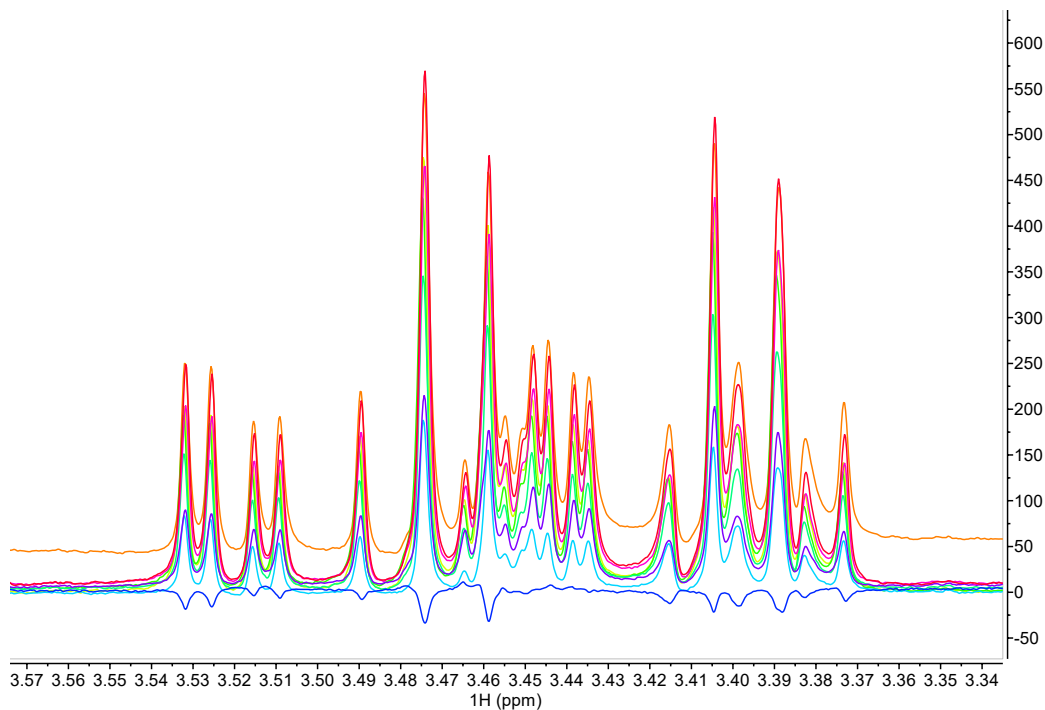


Figure S196. Proton 1D NMR spectrum of 4 mM glucose in the presence of *E. coli* lipid vesicles without the addition of 0.5 mM Mn^{2+} collected with at 298K at different T1 delays (sec): 0.001 (orange), 0.05 (yellow), 0.1 (light green), 0.25 (dark green), 0.5 (light blue), 0.8 (dark blue), 1.5 (purple), 3 (magenta), and 5 (red).

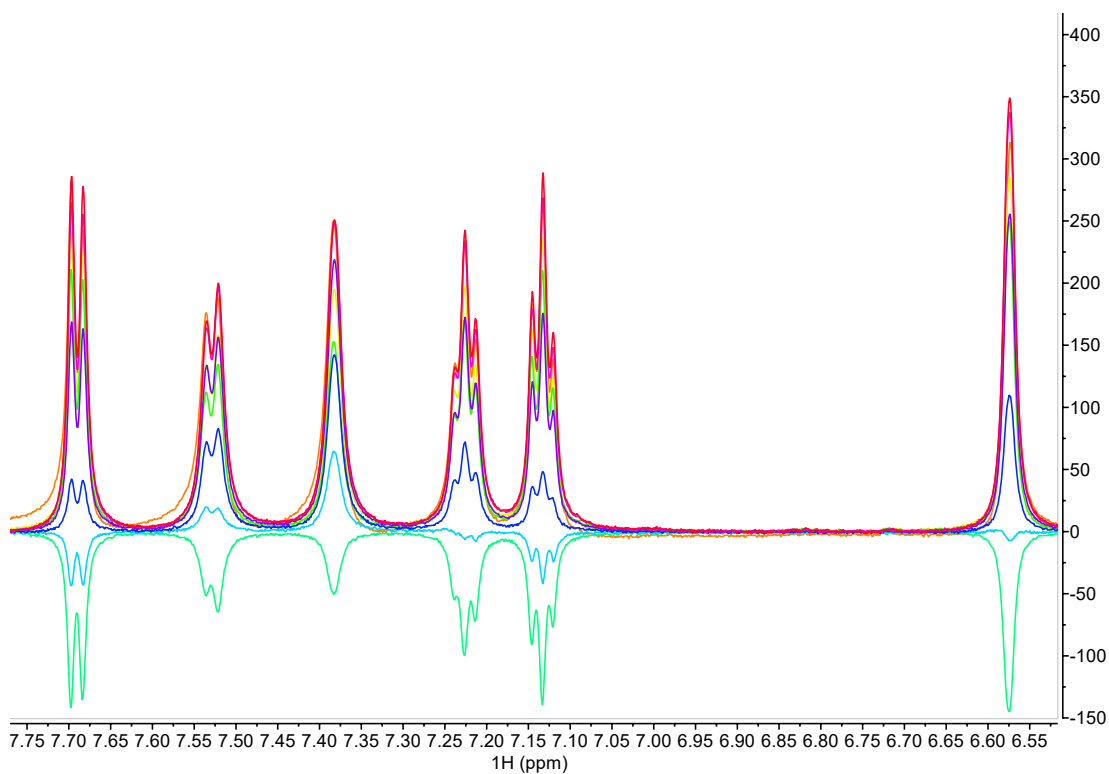


Figure S197. Proton 1D NMR spectrum of 2 mM indole in the presence of *E. coli* lipid vesicles with the addition of 0.5 mM Mn^{2+} collected with at 298K at different T1 delays (sec): 0.001 (orange), 0.05 (yellow), 0.1 (light green), 0.25 (dark green), 0.5 (light blue), 0.8 (dark blue), 1.5 (purple), 3 (magenta), and 5 (red).

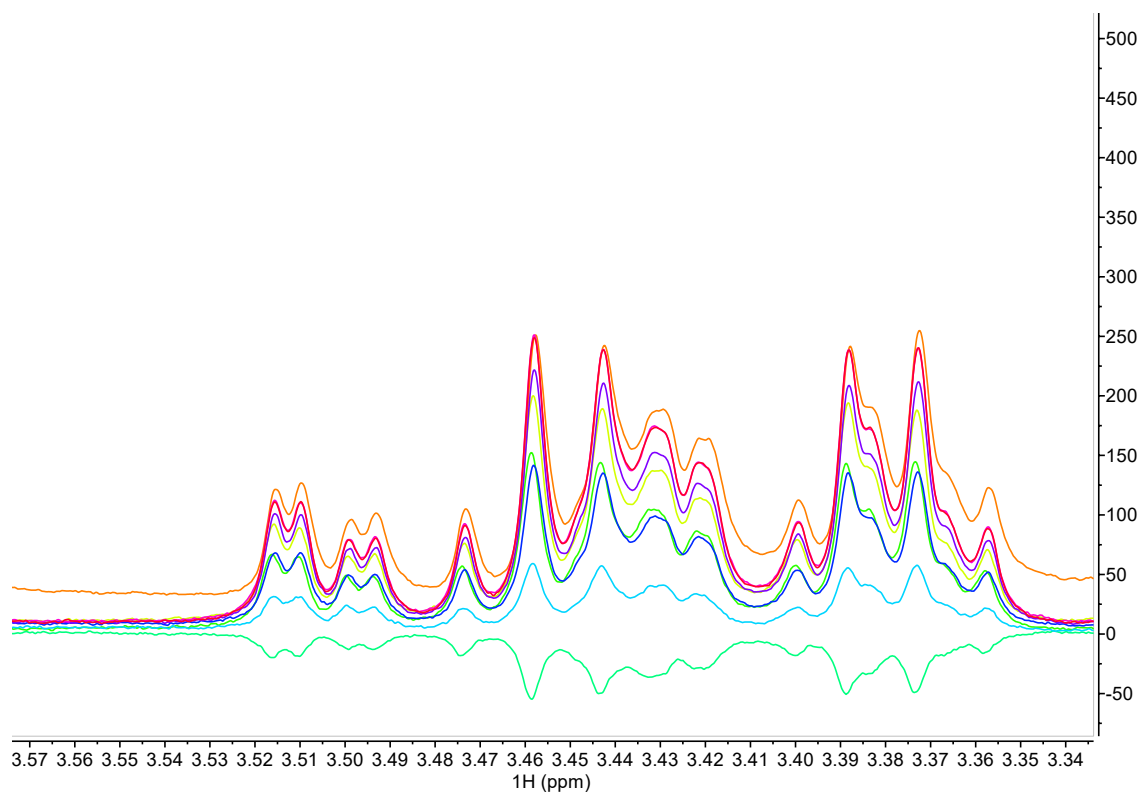


Figure S198. Proton 1D NMR spectrum of 4 mM glucose in the presence of *E. coli* lipid vesicles with the addition of 0.5 mM Mn^{2+} collected with at 298K at different T1 delays (sec): 0.001 (orange), 0.05 (yellow), 0.1 (light green), 0.25 (dark green), 0.5 (light blue), 0.8 (dark blue), 1.5 (purple), 3 (magenta), and 5 (red).

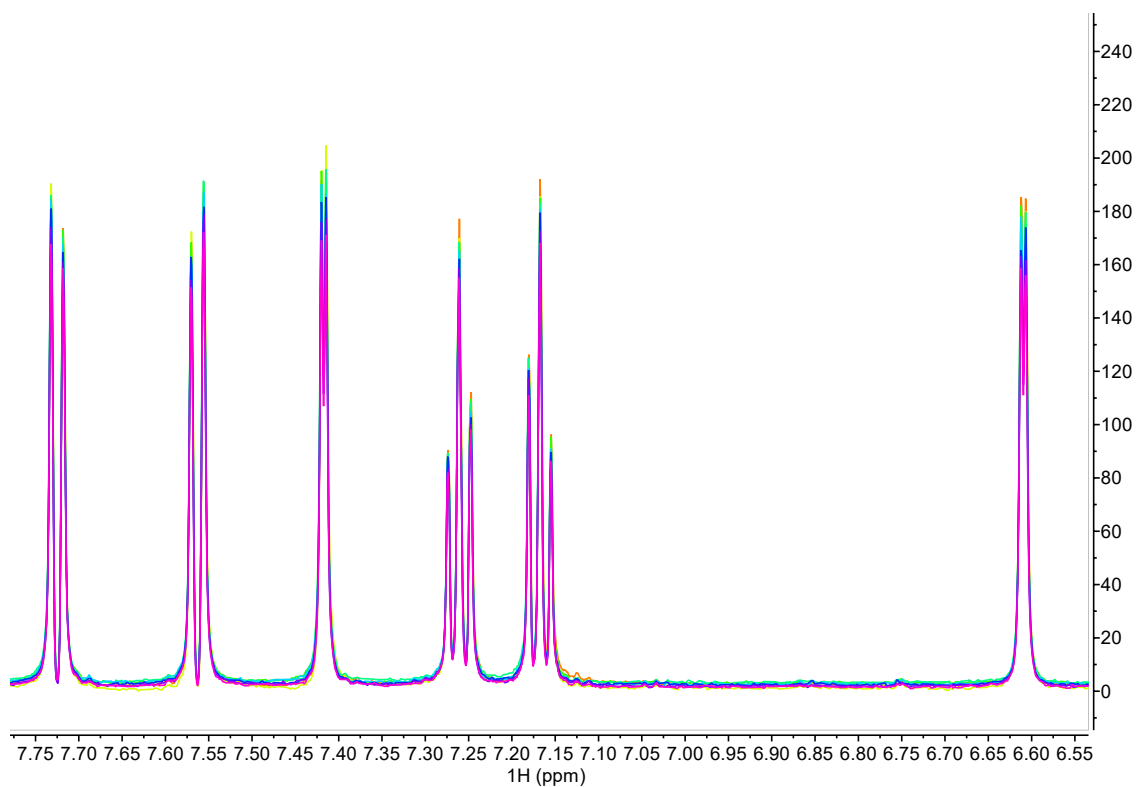


Figure S199. Proton 1D NMR spectrum of 2 mM indole without the addition of 0.5 mM Mn^{2+} collected at 298K at different T2 delays (msec): 5 (orange), 20 (yellow), 40 (light green), 60 (dark green), 80 (light blue), 100 (dark blue), 150 (purple) and 200 (magenta).

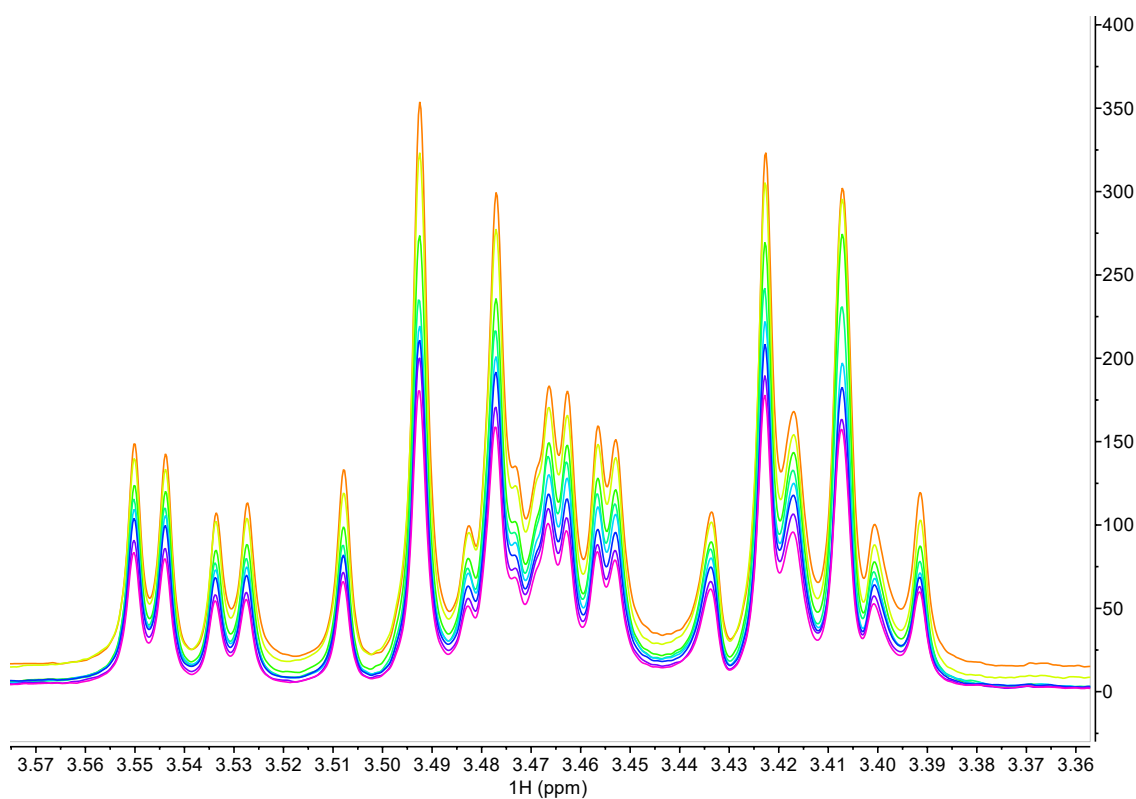


Figure S200. Proton 1D NMR spectrum of 4 mM glucose without the addition of 0.5 mM Mn^{2+} collected at 298K at different T2 delays (msec): 5 (orange), 20 (yellow), 40 (light green), 60 (dark green), 80 (light blue), 100 (dark blue), 150 (purple) and 200 (magenta).

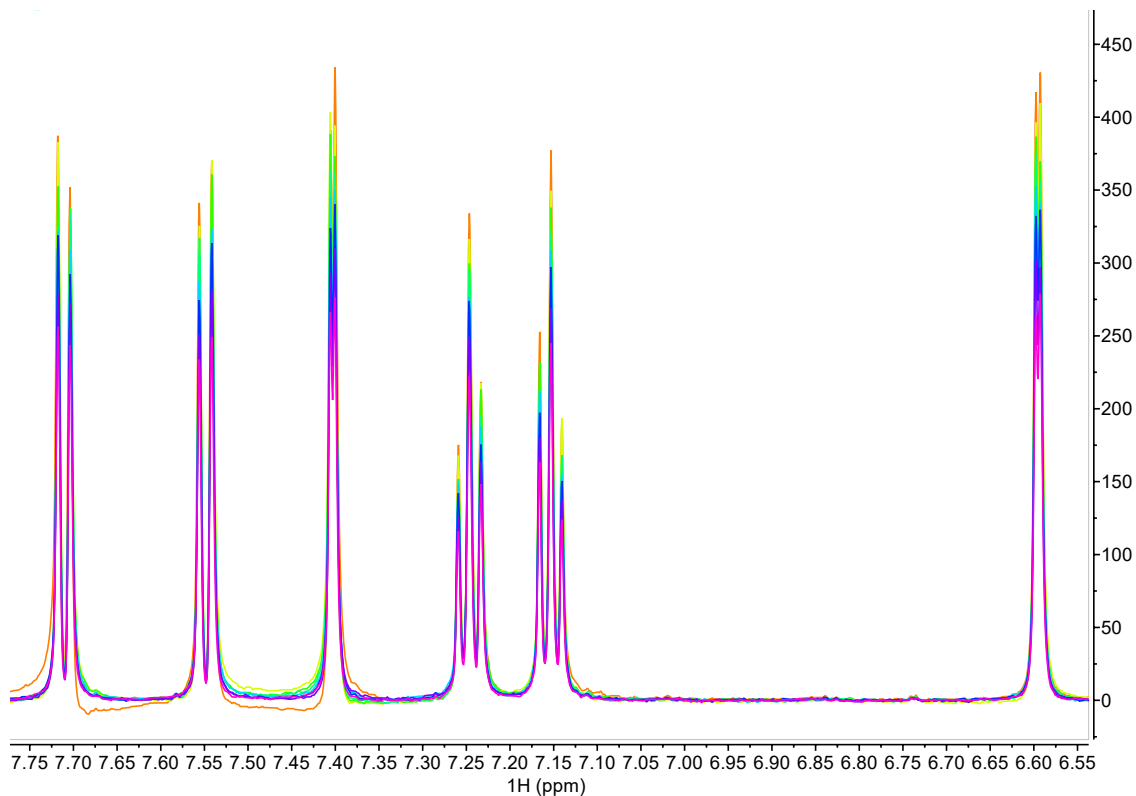


Figure S201. Proton 1D NMR spectrum of 2 mM indole with the addition of 0.5 mM Mn^{2+} collected with at 298K at different T2 delays (sec): 5 (orange), 20 (yellow), 40 (light green), 60 (dark green), 80 (light blue), 100 (dark blue), 150 (purple) and 200 (magenta).

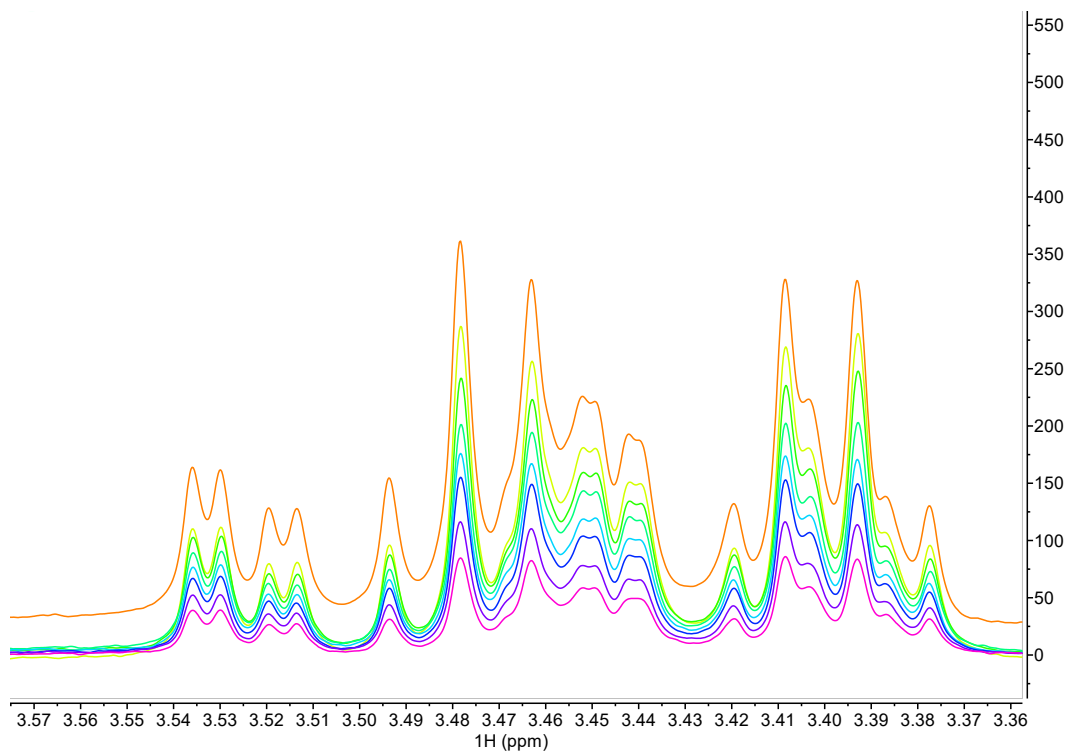


Figure S202. Proton 1D NMR spectrum of 4 mM glucose with the addition of 0.5 mM Mn^{2+} collected with at 298K at different T2 delays (msec): 5 (orange), 20 (yellow), 40 (light green), 60 (dark green), 80 (light blue), 100 (dark blue), 150 (purple) and 200 (magenta).

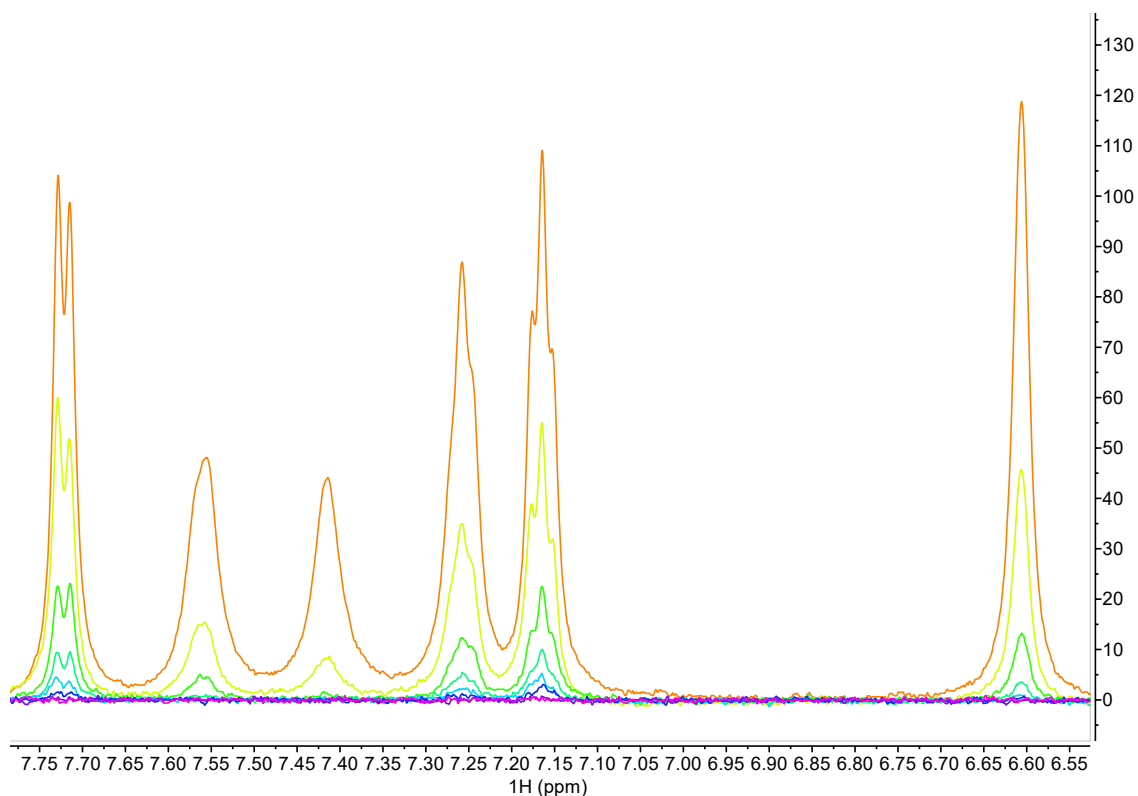


Figure S203. Proton 1D NMR spectrum of 2 mM indole in the presence of *E. coli* lipid vesicles without the addition of 0.5 mM Mn^{2+} collected with at 298K at different T2 delays (msec): 5 (orange), 20 (yellow), 40 (light green), 60 (dark green), 80 (light blue), 100 (dark blue), 150 (purple) and 200 (magenta).

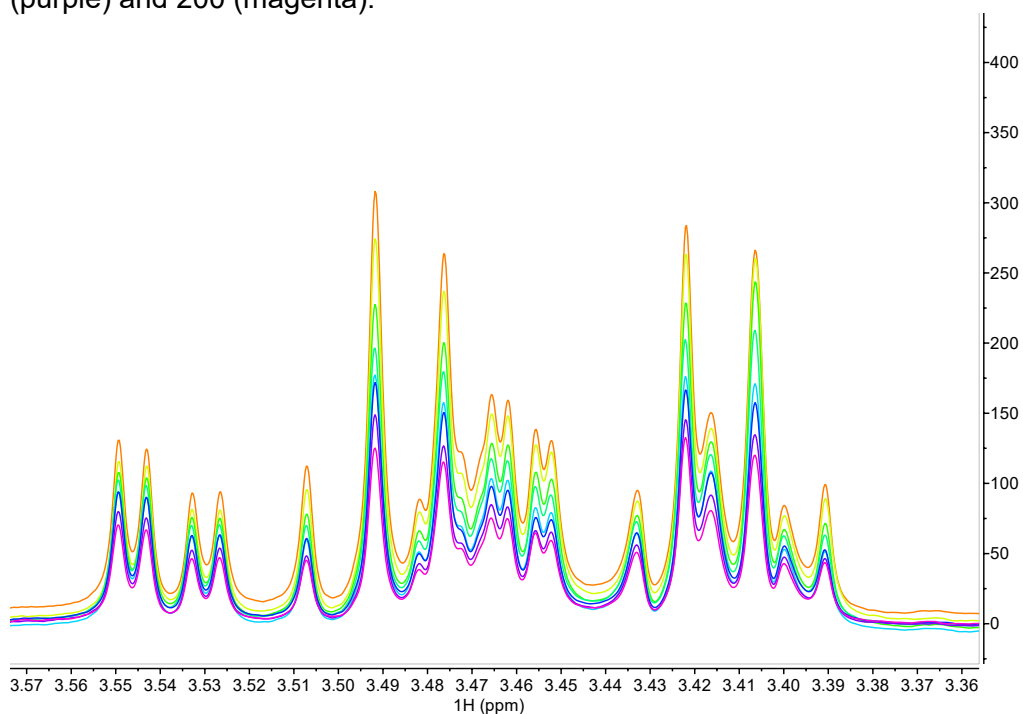


Figure S204. Proton 1D NMR spectrum of 4 mM glucose in the presence of *E. coli* lipid vesicles without the addition of 0.5 mM Mn^{2+} collected with at 298K at different T2 delays (msec): 5 (orange), 20 (yellow), 40 (light green), 60 (dark green), 80 (light blue), 100 (dark blue), 150 (purple) and 200 (magenta).

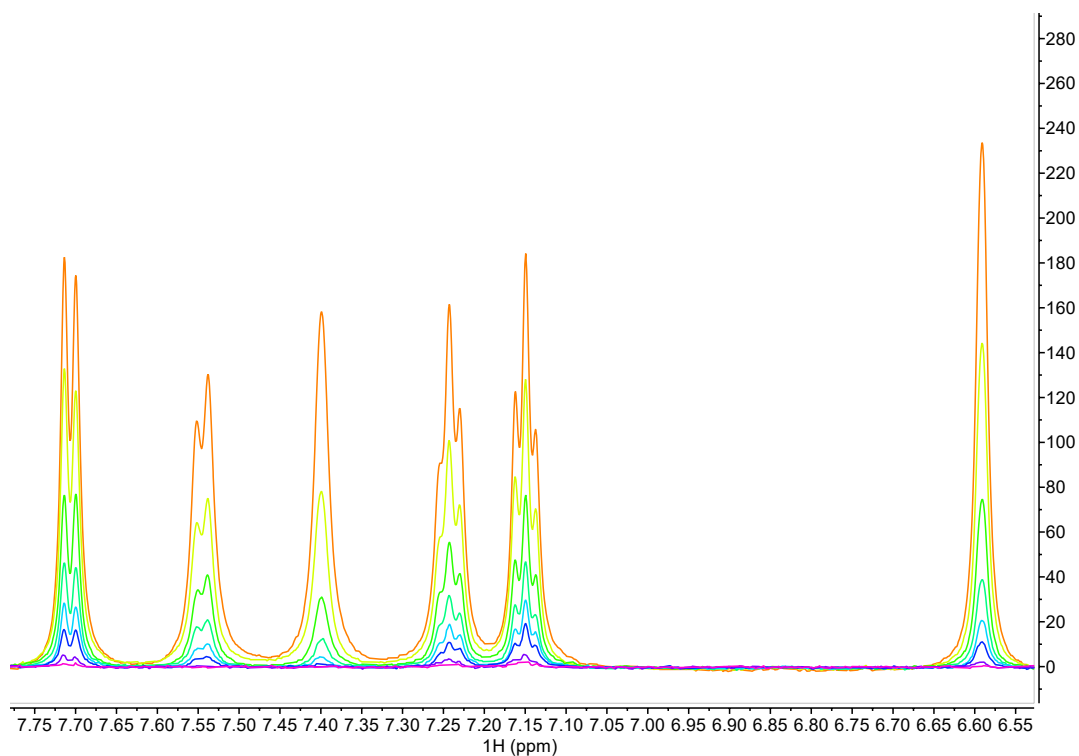


Figure S205. Proton 1D NMR spectrum of 2 mM indole in the presence of *E. coli* lipid vesicles with the addition of 0.5 mM Mn^{2+} collected with at 298K at different T2 delays (msec): 5 (orange), 20 (yellow), 40 (light green), 60 (dark green), 80 (light blue), 100 (dark blue), 150 (purple) and 200 (magenta).

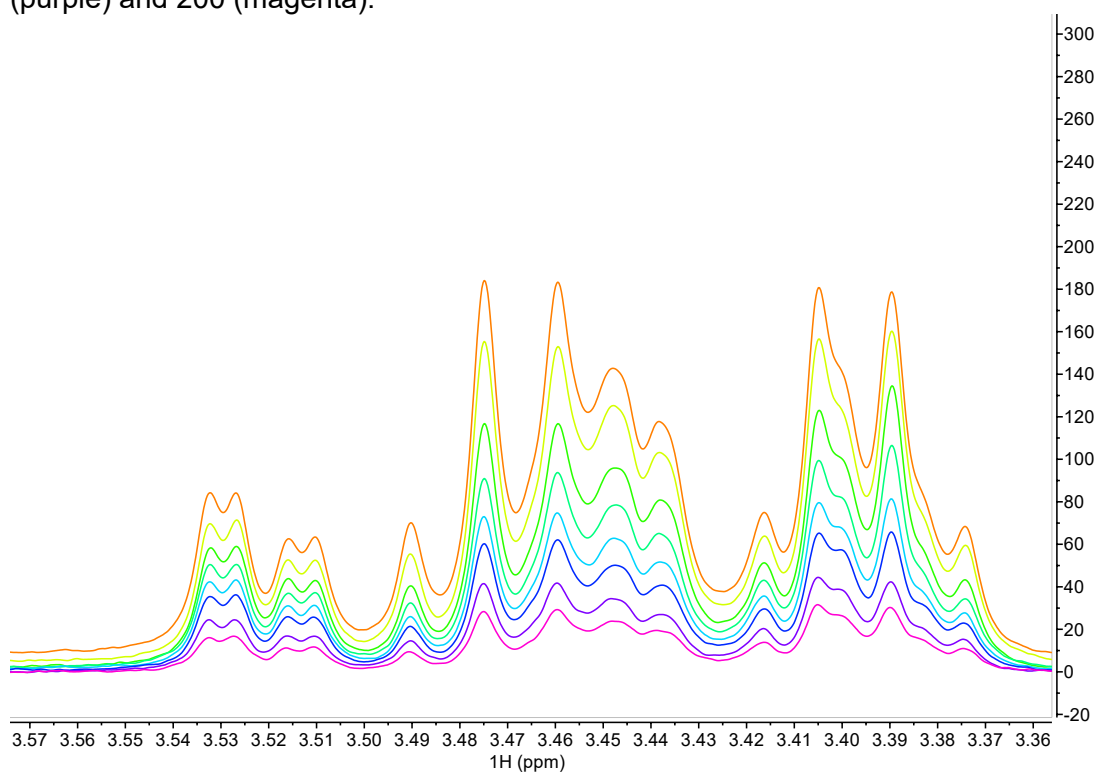


Figure S206. Proton 1D NMR spectrum of 4 mM glucose in the presence of *E. coli* lipid vesicles with the addition of 0.5 mM Mn^{2+} collected with at 298K at different T2 delays (msec): 5 (orange), 20 (yellow), 40 (light green), 60 (dark green), 80 (light blue), 100 (dark blue), 150 (purple) and 200 (magenta).

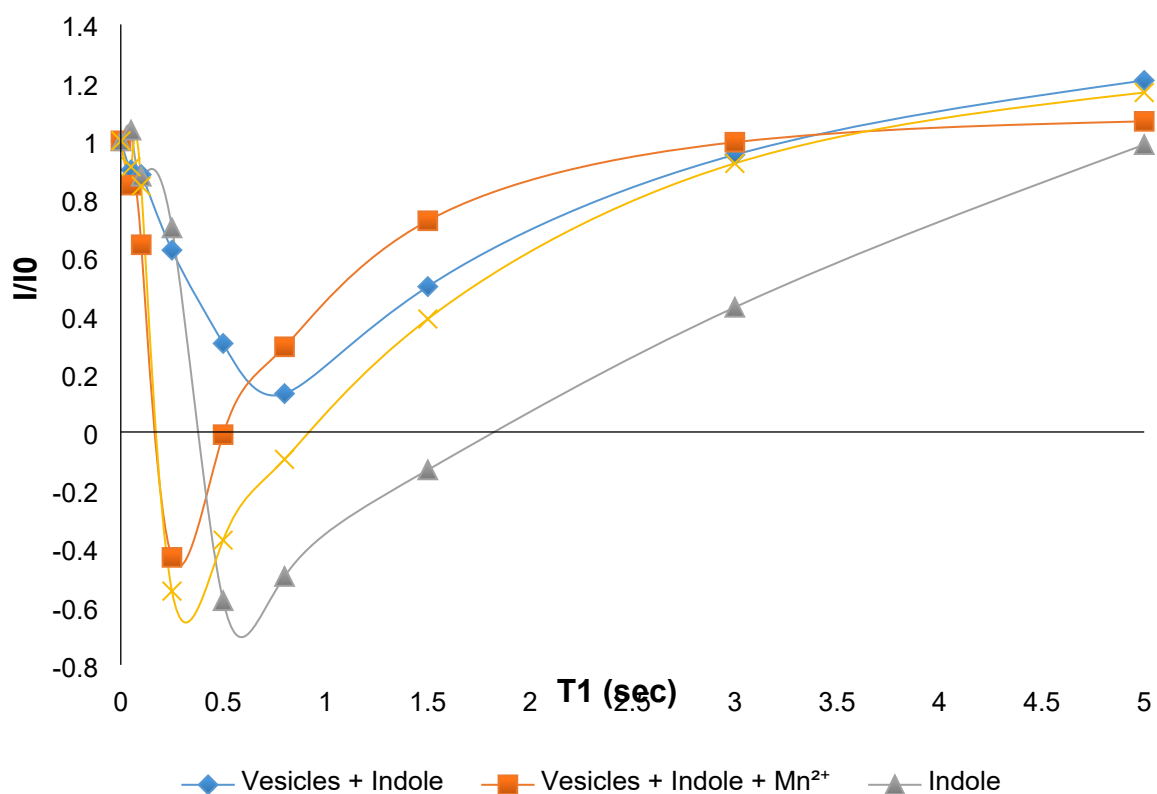


Figure S207. T1 effect on the intensity of 2 mM indole in the presence and absence of *E. coli* lipid vesicles with and without the addition of 0.5 mM Mn²⁺. T1 times calculated are 5.9 s for indole, 1.8 s for indole in the presence of 0.5 mM Mn²⁺, 1.9 s for indole with vesicles, and 0.8 s for indole with vesicles in the presence of 0.5 mM Mn²⁺.

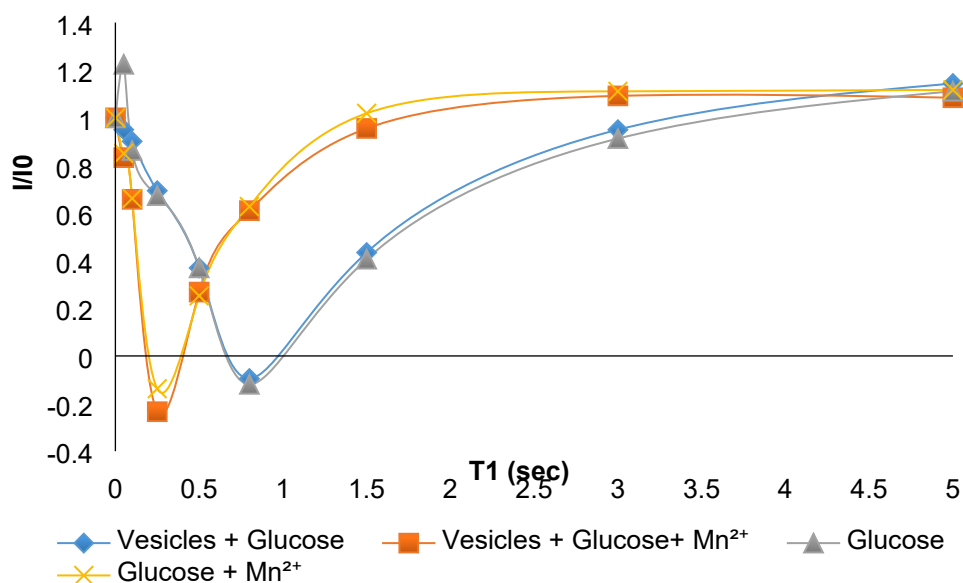


Figure S208. T1 effect on the intensity of 4 mM glucose in the presence and absence of *E. coli* lipid vesicles with and without the addition of 0.5 mM Mn²⁺. T1 times calculated are 1.3 s for glucose, 0.6 s for glucose in the presence of 0.5 mM Mn²⁺, 1.3 s for glucose with vesicles, and 0.5 s for glucose with vesicles in the presence of 0.5 mM Mn²⁺.

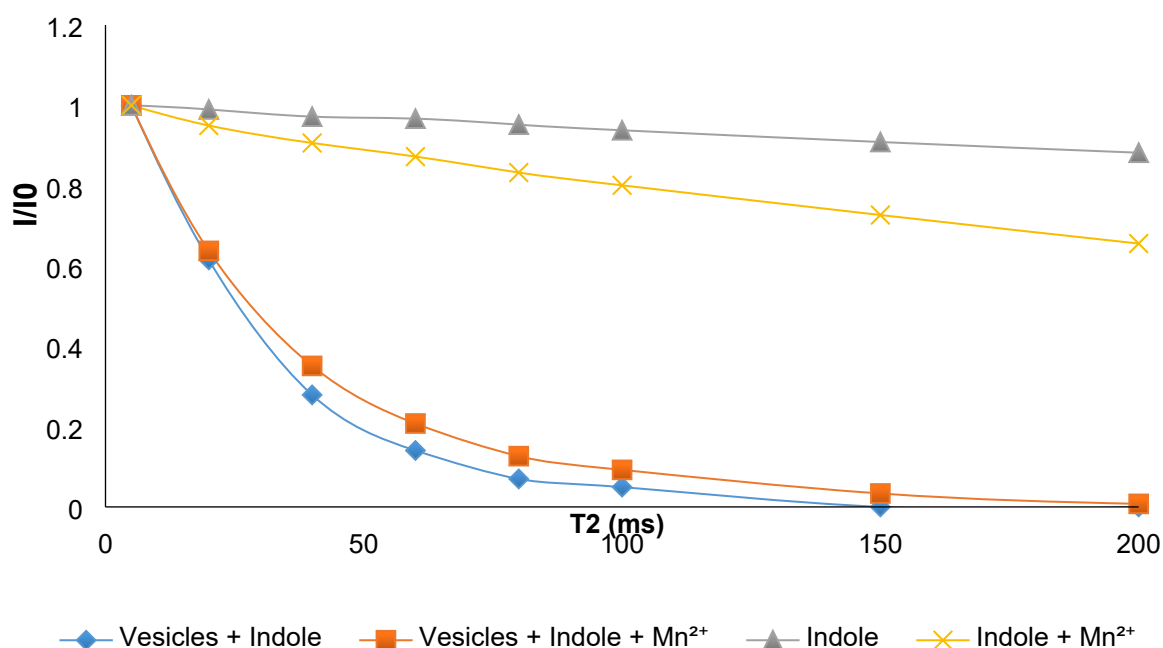


Figure S209. T2 effect on the intensity of 2 mM indole in the presence and absence of *E. coli* lipid vesicles with and without the addition of 0.5 mM Mn²⁺. T2 times calculated are 0.838 ms for indole, 0.253 ms for indole in the presence of 0.5 mM Mn²⁺, 28 ms for indole with vesicles, and 33 ms for indole with vesicles in the presence of 0.5 mM Mn²⁺.

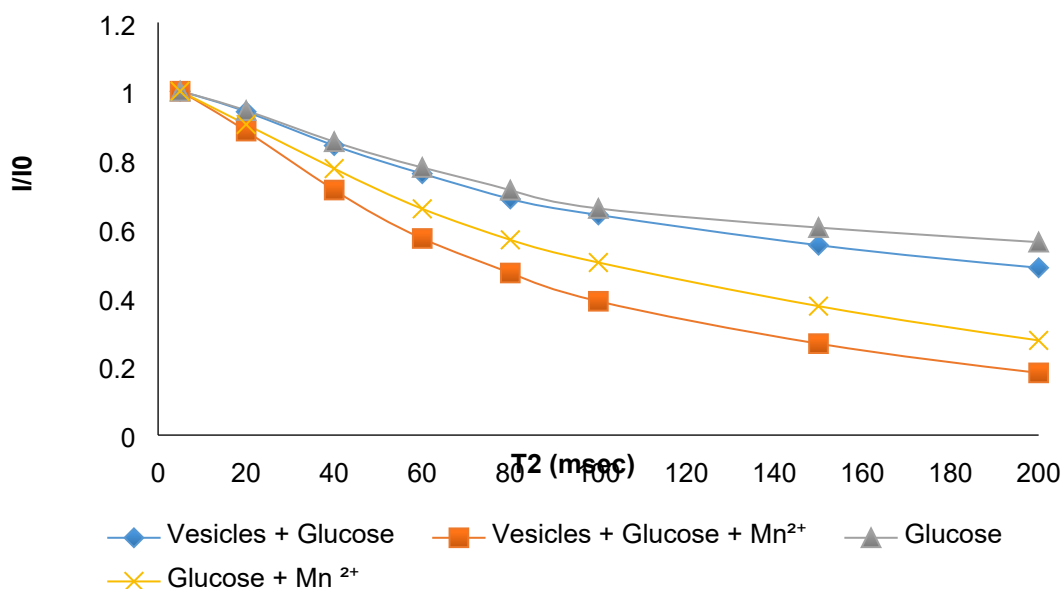


Figure S210. T2 effect on the intensity of 4 mM glucose in the presence and absence of *E. coli* lipid vesicles with and without the addition of 0.5 mM Mn²⁺. T2 times calculated are 300 ms for glucose, 140 ms for glucose in the presence of 0.5 mM Mn²⁺, 250 ms for glucose with vesicles, and 100 ms for glucose with vesicles in the presence of 0.5 mM Mn²⁺.

NMR characterisation

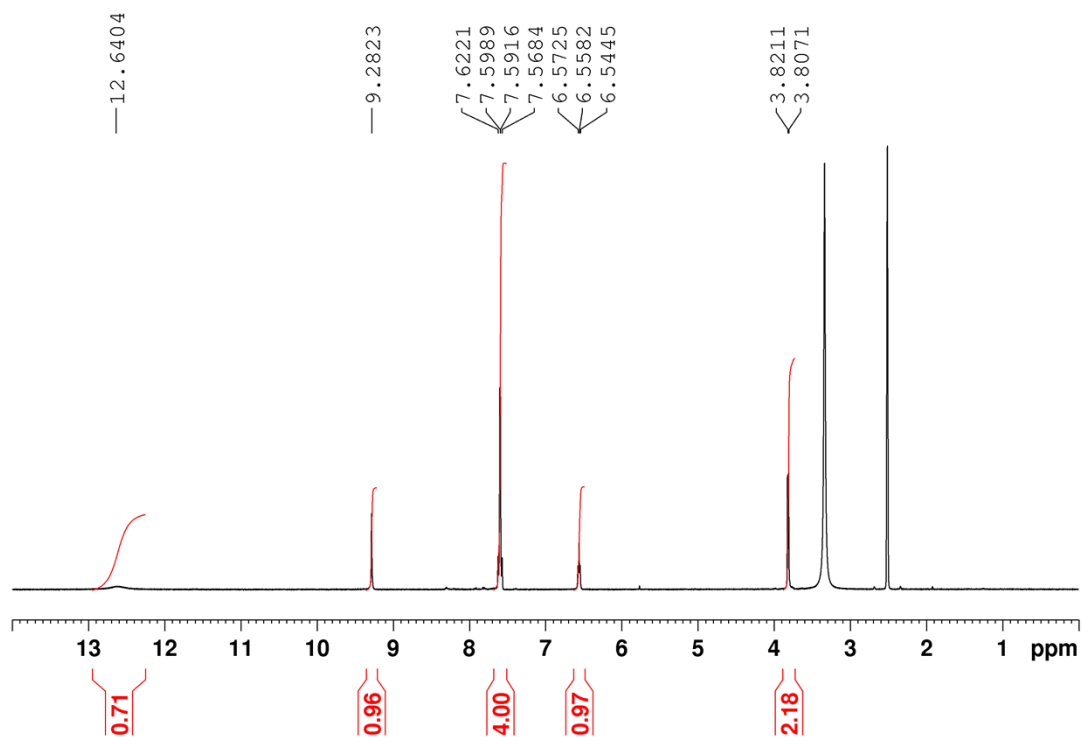


Figure S211. ^1H NMR of compound **29** in $\text{DMSO-}d_6$ conducted at 298 K.

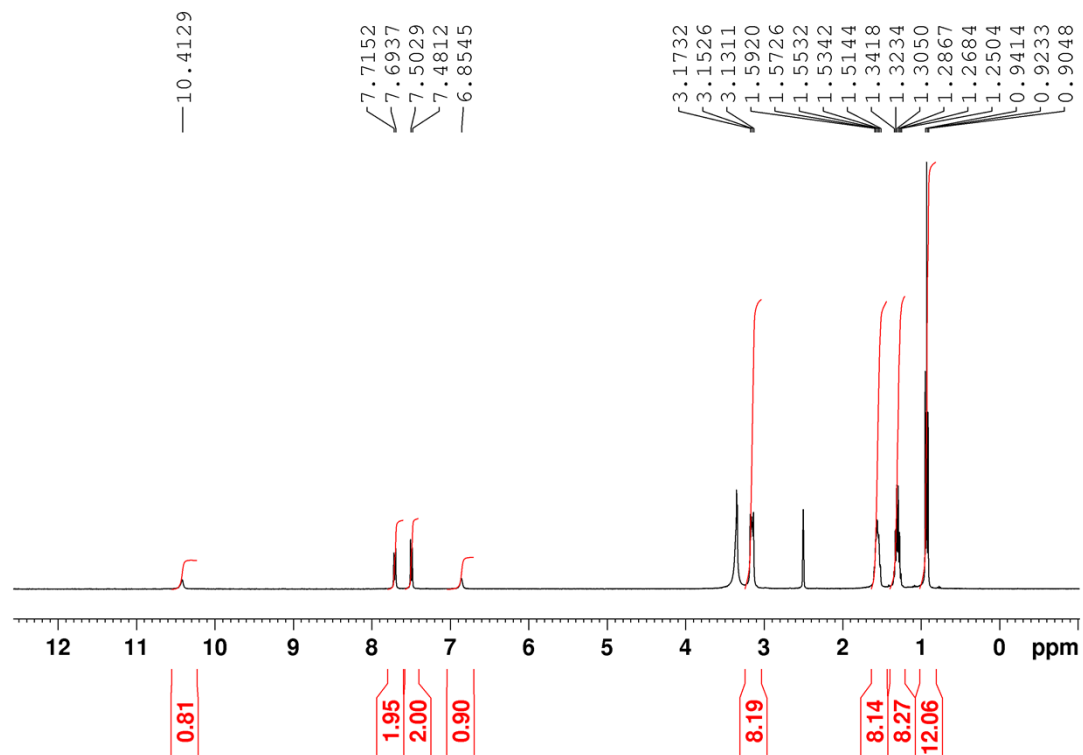


Figure S212. ^1H NMR of compound **30** in $\text{DMSO-}d_6$ conducted at 298 K.

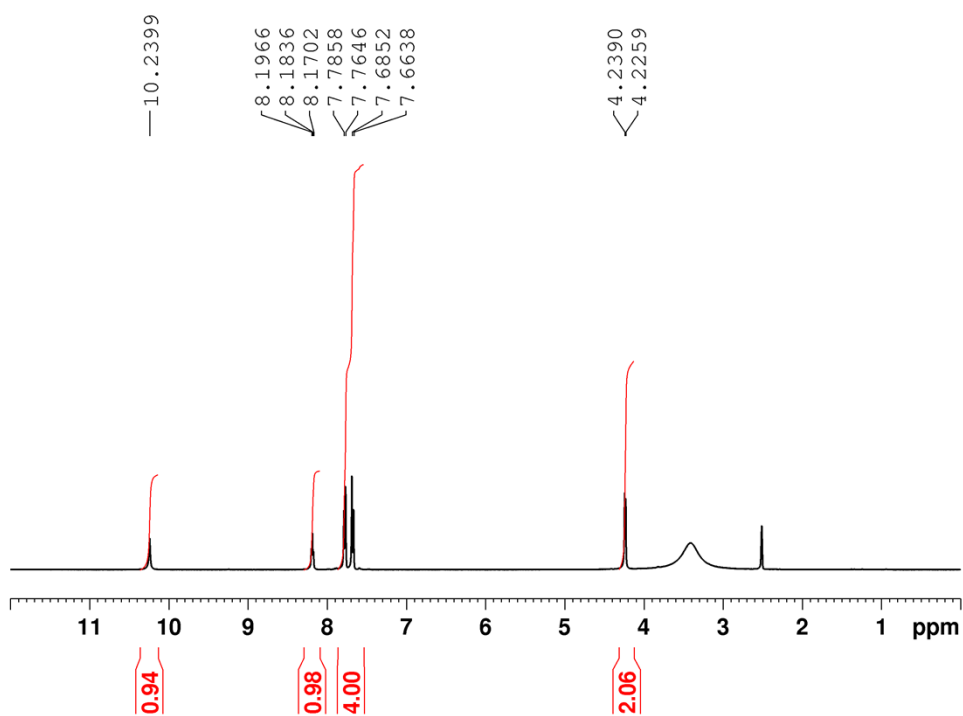


Figure S213. ^1H NMR of compound **32** in $\text{DMSO-}d_6$ conducted at 298 K.

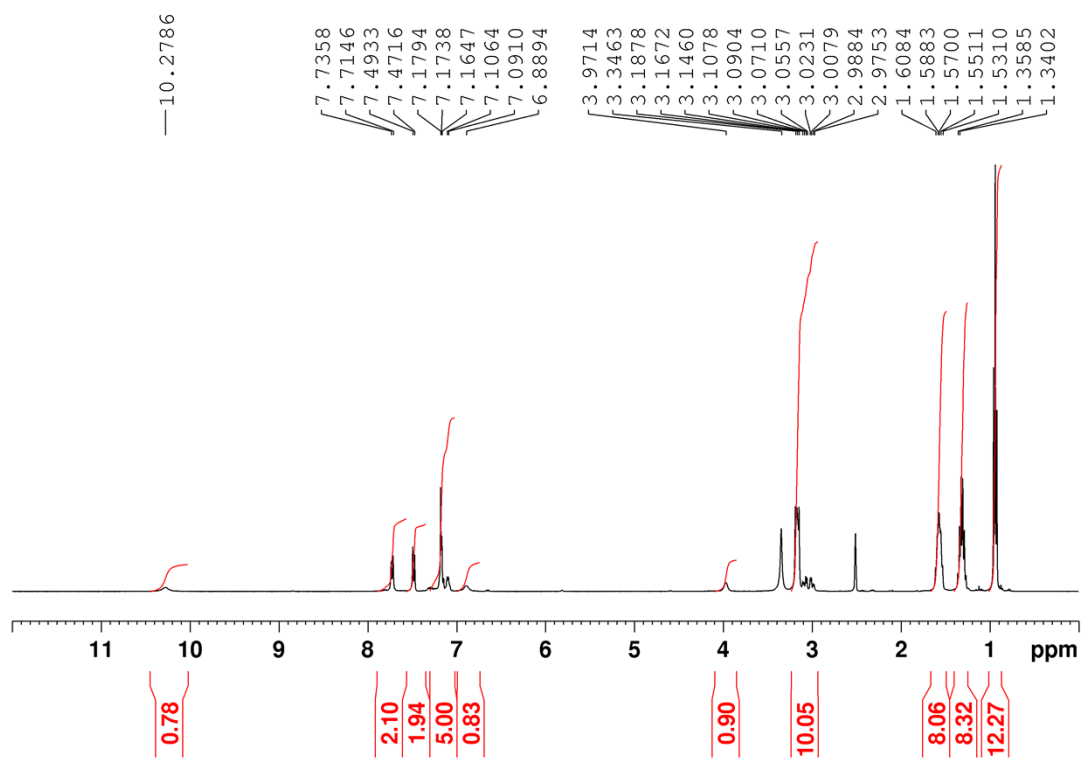


Figure S214. ^1H NMR of compound **57** in $\text{DMSO-}d_6$ conducted at 298 K.

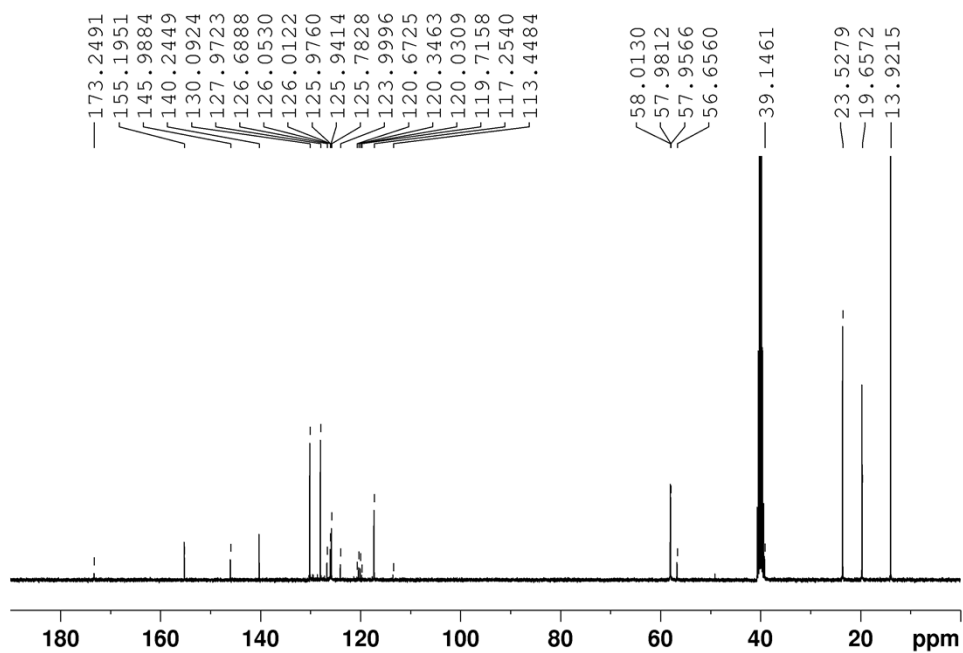


Figure S215. $^{13}\text{C}\{^1\text{H}\}$ NMR of compound **57** in $\text{DMSO-}d_6$ conducted at 298 K.

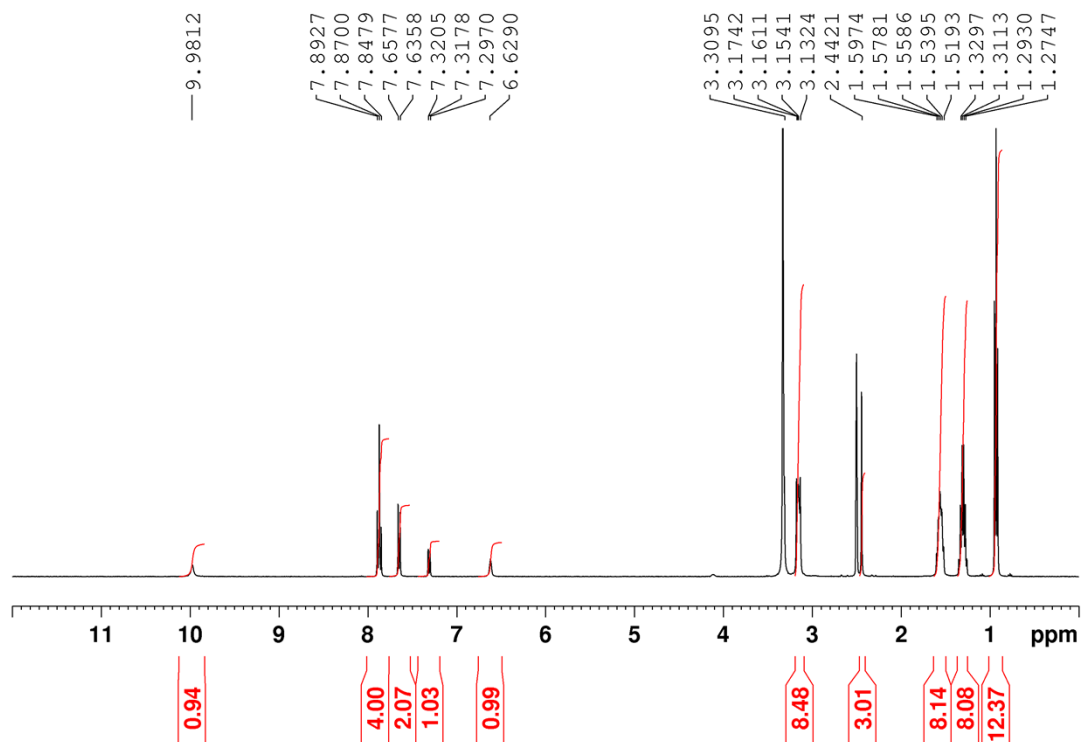


Figure S216. ^1H NMR of compound **60** in $\text{DMSO-}d_6$ conducted at 298 K.

References

- 1 L. J. White, S. N. Tyuleva, B. Wilson, H. J. Shepherd, K. K. L. Ng, S. J. Holder, E. R. Clark and J. R. Hiscock, *Chemistry - European Journal*, 2018, **24**, 7761–7773.
- 2 N. Allen, L. J. White, J. E. Boles, G. T. Williams, D. F. Chu, R. J. Ellaby, H. J. Shepherd, K. K. L. Ng, L. R. Blackholly, B. Wilson, D. P. Mulvihill and J. R. Hiscock, *ChemMedChem*, 2020, **15**, 2193–2205.
- 3 J. E. Boles, C. Bennett, J. Baker, K. L. F. Hilton, H. A. Kotak, E. R. Clark, Y. Long, L. J. White, H. Y. Lai, C. K. Hind, J. M. Sutton, M. D. Garrett, A. Cheasty, J. L. Ortega-Roldan, M. Charles, C. J. E. Haynes and J. R. Hiscock, *Chem Sci*, 2022, **13**, 9761–9773.
- 4 E. Medina-Carmona, L. Varela, A. C. Hendry, G. S. Thompson, L. J. White, J. E. Boles, J. R. Hiscock and J. L. Ortega-Roldan, *Chemical Communications*, 2020, **56**, 11665–11668.